BNL 50276 (T-603)

BNL 50276 (T-60
NCSAC - 33
EANDC(US)-150
INDC(USA)-25 "U

INDC — 38

Reports to . . .

THE AEC NUCLEAR CROSS SECTIONS ADVISORY COMMITTEE

Meeting at

LAWRENCE RADIATION LABORATORY
LIVERMORE, CALIFORNIA

December 1-3, 1970

Compiled by . . .

R.E. Chrien, Secretary, NCSAC

PREFACE

The reports in this document were submitted to the AEC Nuclear Cross Sections Advisory Committee (NCSAC) at the meeting at Livermore, California, on December 1-3, 1970. The reporting laboratories are those having a substantial effort in measuring neutron and nuclear cross sections of relevance to the U. S. applied nuclear energy program. The material contained in these reports is to be regarded as comprised of informal statements of recent developments and preliminary data. Appropriate subjects are listed as follows:

1. Microscopic neutron cross sections relevant to the nuclear energy program, including shielding. Inverse reactions where pertinent are included.

2. Charged particle cross sections, where they are relevant to 1) above, and where relevant to developing and testing nuclear models.

3. Gamma-ray production, radioactive decay, and theoretical developments in nuclear structure which are applicable to nuclear energy programs.

4. Proton and alpha-particle cross sections, at energies of up to 1 GeV, which are of interest to the space program.

These reports cannot be regarded as a complete summary of the nuclear research effort of the AEC. A number of laboratories, whose research is less programmatically oriented do not submit reports; neither do the submitted reports reflect all the work related to nuclear cross sections in progress at the submitting laboratory. Budgetary limitations have made it mandatory to follow more strictly the subject guidelines described above and therefore to restrict the size of this document.

Persons wishing to make use of these data should contact the individual experimenter for futher details. <u>The data which appear in this document should be quoted only by permission of the contributor and should be referenced as private communication, and not by this document number</u>.

This compilation has been produced almost completely from master copies prepared by the individual contributors listed in the Table of Contents. It is a pleasure to acknowledge their help in the preparation of these reports.

R. E. Chrien
Secretary, NCSAC
Brookhaven National Laboratory
Upton, New York 11973

TABLE OF CONTENTS

Previously submitted Reports to the AEC Nuclear Cross Sections Advisory Committee include the following:

May 1970 Meeting at Argonne National Laboratory	NCSAC- 31 EANDC(US)-143U INDC(US)- 22U
September 1969 Meeting at Rice University	WASH-1136 EANDC(US)-122U INDC(US)- 14U
April 1969 Meeting at Oak Ridge, Tennessee	WASH-1127 EANDC(US)-120U INDC(US)- 10U
October 1968 Meeting at Columbia University	WASH-1124 EANDC(US)-111U INDC(US)- 9U
April 1968 Meeting at Los Alamos, New Mexico	WASH-1093 EANDC(US)-105U INDC(US)- 2U
October 1967 Meeting at Idaho Falls, Idaho	WASH-1079 EANDC(US)-104U INDC(US)- 12U
April 1967 Meeting at Brookhaven, New York	WASH-1074 EANDC(US)- 99U INDC(US)- 9U
November 1966 Meeting at Argonne, Illinois	WASH-1071 EANDC(US)- 91U INDC(US)- 5U
March 1966 Meeting at Washington, D.C.	WASH-1068 EANDC(US)- 85U INDC(US)- 3U

The following is an index to measurements in NCSAC-33 pertinent to requests listed in WASH 1144, draft version, "Compilation of Requests for Nuclear Cross Section Measurements" (November 1969). A CINDA-type index has been prepared by L. T. Whitehead of the Division of Technical Information Extension, and follows on page vii.

WASH 1144 Request No.	Material	X-Section	NCSAC 33 page
2	H	ELASTIC	144
4	T	ELASTIC	148
8	HE-3	N-P	78
17	LI-7	TOTAL	200
27	B-10	ELASTIC	6
31,33	C	ELASTIC	164
32	C	ELASTIC	191
39,40	N-14	ELASTIC	226,164
43	N-14	GAMMA PROD	226
44	O	ELASTIC	227,164
47	O	GAMMA PROD	226
55	NA	TOTAL	191,41
61	AL	ELASTIC	227
64	AL	GAMMA PROD	75
66,67	SI	ELASTIC	227
73,74	CA	ELASTIC	227
80,81	TI	GAMMA PROD	171
89	V	ABS	202
92,93,96	CR	CAPT, RES PAR	202
98	MN	GAMMA PROD	95
99,100	FE	ELASTIC	227,164
101	FE	INELASTIC	227,208
104,105,106	FE	GAMMA PROD	75,176
122	NI	RES INT	202
224	MO	CAP SPECTRA	21,16
228	RH-103	N-GAMMA	65,44,41,90
254	SM-152	N-GAMMA	41
265,266	EU-151	N-GAMMA	41
267	EU-153	N-GAMMA	41
274,276	GD	N-GAMMA	68
277	GD-154	RES PAR	41
287,288,289	GD-158	N-GAMMA RES PAR	41,90
290	GD-160	RES INT	90
291	GD-160	RES PAR	41
294	ER-166	N-GAMMA	41
295	ER-167	N-GAMMA	41
300	TM-169	N-GAMMA	44
318	TA	N-GAMMA	68,90
325	W-182	RES PAR	41
327	W-184	RES PAR	41
330	W-186	RES PAR	41
331	AU	N-GAMMA	68,113
343	TH-232	N-GAMMA	44,126
344	TH-232	ABS	41,44
353	U-233	FISSION	59,12
356	U-233	NU BAR	12

WASH 1144 Request No.	Material	X-Section	NCSAC 33 page
358	U-233	ALPHA	12
361	U-233	DELAYED NEUT	155
382,382	U-235	FISSION	182
385	U-235	ETA	87,12
386	U-235	ALPHA	209,182,12
388	U-235	NU	12
389	U-235	FISS YIELD	123,5
390	U-235	DELAYED NEUT	155
391	U-235	CAP SPECTRA	24,152,28
405	U-238	ELASTIC	2
406	U-238	INELASTIC	2
412	U-238	DELAYED NEUT	155
413,414	U-238	N-GAMMA	68,44,182
419	U-238	RES PAR	41,44,21
424	NP-237	N-GAMMA	41,59
441	PU-239	FISSION	12
442	PU-239	FISSION	126
446	PU-239	ETA	12
447	PU-239	ALPHA	126
-	PU-239	NU-BAR	185
459	PU-240	N-GAMMA	203
461	PU-240	RES PAR	203
479	PU-242	N-GAMMA	132
492	AM-243	TOTAL	167
499	CM-244	TOTAL	136
501	CM-244	FISSION	148
503,504	CM-244	N-GAMMA	136
505	CM-245	TOTAL	136
506,507	CM-245	FISSION	136
509,510,511	CM-246	FISSION, N-GAMMA	136
512,513,514	CM-247	FISSION, N-GAMMA	136
516,517,518	CM-248	FISSION, N-GAMMA	136
521	CF-249	FISSION	136
528	CF-252	NU	12

ELEMENT S	A	QUANTITY	TYPE	ENERGY MIN	MAX	DOCUMENTATION REF VOL	PAGE	DATE	LAB	COMMENTS	SERIAL NO.
H	001	ELASTIC	EXPT-PROG	1. 5	3.0 7	NCSAC-33	144	D/70	LAS	HOPKINS+,INTEGRATED SIGS GVN,TBP ND	53387
H	001	DIFF ELASTIC	EXPT-PROG	6. 6	3. 7	NCSAC-33	245	D/70	YAL	FIRK+,POL TO BE MEASURED	53272
H	001	DIFF ELASTIC	EXPT-PROG	1. 5	3.0 7	NCSAC-33	144	D/70	LAS	HOPKINS+,TBL LEGENDRE COEFS,TBP ND	53389
H	001	POLARIZATION	EXPT-PROG	6. 6	3. 7	NCSAC-33	245	D/70	YAL	FIRK+,TO BE DONE	53273
H	001	POLARIZATION	EXPT-PROG	1. 5	3.0 7	NCSAC-33	144	D/70	LAS	HOPKINS+,TBL LEGENDRE COEFS,TBP ND	53388
D	002	TOTAL XSECT	EXPT-PROG	6		NCSAC-33	162	D/70	NBS	SCHWARTZ+,TO BE DONE	53367
D	002	DIFF ELASTIC	EXPT-PROG	5.5 6	2.3 7	NCSAC-33	148	D/70	LAS	SEAGRAVE+,7ES,TBL COS THETA AND SIG	53384
D	002	POLARIZATION	EXPT-PROG	5.5 6	2.3 7	NCSAC-33	148	D/70	LAS	SEAGRAVE+,7ES,TBL COS THETA AND SIG	53383
D	002	GAMMA N	EXPT-PROG	5. 6	3. 7	NCSAC-33	245	D/70	YAL	FIRK+,NEUT POL AT 45-90DEG,TBC,NDG	53271
T	003	DIFF ELASTIC	EXPT-PROG	6.0 6	2.3 7	NCSAC-33	148	D/70	LAS	SEAGRAVE+,6ES,TBL COS THETA AND SIG	53382
T	003	POLARIZATION	EXPT-PROG	6.0 6	2.3 7	NCSAC-33	148	D/70	LAS	SEAGRAVE+,6ES,TBL COS THETA AND SIG	53381
HE	003	N,PROTON	EXPT-PROG	8.5 4	5.2 5	NCSAC-33	78	D/70	GA	COSTELLO+,HE3 PROP DET,TBL+CURV 14ES	53030
HE	004	DIFF ELASTIC	EXPT-PROG	1.8 7	2.4 7	NCSAC-33	146	D/70	LAS	NIILER+,3ES,PHASE SHIFTS GIVEN,TBP	53386
HE	004	POLARIZATION	EXPT-PROG	1.8 7	2.4 7	NCSAC-33	146	D/70	LAS	NIILER+,3ES,PHASE SHIFTS GIVEN,TBP	53385
LI	007	TOTAL XSECT	EXPT-PROG	1.2 5	2. 6	NCSAC-33	200	D/70	RPI	BLOCK+,TRANS,PRELIM CURVS SHOWN	53307
LI	007	RESON PARAMS	EXPT-PROG	2.5 5		NCSAC-33	168	D/70	ORL	ALLEN+,WN AND WG GIVEN,TBP IN PR	53335
LI	007	INELST GAMMA	EXPT-PROG	NDG		NCSAC-33	176	D/70	ORL	PEREY+,SCINT DET,TO BE COMPLETED,NDG	53326
BE	009	TOTAL XSECT	EXPT-PROG	6		NCSAC-33	162	D/70	NBS	SCHWARTZ+,TO BE COMPLETED,NO DATA	53368
BE	009	DIFF ELASTIC	EXPT-PROG	NDG		NCSAC-33	164	D/70	NEL	BUCHER+,TO BE DONE,SMALL-ANGLE SCAT	53345
BE	009	N,GAMMA	EXPT-PROG	5		NCSAC-33	171	D/70	ORL	MACKLIN+,NO DATA GIVEN	53328
B	010	DIFF ELASTIC	EXPT-PROG	7.5 4	2.2 6	NCSAC-33	6	D/70	ANL	ADAMS+,EARLIER DATA ANALYZED,NDG,TBP	53002
B	010	POLARIZATION	EXPT-PROG	7.5 4	2.2 6	NCSAC-33	6	D/70	ANL	ADAMS+,EARLIER DATA ANALYZED,NDG,TBP	53001
B	011	DIFF ELASTIC	EXPT-PROG	7.5 4	2.2 6	NCSAC-33	6	D/70	ANL	ADAMS+,EARLIER DATA ANALYZED,NDG,TBP	53000
B	011	POLARIZATION	EXPT-PROG	7.5 4	2.2 6	NCSAC-33	6	D/70	ANL	ADAMS+,EARLIER DATA ANALYZED,NDG,TBP	52999
C		TOTAL XSECT	EXPT-PROG	5. 5	2.5 7	NCSAC-33	191	D/70	RPI	CLEMENT+,LINAC,CURVES	53308
C		DIFF ELASTIC	EXPT-PROG	7.5 6	9.5 6	NCSAC-33	164	D/70	NEL	BUCHER+,2ES,THETA#3-15DEG,NO DATA	53366
C	012	DIFF ELASTIC	EXPT-PROG	4.0 6	5.6 6	NCSAC-33	34	D/70	CSE	BOSCHUNG+,TBP IN NP,NO DATA GIVEN	52998
C	012	DIFF INELAST	EXPT-PROG	4.0 6	5.6 6	NCSAC-33	34	D/70	CSE	BOSCHUNG+,TBP IN NP,NO DATA GIVEN	52994
C	013	RESON PARAMS	EXPT-PROG	1.5 5		NCSAC-33	168	D/70	ORL	ALLEN+,WN AND WG GIVEN,TBP IN PR	53334
C	013	N,GAMMA	EXPT-PROG	5		NCSAC-33	168	D/70	ORL	ALLEN+,TBP IN PHYSICAL REVIEW,LINAC	53337
N		DIFF ELASTIC	EXPT-PROG	9. 6	1.1 7	NCSAC-33	226	D/70	TNC	BUCHANAN+,15 ANGS 30-120DEG,NO DATA	53258
N		DIFF ELASTIC	EXPT-PROG	7.5 6	9.5 6	NCSAC-33	164	D/70	NEL	BUCHER+,2ES,THETA#3-15DEG,NO DATA	53365
N		NONEL GAMMAS	EXPT-PROG	1.5 7		NCSAC-33	226	D/70	TNC	TUCKER+,GE(LI)+NAI(TL) DET,TBC,NDG	53256
N		DIFF INELAST	EXPT-PROG	9. 6	1.1 7	NCSAC-33	226	D/70	TNC	BUCHANAN+, TOF SPEC SHOWN	53259
O		TOTAL XSECT	EXPT-PROG	2.4 6		NCSAC-33	41	D/70	COL	KALYNA+,ANAL TO BE COMPLTD,VALU GIVN	53179
O		DIFF ELASTIC	EXPT-PROG	9. 6	1.1 7	NCSAC-33	227	D/70	TNC	NELLIS+,TOF SPEC SHOWN,ANAL TBC	53260
O		DIFF ELASTIC	EXPT-PROG	7.5 6	9.5 6	NCSAC-33	164	D/70	NEL	BUCHER+,2ES,THETA#3-15DEG,NO DATA	53364
O		NONEL GAMMAS	EXPT-PROG	1.5 7		NCSAC-33	226	D/70	TNC	TUCKER+,GE(LI)+NAI(TL) DET,TBC,NDG	53257
O		DIFF INELAST	EXPT-PROG	9. 6	1.1 7	NCSAC-33	227	D/70	TNC	NELLIS+,TOF SPEC SHOWN,ANAL TBC	53261
O	016	TOTAL XSECT	EXPT-PROG	2.4 6		NCSAC-33	41	D/70	COL	KALYNA+,ANAL TO BE COMPLTD,VALU GIVN	53180
O	016	TOTAL XSECT	EXPT-PROG	1.7 6	4.4 6	NCSAC-33	165	D/70	ORL	FOWLER+,T(P,N) SOURCE,30KEV RSLN,CRV	53340
O	016	RESON PARAMS	EXPT-PROG	4.3 5		NCSAC-33	168	D/70	ORL	ALLEN+,WN AND WG GIVEN,TBP IN PR	53333
O	016	N,GAMMA	EXPT-PROG	5		NCSAC-33	168	D/70	ORL	ALLEN+,TBP IN PHYSICAL REVIEW,LINAC	53336
F	019	TOTAL XSECT	EXPT-PROG	NDG		NCSAC-33	41	D/70	COL	CAMARDA+,TRANS,NO DATA GIVEN	53178
NE		TOTAL XSECT	EXPT-PROG	NDG		NCSAC-33	41	D/70	COL	CAMARDA+,TRANSMISSION,NO DATA GIVEN	53172

ELEMENT S A	QUANTITY	TYPE	ENERGY MIN	ENERGY MAX	DOCUMENTATION REF VOL PAGE DATE	LAB	COMMENTS	SERIAL NO.
NA 023	TOTAL XSECT	EXPT-PROG	NDG		NCSAC-33 41 D/70	COL	CAMARDA+,TRANS,NO DATA GIVEN	53177
NA 023	TOTAL XSECT	EXPT-PROG	5. 5	4. 7	NCSAC-33 191 D/70	RPI	CLEMENT+,LINAC,CURVS,MUCH STRUCTURE	53309
NA 023	INELST GAMMA	EXPT-PROG	3. 5	1.5 6	NCSAC-33 5 D/70	ANL	SMITH,GE(LI) DET,NO DATA GIVEN	53217
NA 023	INELST GAMMA	EXPT-PROG	NDG		NCSAC-33 176 D/70	ORL	PEREY+,SCINT DET,TO BE COMPLETED,NDG	53325
MG	TOTAL XSECT	EXPT-PROG	NDG		NCSAC-33 41 D/70	COL	CAMARDA+,TRANS,NO DATA GIVEN	53176
AL 027	TOTAL XSECT	EXPT-PROG	NDG		NCSAC-33 41 D/70	COL	CAMARDA+,TRANS,NO DATA GIVEN	53175
AL 027	DIFF ELASTIC	EXPT-PROG	9. 6	1.1 7	NCSAC-33 227 D/70	TNC	WILLIAMS+,ANAL TO BE COMPL.,NO DATA	53264
AL 027	DIFF INELAST	EXPT-PROG	9. 6	1.1 7	NCSAC-33 227 D/70	TNC	WILLIAMS+,ANAL TO BE COMPL,NO DATA	53265
AL 027	INELST GAMMA	EXPT-PROG	8.6 5	1.6 7	NCSAC-33 75 D/70	GA	ORPHAN+,GE(LI),CURV FOR 1013KEV GAM	53032
SI	DIFF ELASTIC	EXPT-PROG	9. 6	1.1 7	NCSAC-33 227 D/70	TNC	WILLIAMS+,ANAL TO BE COMPL,NO DATA	53268
SI	DIFF INELAST	EXPT-PROG	9. 6	1.1 7	NCSAC-33 227 D/70	TNC	WILLIAMS+,ANAL TO BE COMPL,NO DATA	53269
SI	INELST GAMMA	EXPT-PROG	NDG		NCSAC-33 176 D/70	ORL	PEREY+,SCINT DET,TO BE COMPLETED,NDG	53324
S	TOTAL XSECT	EXPT-PROG	NDG		NCSAC-33 41 D/70	COL	CAMARDA+,TRANSMISSION,NO DATA GIVEN	53174
S	DIFF ELASTIC	EXPT-PROG	NDG		NCSAC-33 164 D/70	NEL	BUCHER+,TO BE DONE,SMALL-ANGLE SCAT	53344
CL	TOTAL XSECT	EXPT-PROG	NDG		NCSAC-33 41 D/70	COL	CAMARDA+,TRANSMISSION,NO DATA GIVEN	53169
K	TOTAL XSECT	EXPT-PROG	NDG		NCSAC-33 41 D/70	COL	CAMARDA+,TRANSMISSION,NO DATA GIVEN	53170
K 040	SPECT NGAMMA	EXPT-PROG	THR		NCSAC-33 148 D/70	LAS	SHERA+,GE(LI),K41 LVLS+GAM ES SHOWN	53375
CA	DIFF ELASTIC	EXPT-PROG	9. 6	1.1 7	NCSAC-33 227 D/70	TNC	WILLIAMS+,ANAL TO BE COMPL,NO DATA	53266
CA	DIFF INELAST	EXPT-PROG	9. 6	1.1 7	NCSAC-33 227 D/70	TNC	WILLIAMS+,ANAL TO BE COMPL,NO DATA	53267
TI	DIFF ELASTIC	EXPT-PROG	1. 5	1.5 6	NCSAC-33 1 D/70	ANL	SMITH+,ANAL TO BE COMPLETED,NO DATA	53238
TI	DIFF INELAST	EXPT-PROG	1. 5	1.5 6	NCSAC-33 1 D/70	ANL	SMITH+,ANAL TO BE COMPLETED,NO DATA	53239
TI	N,GAMMA	EXPT-PROG	3. 4	3. 6	NCSAC-33 171 D/70	ORL	ALLEN+,ANAL TO BE COMPLETED,NO DATA	53332
TI	SPECT NGAMMA	EXPT-PROG	3. 4	3. 6	NCSAC-33 171 D/70	ORL	ALLEN+,RELATIVE GAMMA YLD SHOWN	53331
V	RESON PARAMS	EXPT-PROG	1. 2	2. 5	NCSAC-33 202 D/70	RPI	BLOCK+,WN WG CORRELATN COEFS GIVEN	53288
V	RESON PARAMS	EXPT-PROG	1. 2	2. 5	NCSAC-33 202 D/70	RPI	STIEGLITZ+,CAPT+TRANS MEASTS,TBP,NDG	53294
V	STRNTH FNCTN	EXPT-PROG	1. 2	3. 5	NCSAC-33 202 D/70	RPI	STIEGLITZ+,CAPT+TRANS MEASTS,NDG,TBP	53301
V	INELST GAMMA	EXPT-PROG	NDG		NCSAC-33 176 D/70	ORL	PEREY+,SCINT DET,TOF SPEC GIVEN,TBC	53323
V	RES INT ABS	EXPT-PROG	1. 2	3. 5	NCSAC-33 202 D/70	RPI	STIEGLITZ+,CAPT+TRANS MEASTS,NDG,TBP	53295
V	N,GAMMA	EXPT-PROG	1. 2	2. 5	NCSAC-33 202 D/70	RPI	STIEGLITZ+,0.6NS/M RESOL,NDG,TBP NP	53246
V 051	RESON PARAMS	EVAL-PROG	4.2 3	8.8 4	NCSAC-33 213 D/70	RPI	LUBERT+,STIEGLITZ DATA,J+WN GIVEN	53254
V 051	STRNTH FNCTN	EVAL-PROG	4.2 3	8.8 4	NCSAC-33 213 D/70	RPI	LUBERT+,STIEGLITZ DATA,VALUES GIVEN	53255
CR 050	RESON PARAMS	EXPT-PROG	1. 2	2. 5	NCSAC-33 202 D/70	RPI	BLOCK+,WN WG CORRELATN COEFS GIVEN	53286
CR 050	RESON PARAMS	EXPT-PROG	1. 2	2. 5	NCSAC-33 202 D/70	RPI	STIEGLITZ+,CAPT+TRANS MEASTS,TBP,NDG	53292
CR 050	STRNTH FNCTN	EXPT-PROG	1. 2	3. 5	NCSAC-33 202 D/70	RPI	STIEGLITZ+,CAPT+TRANS MEASTS,NDG,TBP	53306
CR 050	RES INT ABS	EXPT-PROG	1. 2	3. 5	NCSAC-33 202 D/70	RPI	STIEGLITZ+,CAPT+TRANS MEASTS,NDG,TBP	53300
CR 050	N,GAMMA	EXPT-PROG	1. 2	2. 5	NCSAC-33 202 D/70	RPI	STIEGLITZ+,0.6NS/M RESOL,NDG,TBP NP	53241
CR 052	RESON PARAMS	EXPT-PROG	1. 2	2. 5	NCSAC-33 202 D/70	RPI	BLOCK+,WN WG CORRELATN COEFS GIVEN	53285
CR 052	RESON PARAMS	EXPT-PROG	1. 2	2. 5	NCSAC-33 202 D/70	RPI	STIEGLITZ+,CAPT+TRANS MEASTS,TBP,NDG	53291
CR 052	STRNTH FNCTN	EXPT-PROG	1. 2	3. 5	NCSAC-33 202 D/70	RPI	STIEGLITZ+,CAPT+TRANS MEASTS,NDG,TBP	53305
CR 052	RES INT ABS	EXPT-PROG	1. 2	3. 5	NCSAC-33 202 D/70	RPI	STIEGLITZ+,CAPT+TRANS MEASTS,NDG,TBP	53299
CR 052	N,GAMMA	EXPT-PROG	1. 2	2. 5	NCSAC-33 202 D/70	RPI	STIEGLITZ+,0.6NS/M RESOL,NDG,TBP NP	53245
CR 053	RESON PARAMS	EXPT-PROG	1. 2	2. 5	NCSAC-33 202 D/70	RPI	BLOCK+,WN WG CORRELATN COEFS GIVEN	53284
CR 053	RESON PARAMS	EXPT-PROG	1. 2	2. 5	NCSAC-33 202 D/70	RPI	STIEGLITZ+,CAPT+TRANS MEASTS,TBP,NDG	53290
CR 053	STRNTH FNCTN	EXPT-PROG	1. 2	3. 5	NCSAC-33 202 D/70	RPI	STIEGLITZ+,CAPT+TRANS MEASTS,NDG,TBP	53304
CR 053	RES INT ABS	EXPT-PROG	1. 2	3. 5	NCSAC-33 202 D/70	RPI	STIEGLITZ+,CAPT+TRANS MEASTS,NDG,TBP	53298
CR 053	N,GAMMA	EXPT-PROG	1. 2	2. 5	NCSAC-33 202 D/70	RPI	STIEGLITZ+,0.6NS/M RESOL,NDG,TBP NP	53244

ELEMENT S A	QUANTITY	TYPE	ENERGY MIN	ENERGY MAX	DOCUMENTATION REF VOL PAGE DATE	LAB	COMMENTS	SERIAL NO.
CR 054	RESON PARAMS	EXPT-PROG	1. 2	2. 5	NCSAC-33 202 D/70	RPI	BLOCK+,WN WG CORRELATN COEFS GIVEN	53283
CR 054	RESON PARAMS	EXPT-PROG	1. 2	2. 5	NCSAC-33 202 D/70	RPI	STIEGLITZ+,CAPT+TRANS MEASTS,TBP,NDG	53289
CR 054	STRNTH FNCTN	EXPT-PROG	1. 2	3. 5	NCSAC-33 202 D/70	RPI	STIEGLITZ+,CAPT+TRANS MEASTS,NDG,TBP	53303
CR 054	RES INT ABS	EXPT-PROG	1. 2	3. 5	NCSAC-33 202 D/70	RPI	STIEGLITZ+,CAPT+TRANS MEASTS,NDG,TBP	53297
CR 054	N,GAMMA	EXPT-PROG	1. 2	2. 5	NCSAC-33 202 D/70	RPI	STIEGLITZ+,0.6NS/M RESOL,NDG,TBP NP	5324[illegible]
MN 055	SPECT NGAMMA	EXPT-PROG	THR	2. 3	NCSAC-33 95 D/70	MTR	GREENWOOD+,2ES,TBL 3.0-7.3MEV GAMMAS	53405
FE	DIFF ELASTIC	EXPT-PROG	9. 6	1.1 7	NCSAC-33 227 D/70	TNC	WILLIAMS+,ANAL TO BE COMPL,NO DATA	53262
FE	DIFF ELASTIC	EXPT-PROG	NDG		NCSAC-33 164 D/70	NEL	BUCHER+,TO BE DONE,SMALL-ANGLE SCAT	53343
FE	DIFF INELAST	EXPT-PROG	9. 6	1.1 7	NCSAC-33 227 D/70	TNC	WILLIAMS+,ANAL TO BE COMPL,NO DATA	53263
FE	DIFF INELAST	EXPT-PROG	3		NCSAC-33 208 D/70	RPI	ZUHR+,TOF,SCINT DET,TO BE COMPL,NDG	53279
FE	INELST GAMMA	EXPT-PROG	8.6 5	1.6 7	NCSAC-33 75 D/70	GA	ORPHAN+,GE(LI),CURV FOR 847KEV GAM	53033
FE	INELST GAMMA	EXPT-PROG	NDG		NCSAC-33 176 D/70	ORL	PEREY+,SCINT DET,TOF SPEC GIVEN,TBC	53322
FE 054	DIFF ELASTIC	EXPT-PROG	4.0 6	5.6 6	NCSAC-33 34 D/70	CSE	BOSCHUNG+,TBP IN NP,NO DATA GIVEN	52997
FE 054	DIFF INELAST	EXPT-PROG	4.0 6	5.6 6	NCSAC-33 34 D/70	CSE	BOSCHUNG+,TBP IN NP,NO DATA GIVEN	52993
FE 054	INELST GAMMA 2	EXPT-PROG	5.3 6	9.0 6	NCSAC-33 178 D/70	ORL	DICKENS+,8NEUT ES,SIGS FOR 2GAMS GVN FULL EXPT SEE ORNL-4592	53319 53318
FE 056	TOTAL XSECT	EVAL-PROG	1.5 6	2.0 6	NCSAC-33 63 D/70	COL	TROUBETZKOY,STRONG FLUCTUATION,NDG	53045
FE 056	ELASTIC	EVAL-PROG	1.5 6	2.0 6	NCSAC-33 63 D/70	COL	TROUBETZKOY,STRONG FLUCTUATION,NDG	53044
FE 056	DIFF ELASTIC	EVAL-PROG	1.5 6	2.0 6	NCSAC-33 63 D/70	COL	TROUBETZKOY, STRONG FLUCTUATION,NDG	53043
FE 056	DIFF INELAST	EVAL-PROG	1.5 6	2.0 6	NCSAC-33 63 D/70	COL	TROUBETZKOY, .85MEV LVL,NO DATA GIVN	53042
FE 56	INELST GAMMA	EXPT-PROG	8.6 5	1.6 7	NCSAC-33 75 D/70	GA	ORPHAN+,GE(LI),CURV FOR 847KEV GAMMA	53031
FE 056	INELST GAMMA 2	EXPT-PROG	5.3 6	9.0 6	NCSAC-33 178 D/70	ORL	DICKENS+,8 NEUT ES,TABLE+CURVES FULL EXPT SEE ORNL-4592	53321 53320
CO 059	TOTAL XSECT	EXPT-PROG	3. 5	1.6 6	NCSAC-33 123 D/70	LOK	FISHER+,DEFORMATN EFFECT,CURVE,TBC	53362
CO 059	TOTAL XSECT	EXPT-PROG	3. 5	8. 6	NCSAC-33 123 D/70	LOK	FISHER+,SPIN-SPIN EFFECT,OPTMDL ANAL	53363
NI	DIFF INELAST	EXPT-PROG	3		NCSAC-33 208 D/70	RPI	ZUHR+,SCINT DET,TOF SPECT GIVEN,TBC	53278
NI 058	DIFF ELASTIC	EXPT-PROG	4.0 6	5.6 6	NCSAC-33 34 D/70	CSE	BOSCHUNG+,TBP IN NP,NO DATA GIVEN	52996
NI 058	DIFF INELAST	EXPT-PROG	4.0 6	5.6 6	NCSAC-33 34 D/70	CSE	BOSCHUNG+,TBP IN NP,NO DATA GIVEN	52992
NI 060	RESON PARAMS	EXPT-PROG	1. 2	2. 5	NCSAC-33 202 D/70	RPI	BLOCK+,WN WG CORRELATN COEFS GIVEN	53287
NI 060	RESON PARAMS	EXPT-PROG	1. 2	2. 5	NCSAC-33 202 D/70	RPI	STIEGLITZ+,CAPT+TRANS MEASTS,TBP,NDG	53293
NI 060	STRNTH FNCTN	EXPT-PROG	1. 2	3. 5	NCSAC-33 202 D/70	RPI	STIEGLITZ+,CAPT+TRANS MEASTS,NDG,TBP	53302
NI 060	DIFF ELASTIC	EXPT-PROG	4.0 6	5.6 6	NCSAC-33 34 D/70	CSE	BOSCHUNG+,TBP IN NP,NO DATA GIVEN	52995
NI 060	DIFF INELAST	EXPT-PROG	4.0 6	5.6 6	NCSAC-33 34 D/70	CSE	BOSCHUNG+,TBP IN NP,NO DATA GIVEN	52991
NI 060	RES INT ABS	EXPT-PROG	1. 2	3. 5	NCSAC-33 202 D/70	RPI	STIEGLITZ+,CAPT+TRANS MEASTS,NDG,TBP	53296
NI 060	N,GAMMA	EXPT-PROG	1. 2	2. 5	NCSAC-33 202 D/70	RPI	STIEGLITZ+,0.6NS/M RESOL,NDG,TBP NP	53242
CU	DIFF ELASTIC	EXPT-PROG	NDG		NCSAC-33 164 D/70	NEL	BUCHER+,TO BE DONE,SMALL-ANGLE SCAT	53342
CU	SPECT NGAMMA	EXPT-PROG	1.4 7		NCSAC-33 64 D/70	COL	STAMATELATOS+,NO DATA GIVEN,TBP	52990
CU	SPECT NGAMMA	EXPT-PROG	THR	2. 3	NCSAC-33 95 D/70	MTR	GREENWOOD+,2ES,TBL+CURV..58-7.9MEV G	53406
CU 063	RES INT ABS	EXPT-PROG	PILE		NCSAC-33 90 D/70	MTR	SCOVILLE+,FAST SPECTRA,VALUE GIVEN	53018
AS 075	INELST GAMMA	EXPT-PROG	3. 5	1.5 6	NCSAC-33 5 D/70	ANL	SMITH,GE(LI) DET,NO DATA GIVEN	53216
SE	TOTAL XSECT	EXPT-PROG	NDG		NCSAC-33 41 D/70	COL	CAMARDA+,TRANSMISSION,NO DATA GIVEN	53171
Y 089	RES INT ABS	EXPT-PROG	PILE		NCSAC-33 90 D/70	MTR	SCOVILLE+,FAST SPECTRA,VALUE GIVEN	53017
ZR	SPECT NGAMMA	EXPT-PROG	1.4 7		NCSAC-33 64 D/70	COL	STAMATELATOS+,NO DATA GIVEN,TBP	52989
NB 093	RESON PARAMS	EXPT-PROG	3.4 1	1.0 4	NCSAC-33 126 D/70	LAS	HARLOW+,NUCL SHOT,FROM N,G. NO DATA	53360
NB 093	RES INT ABS	EXPT-PROG	PILE		NCSAC-33 90 D/70	MTR	SCOVILLE+,FAST SPECTRA,VALUE GIVEN	53016
NB 093	SPECT NGAMMA	EXPT-PROG	3.4 1	1.0 4	NCSAC-33 126 D/70	LAS	HARLOW+,NUCL SHOT,MOXON-RAE DET,NDG	53361

ELEMENT S A	QUANTITY	TYPE	ENERGY MIN	ENERGY MAX	DOCUMENTATION REF VOL	PAGE	DATE	LAB	COMMENTS	SERIAL NO.
MO	N,GAMMA	EXPT-PROG	1. 3	1. 6	NCSAC-33	68	D/70	GA	FRICKE+, CURVE,CFD OTHER DATA	53037
MO 092	TOTAL XSECT	EXPT-PROG	1. 5	1.6 6	NCSAC-33	1	D/70	ANL	SMITH+,NO DATA,ANAL TO BE COMPLETED	53237
MO 092	DIFF ELASTIC	EXPT-PROG	1. 5	1.6 6	NCSAC-33	1	D/70	ANL	SMITH+,NO DATA,ANAL TO BE COMPLETED	53232
MO 092	DIFF INELAST	EXPT-PROG	1. 5	1.6 6	NCSAC-33	1	D/70	ANL	SMITH+,NO DATA,ANAL TO BE COMPLETED	53227
MO 094	TOTAL XSECT	EXPT-PROG	1. 5	1.6 6	NCSAC-33	1	D/70	ANL	SMITH+,NO DATA,ANAL TO BE COMPLETED	53236
MO 094	DIFF ELASTIC	EXPT-PROG	1. 5	1.6 6	NCSAC-33	1	D/70	ANL	SMITH+,NO DATA,ANAL TO BE COMPLETED	53231
MO 094	DIFF INELAST	EXPT-PROG	1. 5	1.6 6	NCSAC-33	1	D/70	ANL	SMITH+,NO DATA,ANAL TO BE COMPLETED	53226
MO 096	TOTAL XSECT	EXPT-PROG	1. 5	1.6 6	NCSAC-33	1	D/70	ANL	SMITH+,NO DATA,ANAL TO BE COMPLETED	53235
MO 096	DIFF ELASTIC	EXPT-PROG	1. 5	1.6 6	NCSAC-33	1	D/70	ANL	SMITH+,NO DATA,ANAL TO BE COMPLETED	53230
MO 096	DIFF INELAST	EXPT-PROG	1. 5	1.6 6	NCSAC-33	1	D/70	ANL	SMITH+,NO DATA,ANAL TO BE COMPLETED	53225
MO 098	TOTAL XSECT	EXPT-PROG	1. 5	1.6 6	NCSAC-33	1	D/70	ANL	SMITH+,NO DATA,ANAL TO BE COMPLETED	53234
MO 098	DIFF ELASTIC	EXPT-PROG	1. 5	1.6 6	NCSAC-33	1	D/70	ANL	SMITH+,NO DATA,ANAL TO BE COMPLETED	53229
MO 098	DIFF INELAST	EXPT-PROG	1. 5	1.6 6	NCSAC-33	1	D/70	ANL	SMITH+,NO DATA,ANAL TO BE COMPLETED	53224
MO 098	RES INT ABS	EXPT-PROG	PILE		NCSAC-33	90	D/70	MTR	SCOVILLE+,FAST SPECTRA,VALUE GIVEN	53015
MO 098	SPECT NGAMMA	EXPT-PROG		1.2 3	NCSAC-33	21	D/70	BNL	CHRIEN+,SPECT FROM 6RES,ONLY 2SHOWN	53188
MO 098	SPECT NGAMMA	EXPT-PROG	1.2 1		NCSAC-33	16	D/70	BNL	CHRIEN+,ABSOL GAMMA INTENSITY REL AU	53197
MO 100	TOTAL XSECT	EXPT-PROG	1. 5	1.6 6	NCSAC-33	1	D/70	ANL	SMITH+,NO DATA,ANAL TO BE COMPLETED	53233
MO 100	DIFF ELASTIC	EXPT-PROG	1. 5	1.6 6	NCSAC-33	1	D/70	ANL	SMITH+,NO DATA,ANAL TO BE COMPLETED	53228
MO 100	DIFF INELAST	EXPT-PROG	1. 5	1.6 6	NCSAC-33	1	D/70	ANL	SMITH+,NO DATA,ANAL TO BE COMPLETED	53223
RH 103	TOTAL XSECT	EXPT-PROG	NDG		NCSAC-33	41	D/70	COL	CAMARDA+,TRANSMISSION,NO DATA GIVEN	53149
RH 103	RESON PARAMS	EXPT-PROG	1.3 0	8.4 2	NCSAC-33	65	D/70	GA	CARLSON+,2G*WN WG J FOR 19 RESON	53041
RH 103	RESON PARAMS	EXPT-PROG	3		NCSAC-33	44	D/70	COL	RAHN+,FROM N,G. ANAL TBC,NO DATA GVN	53054
RH 103	RESON PARAMS	EXPT-PROG	NDG		NCSAC-33	41	D/70	COL	CAMARDA+,TRANSMISSION,NO DATA GIVEN	53131
RH 103	RES INT ABS	EXPT-PROG	PILE		NCSAC-33	90	D/70	MTR	SCOVILLE+,FAST SPECTRA,VALUE GIVEN	53014
RH 103	N,GAMMA	EXPT-PROG	3		NCSAC-33	44	D/70	COL	RAHN+,MOXON-RAE,ANAL TBC,NO DATA	53060
RH 103	N,GAMMA	EXPT-PROG	1. 3	1. 6	NCSAC-33	65	D/70	GA	CARLSON+,CURVE,CFD OTHER DATA	53078
CD	TOTAL XSECT	EXPT-PROG	NDG		NCSAC-33	41	D/70	COL	CAMARDA+,TRANSMISSION,NO DATA GIVEN	53168
CD 110	TOTAL XSECT	EXPT-PROG	NDG		NCSAC-33	41	D/70	COL	CAMARDA+,TRANSMISSION,NO DATA GIVEN	53164
CD 110	RESON PARAMS	EXPT-PROG	NDG		NCSAC-33	41	D/70	COL	CAMARDA+,TRANSMISSION,NO DATA GIVEN	53146
CD 111	RESON PARAMS	EXPT-PROG	8.6 1		NCSAC-33	17	D/70	BNL	CHRIEN+,PRELIM J GIVEN,ANAL TBC	53195
CD 111	SPECT NGAMMA	EXPT-PROG	1. 1	1.5 3	NCSAC-33	17	D/70	BNL	CHRIEN+,ANAL TO BE COMPLETED	53196
CD 111	SPECT NGAMMA	EXPT-PROG	2.8 1		NCSAC-33	16	D/70	BNL	CHRIEN+,ABSOL GAMMA INTENSITY REL AU	53198
CD 112	TOTAL XSECT	EXPT-PROG	NDG		NCSAC-33	41	D/70	COL	CAMARDA+,TRANSMISSION,NO DATA GIVEN	53163
CD 112	RESON PARAMS	EXPT-PROG	NDG		NCSAC-33	41	D/70	COL	CAMARDA+,TRANSMISSION,NO DATA GIVEN	53145
CD 114	TOTAL XSECT	EXPT-PROG	NDG		NCSAC-33	41	D/70	COL	CAMARDA+,TRANSMISSION,NO DATA GIVEN	53162
CD 114	RESON PARAMS	EXPT-PROG	NDG		NCSAC-33	41	D/70	COL	CAMARDA+,TRANSMISSION,NO DATA GIVEN	53144
CD 116	TOTAL XSECT	EXPT-PROG	NDG		NCSAC-33	41	D/70	COL	CAMARDA+,TRANSMISSION,NO DATA GIVEN	53161
CD 116	RESON PARAMS	EXPT-PROG	NDG		NCSAC-33	41	D/70	COL	CAMARDA+,TRANSMISSION,NO DATA GIVEN	53143
IN 113	RESON PARAMS	EXPT-PROG		2.0 3	NCSAC-33	41	D/70	COL	CAMARDA+,1968 MEASTS,AVG D 48 LVLS	53112
IN 113	STRNTH FNCTN	EXPT-PROG		2.0 3	NCSAC-33	41	D/70	COL	CAMARDA+,1968 MEASTS,SO GIVEN	53091
IN 115	RESON PARAMS	EXPT-PROG	2.3 1	2.5 2	NCSAC-33	41	D/70	COL	CAMARDA+,1968 MEASTS,G*WN,WG 15RESON	53081
IN 115	RESON PARAMS	EXPT-PROG	2.3 1	2.0 3	NCSAC-33	41	D/70	COL	CAMARDA+,1968 MEASTS,WN FOR MANY RES	53088
IN 115	RESON PARAMS	EXPT-PROG	2.2 1	2.0 3	NCSAC-33	41	D/70	COL	CAMARDA+,1968 MEASTS,AVG D 145 LVLS	53111
IN 115	STRNTH FNCTN	EXPT-PROG	2.2 1	2.0 3	NCSAC-33	41	D/70	COL	CAMARDA+,1968 MEASTS,SO GIVEN	53090
SB	SPECT NGAMMA	EXPT-PROG	1.4 7		NCSAC-33	64	D/70	COL	STAMATELATOS+,NO DATA GIVEN,TBP	52988

ELEMENT S A	QUANTITY	TYPE	ENERGY MIN	MAX	DOCUMENTATION REF VOL PAGE	DATE	LAB	COMMENTS	SERIAL NO.
XE 124	SPECT NGAMMA	EXPT-PROG	5.2 0		NCSAC-33 30	D/70	BNL	KANE+,TO BE COMPLETED,NO DATA GIVEN	53181
LA 139	RESON PARAMS	EXPT-PROG	6.0 2	1.0 4	NCSAC-33 41	D/70	COL	CAMARDA+,1968 MEASTS,AVG D 66 LVLS	53110
LA 139	STRNTH FNCTN	EXPT-PROG	6.0 2	1.0 4	NCSAC-33 41	D/70	COL	CAMARDA+,1968 MEASTS,SO GIVEN	53089
LA 139	RES INT ABS	EXPT-PROG	PILE		NCSAC-33 90	D/70	MTR	SCOVILLE+,FAST SPECTRA,VALUE GIVEN	53013
CE 140	TOTAL XSECT	EXPT-PROG	NDG		NCSAC-33 41	D/70	COL	CAMARDA+,TRANSMISSION,NO DATA GIVEN	53160
CE 140	RESON PARAMS	EXPT-PROG	NDG		NCSAC-33 41	D/70	COL	CAMARDA+,TRANSMISSION,NO DATA GIVEN	53142
CE 140	RES INT ABS	EXPT-PROG	PILE		NCSAC-33 90	D/70	MTR	SCOVILLE+,FAST SPECTRA,VALUE GIVEN	53012
CE 142	RES INT ABS	EXPT-PROG	PILE		NCSAC-33 90	D/70	MTR	SCOVILLE+,FAST SPECTRA,VALUE GIVEN	53010
PR 141	RES INT ABS	EXPT-PROG	PILE		NCSAC-33 90	D/70	MTR	SCOVILLE+,FAST SPECTRA,VALUE GIVEN	53011
SM 149	RESON PARAMS	EXPT-PROG	6.5 0		NCSAC-33 27	D/70	BNL	BRUNHART+,NUCLEAR POL EXPT PLANNED	53185
SM 149	RESON PARAMS	EXPT-PROG	9.8-2	3.4 1	NCSAC-33 17	D/70	BNL	CHRIEN+,J FOR 16RES+PARTIAL WG DIST	53193
SM 149	SPECT NGAMMA	EXPT-PROG	2. -2	5. 1	NCSAC-33 17	D/70	BNL	CHRIEN+,RESONANCE PARAMS ONLY GIVEN	53194
SM 152	RESON PARAMS	EXPT-PROG	8.8 1	1.3 3	NCSAC-33 41	D/70	COL	CAMARDA+,1968 MEASTS,G*WN,WG 8 RESON	53077
SM 152	RESON PARAMS	EXPT-PROG		1.5 3	NCSAC-33 41	D/70	COL	CAMARDA+,1968 MEASTS,AVG D 29 LVLS	53117
SM 152	STRNTH FNCTN	EXPT-PROG		1.5 3	NCSAC-33 41	D/70	COL	CAMARDA+,1968 MEASTS,SO GIVEN	53096
SM 152	RES INT ABS	EXPT-PROG	-1	UP	NCSAC-33 41	D/70	COL	CAMARDA+,.414 AND .55 LOWER LIMITS	53073
SM 154	RESON PARAMS	EXPT-PROG	3.4 2	1.2 3	NCSAC-33 41	D/70	COL	CAMARDA+,1968 MEASTS,G*WN,WG 3 RESON	53076
SM 154	RESON PARAMS	EXPT-PROG		2.5 3	NCSAC-33 41	D/70	COL	CAMARDA+,1968 MEASTS,AVG D 20 LVLS	53116
SM 154	STRNTH FNCTN	EXPT-PROG		2.5 3	NCSAC-33 41	D/70	COL	CAMARDA+,1968 MEASTS,SO GIVEN	53095
SM 154	RES INT ABS	EXPT-PROG	-1	UP	NCSAC-33 41	D/70	COL	CAMARDA+,.414 AND .55 LOWER LIMITS	53072
EU 151	RESON PARAMS	EXPT-PROG	2.7 0	9.9 1	NCSAC-33 41	D/70	COL	CAMARDA+,1968 MEASTS,G*WN,WG 70RESON	53080
EU 151	RESON PARAMS	EXPT-PROG		9.9 1	NCSAC-33 41	D/70	COL	CAMARDA+,1968 MEASTS,AVG D 88 LVLS	53119
EU 151	STRNTH FNCTN	EXPT-PROG		9.9 1	NCSAC-33 41	D/70	COL	CAMARDA+,1968 MEASTS,SO GIVEN	53098
EU 151	RES INT ABS	EXPT-PROG	-1	UP	NCSAC-33 41	D/70	COL	CAMARDA+,.414 AND .55 LOWER LIMITS	53075
EU 153	RESON PARAMS	EXPT-PROG	1.7 0	9.8 1	NCSAC-33 41	D/70	COL	CAMARDA+,1968 MEASTS,G*WN,WG 47RESON	53079
EU 153	RESON PARAMS	EXPT-PROG		9.8 1	NCSAC-33 41	D/70	COL	CAMARDA+,1968 MEASTS,AVG D 68 LVLS	53118
EU 153	STRNTH FNCTN	EXPT-PROG		9.8 1	NCSAC-33 41	D/70	COL	CAMARDA+,1968 MEASTS,SO GIVEN	53097
EU 153	RES INT ABS	EXPT-PROG	-1	UP	NCSAC-33 41	D/70	COL	CAMARDA+,.414 AND .55 LOWER LIMITS	53074
GD	N,GAMMA	EXPT-PROG	1. 3	1. 6	NCSAC-33 68	D/70	GA	FRICKE+, CURVE,CFD OTHER DATA	53038
GD 154	RESON PARAMS	EXPT-PROG		3.2 3	NCSAC-33 41	D/70	COL	CAMARDA+,1968 MEASTS,AVG D 344 LVLS	53114
GD 154	STRNTH FNCTN	EXPT-PROG		3.2 3	NCSAC-33 41	D/70	COL	CAMARDA+,1968 MEASTS,SO GIVEN	53093
GD 158	TOTAL XSECT	EXPT-PROG	NDG		NCSAC-33 41	D/70	COL	CAMARDA+,TRANSMISSION,NO DATA GIVEN	53159
GD 158	RESON PARAMS	EXPT-PROG	3		NCSAC-33 44	D/70	COL	RAHN+,FROM N,G. ANAL TBC,NO DATA GVN	53052
GD 158	RESON PARAMS	EXPT-PROG	1.6 1	3.0 3	NCSAC-33 41	D/70	COL	CAMARDA+,1968 MEASTS,AVG D 41 LVLS	53113
GD 158	RESON PARAMS	EXPT-PROG	NDG		NCSAC-33 41	D/70	COL	CAMARDA+,TRANSMISSION,NO DATA GIVEN	53141
GD 158	STRNTH FNCTN	EXPT-PROG	1.6 1	3.0 3	NCSAC-33 41	D/70	COL	CAMARDA+,1968 MEASTS,SO GIVEN	53092
GD 158	RES INT ABS	EXPT-PROG	PILE		NCSAC-33 90	D/70	MTR	SCOVILLE+,FAST SPECTRA,VALUE GIVEN	53009
GD 158	N,GAMMA	EXPT-PROG	3		NCSAC-33 44	D/70	COL	RAHN+,HOXON-RAE,ANAL TBC,NO DATA	53058
GD 160	TOTAL XSECT	EXPT-PROG	NDG		NCSAC-33 41	D/70	COL	CAMARDA+,TRANSMISSION,NO DATA GIVEN	53158
GD 160	RESON PARAMS	EXPT-PROG	NDG		NCSAC-33 41	D/70	COL	CAMARDA+,TRANSMISSION,NO DATA GIVEN	53140
GD 160	RES INT ABS	EXPT-PROG	PILE		NCSAC-33 90	D/70	MTR	SCOVILLE+,FAST SPECTRA,VALUE GIVEN	53419
TB 159	RES INT ABS	EXPT-PROG	PILE		NCSAC-33 90	D/70	MTR	SCOVILLE+,FAST SPECTRA,VALUE GIVEN	53420
DY 160	TOTAL XSECT	EXPT-PROG	NDG		NCSAC-33 41	D/70	COL	CAMARDA+,TRANSMISSION,NO DATA GIVEN	53157
DY 160	RESON PARAMS	EXPT-PROG	NDG		NCSAC-33 41	D/70	COL	CAMARDA+,TRANSMISSION,NO DATA GIVEN	53139

ELEMENT A	QUANTITY	TYPE	ENERGY MIN	ENERGY MAX	DOCUMENTATION REF VOL PAGE	DATE	LAB	COMMENTS	SERIAL NO.
DY 161	TOTAL XSECT	EXPT-PROG	NDG		NCSAC-33 41	D/70	COL	CAMARDA+,TRANSMISSION,NO DATA GIVEN	53156
DY 161	RESON PARAMS	EXPT-PROG	3		NCSAC-33 44	D/70	COL	RAHN+,FROM N,G. ANAL TBC,NO DATA GVN	53051
DY 161	RESON PARAMS	EXPT-PROG	NDG		NCSAC-33 41	D/70	COL	CAMARDA+,TRANSMISSION,NO DATA GIVEN	53138
DY 161	N,GAMMA	EXPT-PROG	3		NCSAC-33 44	D/70	COL	RAHN+,MOXON-RAE,ANAL TBC,NO DATA	53057
DY 162	TOTAL XSECT	EXPT-PROG	NDG		NCSAC-33 41	D/70	COL	CAMARDA+,TRANSMISSION,NO DATA GIVEN	53155
DY 162	RESON PARAMS	EXPT-PROG	NDG		NCSAC-33 41	D/70	COL	CAMARDA+,TRANSMISSION,NO DATA GIVEN	53137
DY 163	TOTAL XSECT	EXPT-PROG	NDG		NCSAC-33 41	D/70	COL	CAMARDA+,TRANSMISSION,NO DATA GIVEN	53154
DY 163	RESON PARAMS	EXPT-PROG	NDG		NCSAC-33 41	D/70	COL	CAMARDA+,TRANSMISSION,NO DATA GIVEN	53136
DY 163	RESON PARAMS	EXPT-PROG		3.2 2	NCSAC-33 21	D/70	BNL	CHRIEN+,PARTIAL WG DIST SHOWN	53189
DY 163	SPECT NGAMMA	EXPT-PROG		3.2 2	NCSAC-33 21	D/70	BNL	CHRIEN+,SPECT FROM 23RESON,NO DATA	53190
DY 164	TOTAL XSECT	EXPT-PROG	NDG		NCSAC-33 41	D/70	COL	CAMARDA+,TRANSMISSION,NO DATA GIVEN	53153
DY 164	RESON PARAMS	EXPT-PROG	NDG		NCSAC-33 41	D/70	COL	CAMARDA+,TRANSMISSION,NO DATA GIVEN	53135
HO 165	TOTAL XSECT	EXPT-PROG	1. 5	1.5 6	NCSAC-33 1	D/70	ANL	SMITH+,NO DATA GIVEN,TO BE PUBL ZFP	53008
HO 165	DIFF ELASTIC	EXPT-PROG	3. 5	1.5 6	NCSAC-33 1	D/70	ANL	SMITH+,NO DATA GIVEN,TO BE PUBL ZFP	53007
HO 165	DIFF INELAST	EXPT-PROG	3. 5	1.5 6	NCSAC-33 1	D/70	ANL	SMITH+,NO DATA GIVEN,TO BE PUBL ZFP	53006
HO 165	RES INT ABS	EXPT-PROG	PILE		NCSAC-33 90	D/70	MTR	SCOVILLE+,FAST SPECTRA,VALUE GIVEN	53418
ER 166	RESON PARAMS	EXPT-PROG	1.6 1	3.5 2	NCSAC-33 41	D/70	COL	CAMARDA+,1968 MEASTS,G*WN,WG 8 RESON	53087
ER 166	RESON PARAMS	EXPT-PROG		9.5 3	NCSAC-33 41	D/70	COL	CAMARDA+,1968 MEASTS,AVG D 174 LVLS	53130
ER 166	STRNTH FNCTN	EXPT-PROG		9.5 3	NCSAC-33 4	D/70	COL	CAMARDA+,1968 MEASTS,SO GIVEN	53109
ER 166	RES INT ABS	EXPT-PROG	-1	UP	NCSAC-33 41	D/70	COL	CAMARDA+,.414 AND .55 LOWER LIMITS	53071
ER 167	RESON PARAMS	EXPT-PROG		1.7 3	NCSAC-33 41	D/70	COL	CAMARDA+,1968 MEASTS,AVG D 268 LVLS	53129
ER 167	STRNTH FNCTN	EXPT-PROG		1.7 3	NCSAC-33 4	D/70	COL	CAMARDA+,1968 MEASTS,SO GIVEN	53108
ER 167	RES INT ABS	EXPT-PROG	-1	UP	NCSAC-33 41	D/70	COL	CAMARDA+,.414 AND .55 LOWER LIMITS	53070
ER 168	RESON PARAMS	EXPT-PROG	8.0 1	1.9 2	NCSAC-33 41	D/70	COL	CAMARDA+,1968 MEASTS,G*WN,WG 2 RESON	53086
ER 168	RESON PARAMS	EXPT-PROG		1.5 4	NCSAC-33 41	D/70	COL	CAMARDA+,1968 MEASTS,AVG D 107 LVLS	53128
ER 168	STRNTH FNCTN	EXPT-PROG		1.5 4	NCSAC-33 4	D/70	COL	CAMARDA+,1968 MEASTS,SO AND SI GIVEN	53107
ER 168	RES INT ABS	EXPT-PROG	-1	UP	NCSAC-33 41	D/70	COL	CAMARDA+,.414 AND .55 LOWER LIMITS	53069
ER 170	RESON PARAMS	EXPT-PROG		2.4 4	NCSAC-33 41	D/70	COL	CAMARDA+,1968 MEASTS,AVG D 94 LVLS	53127
ER 170	STRNTH FNCTN	EXPT-PROG		2.4 4	NCSAC-33 4	D/70	COL	CAMARDA+,1968 MEASTS,SO AND SI GIVEN	53106
TM 169	RESON PARAMS	EXPT-PROG	3		NCSAC-33 44	D/70	COL	RAHN+,FROM N,G. ANAL TBC,NO DATA GVN	53053
TM 169	N,GAMMA	EXPT-PROG	3		NCSAC-33 44	D/70	COL	RAHN+,MOXON-RAE,ANAL TBC,NO DATA	53059
YB 171	RESON PARAMS	EXPT-PROG	7.9 0	6.3 2	NCSAC-33 41	D/70	COL	CAMARDA+,1968 MEASTS,G*WN,WG 41RESON	53085
YB 171	RESON PARAMS	EXPT-PROG		1.7 3	NCSAC-33 41	D/70	COL	CAMARDA+,1968 MEASTS,AVG D 165 LVLS	53126
YB 171	STRNTH FNCTN	EXPT-PROG		1.7 3	NCSAC-33 4	D/70	COL	CAMARDA+,1968 MEASTS,SO GIVEN	53105
YB 171	RES INT ABS	EXPT-PROG	-1	UP	NCSAC-33 41	D/70	COL	CAMARDA+,.414 AND .55 LOWER LIMITS	53068
YB 172	RESON PARAMS	EXPT-PROG	1.4 2	5.1 2	NCSAC-33 41	D/70	COL	CAMARDA+,1968 MEASTS,G*WN,WG 4 RESON	53084
YB 172	RESON PARAMS	EXPT-PROG		1.0 4	NCSAC-33 41	D/70	COL	CAMARDA+,1968 MEASTS,AVG D 95 LVLS	53125
YB 172	STRNTH FNCTN	EXPT-PROG		1.0 4	NCSAC-33 4	D/70	COL	CAMARDA+,1968 MEASTS,SO GIVEN	53104
YB 172	RES INT ABS	EXPT-PROG	-1	UP	NCSAC-33 41	D/70	COL	CAMARDA+,.414 AND .55 LOWER LIMITS	53067
YB 174	RESON PARAMS	EXPT-PROG	3.4 2	8.8 2	NCSAC-33 41	D/70	COL	CAMARDA+,1968 MEASTS,G*WN,WG 3 RESON	53083
YB 174	RESON PARAMS	EXPT-PROG		2.5 4	NCSAC-33 41	D/70	COL	CAMARDA+,1968 MEASTS,AVG D 95 LVLS	53124
YB 174	STRNTH FNCTN	EXPT-PROG		2.5 4	NCSAC-33 4	D/70	COL	CAMARDA+,1968 MEASTS,SO GIVEN	53103
YB 174	RES INT ABS	EXPT-PROG	-1	UP	NCSAC-33 41	D/70	COL	CAMARDA+,.414 AND .55 LOWER LIMITS	53066
YB 176	RESON PARAMS	EXPT-PROG	1.5 2		NCSAC-33 41	D/70	COL	CAMARDA+,1968 MEASTS,G*WN,WG	53082
YB 176	RESON PARAMS	EXPT-PROG		2.6 4	NCSAC-33 41	D/70	COL	CAMARDA+,1968 MEASTS,AVG D 77 LVLS	53123
YB 176	STRNTH FNCTN	EXPT-PROG		2.6 4	NCSAC-33 41	D/70	COL	CAMARDA+,1968 MEASTS,SO GIVEN	53102

ELEMENT S A	QUANTITY	TYPE	ENERGY MIN	ENERGY MAX	DOCUMENTATION REF VOL PAGE	DATE	LAB	COMMENTS	SERIAL NO.
LU	TOTAL XSECT	EXPT-PROG	THR		NCSAC-33 89	D/70	MTR	YOUNG,FAST CHOPPER,VALUE GIVEN	53023
LU	N,GAMMA	EXPT-PROG	THR		NCSAC-33 89	D/70	MTR	YOUNG,FAST CHOPPER,VALUE GIVEN	53020
LU 175	TOTAL XSECT	EXPT-PROG	THR		NCSAC-33 89	D/70	MTR	YOUNG,FAST CHOPPER,VALUE GIVEN	53025
LU 175	RESON PARAMS	EXPT-PROG		1.2 3	NCSAC-33 41	D/70	COL	CAMARDA+,1968 MEASTS,AVG D 214 LVLS	53115
LU 175	STRNTH FNCTN	EXPT-PROG		1.2 3	NCSAC-33 41	D/70	COL	CAMARDA+,1968 MEASTS,SO GIVEN	53094
LU 175	N,GAMMA	EXPT-PROG	THR		NCSAC-33 89	D/70	MTR	YOUNG,FAST CHOPPER,VALUE GIVEN	53022
LU 176	TOTAL XSECT	EXPT-PROG	THR		NCSAC-33 89	D/70	MTR	YOUNG,FAST CHOPPER,VALUE GIVEN	53024
LU 176	N,GAMMA	EXPT-PROG	THR		NCSAC-33 89	D/70	MTR	YOUNG,FAST CHOPPER,VALUE GIVEN	53021
TA 181	RES INT ABS	EXPT-PROG	PILE		NCSAC-33 90	D/70	MTR	SCOVILLE+,FAST SPECTRA,VALUE GIVEN	53417
TA 181	N,GAMMA	EXPT-PROG	1. 3	1. 6	NCSAC-33 68	D/70	GA	FRICKE+, CURVE,CFD OTHER DATA	53036
W	N,GAMMA	EXPT-PROG	1. 3	1. 6	NCSAC-33 68	D/70	GA	FRICKE+, CURVE,CFD OTHER DATA	53035
W 182	RESON PARAMS	EXPT-PROG	2.1 1	1.3 4	NCSAC-33 41	D/70	COL	CAMARDA+,1968 MEASTS,WN MANY RESCN	53065
W 182	RESON PARAMS	EXPT-PROG		1.3 4	NCSAC-33 41	D/70	COL	CAMARDA+,1968 MEASTS,AVG D 141 LVLS	53122
W 182	STRNTH FNCTN	EXPT-PROG		1.3 4	NCSAC-33 41	D/70	COL	CAMARDA+,1968 MEASTS,SO GIVEN	53101
W 184	RESON PARAMS	EXPT-PROG	1.0 2	1.6 4	NCSAC-33 41	D/70	COL	CAMARDA+,1968 MEASTS,WN MANY RESCN	53064
W 184	RESON PARAMS	EXPT-PROG		1.5 4	NCSAC-33 41	D/70	COL	CAMARDA+,1968 MEASTS,AVG D 125 LVLS	53121
W 184	STRNTH FNCTN	EXPT-PROG		1.5 4	NCSAC-33 41	D/70	COL	CAMARDA+,1968 MEASTS,SO GIVEN	53100
W 186	RESON PARAMS	EXPT-PROG	1.9 1	1.7 4	NCSAC-33 41	D/70	COL	CAMARDA+,1968 MEASTS,WN MANY RESCN	53063
W 186	RESON PARAMS	EXPT-PROG		1.7 4	NCSAC-33 41	D/70	COL	CAMARDA+,1968 MEASTS,AVG D 102 LVLS	53120
W 186	STRNTH FNCTN	EXPT-PROG		1.7 4	NCSAC-33 41	D/70	COL	CAMARDA+,1968 MEASTS,SO GIVEN	53099
W 186	RES INT ABS	EXPT-PROG	PILE		NCSAC-33 90	D/70	MTR	SCOVILLE+,FAST SPECTRA,VALUE GIVEN	53416
RE	N,GAMMA	EXPT-PROG	1. 3	1. 6	NCSAC-33 68	D/70	GA	FRICKE+, CURVE,CFD OTHER DATA	53034
PT 195	SPECT NGAMMA	EXPT-PROG	1.2 1		NCSAC-33 16	D/70	BNL	CHRIEN+,ABSOL GAMMA INTENSITY REL AU	53200
AU 197	TOTAL XSECT	EXPT-PROG	NDG		NCSAC-33 41	D/70	COL	CAMARDA+,TRANSMISSION,NO DATA GIVEN	53173
AU 197	ACTIVATION	EXPT-PROG	2.5 4		NCSAC-33 100	D/70	MTR	TROMP,NO DATA GIVEN	53407
AU 197	N,GAMMA	EXPT-PROG	1. 3	1. 6	NCSAC-33 68	D/70	GA	FRICKE+, CURVE,CFD OTHER DATA	53040
AU 197	N,GAMMA	EXPT-PROG	1. 4	5.4 6	NCSAC-33 113	D/70	LOK	VAUGHN+,DETAILED DESCRIPTION,CRV+TBL	53411
TL	TOTAL XSECT	EXPT-PROG	NDG		NCSAC-33 41	D/70	COL	CAMARDA+,TRANSMISSION,NO DATA GIVEN	53167
TL 203	TOTAL XSECT	EXPT-PROG	NDG		NCSAC-33 41	D/70	COL	CAMARDA+,TRANSMISSION,NO DATA GIVEN	53152
TL 203	RESON PARAMS	EXPT-PROG	NDG		NCSAC-33 41	D/70	COL	CAMARDA+,TRANSMISSION,NO DATA GIVEN	53134
TL 205	TOTAL XSECT	EXPT-PROG	NDG		NCSAC-33 41	D/70	COL	CAMARDA+,TRANSMISSION,NO DATA GIVEN	53151
TL 205	RESON PARAMS	EXPT-PROG	NDG		NCSAC-33 41	D/70	COL	CAMARDA+,TRANSMISSION,NO DATA GIVEN	53133
PB	TOTAL XSECT	EXPT-PROG	5. 5	2.0 7	NCSAC-33 162	D/70	NBS	SCHWARTZ+,1PC ABSOL ACCURACY,CURVE	53369
PB	DIFF ELASTIC	EXPT-PROG	NDG		NCSAC-33 164	D/70	NEL	BUCHER+,TO BE DONE,SMALL-ANGLE SCAT	53341
PB	DIFF INELAST	EXPT-PROG	3		NCSAC-33 208	D/70	RPI	ZUHR+,SCINT DET,TOF SPECT GIVEN,TBC	53277
PB 204	N,GAMMA	EXPT-PROG	2. 3		NCSAC-33 93	D/70	MTR	GREENWOOD+,TBL OF PARTIAL SIGS SHOWN	53415
PB 204	SPECT NGAMMA	EXPT-PROG	2. 3		NCSAC-33 93	D/70	MTR	GREENWOOD+,HIGH-E PROMPT GAMS SHOWN	53413
PB 206	TOTAL XSECT	EXPT-PROG	1.3 6	1.9 6	NCSAC-33 230	D/70	DKE	MALAN+,C12(D,N) SOURCE,ANAL TBC,NDG	53270
PB 207	N,GAMMA	EXPT-PROG	2.5 4	5. 4	NCSAC-33 171	D/70	ORL	ALLEN+,LINAC,ANAL TBC,NO DATA GIVEN	53330
PB 207	N,GAMMA	EXPT-PROG	2. 3		NCSAC-33 93	D/70	MTR	GREENWOOD+,NO DATA GIVEN	53414
PB 207	SPECT NGAMMA	EXPT-PROG	2.5 4	5. 4	NCSAC-33 171	D/70	ORL	ALLEN+,LINAC,GAMMA YLD SHOWN	53329
TH 229	RESON PARAMS	EXPT-PROG	6.1-1	5.1 1	NCSAC-33 60	D/70	COL	FELVINCI+,SO*WF FOR 29RESON GIVEN	53240
TH 229	FISSION	EXPT-PROG	-2	1	NCSAC-33 60	D/70	COL	FELVINCI+,SO*WF FOR 29RESON GIVEN	53046

ELEMENT S	A	QUANTITY	TYPE	ENERGY MIN	MAX	DOCUMENTATION REF VOL	PAGE	DATE	LAB	COMMENTS	SERIAL NO.
TH	232	TOTAL XSECT	EXPT-PROG	NDG		NCSAC-33	41	D/70	COL	CAMARDA+,TRANSMISSION,NO DATA GIVEN	53165
TH	232	RESON PARAMS	EXPT-PROG	3		NCSAC-33	44	D/70	COL	RAHN+,FROM N,G. ANAL TBC,NO DATA GVN	53055
TH	232	RESON PARAMS	EXPT-PROG	NDG		NCSAC-33	41	D/70	COL	CAMARDA+,TRANSMISSION,NO DATA GIVEN	53147
TH	232	RESON PARAMS	EXPT-PROG	2. 1	2. 3	NCSAC-33	126	D/70	LAS	FORMAN+,NUCL SHOT. FROM N,G. WG TABL	53359
TH	232	N,GAMMA	EXPT-PROG	3		NCSAC-33	44	D/70	COL	RAHN+,MOXON-RAE,ANAL TBC,NO DATA	53061
U	233	FISSION	EXPT-PROG	NDG		NCSAC-33	59	D/70	COL	FELVINCI+,ANAL TO BE COMPLETED,NDG	53049
U	233	FISSION	EVAL-PROG	2.5-2		NCSAC-33	12	D/70	ANL	DE VOLPI,PRELIMINARY VALUE GIVEN	53251
U	233	ETA	EXPT-PROG	6. -2	2.6-1	NCSAC-33	87	D/70	MTR	SMITH+,4 ES,CURVE+TABLE	53028
U	233	ETA	EVAL-PROG	2.5-2		NCSAC-33	12	D/70	ANL	DE VOLPI,PRELIMINARY VALUE GIVEN	53248
U	233	ALPHA	EVAL-PROG	2.5-2		NCSAC-33	12	D/70	ANL	DE VOLPI,PRELIMINARY VALUE GIVEN	53249
U	233	NU	EVAL-PROG	2.5-2		NCSAC-33	12	D/70	ANL	DE VOLPI,PRELIMINARY VALUE GIVEN	53247
U	233	DELAYD NEUTS	EXPT-PROG	1. 5	7. 6	NCSAC-33	155	D/70	LAS	KRICK+,CURV ABSOL NEUT YLD VS. E	53370
U	233	ABSORPTION	EVAL-PROG	2.5-2		NCSAC-33	12	D/70	ANL	DE VOLPI,PRELIMINARY VALUE GIVEN	53215
U	233	N,GAMMA	EVAL-PROG	2.5-2		NCSAC-33	12	D/70	ANL	DE VOLPI,PRELIMINARY VALUE GIVEN	53250
U	234	FISSION	EXPT-PROG	7. 5	2. 6	NCSAC-33	187	D/70	ORL	ROSLER+,LINAC,TO BE COMPLETED,NDG	53311
U	235	SCATTERING	EVAL-PROG	2.5-2		NCSAC-33	12	D/70	ANL	DE VOLPI,PRELIMINARY VALUE GIVEN	53208
U	235	FISSION	EVAL-PROG	2.5-2		NCSAC-33	12	D/70	ANL	DE VOLPI,PRELIMINARY VALUE GIVEN	53213
U	235	FISSION	THEO-PROG		2.5 3	NCSAC-33	209	D/70	RPI	SHEA,AVG SIG CALCTD,OKS EXPT,NO DATA	53252
U	235	FISSION	THEO-PROG	1.8 1	6.6 1	NCSAC-33	209	D/70	RPI	SHEA,TRIPLET APPROX,OKS EXPT,NO DATA	53276
U	235	FISSION	EXPT-PROG		1. 5	NCSAC-33	182	D/70	ORL	DE SAUSSURE+,NO DATA GIVEN,TBC	53314
U	235	ETA	EXPT-PROG	6. -2	1.6-1	NCSAC-33	87	D/70	MTR	SMITH+,2 ES,VALUES GIVEN	53027
U	235	ETA	EVAL-PROG	2.5-2		NCSAC-33	12	D/70	ANL	DE VOLPI,PRELIMINARY VALUE GIVEN	53210
U	235	ALPHA	EVAL-PROG	2.5-2		NCSAC-33	12	D/70	ANL	DE VOLPI,PRELIMINARY VALUE GIVEN	53211
U	235	ALPHA	THEO-PROG		2.5 3	NCSAC-33	209	D/70	RPI	SHEA,AVG ALFA CALCTD,OKS EXPT,NDG	53253
U	235	ALPHA	EXPT-PROG		1. 5	NCSAC-33	182	D/70	ORL	DE SAUSSURE+,NO DATA GIVEN,TBC	53315
U	235	NU	EVAL-PROG	2.5-2		NCSAC-33	12	D/70	ANL	DE VOLPI,PRELIMINARY VALUE GIVEN	53209
U	235	DELAYD NEUTS	EXPT-PROG	1. 5	7. 6	NCSAC-33	155	D/70	LAS	KRICK+,CURV ABSOL NEUT YLD VS. E	53371
U	235	SPECT FISS N	EXPT-PROG	NDG		NCSAC-33	5	D/70	ANL	SMITH,ANALYSIS TO BE COMPL,NO DATA	53219
U	235	SPECT FISS G	EXPT-PROG	THR		NCSAC-33	185	D/70	ORL	PLEASONTON,PRELIM TOTAL YLD+E GIVEN	53312
U	235	FISS YIELD	EXPT-PROG	THR	1.5 7	NCSAC-33	123	D/70	LOK	IMHOF+,11 ES,NO DATA GIVEN	53403
U	235	FISS PROD GS	EXPT-PROG	THR	1	NCSAC-33	27	D/70	BNL	SAILOR+,DELAYED GAM YLDS TO BE MEASD	53184
U	235	FISS PROD GS	EXPT-PROG	THR	1.5 7	NCSAC-33	123	D/70	LOK	IMHOF+,GE(LI) DET,NO DATA GIVEN	53412
U	235	RES INT FISS	THEO-PROG	1.8 1	6.6 1	NCSAC-33	209	D/70	RPI	SHEA,TRIPLET APPROX,OKS EXPT,NO DATA	53275
U	235	ABSORPTION	EVAL-PROG	2.5-2		NCSAC-33	12	D/70	ANL	DE VOLPI,PRELIMINARY VALUE GIVEN	53214
U	235	N,GAMMA	EVAL-PROG	2.5-2		NCSAC-33	12	D/70	ANL	DE VOLPI,PRELIMINARY VALUE GIVEN	53212
U	235	N,GAMMA	THEO-PROG		2.5 3	NCSAC-33	209	D/70	RPI	SHEA,AVG SIG CALCTD,OKS EXPT,NO DATA	53274
U	235	N,GAMMA	EXPT-PROG		1. 5	NCSAC-33	182	D/70	ORL	DE SAUSSURE+,NO DATA GIVEN,TBC	53316
U	235	SPECT NGAMMA	EXPT-PROG	1.1 0	6.4 0	NCSAC-33	28	D/70	BNL	KANE,TABLE SPECTRA FOR 4 RESON ES	53182
U	235	SPECT NGAMMA	EXPT-PROG	2. 0	3.4 1	NCSAC-33	24	D/70	BNL	CHRIEN+,642KEV TRANSITION SHOWN	53186
U	235	SPECT NGAMMA	EXPT-PROG	THR		NCSAC-33	152	D/70	LAS	JURNEY,PRELIM GAM ES 4.4-6.8MEV GIVN	53374
U	236	FISSION	EXPT-PROG	7. 5	2. 6	NCSAC-33	187	D/70	ORL	ROSLER+,LINAC,TO BE COMPLETED,NDG	53310
U	238	TOTAL XSECT	EXTH-PROG	1. 5	1. 7	NCSAC-33	2	D/70	ANL	SMITH+,NO DATA,TO BE PUBL IN NSE	53005
U	238	TOTAL XSECT	EXPT-PROG	NDG		NCSAC-33	41	D/70	COL	CAMARDA+,TRANSMISSION,NO DATA GIVEN	53166
U	238	RESON PARAMS	EXPT-PROG	3		NCSAC-33	44	D/70	COL	RAHN+,FROM N,G. ANAL TBC,NO DATA GVN	53056
U	238	RESON PARAMS	EXPT-PROG	NDG		NCSAC-33	41	D/70	COL	CAMARDA+,TRANSMISSION,NO DATA GIVEN	53148

ELEMENT S	A	QUANTITY	TYPE	ENERGY MIN	MAX	DOCUMENTATION REF VOL	PAGE	DATE	LAB	COMMENTS	SERIAL NO.
U	238	RESON PARAMS	EXPT-PROG	1	2	NCSAC-33	21	0/70	BNL	CHRIEN+,PARTIAL WG DIST,NO DATA GIVN	53191
U	238	ELASTIC	EXTH-PROG	1. 5	1. 7	NCSAC-33	2	0/70	ANL	SMITH+,NO DATA,TO BE PUBL IN NSE	53003
U	238	TOT INELASTC	EXTH-PROG	1. 5	1. 7	NCSAC-33	2	0/70	ANL	SMITH+,CURVE TO 2 MEV,TBP IN NSE	53004
U	238	DELAYD NEUTS	EXPT-PROG	1. 5	7. 6	NCSAC-33	155	0/70	LAS	KRICK+,CURV ABSOL NEUT YLD VS. E	53372
U	238	FISS PROD GS	EXPT-PROG	THR	1	NCSAC-33	27	0/70	BNL	SAILOR+,DELAYED GAM YLDS TO BE MEASD	53183
U	238	N,GAMMA	EXPT-PROG	1. 3	1. 6	NCSAC-33	68	0/70	GA	FRICKE+, CURVE,CFD OTHER DATA	53039
U	238	N,GAMMA	EXPT-PROG	3		NCSAC-33	44	0/70	COL	RAHN+,MOXON-RAE,ANAL TBC,NO DATA	53062
U	238	N,GAMMA	EXPT-PROG	5. 2	1. 5	NCSAC-33	182	0/70	ORL	DE SAUSSURE+,TABLE+CURVE,TBC	53317
U	238	SPECT NGAMMA	EXPT-PROG	5.6 0	1.0 5	NCSAC-33	82	0/70	GA	JOHN+,GE(LI)-NAI(TL) SPECT,CURVES	53029
U	238	SPECT NGAMMA	EXPT-PROG	0	2	NCSAC-33	59	0/70	COL	DERENGOWSKI+,GE DET,1-8MEV GAMS,NDG	53050
U	238	SPECT NGAMMA	EXPT-PROG	5. 0	1.3 3	NCSAC-33	21	0/70	BNL	CHRIEN+,SUMMED SPECT 6-600EV SHOWN	53192
U	238	SPECT NGAMMA	EXPT-PROG	6.7 0		NCSAC-33	16	0/70	BNL	CHRIEN+,ABSOL GAMMA INTENSITY REL AU	53199
U	238	SPECT NGAMMA	EXPT-PROG		6. 2	NCSAC-33	174	0/70	ORL	WASSON+,GE(LI),TOF SPECTRA SHOWN	53327
NP	237	TOTAL XSECT	EXPT-PROG	NDG		NCSAC-33	41	0/70	COL	CAMARDA+,TRANSMISSION,NO DATA GIVEN	53150
NP	237	RESON PARAMS	EXPT-PROG	3.9 1		NCSAC-33	59	0/70	COL	FELVINCI+,PRELIM WF GVN,ANAL TBC	53047
NP	237	RESON PARAMS	EXPT-PROG	NDG		NCSAC-33	41	0/70	COL	CAMARDA+,TRANSMISSION,NO DATA GIVEN	53132
NP	237	FISSION	EXPT-PROG	0	1	NCSAC-33	59	0/70	COL	FELVINCI+,RESON AT 39.07EV,ANAL TBC	53048
PU	239	SCATTERING	EXPT-PROG	2. 1	6. 3	NCSAC-33	126	0/70	LAS	FARRELL+,NUCL SHOT,CURV 20-60EV	53354
PU	239	FISSION	EVAL-PROG	2.5-2		NCSAC-33	12	0/70	ANL	DE VOLPI,PRELIMINARY VALUE GIVEN	53206
PU	239	FISSION	EXPT-PROG	2. 1	3. 3	NCSAC-33	126	0/70	LAS	FARRELL+,NUCL SHOT,TABLE+CURVE	53358
PU	239	ETA	EVAL-PROG	2.5-2		NCSAC-33	12	0/70	ANL	DE VOLPI,PRELIMINARY VALUE GIVEN	53203
PU	239	ALPHA	EVAL-PROG	2.5-2		NCSAC-33	12	0/70	ANL	DE VOLPI,PRELIMINARY VALUE GIVEN	53204
PU	239	ALPHA	EXPT-PROG	1. 2	1. 4	NCSAC-33	126	0/70	LAS	FARRELL+,NUCL SHOT,TBL+CRV,CFD OTHRS	53357
PU	239	NU	EVAL-PROG	2.5-2		NCSAC-33	12	0/70	ANL	DE VOLPI,PRELIMINARY VALUE GIVEN	53202
PU	239	NU	EXPT-PROG	0.	1. 2	NCSAC-33	185	0/70	ORL	WESTON+,PRELIMINARY CURV SHOWN,TBC	53313
PU	239	SPECT FISS N	EXPT-PROG	NDG		NCSAC-33	5	0/70	ANL	SMITH,ANALYSIS TO BE COMPL,NO DATA	53218
PU	239	FISS YIELD	EXPT-PROG	THR	1.5 7	NCSAC-33	123	0/70	LOK	IMHOF+,11 ES,NO DATA GIVEN	53402
PU	239	FISS PROD GS	EXPT-PROG	THR	1.5 7	NCSAC-33	123	0/70	LOK	IMHOF+,GE(LI) DET,NO DATA GIVEN	53404
PU	239	ABSORPTION	EVAL-PROG	2.5-2		NCSAC-33	12	0/70	ANL	DE VOLPI,PRELIMINARY VALUE GIVEN	53207
PU	239	N,GAMMA	EVAL-PROG	2.5-2		NCSAC-33	12	0/70	ANL	DE VOLPI,PRELIMINARY VALUE GIVEN	53205
PU	239	SPECT NGAMMA	EXPT-PROG	3. -1	5.8 1	NCSAC-33	24	0/70	BNL	CHRIEN+,LOW-E GAMS GIVN FOR 12 RESON	53187
PU	239	SPECT NGAMMA	EXPT-PROG	THR		NCSAC-33	152	0/70	LAS	JURNEY,PRELIM GAM ES 4.4-6.8MEV GIVN	53373
PU	240	TOTAL XSECT	EXPT-PROG	1. -2	3. -1	NCSAC-33	89	0/70	MTR	KROGER+,FAST CHOPPER,ANAL TBC,NDG	53019
PU	240	TOTAL XSECT	EXPT-PROG	1. 5	1.5 6	NCSAC-33	2	0/70	ANL	SMITH+,ANAL TO BE COMPLETED,CURVE	53222
PU	240	RESON PARAMS	EXPT-PROG	4. 3	3. 4	NCSAC-33	203	0/70	RPI	HOCKENBURY+,CAPT+FISS MEASTS,NO DATA	53280
PU	240	ELASTIC	EXPT-PROG	3. 5	1.5 6	NCSAC-33	2	0/70	ANL	SMITH+,ANAL TO BE COMPLETED,CURVE	53221
PU	240	TOT INELASTC	EXPT-PROG	3. 5	1.5 6	NCSAC-33	2	0/70	ANL	SMITH+,ANAL TO BE COMPLETED,NO DATA	53220
PU	240	FISSION	EXPT-PROG	4. 3	3. 4	NCSAC-33	203	0/70	RPI	HOCKENBURY+,FISS YLDS+SIG CURVS GIVN	53281
PU	240	N,GAMMA	EXPT-PROG	4. 3	3. 4	NCSAC-33	203	0/70	RPI	HOCKENBURY+,CAPT YLDS+SIG CURVS GIVN	53282
PU	241	ETA	EXPT-PROG	6. -2	9.1-1	NCSAC-33	87	0/70	MTR	SMITH+,3 ES,VALUES GIVEN	53026
PU	242	RESON PARAMS	EXPT-PROG	3.7 2	4.6 4	NCSAC-33	132	0/70	LAS	BERGEN+,NUCL SHOT,TBL SUM FISSN AREA	53353
PU	242	FISSION	EXPT-PROG	2. 1	8. 6	NCSAC-33	132	0/70	LAS	BERGEN+,NUCL SHOT,CURV 0.2-8MEV	53356
PU	244	RESON PARAMS	EXPT-PROG	1.2 3	1.8 4	NCSAC-33	132	0/70	LAS	BERGEN+,NUCL SHOT,TBL SUM FISSN AREA	53352
PU	244	FISSION	EXPT-PROG	2. 1	8. 6	NCSAC-33	132	0/70	LAS	BERGEN+,NUCL SHOT,CURV 0.2-8MEV	53355

ELEMENT S A	QUANTITY	TYPE	ENERGY MIN	ENERGY MAX	DOCUMENTATION REF VOL	PAGE	DATE	LAB	COMMENTS	SERIAL NO.
AM 243	RESON PARAMS	EXPT-PROG	5. -1	1.8 2	NCSAC-33	167	D/70	ORL	HARVEY+,TRANS,156RESON,SO+D ONLY GVN	53339
AM 243	STRNTH FNCTN	EXPT-PROG	5. -1	1.8 2	NCSAC-33	167	D/70	ORL	HARVEY+,TRANS,SO VALUE GIVEN	53338
CM 244	RESON PARAMS	EXPT-PROG	2.3 1	9.7 2	NCSAC-33	136	D/70	LAS	MOORE+,NUCL SHOT,SO*WF,SO*WG,WF,WG	53351
CM 244	FISSION	EXPT-PROG	1. 6	1.5 7	NCSAC-33	148	D/70	LAS	BARTON+,NO DATA GIVEN,TO BE PUBLISHD	53380
CM 244	FISSION	EXPT-PROG	1	3	NCSAC-33	136	D/70	LAS	MOORE+,NUCL SHOT,RESON PARS+ALFA GVN	53401
CM 244	ALPHA	EXPT-PROG	1. 2	5. 3	NCSAC-33	136	D/70	LAS	MOORE+,NUCL SHOT,CURVE,TBP	53346
CM 244	N,GAMMA	EXPT-PROG	1	3	NCSAC-33	136	D/70	LAS	MOORE+,NUCL SHOT,RESON PARS+ALFA GVN	53396
CM 245	RESON PARAMS	EXPT-PROG	2.2 1	6.0 1	NCSAC-33	136	D/70	LAS	MOORE+,NUCL SHOT,2G*WN WF 26RESON	53348
CM 245	FISSION	EXPT-PROG	1. 6	1.5 7	NCSAC-33	148	D/70	LAS	BARTON+,TO BE DONE	53379
CM 245	FISSION	EXPT-PROG	1	3	NCSAC-33	136	D/70	LAS	MOOPE+,NUCL SHOT,RESON PARS ONLY GVN	53400
CM 245	N,GAMMA	EXPT-PROG	1	3	NCSAC-33	136	D/70	LAS	MOORE+,NUCL SHOT,RESON PARS ONLY GVN	53395
CM 246	RESON PARAMS	EXPT-PROG	8.4 1	3.8 2	NCSAC-33	136	D/70	LAS	MOORE+,NUCL SHOT,SO*WF,SO*WG,WF,WG	53350
CM 246	FISSION	EXPT-PROG	1. 6	1.5 7	NCSAC-33	148	D/70	LAS	BARTON+,TO BE DONE	53378
CM 246	FISSION	EXPT-PROG	1	3	NCSAC-33	136	D/70	LAS	MOORE+,NUCL SHOT,RESON PARS ONLY GVN	53399
CM 246	N,GAMMA	EXPT-PROG	1	3	NCSAC-33	136	D/70	LAS	MOORE+,NUCL SHOT,RESON PARS ONLY GVN	53394
CM 247	RESON PARAMS	EXPT-PROG	2.1 1	6.0 1	NCSAC-33	136	D/70	LAS	MOORE+,NUCL SHOT,2G*WN WF 26RESON	53347
CM 247	FISSION	EXPT-PROG	1	3	NCSAC-33	136	D/70	LAS	MOORE+,NUCL SHOT,RESON PARS ONLY GVN	53398
CM 247	N,GAMMA	EXPT-PROG	1	3	NCSAC-33	136	D/70	LAS	MOORE+,NUCL SHOT,RESON PARS ONLY GVN	53393
CM 248	RESON PARAMS	EXPT-PROG	2.7 1	4.2 2	NCSAC-33	136	D/70	LAS	MOORE+,NUCL SHOT,SO*WF,SO*WG,WF,WG	53349
CM 248	FISSION	EXPT-PROG	1. 6	1.5 7	NCSAC-33	148	D/70	LAS	BARTON+,TO BE COMPLETED,NO DATA GIVN	53377
CM 248	FISSION	EXPT-PROG	1	3	NCSAC-33	136	D/70	LAS	MOORE+,NUCL SHOT,RESON PARS ONLY GVN	53397
CM 248	N,GAMMA	EXPT-PROG	1	3	NCSAC-33	136	D/70	LAS	MOORE+,NUCL SHOT,RESON PARS ONLY GVN	53392
CF 249	FISSION	EXPT-PROG	1. 6	1.5 7	NCSAC-33	148	D/70	LAS	BARTON+,TO BE DONE	53376
CF 249	FISSION	EXPT-PROG	1.5 1	3. 6	NCSAC-33	136	D/70	LAS	SILBERT+,PRELIM SIG CURV,ANAL TBC	53391
CF 249	RES INT FISS	EXPT-PROG	2. 1	3. 66	NCSAC-33	136	D/70	LAS	SILBERT+,TBL RIF 10 ENERGY INTERVALS	53390
CF 252	NU	EVAL-PROG	2.5-2		NCSAC-33	12	D/70	ANL	DE VOLPI,PRELIMINARY VALUE GIVEN	53201
FM 257	FISSION	EXPT-PROG	THR		NCSAC-33	103	D/70	LRL	WILD,PRELIMINARY VALUE GIVEN	53410
FM 257	FISS YIELD	EXPT-PROG	SPON	THR	NCSAC 33	103	D/70	LRL	JOHN+,MASS DIST CURVE SHOWN,3 PEAKS	53408

ARGONNE NATIONAL LABORATORY

ACCELERATOR PROGRAMS

A. Fast Neutron Physics

1. Fast Neutron Cross Sections of Titanium

(A. Smith, P. Moldauer, J. Whalen, E. Barnard,* J. deVilliers,* and D. Reitmann*)

All measurements have been completed and the results incorporated in a revised version of the ENDF/B evaluated file. This revised file has been formally transmitted to the NNCSC, BNL. Final theoretical interpretation of the data is nearing completion employing a picket fence model.

2. Fast Neutron Cross Sections of ^{165}Ho

(A. Smith, J. Whalen, J. Meadows and T. Beynon**)

This work has been completed and a formal manuscript submitted for publication in Zeits. für Physik.

3. Fast Neutron Total and Scattering Cross Sections of the Even Molybdenum Isotopes

(P. Lambropoulos, J. Whalen, and A. Smith)

The elastic and inelastic scattering cross sections and the total cross sections of the isotopes Mo-92, 94, 96, 98 and 100 were determined from incident neutron energies of 0.1 to 1.6 MeV. A detailed analysis of these experimental results has been undertaken based on the Davydov-Fillippov model. The cross sections have been calculated using the optical model computer code ABACUS-2. Spins have been assigned to the experimentally observed excited states. The results are consistent with the theoretical model as well as with γ-ray experi-

---

*South African Atomic Energy Board, Pelindaba, Transvaal, Republic of South Africa.

**University of Birmingham, Birmingham, England.

mental results and analyses recently reported by other authors. Several new levels have been observed. (Pertinent to request #221, WASH-1144)

4. Fast Neutron Total and Scattering Cross Sections of ^{238}U
(P. Lambropoulos, A. Smith, J. Whalen, and J. Meadows)

The results of recent measurements are complete and, combined with previously reported values, have been interpreted from 0.1 to 10.0 MeV in terms of a local, energy-dependent, spherical optical potential with spin orbit coupling. Total cross sections and elastic and inelastic scattering cross sections were calculated and compared in detail with the experimental results. The statistical model was used in calculating elastic and inelastic scattering processes and capture and fission reactions were taken into account. The effects of resonance width fluctuations and correlations, and of deformation were examined. Generally, satisfactory agreement was achieved between calculation and experiment. An interesting result of the work was the conclusion that the inelastic scattering cross section in the region near 1.5 MeV is appreciably smaller than that given in some of the more widely used evaluations. This is illustrated in Fig. A-1. Shown is the total inelastic scattering cross section of ^{238}U. The solid curve indicates the results of the present work. The other curves indicate the values given in various evaluations, particularly, —·· ·—··· ENDF/B, and — — — ENDF/B, version II.

A formal report of the above work has been submitted for publication in Nuclear Science and Engineering. (Pertinent to request #405 and 406, WASH-1144)

5. Fast Neutron Total and Scattering Cross Sections of Pu-240; 0.1 to 1.5 MeV
(P. Lambropoulos, J. Whalen, and A. Smith)

Experimental determination of the total cross sections and of the elastic and inelastic scattering cross sections of Pu-240 has been completed for neutron energies from 0.1 to 1.5 MeV.

Representative experimental results are shown in Fig. A-2; namely, total and elastic scattering cross sections of Pu-240. The dashed curves indicate "eye guides" through the experimental points. The solid curve is the result of preliminary optical-model analysis. The total cross section displays appreciable structure. This effect is believed anomalous, arising from the contribution of aluminum reson-

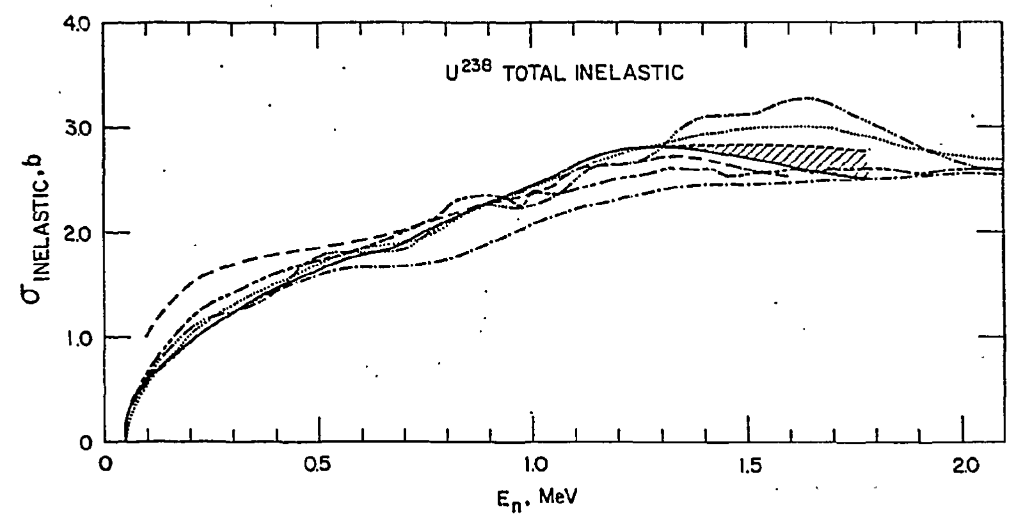

Fig. A-1

DATA NOT FOR QUOTATION

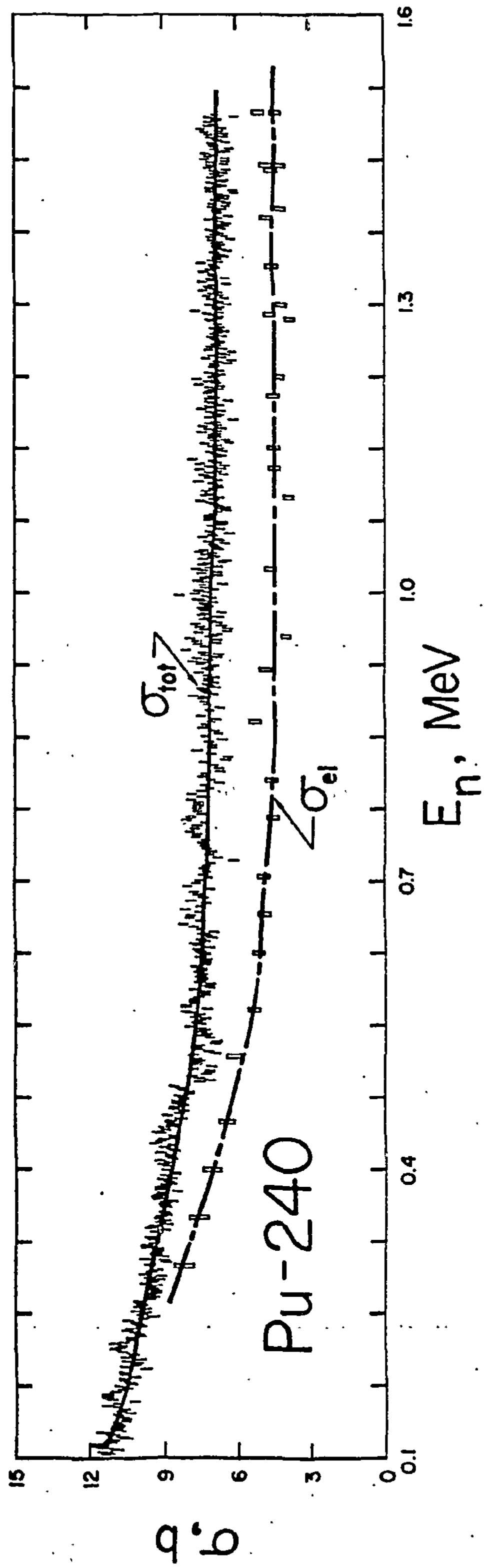

Fig. A-2

DATA NOT FOR QUOTATION

ances. Corrections were applied but small differences in energy resolution and/or incident energy calibration can easily lead to the structured behavior. Averages over energy intervals large compared to that of the structure should result in reliable average cross section values. The figure also indicates the measured elastic scattering cross sections. These, combined with the measured inelastic scattering cross sections, are consistent with the observed total cross sections. A preliminary result of theoretical interpretation based on the optical-model is indicated on the figure. Further analysis now in progress is based upon the compound nucleus processes, channel coupling effects and resonance interference properties. The measurements and the interpretation constitute the only known detailed study of fast neutron processes in Pu-240, a major constituent of many fast reactor systems.

6. Prompt Fission Neutron Spectra of ^{235}U and ^{239}Pu
(A. Smith)

The final reduction of the experimental results is nearing completion. The ratio of the spectral distribution from ^{235}U and ^{239}Pu are very clearly defined and the absolute spectral shapes derived to neutron energies of 1.5 MeV. All data are presently in the form of energy spectra which must be combined to obtain the final values. Careful assay of the accuracy of the results is difficult and has slowed the analysis of the experimental values. (Pertinent to request #389, WASH-1144)

7. Fast Neutron Inelastic Gamma Ray Studies in Arsenic and Sodium
(D. L. Smith)

Inelastic neutron scattering gamma-ray production measurements for ^{75}As and ^{23}Na were made at several neutron energies between 300 keV and 1500 keV with the Ge(Li) detector at 90° to the incident neutron flux.

Angular distribution measurements were made for the 440 keV gamma ray from the $^{23}Na(n,n'\gamma)$ reaction at neutron energies of 780, 910, 1070, 1150 and 1230 keV. Preliminary experimental results are available from the author.

8. Resonance Scattering of Neutrons by B^{10} and B^{11}
(J. L. Adams,* R. O. Lane,* S. L. Hausladen,* C. E. Nelson,* A. J. Elwyn, J. E. Monahan, F. P. Mooring, and A. Langsdorf, Jr.)

The polarization and differential cross sections for neutrons scattered by B^{10} and B^{11} for energies in the interval 0.075—2.2 MeV were measured at Argonne several years ago. Recently we have analyzed these data to obtain spectroscopic information about the resonances excited in these reactions. One report of this work is in press,** and another is in preparation. In the case of neutron scattering from B^{11}, an attempt has been made to interpret the spectra in terms of particle-hole shell model configurations. In the case of neutron scattering from B^{10}, the results of most of the neutron scattering, (n,α) reaction cross sections, and total cross sections have been interpreted in one consistent R-matrix calculation. Furthermore, quantitative explanation of the large 1/v $B^{10}(n,\alpha)Li^7$ cross section as well as the α_0/α_1 branching ratio is given. (Pertinent to request #27, WASH-1144)

9. Facilities
(Applied Nuclear Physics Division)

The Dynamitron Tandem Accelerator is now fully operational. The dc proton beam current obtained at 8.0 MeV is ~55 μA. Peak pulsed proton and deuteron currents measured with a fast Faraday cup are > 1000 μA at 1.3 nsec FWHM and 700 μA at 2.0 nsec FWHM, respectively. Beam energy stability ($\Delta E/E$) is less than 140 eV at 1.88 MeV and 820 eV at 6.00 MeV as indicated by the thin target yield of $^7Li(p,n)^7Be$ and $^{27}Al(p,n)^{27}Si$.

The facility is in routine production at this time. New instrumentation includes a 7 meter rotary collimator system permitting the determination on scattered neutron angular distributions at ten angles concurrently and a large liquid scintillation tank for capture

---

*Ohio University, Athens, Ohio.

**J. L. Adams, R. O. Lane, C. E. Nelson, J. E. Monahan, A. J. Elwyn, F. P. Mooring, and A. Langsdorf, Jr., Phys. Rev. (in press).

gamma-ray measurements. A complement of on-line computers has been put into operation including two 16k 24 bit machines and two 12 bit machines with a total of 24k words of core storage. Software development has progressed to the point of production use.

10. Facilities
(Physics Division)

Installation of a nanosecond beam-pulsing system in the high voltage terminal of the 4-MeV Dynamitron has been completed. The ORTEC system passed its acceptance tests early in 1970. The system consists of three basic parts—a conventional duoplasmatron ion source followed by a beam chopper and finally a Klystron buncher. Without bunching beam pulses as short as 14 nsec FWHM and with peak currents up to 800 μA have been produced. Typically such pulses, when bunched, shorten to 1.3—1.5 nsec FWHM with peak currents of 2—3 mA. The shortest pulses produced to date were 1.0 nsec FWHM, with a peak current of 1.6 mA. The repetition rate can be varied by successive factors of $\frac{1}{2}$ from 2 MHz down to 31.25 KHz. The system is now being used routinely in a series of investigations of nuclear properties.

B. Charged Particle Physics

1. Neutron Differential Cross Sections in the ^{48}Ca(p,n)^{48}Sc Reaction
(A. J. Elwyn, F. T. Kuchnir, F. P. Mooring, J. Lemming, and W. G. Stoppenhagen)

We have measured the relative differential cross sections to a number of final states in ^{48}Sc in the ^{48}Ca(p,n)^{48}Sc reaction at proton energies near 2 MeV. This range of proton energies corresponds to the excitation of the $T=\frac{9}{2}$ state in ^{49}Sc at 11.56 MeV which is the analog of the ^{49}Ca ground state. The yields of neutrons leading to the 0.131, 0.252, 0.624, and 1.140 MeV states in ^{48}Sc have been obtained at 7 angles between 0 and 135° and at 11 proton energies from 1.95 to 2.0 MeV. The newly-installed pulsed and bunched source of the 4-MeV Dynamitron producing proton beam bursts 1.3—1.5 nsec wide with peak currents of about 2.2 mA was used and the various neutron groups were separated by measuring the time-of-flight over a 1m flight path. Neutrons were detected simultaneously at 4 angles using 2" diameter by 1" thick stilbene scintillators coupled to

RCA 8575 photo tubes. Pulse-shape discrimination was employed to suppress the gamma rays. The energy resolution was 7% and 6% (FWHM) for neutron energies of 300 keV and 1.2 MeV, respectively. Analysis of the observed angular distributions in terms of the partial waves involved in the reaction is in progress.

2. $Ru^{103,105}$ States Observed in the Reactions $Ru^{102,104}(d,p)$
(H. T. Fortune, G. C. Morrison, J. A. Nolen, Jr., and P. Kienle)

The (d, p) reaction on Ru^{102} and Ru^{104} has been studied at an incident deuteron energy of 14 MeV. Proton spectra were recorded in a broad-range magnetic spectrograph. Transferred ℓ values and spectroscopic factors were obtained by comparing the measured angular distributions with DWBA predictions. The summed spectroscopic factors give information on the extent of filling of the neutron orbitals in the targets, and these results are in reasonable agreement with results from the (d, t) reaction and for other nuclei in this region.

C. Threshold Photoneutron Studies

1. Possible Nonresonant (γ, n) cross section in ^{207}Pb and ^{208}Pb

Using the ANL high-intensity photoneutron source (see NCSAC-31, page 10, for a brief description) we have attempted to verify the existence of an anomously large non-resonant (γ, n) cross section near threshold in ^{208}Pb reported earlier in Livermore measurements.* The shape of the 40.4 keV resonance in the reaction $^{208}Pb(\gamma,n)^{207}Pb$ was examined for evidence of resonance-non-resonant amplitude interference and a direct measurement of the non-resonant cross section was made at 25 keV in both ^{207}Pb and ^{208}Pb. The direct measurement was made by inserting an iron filter in the photoneutron beam near the ^{208}Pb target and observing the strength of the transmission dip in the neutron time-of-flight spectrum at 27.9 keV. This dip, due to a strong resonance in the iron filter at that energy,

*Bowman, Baglan, and Berman, Phys. Rev. Letters 23, 796 (1969).

is assumed to arise from the attenuation of the neutron continuum produced by the non-resonant (γ, n) amplitude. Although the shape of 40.4 keV resonance is distinctly different from that of earlier experiments, the results for ^{208}Pb are consistent with a non-resonant amplitude of 1—1.5 mb/sr. in the range 25—40 keV. However, no detectable non-resonant amplitude is observed for ^{207}Pb(γ, n) in the same energy range. Three points suggest that the non-resonant cross section reported for ^{208}Pb is in fact an instrumental effect: 1) the value observed at 25 keV for ^{208}Pb is an order of magnitude larger than the upper limit inferred from the 25 keV capture cross section for ^{207}Pb, 2) The observed ^{208}Pb cross sections when extrapolated to thermal are not consistent with the known cross section for the inverse process, ^{207}Pb(n, γ_0), 3) Although a similar phenomenon is expected for the other Pb isotopes none is observed for ^{207}Pb. Efforts to understand the (γ, n) results are continuing.

2. M1 Radiative Strength in ^{53}Cr
(H. E. Jackson)

We have studied the reaction ^{53}Cr(γ, n) near threshold. Time-of-flight spectra for the photoneutron spectra were observed for neutrons emitted at 90° and 135° to the incident photon beam and from the observed angular distributions angular momentum assignments of the resonances shown in table C-1 were made. The spectra for θ = 135° are shown in fig. C-1. The data are characterized by an intense p-wave component which suggests exceptionally strong M1 radiative transitions. A report of this work is in preparation.

3. Monte Carlo Program for ^{6}Li Glass Detectors
(E. N. Strait, W. J. Snow, and J. W. Tippie)

The capture of neutrons in a ^{6}Li glass scintillator has been investigated by a Monte Carlo computer program. The program randomizes the neutron point of entry at the face of a finite geometry cylindrical detector and traces its progress via scattering, which is assumed to be isotropic, until capture or escape from the glass. Ten incident energies have been treated in the range 10 keV to 800 keV with sufficient number of neutrons to produce 5000 captures in each case. At each energy the output of the program gives spectra of the transport times within the glass for neutrons which are captures before scattering, for those captured after one or more scattering

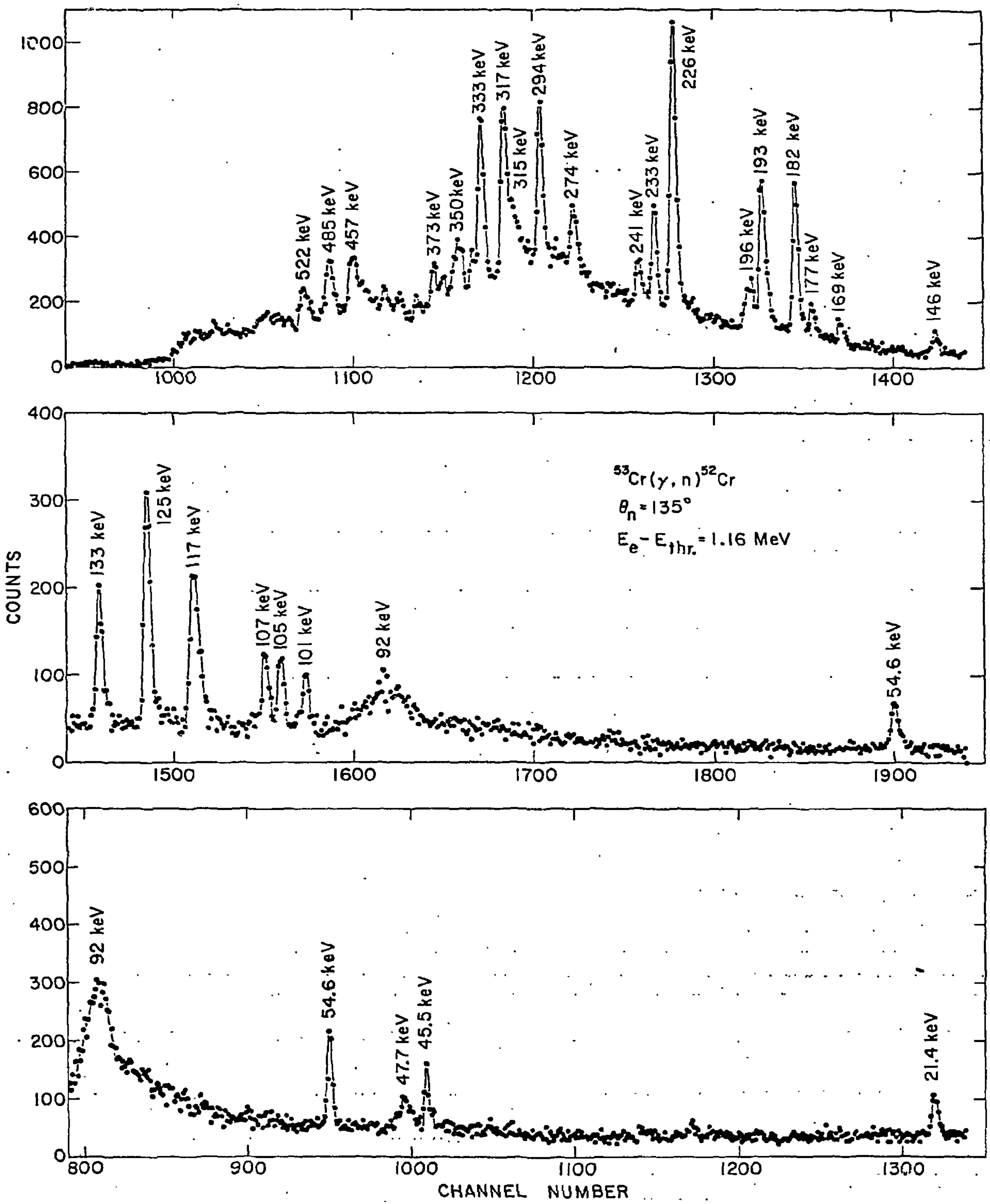

Fig. C-1

DATA NOT FOR QUOTATION

E_n (MeV)	J	E_n (MeV)	J
.373	$\frac{1}{2}$	.169	...
.350	$\frac{3}{2}$	.146	$\frac{1}{2}$
.333	$\frac{1}{2}$	.133	$\frac{3}{2}$
.317	$\frac{3}{2}$	.125	$\frac{3}{2}$
.315	$\frac{1}{2}^+$	.117	$\frac{1}{2}^+$
.294	$\frac{1}{2}$	.107	$\frac{3}{2}$
.274	$\frac{3}{2}$	.105	$\frac{3}{2}$
.241	$\frac{3}{2}$	.101	$\frac{3}{2}$
.233	$\frac{1}{2}$	.092	$\frac{1}{2}^+$
.226	$\frac{1}{2}^+$	.0546	...
.196	$\frac{3}{2}$	.0477	$\frac{1}{2}^+$
.193	$\frac{1}{2}$	.0455	...
.182	$\frac{1}{2}$	.0214	...
.177	...		

Table C-1. Angular momentum assignments for resonances in the reaction $^{53}Cr(\gamma, n)$.

events, the composite time spectrum of these two types of histories, the efficiency of the detector, and the number of scatterings from each nuclide within the glass. The program contains options for various neutron source geometries. For a parallel beam of neutrons incident normally upon the face of a 0.375 inch thick by 5 inch diameter NE913 scintillator (18% $^6Li_2O$, 1% $^7Li_2O$, 76% SiO_2, 5% CeO_3) efficiencies range between 0.9% and 4.8% in the energy range treated. Multiple scattering is significant, contributing 20% to 35% of the events leading to capture.

DATA NOT FOR QUOTATION

4. Photoneutrons from ^{235}U
(H. E. Jackson)

The use of the threshold photoneutron technique has been proposed as a possible means of nondestructive analysis for fissile material. In a search for a possible prominent spectral feature which could serve as a signature for ^{235}U we irradiated a 200g sample of ^{235}U with a pulsed bremsstrahlung beam whose end point energy was 7.0 MeV. The photoneutron spectrum was measured by time-of-flight over a 5 meter flight path at a emission angle of 135^{o}. Initial results are negative. No detectable evidence for photoneutron resonances was observed in an 8 hour run with an average electron beam of approximately 20 microamps.

D. Slow Neutron Physics

1. CP-5 Reactor

The CP-5 reactor returned to normal operation in October after an extended shutdown for extensive modification and rehabilitation. Research activity has been limited in this period to analysis of data obtained before the shutdown.

2. Current Values of the Fundamental Fission Parameters, The 2200 m/s Constants
(A. De Volpi).

A review* has been made of the status of 2200 m/s fission constants, focused mainly on ^{235}U, ^{239}Pu, and ^{233}U. The most recent work in this field has been by the IAEA published in 1969. Depending very much on a partially subjective view towards experimental credibility, a significantly different set of parameters can be developed. The points of departure are the acceptance by the reviewer of the more recent low measurements of the ^{233}U and ^{234}U half-lives and of reduced downweighting of some absolute measurements of $\nu(^{252}Cf)$ which have been the object of extensive verification procedures. This results in 1% lower ν values for the fissile isotopes. In addition, some reductions in η values are experimentally justified. The half-life revisions augment evidence that the fission cross-sections for ^{233}U and ^{235}U should be higher than the IAEA

*for Reactor Technology

DATA NOT FOR QUOTATION

average. As a result of this study, an adjusted set of fission parameters has been generated with substantive support from the revised experimental input data, see Table D-1. A uniform constraint of constant product $\nu\sigma_f = \eta\sigma_a$ is applied, which makes most integral experiments insensitive to the modifications. The ^{239}Pu set has additional ambiguities due to inadequate input data.

Table D-1. Revised Values for 2200 m/s constants*

	^{233}U		^{235}U	
	Experiment	Adjusted	Experiment	Adjusted
σ_a	575.6 ± 1.6 (0%)**	582.5 ± 1.8 (+0.85%)	680.5 ± 2.7 (+0.15%)	683.0 ± 1.9 (+0.66%)
σ_f	539.3 ± 4.8 (+1.6%)	537.9 ± 1.9 (+1.0%)	587.4 ± 2.5 (+1.0%)	585.7 ± 1.8 (+0.95%)
σ_γ	50.6 ± 3.2 (0%)	44.6 ± 0.9 (-12%)	— —	97.3 ± 1.1 (-1.0%)
α	0.0900 ± 0.0004 (0%)	0.0830 ± 0.0018 (-6.6%)	0.1691 ± 0.0021 (-0.59%)	0.1661 ± 0.00[illegible] (-2.0%)
η	2.278 ± 0.008 (-0.44%)	2.265 ± 0.006 (-0.86%)	2.067 ± 0.009 (-0.48%)	2.058 ± 0.006 (-0.68%)
ν_t	2.453 ± 0.050 —	2.453 ± 0.007 (-1.4%)	2.393 ± 0.008 —	2.400 ± 0.007 (-0.92%)
σ_s	—		14.3 ± 0.5 (-7.0%)	13.6 ± 1.5 —

*Preliminary, 7 October 1970

**In parentheses are percentage differences comparing Hanna et al. (1970) input-experimental and output-adjusted data.

DATA NOT FOR QUOTATION

^{239}Pu

	Experiment	Adjustment A*	Adjustment B*
σ_a	1012.1 ± 6.2 (0%)	1021.6 (+0.86%)	1013.4 ± 4.6 (0.13%)
σ_f	742.5 ± 2.8 (+0.26%)	742.5 (+0.26%)	742.5 ± 3.1 (+0.26%)
σ_γ	275.5 ± 7.8 (0%)	279.1 (+2.9%)	270.9 ± 2.6 (-1.7%)
α	0.3598 (0%)	0.376 (+2.8%)	0.365 ± 0.004 (+1.4%)
η	2.100 ± 0.009 (-0.48%)	2.091 (-0.84%)	2.091 ± 0.007 (-0.84%)
ν_t	2.854 ± 0.008 —	2.877 (-0.10%)	2.854 ± 0.007 (-0.91%)

*For ^{239}Pu Adjustment A, $\nu_t(^{239}Pu)\sigma_f(^{239}Pu) = 2136.2$ (as Hanna et al., 1970); for B the product is 2119.1.

$\nu_t(^{252}Cf) = 3.730 \pm 0.008$ (Experiment) (-0.35%)
3.730 ± 0.008 (Adjusted) (-0.94%)

$\sigma_f(^{239}Pu/^{235}U) = 1.2615 \pm 0.0081$ (Experiment) (-1.6%)
1.2615 ± 0.0081 (Adjusted) (-1.3%)

$\tau_{1/2}(^{233}U) = 1.554 \pm 0.003 \times 10^5$ y (-2.5%)
$\tau_{1/2}(^{234}U) = 2.444 \pm 0.005 \times 10^5$ y (-1.8%)
Experiment

Table D-1 (continued)

DATA NOT FOR QUOTATION

$\nu_t(^{235}U/^{252}Cf)$	$= 0.6417 \pm 0.0018$	(Experiment)	(0%)
	$= 0.6434 \pm 0.0015$	(Adjusted)	(0%)
$\nu_t(^{239}Pu/^{252}Cf)$	$= 0.7648 \pm 0.0067$	(Experiment)	(0%)
	$= 0.7713 \pm 0.0022$	(Adjusted)	(+0.85%)
$\nu_t(^{235}U)\sigma_f(^{235}U)$	$= 1405.6$	(Experiment)	(-0.01%)
	$= 1405.7$	(Adjusted)	(-0.01%)
$\eta(^{235}U)\sigma_a(^{235}U)$	$= 1406.6$	(Experiment)	(+0.06%)
	$= 1405.7$	(Adjusted)	(-0.01%)
$\nu_t(^{233}U)\sigma_f(^{233}U)$	$= 1322.9$	(Experiment)	(+0.26%)
	$= 1319.5$	(Adjusted)	(0%)
$\eta(^{233}U)\sigma_a(^{233}U)$	$= 1311.2$	(Experiment)	(-0.63%)
	$= 1319.4$	(Adjusted)	(0%)
$\nu_t(^{239}Pu)\sigma_f(^{239}Pu)$	$= 2119.1^{A}$	(Experiment)	(-0.81%)
	$= 2136.2^{B}$	(Adjusted)	(0%)
$\eta(^{239}Pu)\sigma_a(^{239}Pu)$	$= 2125.4$	(Experiment)	(-0.51%)
	2136.2	(Adjusted)	(0%)
$\dfrac{\eta(^{239}Pu)\sigma_a(^{239}Pu)}{\eta(^{235}U)\sigma_a(^{235}U)}$	$= 1.5110$	(Experiment)	(+0.15%)
	$= 1.5197^{A}$	(Adjusted)	(+0.03%)
	$= 1.5075^{B}$	vs. 1.5087 ± 0.025	(Magnuson 1970)
$\dfrac{(\eta-1)(^{239}Pu)\sigma_a(^{239}Pu)}{(\eta-1)(^{235}U)\sigma_a(^{235}U)}$	$= 1.5333$	(Experiment)	(+3.6%)
	$= 1.5424^{A}$	(Adjusted)	(-0.09%)
	$= 1.5300^{B}$	vs. 1.4803	(Experiment Average)
$\eta(^{239}Pu)/\eta(^{235}U)$	$= 1.0160$	(Experiment)	(+0.13%)
	$= 1.0160$	(Adjusted)	(-0.16%)
$\eta(^{233}U)/\eta(^{235}U)$	$= 1.1021$	(Experiment)	(-0.05%)
	$= 1.1006$	(Adjusted)	(-0.17%)
$\dfrac{\eta(^{233}U)\sigma_a(^{233}U)}{\eta(^{235}U)\sigma_a(^{235}U)}$	$= 0.9322$	(Experiment)	(-0.19%)
	$= 0.9386$	(Adjusted)	(0%) vs 0.934 ± 0.014 (Magnuson 1970)

Table D-1 (continued)

DATA NOT FOR QUOTATION

BROOKHAVEN NATIONAL LABORATORY

A. NEUTRON PHYSICS

1. Fast Chopper (R. E. Chrien, O. A. Wasson, G. Cole, R. G. Graves,** M. R. Bhat,* S. F. Mughabghab,* S. Dritsa,† F. Becvar,†† R. Moreh,††† P. Liaud††††

a) Instrumental

Development of a spectrometer to measure the resonant neutron capture γ rays in the fissile nuclei continues. A special Ge(Li) γ-ray detector is surrounded by an annular liquid scintillator, which detects fission neutrons, and thereby separates capture from fission events. Events detected in the Ge(Li) detector are tagged if the events from the fission detector occur in coincidence. The tagged and untagged events are written in tape and sorted off-line. Tests of the fission detection efficiency of the liquid scintillator using resonant neutron absorption in U^{235} are in progress.

b) Experimental

1) Measurement of absolute γ-ray intensities in resonances of U^{238}, Pt^{195}, Mo^{98}, and Cd^{111} relative to Au^{198}. In order to determine absolute γ-ray intensities for those elements for which thermal capture spectra are difficult to obtain due to isotopic contamination or low cross sections, we have measured these intensities relative to those of the 4.9 eV resonance in gold. Since it is known in our previous work that the summed γ-ray intensities for $E_\gamma > 6200$ keV are the same for capture of both thermal and 4.9 eV neutrons, we have used as a standard the value of 10.6 photons per 100 captures measured for these γ-rays in thermal capture by Groshev et al. We have run composite samples of different elements using the measured neutron flux shape and the known resonance parameters to calculate the number of neutrons absorbed in each resonance. The resultant γ-ray intensities for the lowest energy resonances in these nuclei are listed in Table I.

---

* Department of Applied Science, BNL.

** State University of New York, Stony Brook.

† IAEA Fellow, NRC Democritos, Athens, Greece.

†† On leave from JINR, Dubna, USSR.

††† Summer visitor from Nuclear Research Center - Negev, Beer Sheva, Israel.

†††† Guest Scientist, Centre d'Etudes Nucleaires, Grenoble, France.

DATA NOT FOR QUOTATION

Table I

Absolute γ-ray Intensities Relative to Gold

Target	E_γ(eV)	E_γ(MeV)	I_j (photons per capture)
Au^{198}	4.9 [illegible]	6.2-6.5	0.106
Pt^{195}	1[illegible]	7.92	0.062 ± .006
U^{238}	[illegible]	3.991 + 3.982	0.039 ± .004
Cd^{111}	2[illegible]	6.888	0.0059 ± .001
		6.565	0.119 ± .002
Mo^{98}	12.0	5.926	0.031 ± .006
		5.575	0.021 ± .006
		5.379	0.028 ± .007
		5.133	0.053 ± .008

The results for U^{238} are significantly lower than reported in previous BNL chopper measurements (D. L. Price et al, Nuc. Phys. A121, 630-654 (1968), and are now in good agreement with measurements at Gulf General Atomic (GGA Report GA-10186)

2) Resonant neutron capture in $^{111}Cd(n,\gamma)^{112}Cd$. Analysis of a previous experiment using the $^{112}Cd\ (\gamma,\gamma')^{112}Cd$ reaction demonstrated a correlation between the γ-ray transition rates from a negative parity level near 7.6 MeV excitation to low-lying positive parity states and the (d,p) spectroscopic factors of the final states. A search for a similar correlation from the higher excited states above the neutron binding energy formed by P-wave neutron capture in ^{111}Cd was undertaken using the Fast Chopper at BNL. The neutron energy region extended from 10 to 1500 eV, yielding γ-ray spectra from 5 resolved neutron resonances below 200 eV as well as from the unresolved region at higher energies. There is strong evidence that the spin of the 86 eV resonance is 0. The average γ-ray intensities from the unresolved neutron energy region above 300 eV are at nearly equal strength for transitions to both positive and negative parity final states, suggesting the presence of both S-and P-wave resonances in that energy region. A determination of the correlation coefficient is in progress.

3) Study of resonance neutron capture in ^{149}Sm. The capture γ-ray spectrum from an enriched sample in ^{149}Sm was studied throughout the neutron energy interval from 0.02 to 50 eV. The resonance spins were determined from the γ-ray decay of the capturing states and are listed in Table II. In addition to the spectra measured

DATA NOT FOR QUOTATION

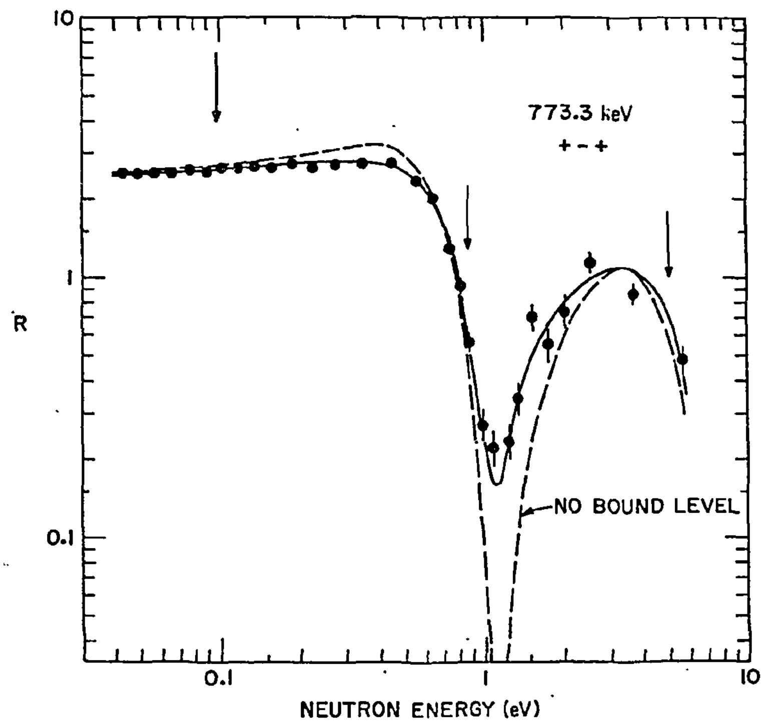

Figure 1

on the resonances, the intensity variation of 41 γ-rays were also measured in the off-resonance region from 0.02 to 10.0 eV. A representative intensity variation for the primary transition to a final state at 223 keV is shown in Fig. 1 where the arrows indicate the positions of the resonances. The variation results from resonance-resonance interference. The importance of postulating a 3- bound level is apparent from the curve. From the interference analysis, the partial radiation widths for 41 γ-rays from the bound level were determined and found to follow the same fluctuations as the positive energy resonances. An analysis of the statistical properties of the partial radiation widths from 16 positive energy resonances to 41 final states was done. The distribution of partial widths is shown in Fig.2 and was fitted to a chi-squared distribution with $1.64^{+0.23}_{-0.18}$ degrees of freedom which is inconsistent with the predicted value of 1.0. However there is no significant correlation between either resonant neutron widths and partial radiation widths or between pairs of partial radiation widths, which is in agreement with the predictions of the statistical model.

TABLE II

Resonance spin assignment for ^{149}Sm target

E_{res} (eV)	BNL-325	J^{π} present work
0.0976	4^-	4^-
0.873	4^-	4^-
4.98	4^-	4^-
6.48	4^-	3^-
9.0	4^-	3^-
12.2		3^-
14.9		3^-
16.0		3^-
17.2		4^-
23.3		4^-
25.3		3^-
26.1		3^-
28.1		3^-
29.8		3^-
30.9		4^-
34.0		4^-

DATA NOT FOR QUOTATION

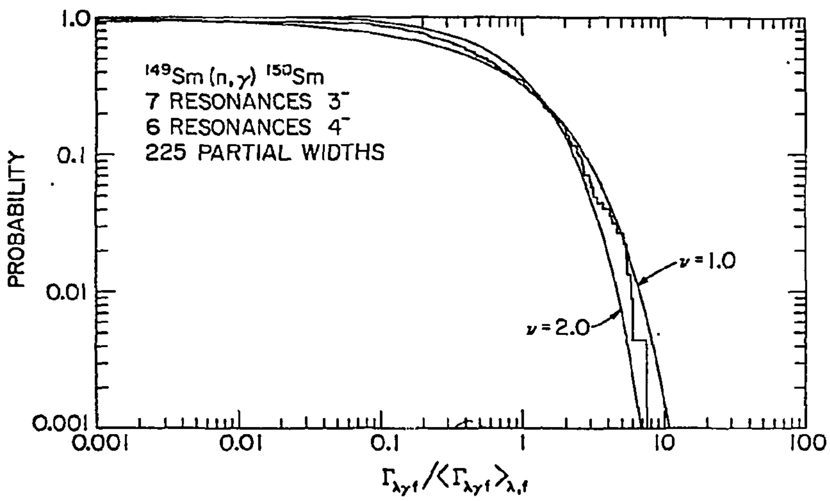

1.0
0.1
0.01
0.001
PROBABILITY
^{149}Sm (n,γ) ^{150}Sm
7 RESONANCES 3$^-$
6 RESONANCES 4$^-$
225 PARTIAL WIDTHS
ν = 1.0
ν = 2.0
0.001
0.01
0.1
1
10
100
$\Gamma_{\lambda\gamma f}/\langle\Gamma_{\lambda\gamma f}\rangle_{\lambda,f}$

Figure 2

4) <u>Distribution of Partial Radiation Widths in $^{238}U(n,\gamma)^{239}U$.</u> (In collaboration with G. G. Slaughter and J. A. Harvey of Oak Ridge National Laboratory) The neutron capture γ-ray spectra from U^{238} were measured throughout the neutron energy interval from 5 to 1300 eV using ORELA. Below 600 eV 23 of the resolved resonances were strong enough to determine the intensities of the high energy γ-rays. The summed spectrum from 6 to 600 eV for the 10 day run is shown in Fig. 3 where the double escape peaks of the uranium γ-rays are indicated by vertical lines. The distribution of partial radiation widths was fitted to a chi squared distribution function with a variable number of degrees of freedom. The γ-rays below 4.0 MeV are consistent with 1 degree of freedom while the γ-rays at higher energy are not. The departures from 1 degree of freedom are apparently not dependent on the multipolarity of the γ-ray transition but depend only on γ-ray energy. In addition the intensities of the 3991 and 3982 keV γ-rays are strongly correlated over resonances while the remaining γ-rays show no correlations. (Pertinent to Request #415 WASH 1144)

5) <u>Non-Statistical Effects in $^{163}Dy(n,\gamma)^{164}Dy$.</u> The capture γ-ray spectra from 23 resonances below 325 eV were measured. The γ-ray intensities from 17 resonances with J = 3 to 22 final states in ^{164}Dy reveal that these are significant correlations between partial radiation widths and resonant reduced neutron widths as was first observed in ^{169}Tm. However no correlation is observed for the 8 resonances of spin 2. The average correlation coefficient of +0.223 for the entire set of γ-rays from J = 3 resonances is shown in Fig. 4 where the histogram represents the distribution for zero correlation. This correlation in the J = 3 channel is attributed to non-statistical effects produced by both channel capture and the presence of doorway states near the neutron binding energy.

6) <u>Non-Statistical Effects in P-Wave Neutron Capture in ^{98}Mo.</u> The capture γ-ray spectra from P-wave neutron capture in 6 resonances of ^{98}Mo below 1200 eV were obtained at the 48 m flight path of the Fast Chopper. The spectra from the 612 eV and 429 eV resonances (Fig. 5) are strikingly similar suggesting a strong correlation between pairs of γ-ray intensities. The resulting average correlation coefficient between pairs of γ-rays for the 4 P-wave resonances and 5 lowest lying states is +0.54 and is highly significant. In addition the γ-ray reduced intensities are strongly correlated with the (d,p) spectroscopic factors of the final states. These results are similar to those reported for ^{92}Mo and ^{93}Nb and suggests that doorway states are influencing P-wave neutron capture in this mass region.

(Pertinent to Requests 224, 225, WASH 1144)

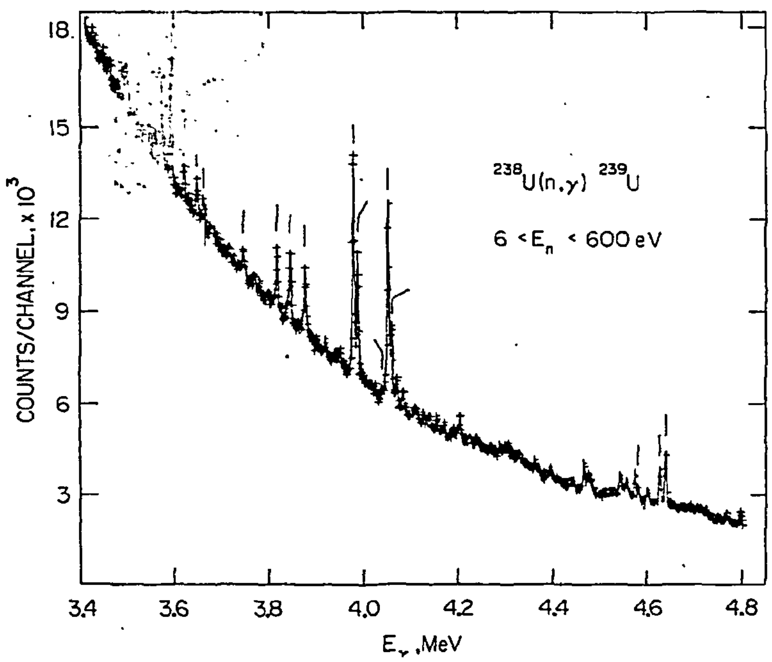

Figure 3

DATA NOT FOR QUOTATION

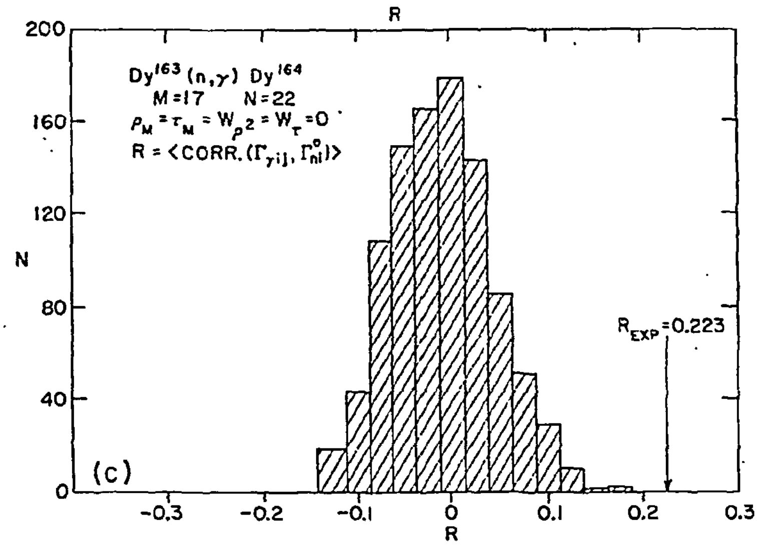

Figure 4

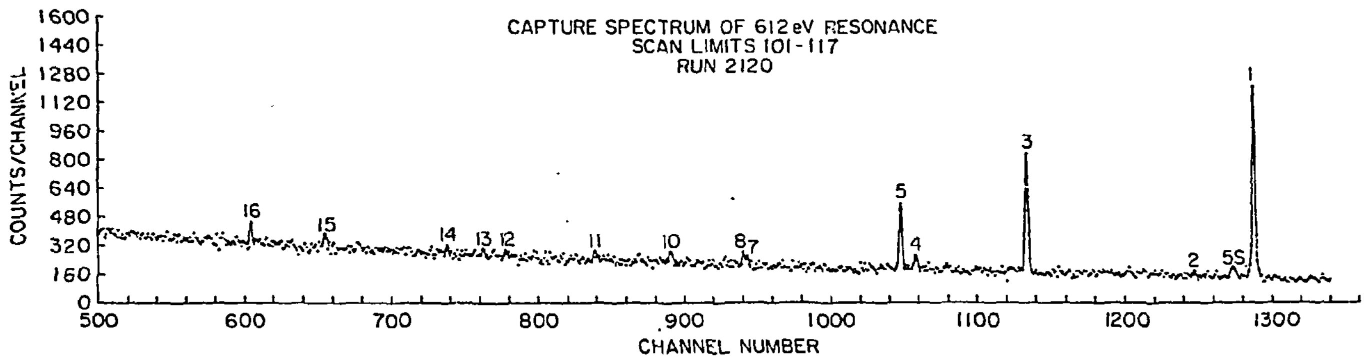

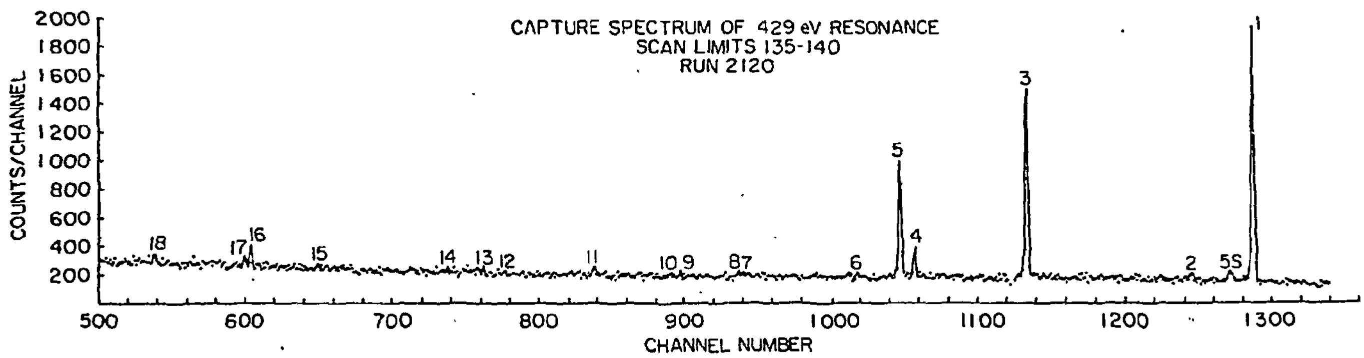

Figure 5

DATA NOT FOR QUOTATION

7) Low energy γ-rays from thermal and resonance capture in ^{239}Pu and ^{235}U. Low energy gamma rays following neutron capture in ^{235}U and ^{239}Pu have been examined. In the ^{235}U case most resonances between 2 and 34 eV were adequately separated. However, due to the high fission gamma ray background, only a few radiative transitions to the ground state band were observed. The intensity of these transitions fluctuates from resonance to resonance and is roughly proportional to the ratio of capture to fission width. An attempt to correlate the spin of the capturing resonances to the values of the relative intensity of a certain transition gave negative results. Namely for the 642 keV transition, from the 2^- level at 687 keV to the first excited 2^+ state, no grouping was observed according to the spin values, as is shown in Fig. 6. In the case of ^{239}Pu where the radiative transitions are stronger a number of resonances from 0.3 eV to 58 eV were examined. For one resonance, the 7.8 eV, measurements were also taken with the crystal neutron diffraction monochromator, and the results were compared with those from the Fast Chopper measurements. Several transitions were observed strongly in most of the resonances examined. These transitions populate energy levels of ^{240}Pu known from the decays of neighboring nuclei. The relative intensities of the stronger transitions are listed in Table III. These intensities have been normalized against the mean value intensity for each resonance. (Pertinent to Request #391, WASH 1144)

8) Neutron capture γ-rays from the 2.85 keV Na resonance. It has been recently reported by workers at RPI and Harwell that the radiation width of the 2.85 keV resonance in Na^{23} is too large to be consistent with the known thermal capture cross section, 0.534 ± 0.005 barns. For example, the RPI result $\Gamma_\gamma = 0.47$ eV, is about 50% larger than is expected. To determine whether multilevel interference effects in the radiative channels can be responsible for this departure, we have measured the spectrum from the 2.85 keV resonance and compared it to thermal capture. Although the background, caused by the high ratio of scattering to capture, is high, we have been able to determine that quantitative differences in the spectra do exist, particularly for the 6395.1 γ-ray, which has a 20% intensity at thermal. Destructive interference for this transition could depress the cross section sufficiently to account for the discrepancy. The interfering amplitude does not appear to result from a bound state, hence direct capture is a plausible alternative. A direct capture cross section of 77 mb at E = 0.0253 could be consistent with the observed results.

1. Yanamuro et al, Nuc. Sci. & Engineering 41, 445 (1970)
2. Moxon and Pattenden, Proc. Conf. on Nuc. Data for Reactors, IAEA Vienna, paper CN-23/27 (1967)

Table III

Low Energy γ-Ray Intensities from $^{239}Pu(n,\gamma)^{240}Pu$

Relative Intensities

Resonance Energy, eV

E_γ (keV)	0.3	7.8	10.95	11.9	14.68	17.7
554±1.5	2.75±.24	2.96±.16	2.80±.24	3.30±.36	2.20±.26	2.84±.46
597	2.23±.23	2.00±.36	1.68±.56	2.30±.43	2.13±.25	1.90±.31
607	1.21±.13	1.21±.25	1.30±.50	2.10±.37	1.50±.20	.65±.18
814	.77±.20	.56±.03	.81±.07	.25±.04	.81±.16	.54±.10
916	1.10±.08	.63±.16	.82±.22	--------	--------	--------
937	--------	1.50±.13	.37±.09	1.52±.21	.87±.18	1.40±.33
973	.54±.10	--------	.65±.16	.10±.04	.62±.24	.33±.08
986	.70±.10	.95±.23	.62±.19	.82±.13	1.0 ±.23	1.24±.38
1131	.85±.08	.37±.11	.91±.21	--------	.50±.13	.18±.06
1134	.75±.05	.31±.10	--------	.28±.07	.53±.12	.77±.15
1216	.45±.06	.66±.20	.63±.23	.33±.10	.67±.25	.71±.12
1220	.44±.06	.53±.18	1.42±.27	.36±.11	.46±.08	.68±.12

E_γ (keV)	22.2	26.2	41.7	44.	52.7	58.
554±1.5	3.00±.57	2.35±.41	3.34±.56	3.54±.40	3.23±.59	2.21±.38
597	2.32±.33	2.46±.66	1.90±.41	1.50±.30	2.21±.32	2.66±.50
607	1.60±.27	1.50±.50	1.40±.32	1.15±.25	1.03±.21	1.10±.33
814	.93±.40	2.22±.55	--------	1.11±.23	.62±.21	1.18±.20
916	--------	--------	1.61±.43	.82±.20	1.40±.23	--------
937	.60±.20	1.04±.19	1.42±.29	1.00±.23	.80±.12	--------
973	2.03±.68	.48±.14	.18±.06	--------	.35±.11	.92±.33
986	.31±.05	--------	1.04±.31	.60±.08	.90±.14	.28±.07
1131	.40±.06	--------	.30±.06	1.16±.30	.32±.08	.65±.20
1134	.20±.06	.50±.20	.32±.06	.66±.24	.38±.08	.51±.18
1216	.40±.16	--------	.23±.06	.38±.05	.54±.05	.40±.10
1220	1.04±.25	--------	.26±.04	.12±.02	--------	1.09±.26

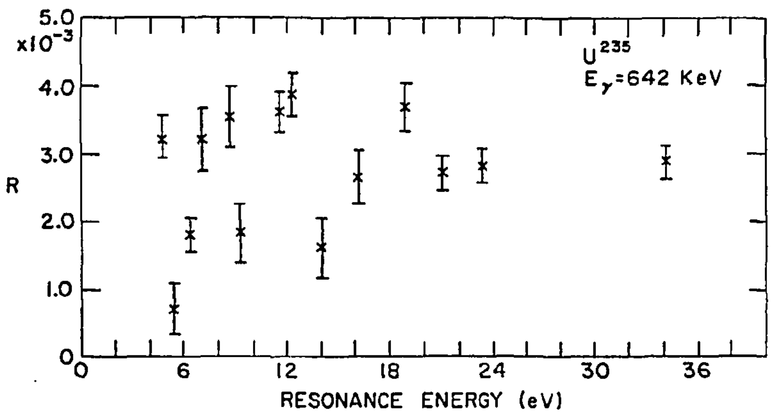

Figure 6

DATA NOT FOR QUOTATION

2. Nuclear Cryogenics

a) Multiple scattering corrections in neutron capture cross section measurements (G. Brunhart and S.S. Malik)

A simple approximate correction method for multiple scattering in neutron capture cross sections has been developed for slab geometries assuming only incoherent, elastic, and isotropic scattering. The method is applicable whenever the capture cross section is a slowly varying function of the incident neutron energy, i.e. in the non-resonant region and in between resonances. The accuracy of the method is discussed in terms of Monte Carlo and analytical calculations that are performed under the same restricting assumptions given above.

b) Slow neutron capture cross section measurements (G. Brunhart, S. S. Malik, D. C. Rorer and V. L. Sailor)

An extensive study of the practicality of using a simple Moxon-Rae detector for precision measurements of slow neutron capture cross sections has been made.* A continuation of this work is planned and is to include measurements on separated isotopes pertinent to requests listed in WASH 1144.

*S.S. Malik, G. Brunhart, F. J. Shore and V. L. Sailor, Nucl. Instr. and Meth. 86, 83 (1970).

c) Spin assignment of Sm^{149} neutron resonances by nuclear polarization (G. Brunhart, D. C. Rorer, V. L. Sailor)

Recent neutron resonance capture studies* of Sm^{149} have led to a disagreement with earlier spin assignments of the 6.48 eV neutron resonance.** It is planned to do a polarization measurement with a Sm-Ho alloy target in order to resolve the discrepancy. There is previous evidence that large nuclear polarizations of otherwise antiferromagnetic samarium in a Sm-Ho alloy can be achieved.

*F. Becvar, Contributed paper at APS Meeting, Houston, Oct. 1970.

**H. Marshak, H. Postma, V. L. Sailor, and C. A. Reynolds, Phys. Rev. 128, 1287 (1962).

d) Delayed gamma-ray yield from U^{235} and U^{238} (V. L. Sailor, G. Brunhart, and D. C. Rorer)

Plans are being made for the measurement of the delayed gamma-ray yield induced in U^{235} and U^{238} targets irradiated in a monochromatic neutron beam of energies in the thermal and eV region. These measurements are pertinent to requests 392 and 417, WASH 1144.

3. Nuclear Structure

a) Gamma-Rays from Resonances in ^{235}U. (W. R. Kane)

The HFBR crystal diffraction neutron monochromater has been used to study high and low energy capture γ-rays following capture in resonances of ^{235}U. In addition to known levels at 149 and 688 keV, six previously unobserved levels are populated, four of which appear to be members of the beta and gamma vibrational bonds. The neutron separation energy of ^{236}U is 6545±2 keV. Direct transition to spin 2 final states indicate that the 2.04 and 6.39 eV resonances have spin 3. For the 4.845 eV resonance, the absence of transitions to spin 2 final states suggests that a $J^{\pi}=4^-$ assignment is likely.

The deduced level scheme for ^{236}U derived from the resonance capture data and internal conversion data is shown in fig. 7. The intensities of the high energy lines are shown in Table IV. (Pertinent to Request 391, WASH 1144)

1. A. Backlin, B. Fogelberg and E. Falkström - Lund, Proc. Intern. Symposium on Neutron Capture Gamma Ray Spectroscopy, Studsvik (IAEA, Vienna 1969) p. 141.

Table IV.

High energy gamma rays from resonance neutron capture in U^{235}. Gamma-ray intensities are given relative to the 642 keV transition in U^{236}.

	$I_\gamma(I_{642} = 100)$				
E_γ	1.135 eV	2.040 eV	4.845 eV	6.39 eV	Assignment
6395	0.05	0.03	0.3	----	6545 → 148.7
5857	----	----	---	0.09	6545 → 687.7
5585	----	1.2	---	0.5	6545 → 956 or 958
5544	----	----	---	0.7	6545 → 1001
5517	1.7	0.3	0.4	0.3	Fission
5494	----	----	0.8	----	6545 → 1051
5487	----	0.9	---	----	6545 → 1058
5475	3.1	0.9	0.6	0.6	Fission
5400	1.8	0.6	0.6	0.7	Fission
5289	----	0.7	0.5	----	6545 → 1256
5205	----	1.0	---	----	6545 → 1340

DATA NOT FOR QUOTATION

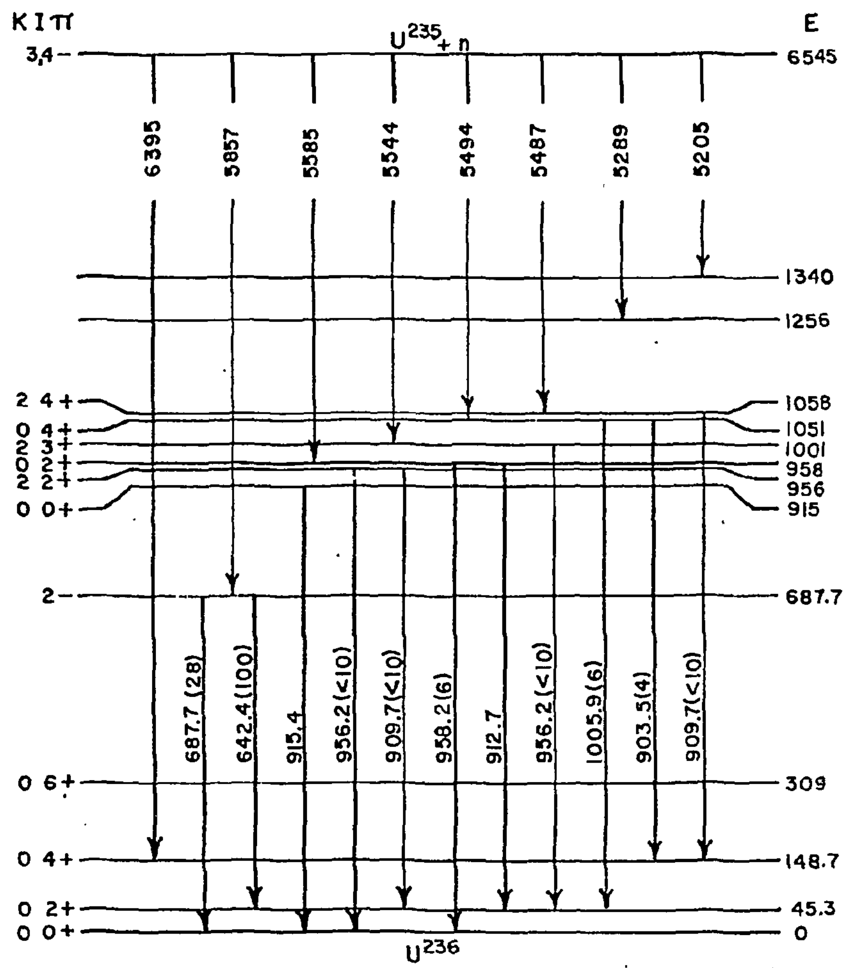

Figure 7

DATA NOT FOR QUOTATION

b) <u>Neutron Capture in the 5.16 eV Resonance of Xe^{124}</u> (W. R. Kane, W. Gelletly, and D. R. MacKenzie.†

In a continuation of work on neutron capture by xenon isotopes in the resonance region (see status report to the NCSAC, May 1970) the gamma rays emitted after neutron capture in the 5.16 eV resonance of Xe^{124} are being investigated. Although Xe^{124} is only $\sim$ 0.1% abundant in the normal Na_4XeO target employed in this work, so that the target contains only $\sim$ 2 mg. of Xe^{124}, the sensitivity of the neutron monochromator system is such that a number of gamma rays attributable to the product nucleus Xe^{125} are observed at the 5.16 eV resonance. In addition, since the monochromator provides a continuous beam of neutrons at one energy, the data obtained are readily normalized to the gamma rays from the $Xe^{125} \rightarrow I^{125}$ decay, aiding further in the unambiguous identification of the Xe^{124} capture gamma rays. These results should be particularly interesting with respect to the level structure of Xe^{125} since this nucleus lies at the edge of a region of deformation. So far, only high spin levels of Xe^{125} are known, from studies of the $Te^{123}(\alpha,2n)Xe^{125}$ reaction.

B. <u>NATIONAL NEUTRON CROSS SECTION CENTER</u> (S. Pearlstein, M. D. Goldberg, M. K. Drake, D. E. Cullen, T. J. Krieger, J. R. Stehn, M. R. Bhat, H. R. Connell, D. I. Garber, W. H. Kropp, B. A. Mugurno, V. May, S. F. Mughabghab, O. Ozer, A. Prince, F. M. Scheffel, H. Takahashi, M. Raymund)

After a trial exchange of tapes, formal transmission of data in an international exchange format (EXFOR) began July 1, 1970. At the recent 4-Center meeting in Paris the NNCSC transmission was examined in detail. No serious problems in the transmission of experimental data have been noted so far.

Trial transmission of data from experimenters in a format approximating EXFOR are underway at AEC laboratories. These procedures will minimize the time required for the generation of author proofs and the entry of data into the files.

The compilation BNL-400, "Angular Distributions in Neutron-Induced Reactions, Volume I, Z = 1 to 20" has been issued. Volume II is in press. Computerized techniques were used in preparation of the material for publication. These techniques will reduce the costs and time required for future publications.

Version II of the ENDF/B library has been distributed. An intensive effort to test the data in benchmark calculations is being performed by the Cross Section Evaluation Working Group, a cooperative effort among several laboratories. An ENDF Formats and Procedures

Manual will be issued soon.

Programming has been started on a physics checking code, PSYCHE, for ENDF data. The code will use a library of basic data, such as masses, spin, decay properties, etc., to check input data. In addition statistical properties and spectrum averages will be calculated from the data file for comparison with experimental values such as strength functions, resonances integrals, fission and Maxwellian spectrum averages, etc.

Increasing attention is being given to nuclear model codes for use in evaluation studies. The NNCSC is attempting to assist studies that will determine the availability, code size, programming language, capabilities, and documentation of useful codes.

The PDP-10 computer has been operating with two disc-pack units allowing sixty (60) million bytes of on-line fast storage. The evaluated data library is now stored on discs. Steps are being taken to also place the experimental library on disc pacs. Interactive graphics equipment is scheduled for delivery in December 1970.

C. BROOKHAVEN LINAC ISOTOPE PRODUCER (L. G. Stang)

Planned for construction at Brookhaven is a facility to be known as the Brookhaven Linac Isotope Producer (BLIP). It will be located adjacent to the 200 MeV proton LINAC that is being constructed for use as an injector for the Alternating Gradient Synchrotron. The LINAC is expected to provide the BLIP with a time-averaged DC current of 180 microamperes of 200-MeV protons in the form of nine 200-microsecond pulses per second on a continuous 24 hr/day, 7 days/week basis.

The BLIP will provide for the irradiation of a variety of targets, each selected to be the optimum for producing specific products of interest. The number and thickness of each target will be such that virtually all of the protons are absorbed in the targets at all times with essentially none of the protons being wasted. For example, when short-lived products (requiring only short-term irradiations) are not being produced their places will be taken by targets requiring long-term irradiations (for producing long-lived products).

An idea of the capacity of this facility can be had by noting that the following amounts could be made sequentially, provided that the entire beam is used for producing each of the products one at a time; (proportionately, less would, of course, be available if several different targets were irradiated simultaneously, which is the actual mode of operation proposed, the amount of each depending on the fraction of the beam that each target intercepts):

Isotope	Half-Life	Production Rate
Ta-179	1.7 years	100 curies/year
Ar-42	33 years	200 millicuries/year
Al-26	740,000 years	30 milligrams/year
Y-88	107 days	3 curies/day
Ga-67	78 hours	280 curies/day
Mg-28	21.3 hours	16 curies/day
I-123	13 hours	800 curies/day
Fe-52	8.3 hours	4 curies/day
C-11	20.5 minutes	100 curies/20 minutes
N-13	9.96 minutes	85 curies/10 minutes

The above are just a few examples of some of the products. It will be noticed that most, but not all, of them are neutron-deficient. This is because most, but not all, of the production reactions to be utilized are spallation reactions, although spallation reactions will also be used to produce neutron-rich isotopes such as magnesium-28, their most effective utilization involves production of neutron-deficient nuclides. All of the products will be virtually carrier-free. Product mass numbers can range from one up to the mass number of the target used, and the atomic numbers of the products can range from one up to one more than the atomic number of the target, although the optimum yields decrease as the product nuclide of interest gets farther from the line of stability. In many cases by proper choice of irradiation and cooling times, method of processing, production route, etc. it will be possible to produce particular nuclides free of other isotopes of the same element, although there will, of course, be some cases in which objectionable by-product isotopes can not be excluded.

Although it is still too early to predict schedules with certainty, the first irradiations might commence as early as October 1971. A more likely estimate is some time in 1972.

It would be helpful for planning purposes if people needing specific nuclides that can not be made in satisfactory quantity or purity by present methods would contact Lou Stang, Brookhaven. Although the primary objectives of the BLIP are to assist in an exploratory program at Brookhaven involved in developing medical applications of isotopes and isotopes for medical applications, it may well be possible to provide other kinds of isotopes, especially with proper scheduling.

D. TANDEM VAN DE GRAAFF (H. E. Wegner)

The new 30 MeV three-stage tandem is now in operation and various research programs have been initiated. The facility can provide

30 MeV protons with utilization of all three stages and many types of heavy ions at various energies with two stage acceleration. At present, special modifications are being made in the terminal ion source so that all two-stage ions presently available will also be available on a three-stage basis with ion energies 20-40 MeV higher than the maximum possible with two-stage acceleration.

Many types of heavy ion reactions are presently under study and in a number of cases the heavy ion is used to bombard a light target of deuterium, tritium, helium-3, or helium-4. This technique allows nuclear reactions customarily carried out with the light particle being accelerated to be accomplished by accelerating the target into the light particle. The accelerated target is automatically magnetically analyzed by the energy control system of the accelerator, thereby providing a 100% pure isotopic target and in addition the gamma background from the interaction of the accelerated target particles with other parts of the apparatus such as collimators and Faraday cups is reduced to almost zero in most cases. For example, in the $^{32}S(d,n)^{33}Cl$ reaction the deuterons produce neutrons and gamma rays from many parts of the apparatus and from contaminants in the ^{32}S target while with the $d(^{32}S,^{33}Cl)n$ reaction at energies like 50 or 60 MeV the only neutrons produced are from this specific reaction with no background of any kind.

There are no immediate plans for any specific neutron cross-section-type measurements; however, fast pulse systems are being planned for the facility and almost any type of nuclear cross section will be measurable in the future. It is possible that certain nuclear cross sections important to the AEC could be measured with this facility in a unique way. However, the facility will have to be further instrumented in a more complete fashion than it is at present in order to carry out sophisticated and special measurements more easily here than at other existing laboratories.

CASE WESTERN RESERVE UNIVERSITY

A. NEUTRON PHYSICS

1. Elastic and Inelastic Neutron Scattering (P. Boschung*, J. T. Lindow**, and E. F. Shrader**)

Accurate differential elastic (typically 3 to 5%) and inelastic (typically 10 to 20%) neutron scattering cross sections have been determined for ^{12}C, ^{54}Fe, ^{58}Ni, and ^{60}Ni between 4.0 and 5.6 MeV. The iron and nickel elastic cross sections have been compared with predictions of the optical model using standard sets of parameters for the potential.[1] Calculations using the average potential of Rosen *et al*. predict the differential cross sections fairly well, with agreement somewhat better for the two nickel isotopes. Coupled-channel calculations for the elastic scattering of neutrons by carbon agree very well with the measurements.

Inelastic scattering to single levels in the residual nucleus can be described adequately with the statistical model. In the case of the first excited levels of the nickel and iron isotopes, which are 2^+ collective states, there is significant evidence for the existence of direct reaction contributions. The data for these states agree well with the sum of predictions of the statistical model and DWBA calculations of direct reaction contributions.

This work is now complete, and a paper titled "scattering of Fast Neutrons by ^{12}C, ^{54}Fe, ^{56}Fe, ^{58}Ni and ^{60}Ni" has been accepted for publication in Nuclear Physics. A Ph.D. dissertation[2] describing the work has been accepted by the university.

---

*Presently at Institut de Physique de l'Universite'de Neuchâtel, Neuchâtel, Switzerland.

**Presently at Harshaw Chemical Company, Solon, Ohio.

[1] L. Rosen, J. G. Beery, A. S. Goldhaber and E. H. Auerbach, Ann. Phys. 34 (1965) 96; P. A. Moldauer, Nucl. Phys. 47 (1963) 65; F. Perey and B. Buck, Nucl. Phys. 32 (1962) 353; F. G. Perey, Phys. Rev. 131 (1963) 745; D. Wilmore and P. E. Hodgson, Nucl. Phys. 55 (1964) 673.

[2] J. T. Lindow, unpublished Ph.D. dissertation, CWRU (1970).

2. Normalization of Neutron Scattering Cross Sections
(J. T. Lindow, P. Boschung, and E. F. Shrader)

Work has been completed on a technique for absolute normalization of the cross section data from neutron scattering. A paper titled "Absolute Normalization of Neutron Scattering Cross Section Data Using Organic Scintillators as Scatterers"[1] has been published.

B. STRIPPING REACTIONS AND POLARIZATION

1. Polarization of Neutrons from the $^{13}C(d,n)$ Reaction
(W. W. Lindstrom* and E. F. Shrader)

The reduction of data from measurements of the polarization of neutrons produced by the $^{13}C(d,n)$ reaction is now completed. The feasibility of analyzing the data by comparison with DWBA calculations is being investigated.

A Ph.D. dissertation[2] describing the experimental methods and results has been accepted by the university.

2. $^{16}O(d,n)^{17}F$ Differential Cross Sections (D. E. Velkley, B. D. Anderson, and H. B. Willard)

Preparations are almost complete for a measurement of the absolute differential cross sections for excitation of the ground and first excited state of ^{17}F via the $^{16}O(d,n)^{17}F$ reaction over the deuteron energy range of 2.8 to 3.8 MeV. Excitation functions will be measured at two angles in intervals of 100 keV, and angular distributions will be taken at average deuteron energies of 3.05, 3.34 and 3.60 MeV, corresponding to the same incident deuteron energies and target thickness as the polarization measurements described below. These results are expected to provide additional information regarding the reaction mechanism which may be pertinent to interpretation of the

---

*Presently at Physikalisches Institut der Universitat Basel, Basel, Switzerland.

[1] J. T. Lindow, P. Boschung, and E. F. Shrader, Nucl. Instr. and Meth. 85 (1970) 151.

[2] W. W. Lindstrom, unpublished Ph.D. dissertation, CWRU (1970).

polarization results. Measurements of cross sections in this energy region have been reported[1] but not at the exact energies and angles appropriate for the desired analysis.

The necessary equipment including an oxygen gas target chamber and neutron detection system has been assembled and the measurements are expected to be made in the very near future.

3. Polarization of Neutrons from the $^{16}O(d,n)^{17}F$ Reaction (B. D. Anderson, D. E. Velkley, R. C. Nerbun, Jr., and H. B. Willard)

Experimental data have been taken to determine the polarization of neutrons from the $^{16}O(d,n)^{17}F$ reaction. Asymmetries in the scattering by helium of the ground and first excited state neutron groups have been measured for a deuteron energy range of 3 to 4 MeV. Three angular distributions and one excitation function have been measured in this region. The experimental apparatus used has been described previously.

As in previous $^{13}C(d,n)$ neutron polarization measurements performed at this laboratory, the data were stored in a two-dimensional array. The first dimension was time-of-flight (TOF) from the target to a He-Xe cell and the second dimension was the pulse height output of the He-Xe cell derived from the alpha recoils produced by the neutrons scattered into side detectors. Periodic checks for false asymmetries were performed throughout the data taking and were considered to be satisfactory in all cases.

An existing program to determine effective average analyzing power has been modified to take into account a change in the side detector scintillators from NE-213 to NE-102. This modification consists of an improved calculation of the absolute neutron detection efficiencies and was aided by comparison with the results of a Monte-Carlo code which simulates events in a proton-recoil neutron detector.

---

[1] Dietzsch, et al., Nuclear Physics A114 (1968) 330. Bahnsen, et al. Phys. Rev. C2 (1970) 859.

It is expected that polarizations will be determined late this fall. A DWBA analysis with the program DWUCK[1] is in preliminary stages.

4. Detector Efficiency Measurements and Calculations
(W. W. Lindstrom, B. D. Anderson, and E. F. Shrader)

Relative neutron detection efficiencies of cylinders of NE-102 and NE-213 uniformly illuminated perpendicular to their axes have been measured. The $T(p,n)^3He$ reaction was the source of neutrons.[2] Data were obtained for both scintillators simultaneously with the same target filling of tritium gas, thus determining the relative ratios of NE-102 and NE-213 detection efficiencies consistently. Data were obtained using time-of-flight techniques with a discriminator bias to reject all events producing a linear output from the detector smaller than a minimum pulse height.

A published proton recoil detector efficiency code[3] has been modified to include the effects of C(n,n) angular distribution and scintillator photomultiplier resolution. New data for recoil-proton light output of Smith _et al._[4] were used. Carbon recoil pulse heights were obtained by extrapolation of data of Steuer and Wenzel.[5] This code was used to fit the observed data described above. The scale factor for the experimental data and the program parameter of "average photoelectrons per light unit" were varied until the rapid rise near "cutoff" was reproduced for the NE-213 data. The NE-102 data were then reproduced by changing the scintillator density, the H/C ratio, and the relative light output curves in the code. The scale factor was not changed. The results for NE-102 are shown below.

---

[1] P. D. Kunz, University of Colorado.

[2] G. A. Jarvis, A. Hemmendinger, H. V. Argo and R. F. Taschek, Phys. Rev. _79_ (1950) 929-935.

[3] B. Gustafsson and O. Aspelund, Nucl. Instr. and Meth. _48_ (1967) 77-86.

[4] D. L. Smith, R. G. Polk, and T. G. Miller, Nucl. Instr. and Meth. _64_ (1968) 157-166.

[5] M. F. Steuer and B. E. Wenzel, Nucl. Instr. and Meth. _33_ (1965) 131-135.

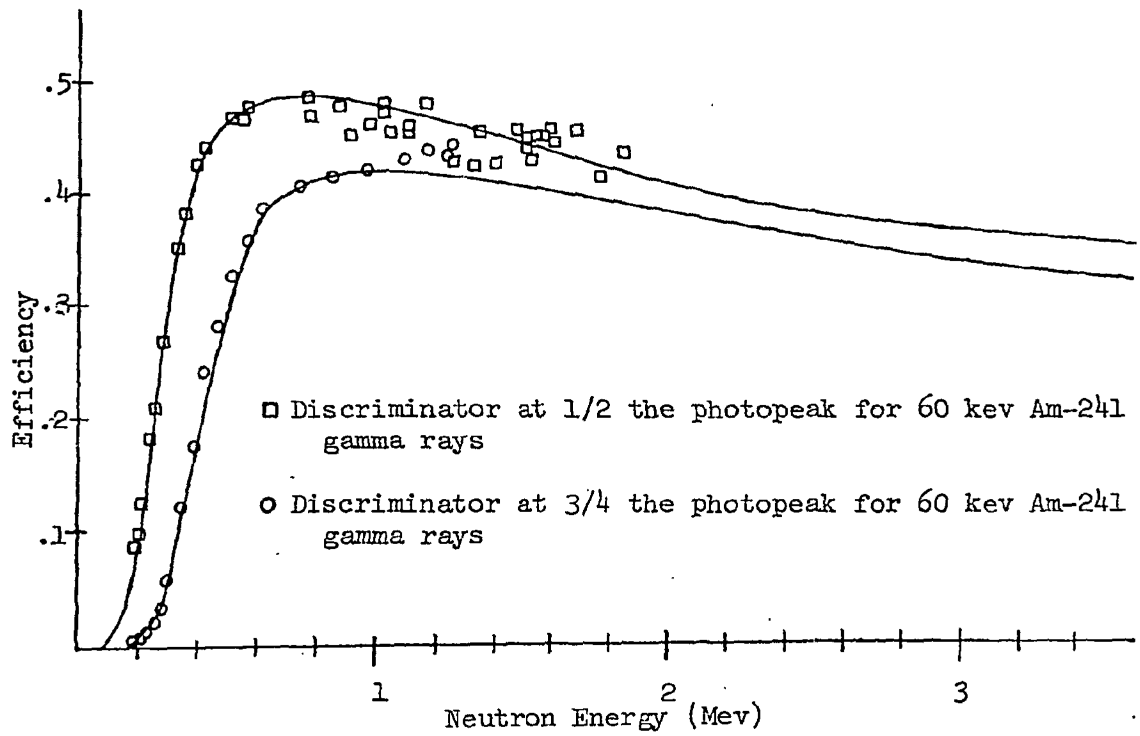

This figure shows the comparison of measured relative efficiency (data points) and calculated absolute efficiency (solid lines) for a 5.08 cm dia. x 5.08 cm high cylinder. The agreement of the code with the observed data is seen to be excellent. The accurate simulation of efficiencies for different scintillators and different discriminator biases indicates that most of the major physical processes are being handled correctly.

5. Cross Section Measurements of the (^3He,n) Reaction
(S. K. Bose, A. Kogan, and P. R. Bevington)

An investigation of the cross sections for (^3He,n) reactions for target nuclei in the s-d shell region is in progress. Almost all modifications to existing apparatus necessary for these measurements have been completed. Measurements of $^{20}Ne(^3He,n)$ cross sections are scheduled to begin in February, 1971.

A liquid NE-213 bubble-free scintillator 5 in. in diameter and 3 in. long has been obtained which is larger than that used in preliminary measurements and is expected to increase the counting rate by nearly an order of magnitude. The complete assembly of scintillator, photomultiplier tube, and electronics is being constructed with low mass and with considerable attention to optimizing scintillator response.

For timing with double charged $^3He^{++}$ ions at energies above 4 MeV, a pick-up loop to synchronize external bunching of the beam with internal burst times has been installed ahead of the energy-stabilizing magnet; it takes advantage of the higher current of the single charged $^3He^+$ ions in the beam before they are separated out by the magnet.

One of the experimental problems encountered in preliminary measurements of (^{3}He,n) cross sections was that of carbon contamination of the target system, including apertures and target backings. Various methods of cleaning Ta were evaluated, using the ^{12}C(d,n) yield to determine the level of contamination. Best results were achieved by dipping the Ta into a mixture of nitric, sulfuric, and hydrofluoric acids in the proportion 9:24:8 for about fifteen seconds. Apertures in the gas target have been cleaned and enlarged to reduce contributions from carbon in (^{3}He,n) spectra.

6. <u>Polarization of Neutrons from (^{3}He,n) Reactions</u>
(R. C. Nerbun, Jr., V. B. Burke, and P. R. Bevington)

A thorough study was undertaken of s-d shell nuclei as targets for diproton stripping via (^{3}He,n) reactions. Simulated time-of-flight (TOF) spectra were observed on the oscilloscope of the CWRUNCH computer calculated by the program RATE (Reaction Analyzer for Time-of-Flight vs. Energy). The reaction ^{20}Ne(^{3}He,n)^{22}Mg was found to have well resolved neutron groups. Preliminary work is now under way to measure the neutron polarization for this reaction.

7. <u>Study of the (^{4}He,^{6}He) Reaction on s-d Shell Nuclei</u>
(J. Arnold* and H. B. Willard)

The (^{4}He,^{6}He) reaction on s-d shell nuclei was investigated by measuring the energy spectra of ^{6}He nuclei emitted after bombardment of various targets by alpha particles. Targets of ^{18}O, ^{22}Ne, and ^{26}Mg were bombarded with the 42 MeV alpha particle beam from the 60-inch fixed-energy cyclotron of the Lewis Research Center of NASA[1]. Energy spectra were measured over the angular range of 15° to 70° in steps of 2.5° using a particle-identifier system containing four detectors. Cross sections accurate to about 10% were extracted from the data with the help of an interactive display program written for the CWRUNCH computer.

---

*Presently at Lewis Research Center, NASA, Cleveland, Ohio

[1] Work supported in part by the National Aeronautics and Space Administration; research conducted in part under the direction of R. Bercaw, Lewis Research Center, NASA.

Angular distributions for half of the energy groups detected appear quite smooth, varying by only about one order of magnitude over the angular range studied, while the rest of the angular distributions are quite oscillatory in nature, with very pronounced minima. In general, those for the excited states tend to have less structure. The average magnitude of all cross sections for states in the same nucleus are approximately the same. That is, no one state is excited preferentially over the angular range studied, and in particular the ground state cross section is of the same order of magnitude as that of the first several excited states, which is not the case for (p,t) stripping reactions. This difference may be attributable to the effects of inelastic scattering in the entrance and exit channels, or the structure of the neutron pair in the outgoing particle.

DWBA predictions were calculated for two-neutron pickup on ^{18}O using a computer code[1] for zero-range approximation and one-particle transfer, modified by the inclusion of a form factor describing the nuclear structure information. Given a Woods-Saxon potential which reproduces the single-particle levels in ^{17}O, a set of two-particle states were found, and the residual interaction (of Yukawa form) was diagonalized in this set of states. Optical potential parameters for ^{6}He were extrapolated from data for elastic scattering of ^{6}Li, but the resulting ^{6}He-^{16}O potential, which is the least reliable potential used in the calculations, appears to have the most influence on the calculated angular distributions.

DWBA predictions for the $^{18}O(^{4}He,^{6}He)^{16}O$ reaction could not even reproduce qualitatively the main features of the experimental data, even with considerable freedom in choice of the ^{6}He parameters, although this 0^{+} - 0^{+} transition should be the simplest to describe. Possible reasons for the discrepancy include: 1) finite-range effects may be important for two-nucleon transfer; 2) correlations of the transferred neutrons with the alpha particle may be important; 3) shell model continuum states included in the calculation of two-particle form factors may significantly alter their shape in the region extending outward from the nuclear surface; and 4) there may be a sizable compound nuclear contribution to the reaction.

A Ph.D. dissertation[2] describing the work has been accepted by the university.

---

[1] W. R. Gibbs, V. A. Madsen, J. A. Miller, W. Tobocman, E. C. Cox, and C. Mowry, unpublished NASA Technical Note No. D-2170 (1964).

[2] J. Arnold, unpublished Ph.D. dissertation, CWRU (1970).

COLUMBIA UNIVERSITY

A. FAST NEUTRON SPECTROSCOPY

Total Cross Section of O^{16} at 2.362 Mev. (J. Kalyna, Ivor Taylor L. J. Lidofsky)

The experiment has been completed and a first analysis of all data completed. After making corrections for known effects (in scattering, isotopic composition of sample, sample holder, 2nd energy group, etc.) the resultant cross sections for O^{16} for the minimum of the 2.362 Mev dip lie between 60 and 80 mb. The final analysis is nearly complete and a paper is being prepared for publication. Our present best value for the cross section at the minimum is 70±15 mb.- for O^{16} and 80±15 mb for normal oxygen.

B. SLOW NEUTRON PHYSICS

1. Neutron Resonance Cross Section Measurements (H. Camarda, G. Hacken, F. Rahn, H.I. Liou, S. Wynchank, M. Slagowitz, W.W. Havens, Jr., and J. Rainwater)

a. New Data

The 1970 neutron spectrometer run produced a large amount of new data for both natural samples and separated isotopes. The first part of the run used 3" x 4" iron as a reference sample. The iron reference sample has large sharp structure features which can be used to give the transmission of other samples in the energy region of the iron structure without need of further normalization.
Other reference samples used were 1/2" Co and 1/2" Cu.
This made it possible to determine the transmission of various samples under investigation at places where the cross section was not rapidly varying and provided systematic information for later use in data normalization and background corrections. Also it was possible to run 0.1" Ta as a reference sample with D-only samples to get T values at the Ta resonance for the sample in 40 meter runs.

The natural samples studied were F, Na, Mg, Al, S, Au, Ne, Se, K, Cl, Cd, and Tl. Highly enriched samples obtained from ORNL of the following separated isotopes were run U^{238}, Th^{232}, $Cd^{110,112,114,116}$, Ce^{140}, $Gd^{158,160}$, $Dy^{160,161,162,163,164}$, $Tl^{203,205}$, Np^{237}, and Rh^{103}. Many new resonances were observed, especially in the separated isotopes, and the data obtained are analyzed for the resonance parameters to higher energies than previously reported. The data were obtained by a new time of flight system, capable of 16,000 channels, operating in conjunction with the on-line EMR-6130 computer. The best resolution obtained was .1 n sec/meter at the 200 meter station and .5 n sec/meter at the 40 meter station. A display scope was used to study portions of the histogram during data taking, in order to insure the proper functioning of experimental equipment and to allow planning of the experiment as the data were received.

At present, the Nevis synchrocyclotron is under modification. The machine is being converted to a three-fold symmetry spiral sector focusing AVF synchrocyclotron, with a long duty factor 550 MeV beam. The time averaged external beam intensity will increase to between 5 and 40 μa. The modification program is scheduled for completion late in 1971.

b. Analysis of Results

During 1970 much work was done in completing the analysis of results obtained from the 1968 run, especially for isotopes in the mass region $140 \leq A \leq 186$. This region is especially interesting in that it corresponds to a maximum in S_0 and it is expected to have a minimum in S_1. There are many even-even I = 0 nuclei having strong resonances suitably spaced for observation of essentially all resonances over a large energy range. From this is obtained a large sample size of single population $\ell = 0$ resonances, with few $\ell = 1$ resonances. We have found an especially clean test case to be Er^{166}.

The new results are summarized in Table I, which shows the energy interval investigated for each isotope and the number of analyzed resonances. The $\langle D \rangle$ values are generally best estimates for the $\ell = 0$ population. The $\ell = 0$ strength, S_0, is not sensitive to missing weak levels, so a larger range can be used for it than for detailed statistical tests where one would like to include all $\ell = 0$ resonances.

Table II lists the $g\Gamma_n^0$ values for In^{115} and Table III gives information for cases in which Γ_γ and some spin values J were obtained in the isotopes $Er^{166,168}$, $Yb^{171,172,174,176}$, $Eu^{151,153}$, $Sm^{152,154}$, and In^{115}. The infinite dilution capture integrals for $Eu^{151,153}$, $Sm^{152,154}$, $Er^{166,167,168}$, and $Yb^{171,172,174}$ are presented in Table IV.[1] Table V lists values of Γ_n^0 for the tungsten isotopes $W^{182,184,186}$.

---

[1]Resonance Capture Integrals of $Er^{166,167,168}$ and $Yb^{171,172,174}$, H. Liou et.al., American Nuclear Society Summer Meeting, 1970.

DATA NOT FOR QUOTATION

For nearest neighbor level spacings, the Wigner distribution is expected to apply. This predicts the distribution of level spacings near the mean, but does not predict the covariance of a given nearest level spacing and adjacent, or further removed spacings. Thus the Wigner function inplies a variance of $n\pi/4$ in n if n levels are observed in an energy interval ΔE. By treating random matrices, it has been shown by Porter, Rosenzweig, Gunson, Kahn, Garrison, and others that the covariance of neighboring level spacings should be about (-0.25), which implies a longer range ordering of level spacings.

Dyson and Dyson and Mehta[2] formulated a test in which a prediction was made as to the expected mean square deviation between observed level number N(E), for $\leq$E and a best fit straight line

$$\Delta = \min_{A,B} \; 1/E \int_0^E [N(E) - AE - B]^2 \, dE$$

Dyson and Mehta obtained the predicted results for large n

$$<n> \approx n$$
$$V_n = 0.2026 \; (\ln \; n + 2.181)$$
$$<\Delta> = 1/\pi^2 \; (\ln \; n - 0.0687)$$
$$V_\Delta = 1.1690/\pi^4$$

where V is the variance. The small value of $<\Delta>$ for large n increasing only as ($\ln$ n) implies an almost crystal lattice long range ordering of level positions.

For the Er^{166} isotope, with 109 observed levels up to E=4200 eV., the observed histogram of the number of levels N seen up to an energy E (vs. E) gives an excellent ladder for a match with Dyson-Mehta long range order. (Δ_{exp} = 0.4545 compared with a predicted value of Dyson = 0.4684). It was found that the quantity [C_{OV} + Δ] where C_{OV} is the covariance(S_j, S_{j+1}) is a more sensitive quantity for testing the theory. For an uncorrelated sequence of Wigner distributed spacings, the expected $C_{OV} = 0.0 \pm \sqrt{1/m}$ where m is the number of adjacent spacing pairs. For Er^{166}, the experimental C_{OV} was -0.22 and the observed (C_{OV} + Δ) was 0.2345.
The probability of achieving less than this observed (C_{OV} + Δ) with an uncorrelated Wigner distribution is 0.00055. Other test cases in the rare earth region are being completed.

---

[2] J. Math. Phys. 4, 701 and 713 (1963).

DATA NOT FOR QUOTATION

Preliminary processing of the $Dy^{160,161,162,163,164}$ isotopes has been completed. The total cross section and resonance parameters are in the final stages of evaluation. The energy range covered for the parameter evaluation is greater by a factor of ten than for previously available information and extends to greater than 3 kev. Measurements of the total neutron cross sections of U^{238} and Th^{232} have been completed. These isotopes have been investigated in far greater detail than before, with a considerable amount of 1970 running time being devoted to obtaining a complete set of transmission, and self-indication measurements. In view of the interest in the Γ_γ values of these isotopes, these measurements were combined with capture measurements to determine as accurately as possible the value Γ_γ in as many resonances as possible and its fluctuation from resonance to resonance.

2. <u>Radiative Capture Cross Section Measurements in the Low KeV. Region</u> (F. Rahn, J. Rainwater, C. Ho, E. Melkonian, J. Arbo, J. Felvinci, and W. W. Havens, Jr.)

The latest series of experiments at the Nevis neutron velocity spectrometer obtained capture cross section data for the isotopes U^{238}, Th^{232}, Rh^{103}, Tm^{169}, Gd^{158}, and Dy^{161}. These data were of high quality, with a good signal to noise ratio. The $\Gamma(n,\gamma)$ of Th^{232} was successfully measured despite the high gamma background from the Th^{228} decay product. In addition to the above isotopes, an extensive amount of running time was used on B^{10}, C, and Au^{197} samples in order to determine accurately open beam and background spectra, and, in the case of Au^{197}, to establish the "saturated open" beam times the detector efficiency at a given neutron energy. This energy dependent count rate, which would result from the total capture of all the neutrons in the sample, is determined by looking at the resonances in Au^{197} for which the resonance parameters are accurately known. The running of the sample of interest simultaneously with the Au^{197} samples gives the relative normalization for this sample. As a cross check, a saturated open can be determined by assuming an average $\langle\Gamma_\gamma\rangle$ for the sample being studied, and by relying on previously obtained values of $g\Gamma_n$. As a further check, this is compared with peaks corrected for multiple scattering which have been saturated in various sample thicknesses.

The calibration of detection efficiency <u>vs</u> gamma ray energy for the Moxon-Rae detectors is still being refined. Previously reported measurements made on a single detector unit showed efficiency to be linear with gamma energy from 0.5 to 4 MeV. A calibration point taken with the single detectors at 7.367 MeV using a Pb-207 target in a thermal

TABLE I (1968 Measurements)

Partial Summary of Information Obtained from Analyses

Isotope	Energy Interval (keV)	No. Of Levels	<D> (eV)	10^4 S_o	10^4 S_1
Er^{166}	0-9.5	174	38.3*	1.70±0.24	-
Er^{167}	0-1.7	268	4.10*	1.89±0.22	-
Er^{168}	0-15.0	107	95.6*	1.50±0.25	0.9±0.3
Er^{170}	0-24.0	94	152*	1.44±0.25	1.4±0.4
Yb^{168}	0-1.0	6	-	-	-
Yb^{170}	0-1.3	20	-	-	-
Yb^{171}	0-1.7	165	6.3*	1.86±0.24	-
Yb^{172}	0-10.1	95	64.7*	1.48±0.24	-
Yb^{174}	0-25.0	95	180*	1.36±0.24	-
Yb^{176}	0-26.2	77	196*	1.90±0.37	-
W^{182}	0 ~ 13	141	66.4*	2.42±0.29	-
W^{184}	0 ~ 15	125	94.8*	2.37±0.30	-
W^{186}	0 ~ 17	102	123.0*	2.22±0.29	-
Eu^{151}	0-0.0986	88	1.04	3.25±0.51	
Eu^{153}	0-0.0976	68	1.45	2.42±0.47	
Sm^{152}	0-1.501	29	52.5	2.72±0.83	
Sm^{154}	0-2.492	20	125.	1.90±0.66	
Lu^{175}	0-1.20	214	5.6	1.36±0.32	
Gd^{154}	0-3.20	344	9.2		
Gd^{158}	0.016-3.00	41	71.0		
In^{113}	0-2.0	48	~11 *	0.28±0.06	
In^{115}	0.022-1.98	145	10.7*	0.24±0.04	
La^{139}	0.60-10.23	66	148	0.67±0.12	

* Best evaluation for ℓ=0 population including comparison with Wigner and Porter-Thomas distributions.

TABLE II

Resonance Parameters Γ_n^o Values for In^{115}

E	ΔE	$g\Gamma_n$	$\Delta g\Gamma_n$	E	ΔE	$g\Gamma_n$	$\Delta g\Gamma_n$
22.733	0.012	0.51	0.020	551.10	0.35	0.84	0.05
26.777	0.015	0.005	0.001	562.61	0.36	0.47	0.04
39.599	0.027	2.1	0.1	571.86	0.37	17.8	1.0
46.363	0.035	0.125	0.005	580.19	0.38	4.0	0.2
48.142	0.037	0.25	0.05	582.87	0.38	2.5	0.1
62.976	0.027	0.37	0.05	589.09	0.39	3.3	0.1
69.491	0.032	0.20	0.05	602.22	0.40	1.04	0.21
80.874	0.04	0.75	0.05	609.99	0.41	0.42	0.03
83.276	0.042	3.3	0.4	614.13	0.42	18.8	1.0
94.341	0.05	1.45	0.15	619.59	0.42	8.36	0.52
120.71	0.073	0.004	0.002	643.93	0.45	2.4	0.1
125.89	0.077	1.9	0.1	654.81	0.46	4.5	0.1
132.81	0.084	2.7	0.5	674.03	0.48	5.64	0.11
138.88	0.090	0.011	0.003	683.23	0.49	1.6	0.1
150.29	0.10	2.3	0.1	694.62	0.50	2.1	0.1
164.67	0.12	9.0	0.5	704.75	0.51	1.15	0.10
168.08	0.12	1.05	0.05	707.83	0.52	2.9	0.5
177.92	0.13	1.5	0.3	719.85	0.53	1.57	0.1
186.955	0.14	10.	1.	727.84	0.54	1.67	0.1
205.60	0.16	11.5	3.	733.25	0.54	6.17	0.1
224.03	0.18	16.	3.	752.66	0.57	1.15	0.1
226.81	0.19	0.66	0.40	769.91	0.59	1.67	0.1
250.17	0.22	30.	2.	774.02	0.59	10.5	1.0
266.955	0.12	2.	0.1	783.54	0.60	7.94	0.21
288.88	0.13	10.	1.	785.35	0.60	0.92	0.02
294.34	0.14	22.	5.	789.58	0.61	8.36	0.52
319.49	0.16	7.5	0.5	815.73	0.64	1.67	0.31
339.795	0.17	0.95	0.05	819.41	0.32	4.2	0.5
354.13	0.18	3.1	1.0	829.79	0.33	5.4	0.3
362.10	0.19	5.4	0.2	836.70	0.33	8.9	0.3
370.94	0.20	3.4	0.2	853.52	0.34	29.3	2.1
379.095	0.20	0.31	0.05	861.08	0.35	11.5	2.1
384.20	0.21	2.9	0.3	863.85	0.35	9.4	2.1
402.345	0.22	15.6	3.1	875.09	0.35	3.45	0.21
411.56	0.23	15.7	3.1	891.62	0.37	7.94	0.21
423.00	0.24	5.2	0.5	898.96	0.37	1.78	0.21
437.16	0.25	0.52	0.05	913.90	0.38	6.9	0.3
448.90	0.26	6.3	1.0	923.43	0.38	3.1	0.7
453.89	0.27	10.4	2.1	948.12	0.40	26.1	1.0
456.82	0.27	9.6	1.0	956.57	0.40	15.7	1.0
469.65	0.28	2.7	0.3	977.99	0.42	18.3	1.0
477.55	0.29	1.6	0.1	997.97	0.43	16.7	1.0
498.20	0.30	1.46	0.11	1035.7	0.46	3.45	0.52
503.73	0.31	12.5	2.1	1043.0	0.46	26.1	2.1
511.56	0.32	0.89	0.11	1049.1	0.46	2.6	0.3
515.38	0.32	1.67	0.10	1060.3	0.47	6.5	0.3
525.46	0.33	7.1	1.0	1075.1	0.48	17.7	2.1
530.11	0.33	0.47	0.05	1085.8	0.49	16.7	1.0
544.78	0.35	1.88	0.10	1111.7	0.51	6.6	0.3
547.92	0.35	2.7	0.1	1140.2	0.53	9.61	0.42

DATA NOT FOR QUOTATION

TABLE II (Continued)

E	ΔE	$g\Gamma_n$	$\Delta g\Gamma_n$
1170.3	0.55	8.36	1.05
1179.7	0.56	9.6	0.3
1190.8	0.56	1.67	0.21
1213.1	0.58	24.0	3.1
1224.2	0.59	19.9	2.1
1230.0	0.59	2.51	0.21
1243.1	0.60	10.5	1.
1281.2	0.63	8.26	0.31
1309.3	0.65	7.12	0.31
1325.0	0.66	5.7	2.1
1330.9	0.66	6.5	0.4
1334.3	0.67	3.97	0.31
1342.3	0.67	4.08	0.31
1349.8	0.68	14.6	2.1
1357.9	0.69	3.7	0.3
1389.3	0.71	5.1	0.42
1397.9	0.72	6.5	0.5
1402.2	0.72	3.66	0.21
1415.9	0.73	12.5	1.
1448.6	0.76	1.57	0.31
1468.4	0.77	14.6	2.1
1480.0	0.78	3.4	0.3
1520.6	0.81	22.0	1.0
1546.1	0.83	13.6	1.0
1567.1	0.85	10.5	1.0
1595.5	0.87	15.7	1.
1614.0	0.89	18.8	2.1
1619.3	0.89	94.1	10.5
1640.9	0.91	23.0	1.
1664.8	0.93	78.4	3.
1679.8	0.94	7.1	0.21
1688.4	0.95	83.6	1.0
1711.4	0.97	29.3	3.1
1724.1	0.98	4.5	0.21
1735.9	0.99	36.6	5.2
1780.3	1.0	2.6	0.2
1796.8	1.0	19.9	1.0
1854.5	1.1	27.2	3.1
1865.5	1.1	6.8	0.5
1891.1	1.1	64.8	3.1
1918.5	1.1	17.8	3.1
1946.4	1.2	16.7	1.0
1959.4	1.2	15.7	1.0
1967.7	1.2	8.4	2.1
1980.9	1.2	20.9	3.4

TABLE III

Resonance Levels for which Γ_γ is also evaluated

E(eV)	$g\Gamma_n$(MeV)	$\Delta\Gamma_n$(MeV)	Γ_γ(MeV)	$\Delta\Gamma_\gamma$(MeV)	
Er^{166}					
15.56	2.2	0.2	88	10	
73.79	62	4	82	16	
81.74	10	0.5	85	10	
154.15	7.0	0.4	88	12	
243.59	30	3	110	25	
301.15	195	15	100	18	
315.70	360	30	95	20	
352.23	91	7	90	15	
Er^{168}					
79.70	38	2	82	15	
188.94	78	4	87	12	
Yb^{171}					
7.91	1.7	0.1	75	10	
13.04	2.5	0.2	82	10	
28.13	1.8	0.1	79	10	
34.54	3.6	0.2	84	8	(J=0)
41.36	7.6	0.3	64	10	(J=0)
52.87	5.0	0.2	77	14	(J=1)
54.07	15.5	1.0	75	12	(J=1)
60.09	4.2	0.2	78	10	(J=0)
64.70	7.1	0.2	80	12	(J=1)
76.94	9.6	0.7	71	12	(J=1)
96.05	2.8	0.2	74	15	(J=0)
107.61	37	2	80	12	(J=1)
112.10	16.0	1.5	85	14	(J=0)
127.57	15.	1.	70	14	(J=1)
145.90	7.3	0.3	60	18	(J=1)
160.41	63	5	80	14	(J=1)
164.61	39	2	70	10	(J=1)
175.61	11	1	68	15	(J=1)
226.81	21	2	74	10	(J=1)
250.06	24	3	82	12	(J=1)
255.26	28.5	4.0	95	20	(J=1)
287.49	17.2	2	79	20	(J=1)
290.58	82	6	86	20	(J=1)
302.32	20.3	3.0	58	18	(J=1)
310.10	32	4	84	15	(J=0)
341.61	15	3	80	20	(J=0)
354.41	165	25	82	14	(J=1)
387.21	125	15	100	25	(J=0)

TABLE III
(Continued)

434.56	42.	5	90	25	(J=0)
444.78	61	7	78	14	(J=1)
470.78	30	3	67	12	(J=1)
483.62	23	3	60	15	(J=1)
499.12	83	9	76	20	(J=1)
512.86	93	10	80	20	(J=1)
524.80	63	7	75	18	(J=1)
538.90	239	30	74	15	(J=0)
577.74	43	5	67	15	(J=1)
598.23	31	5	88	25	(J=1)
603.88	67	9	72	22	(J=1)
612.50	43	5	66	20	(J=1)
628.58	62	8	85	22	(J=1)
Yb^{172}					
139.82	130	8	64	15	
180.28	215	14	72	20	
201.48	12.5	0.9	90	18	
508.72	240	15	60	20	
Yb^{174}					
342.98	450	30	80	20	
585.42	105	10	72	18	
880.23	420	30	88	20	
Yb^{176}					
148.45	8.6	0.7	82	15	
In^{115}					
22.733	0.51	0.02	81	5	
39.599	2.1	0.1	76	5	
48.142	0.25	0.05	90	5	
62.976	0.37	0.05	95	10	
80.874	0.75	0.05	70	10	
83.276	3.3	0.4	73	5	
94.341	1.45	0.15	90	10	
125.89	1.9	0.1	65	20	
132.81	2.7	0.5	180	50	
150.29	2.3	0.1	85	10	
164.67	9.0	0.5	82	10	
177.92	1.5	0.3	80	20	
186.955	10.	1.	100	20	
224.03	16.	3.	60	15	
250.17	30.	2.	85	10	

DATA NOT FOR QUOTATION

TABLE III
(Continued)

Eu^{151}

2.715	0.13	0.02	97	5
3.362	0.45	0.1	97	6
3.707	0.40	0.05	89	6
5.382	0.095	0.01	108	12
5.984	0.16	0.02	100	15
7.291	1.10	0.15	88	12
7.443	0.85	0.15	85	9
9.072	0.53	0.05	104	12
10.47	1.05	0.10	91	9
10.94	0.32	0.03	98	11
12.23	0.47	0.04	88	9
12.64	1.20	0.10	88	7
13.66	0.22	0.04	115	12
14.76	0.96	0.04	76	9
15.18	1.00	0.10	79	9
17.75	0.69	0.04	104	11
19.10	2.6	0.2	133	19
21.69	0.97	0.08	82	12
22.21	1.40	0.18	66	15
22.75	0.74	0.05	89	9
24.58	4.2	0.3	99	10
25.60	0.25	0.08	89	17
26.72	3.5	0.3	78	10
27.43	0.32	0.03	97	8
28.09	0.15	0.04	90	15
29.23	2.25	0.15	79	11
30.22	1.80	0.15	86	6
30.81	0.33	0.05	99	14
31.59	0.87	0.05	97	7
35.05	1.6	0.2	90	8
36.09	2.5	0.2	78	8
37.01	2.8	0.2	78	9
37.78	1.70	0.15	92	7
39.23	2.9	0.2	98	10
39.94	0.62	0.3	79	9
41.35	13.5	1.5	80	13
43.19	2.8	0.2	84	9
44.43	1.8	0.2	89	8
45.42	0.70	0.15	99	18
46.41	5.2	1.5	85	19
47.04	8.5	1.0	99	12
50.58	11.5	1.0	102	11
52.41	5.0	0.4	112	15
53.94	2.25	0.15	88	10
55.26	1.90	0.15	96	9
56.18	1.75	0.15	98	9
57.36	9.5	0.8	83	9
58.85	3.2	0.3	108	11
60.85	2.9	0.3	96	9
62.41	2.0	0.2	86	8
63.19	1.25	0.20	100	11
67.91	9.0	0.4	100	10
70.75	2.3	0.3	78	10

TABLE III
(Continued)

71.41	3.0	0.3	84	10
72.41	1.1	0.2	93	11
75.76	2.1	0.3	90	11
77.45	4.4	0.3	99	10
78.66	8.5	0.8	73	9
79.51	2.8	0.4	64	13
80.29	4.1	0.5	81	10
81.08	12.	1.	101	13
83.07	1.6	0.2	95	11
84.00	7.4	0.4	99	12
85.67	2.4	0.3	84	18
89.34	7.3	0.4	104	13
90.18	2.5	0.3	85	14
91.13	2.4	0.3	94	11
93.36	14.	1.	112	13
96.29	9.2	1.0	112	13
98.61	7.7	0.5	108	13
Eu^{153}				
1.73	0.030	0.003	91	9
3.94	0.53	0.03	94	5
6.16	0.32	0.03	109	10
8.85	1.7	0.15	114	11
11.61	2.2	0.2	96	10
12.45	0.08	0.003	90	25
16.73	0.70	0.15	89	15
18.01	2.5	0.2	92	15
18.73	1.5	0.2	100	11
20.02	4.7	0.3	101	16
22.54	1.4	0.2	84	12
23.66	1.3	0.2	86	12
28.63	0.90	0.05	79	15
31.21	1.15	0.1	118	13
34.53	2.6	0.3	90	12
36.62	2.1	0.3	106	14
37.76	2.2	0.3	94	12
38.30	3.0	0.2	81	11
41.15	0.73	0.04	69	20
42.15	2.4	0.3	77	14
43.16	1.6	0.2	96	9
45.79	0.70	0.10	99	15
47.11	1.05	0.10	94	11
49.30	0.27	0.05	89	8
50.00	1.45	0.15	92	8
50.74	3.7	0.3	113	14
52.31	6.1	0.4	108	15
53.07	1.4	0.2		
55.19	0.13	0.05	95	20
58.97	0.58	0.1	85	9
59.72	1.40	0.15	102	15
60.92	16.	1.	78	14
62.55	2.6	0.3	105	13
63.70	3.7	0.4	93	20
64.09	7.0	0.5	116	15

DATA NOT FOR QUOTATION

TABLE III
(Continued)

66.94	1.9	0.3	86	17
68.15	2.6	0.3	87	12
70.04	1.5	0.2	100	14
76.93	7.2	0.3	105	13
80.29	2.4	0.3	103	19
81.24	2.0	0.3	96	14
82.99	1.8	0.3	86	9
86.99	6.2	0.3	68	8
87.70	2.4	0.2	105	16
90.75	2.1	0.2	79	13
93.26	25.	2.	105	25
97.60	13.	3.	101	15
Sm^{152}				
8.06	130*	5*	60	11
87.70	205	18	65	25
154.1	142	18	93	23
185.2	19	2	51	10
385.1	40	6	45	9
415.8	57	5	58	10
587.1	159	16	81	24
792.5	115	8	60	14
1314.4	245	20	73	25

*BNL-325 value assumed in analysis

Sm^{154}				
341.5	15	3	65	15
457.3	160	20	90	25
1181.5	72	4	83	23

TABLE IV
RESONANCE CAPTURE INTEGRALS

ISOTOPE	$I_c^{0.414}$	$I_c^{0.55}$	I_c comparison
Eu^{151}	6559±687	3300±350	3741[1]
Eu^{153}	2332±205	2198±175	1833[1]
Sm^{152}	2644±604	2635±541	3100[2],3163[3],2850[4]
Sm^{154}	54±14	50±14	----
Er^{166}	123±13	122±13	56.5±11.3[6]
Er^{167}	4899±605	2524±308	----
Er^{168}	36±7	35±7	----
Yb^{171}	345±39	343±39	313[5]
Yb^{172}	26±6	26±6	23[5],18±7[6]
Yb^{174}	27±6	25±6	33.8[5]

TABLE V

Resonance Parameters W^{182}

E(ev)	ΔE	Γ_n^o	$\Delta\Gamma_n^o$	E(ev)	ΔE	Γ_n^o	$\Delta\Gamma_n^o$
21.03	.06	7.85	1.09	3494.	1.4	28.93	2.54
114.4	.13	22.91	2.81	3523.	1.5	8.59	1.01
212.8	.18	.17	.034	3564.	1.5	7.20	.67
248.0	.22	57.15	3.81	3602.	1.5	20.83	2.50
341.6	.35	.314	.054	3786.	1.6	1.54	.33
376.2	.40	7.42	1.03	3846.	1.7	74.17	9.68
428.5	.25	12.08	1.21	3879.	1.7	31.31	4.01
484.2	.30	20.00	1.82	3975.	1.7	26.57	3.17
578.2	.39	11.23	1.04	3996.	1.7	4.59	.79
655.2	.46	5.16	.78	4062.	1.8	17.89	2.75
759.4	.58	3.52	.73	4212.	1.9	4.47	.46
781.7	.60	.329	.089	4266.	1.9	3.22	.46
862.8	.34	.14	.051	4313.	2.0	30.45	3.06
918.8	.38	11.38	1.32	4367.	2.0	1.29	.30
947.3	.40	64.98	6.50	4431.	2.0	43.81	3.76
1007.	0.4	16.07	1.58	4492.	2.0	6.57	.75
1095.	0.5	43.67	6.04	4715.	2.2	13.84	1.46
1161.	0.6	14.21	.73	4832.	2.3	43.16	5.04
1275.	0.6	1.09	.17	4846.	2.3	2.20	.50
1287.	0.7	2.51	.56	4911.	2.4	19.41	2.85
1326.	0.7	.69	.22	4961.	2.4	5.40	.71
1408.	0.7	3.47	.80	5138.	2.5	15.53	2.09
1502.	0.8	11.35	.77	5199.	2.6	72.40	5.55
1514.	0.8	10.54	1.54	5435.	2.8	85.46	8.14
1582.	0.9	1.96	.38	5538.	2.9	7.73	2.02
1646.	0.9	1.53	.37	5563.	2.9	9.39	1.34
1772.	0.5	71.23	5.94	5656.	3.0	186.15	26.59
1793.	0.5	5.90	.95	5884.	3.1	5.02	1.30
1921.	2.0			6019.	3.2	3.09	1.29
2006.	0.6	31.82	3.35	6189.	3.4	57.84	5.09
2061.	0.7	29.19	3.30	6259.	3.4	32.74	3.79
2104.	0.7	6.89	.55	6404.	3.5	47.49	5.00
2180.	0.7	12.74	1.07	6514.	3.6	11.26	1.86
2226.	0.7	16.96	1.70	6536.	3.6	23.38	2.47
2328.	0.8	11.67	1.24	6605.	3.7	4.68	.98
2384.	0.8	18.95	2.05	6667.	3.8	58.79	6.12
2412.	0.8	4.34	.61	6732.	3.8	5.67	1.22
2530.	0.9	4.47	.60	6743.	3.8	7.71	1.22
2576.	0.9	17.73	1.97	6858.	3.9	15.09	1.81
2607.	0.9	4.11	.59	6961.	4.0	33.56	3.60
2790.	1.0	53.96	4.73	7012.	4.0	7.05	1.19
2871.	1.1	4.72	.75	7102.	4.1	5.76	1.19
2941.	1.1	5.44	.74	7155.	4.1	24.00	3.55
3048.	1.2	26.45	2.72	7243.	4.2	12.69	1.76
3119.	1.2	2.95	.54	7286.	4.3	4.03	1.17
3203.	1.3	5.12	.53	7472.	4.4	45.12	3.47
3257.	1.3	10.51	.88	7552.	4.5	38.55	3.45
3306.	1.3	27.22	2.61	7586.	4.5	6.20	1.15
3343.	1.3	2.94	.52	7694.	4.7	44.46	3.42
3413.	1.4	44.85	5.14	7745.	4.8	14.03	1.70

TABLE V

Resonance Parameters W^{182}

E(ev)	ΔE	Γ_n^o	$\Delta\Gamma_n^o$
7810.	4.8	33.95	2.83
7834.	4.8	14.69	2.83
8013.	4.9	14.75	2.23
8192.	5.1	18.12	2.21
8394.	5.3	19.87	2.73
8506.	5.3	6.61	1.63
8533.	5.3	6.55	1.62
8725.	5.5	47.96	4.28
8815.	5.7	20.02	2.66
9005.	5.9	9.06	1.58
9231.	6.1	42.15	4.16
9454.	6.3	36.51	4.63
9472.	6.3	12.84	3.60
9823.	6.6	25.22	2.52
9896.	6.6	16.49	2.01
9944.	6.7	6.62	2.00
9998.	6.8	32.00	6.00
10025.	6.9	32.96	6.00
10140.	7.0	16.49	1.99
10260.	7.1	36.73	3.46
10630.	7.5	18.23	2.43
10900.	7.7	8.52	2.87
11000.	7.9	17.50	1.91
11174.	8.0	12.30	2.37
11310.	8.3	29.62	2.82
11380.	8.4	56.25	5.62
11560.	8.4	23.76	2.79
11710.	8.6	34.56	3.23
11780.	8.6	5.90	1.38
11820.	8.7	25.20	2.76
11890.	8.8	28.89	2.75
11910.	8.8	23.27	2.75
12210.	9.1	17.56	2.72
12361.	9.3	9.89	2.70
12490.	9.5	28.63	2.68
12540.	9.5	25.54	2.68
12680.	9.7	17.76	2.66
13057.	10.0	26.69	2.63
13180.	10.3	43.55	6.10
13253.	10.4	28.67	3.04

TABLE V

Resonance Parameters W^{184}

E(ev)	ΔE	Γ_n^o	$\Delta\Gamma_n^o$	E(ev)	ΔE	Γ_n^o	$\Delta\Gamma_n^o$
101.7	.12	.357	.050	5807.	3.0	5.91	.98
184.2	.14	81.05	7.37	5884.	3.1	67.01	9.12
242.8	.21	.128	.026	6067.	3.2	5.07	.77
310.7	.30	4.26	.34	6127.	3.3	145.64	31.94
422.8	.24	2.14	.24	6232.	3.4	12.16	2.53
681.2	.49	24.90	1.92	6411.	3.5	2.75	1.00
703.7	.51	.237	.038	6475.	3.6	9.32	1.24
784.1	.60	.57	.11	6548.	3.6	8.40	1.24
799.3	.62	62.25	5.31	6789.	3.8	12.02	1.82
957.3	.40	45.25	4.85	6913.	3.9	4.45	1.20
998.5	.43	2.60	.32	6964.	4.0	11.62	1.80
1086.	0.5	94.07	9.10	7049.	4.0	73.85	8.34
1132.	0.5	10.11	1.49	7122.	4.1	18.60	3.56
1261.	0.6	36.61	2.82	7205.	4.2	5.13	1.18
1335.	0.7	.421	.109	7303.	4.3	21.53	2.93
1400.	0.7	85.52	5.35	7334.	4.4	9.81	1.75
1424.	0.8	20.14	1.33	7472.	4.5	75.77	6.94
1514.	0.8	36.75	3.86	7552.	4.5	71.35	6.90
1552.	0.9	2.16	1.02	7777.	4.7	13.50	2.84
1655.	0.9	6.39	.74	8167.	5.0	40.39	4.43
1792.	0.5	28.58	3.54	8310.	5.1	16.62	2.74
1920.	0.6	5.48	.69	8458.	5.3	58.17	6.52
2045.	0.6	26.54	2.21	8549.	5.4	54.62	5.41
2092.	0.7	101.23	8.75	8603.	5.5	12.29	2.16
2211.	0.7	5.85	.64	8741.	5.6	11.66	2.14
2252.	0.7	10.54	.84	8889.	5.7	19.94	2.12
2411.	0.8	26.99	3.06	8987.	5.9	12.66	2.64
2459.	0.8	11.80	1.41	9046.	5.9	89.96	7.36
2540.	0.9	13.10	1.59	9286.	6.1	21.59	2.59
2621.	0.9	25.20	1.95	9372.	6.2	66.42	6.20
2836.	2.0			9665.	6.5	6.05	1.53
2922.	1.1	38.85	3.70	9816.	6.6	14.74	3.53
2982.	1.1	15.20	1.65	9843.	6.7	33.46	4.03
3133.	1.2	8.04	1.07	10050.	6.9	49.88	4.99
3182.	1.2	17.73	2.66	10250.	7.1	101.74	8.89
3203.	1.2	38.70	3.53	10420.	7.3	10.87	2.45
3232.	1.3	5.81	.53	10680.	7.5	32.51	3.87
3457.	1.4	38.78	3.40	10740.	7.6	8.88	2.41
3539.	1.4	22.02	2.52	11070.	7.9	86.49	9.50
3596.	1.5	1.42	.33	11280.	8.2	29.66	3.77
3736.	1.6	52.76	4.09	11370.	8.3	9.10	2.35
3807.	1.6	67.26	6.48	11450.	8.4	8.41	2.34
3941.	1.8	4.46	.80	11650.	8.5	10.56	1.85
4008.	1.8	6.16	1.58	11710.	8.6	63.76	6.47
4186.	1.8	39.57	3.86	11820.	8.7	50.13	6.44
4249.	1.9	16.26	2.30	11850.	8.7	83.60	9.19
4547.	2.1	8.75	1.48	12020.	8.9	10.22	3.19
4614.	2.2	4.86	.88	21270.	9.2	12.15	2.27
4802.	2.3	26.70	2.89	12430.	9.4	20.63	2.24
4928.	2.3	24.22	3.56	12660.	9.6	13.73	2.22
5053.	2.4	6.68	.99	13000.	10.0	36.83	3.51
5090.	2.5	39.25	4.21	13080.	10.0	8.39	2.19
5189.	2.6	22.49	2.78	13200.	10.3	174.08	21.76

TABLE V

Resonance Parameters W^{184}

E(ev)	ΔE	Γ_n^o	$\Delta\Gamma_n^o$
13360.	5.2	29.42	3.46
13390.	5.3	31.76	4.32
13480.	5.3	60.29	7.75
13500.	5.3	3.62	1.38
13610.	5.4	6.69	1.71
13680.	5.4	14.88	2.14
13930.	5.5	30.50	3.39
14420.	5.9	91.60	12.49
14860.	6.1	50.04	5.74
15070.	6.2	11.32	2.04
15170.	6.4	16.24	2.03
15250.	6.4	18.22	2.02
15350.	6.5	14.53	2.02
15450.	6.5	74.02	12.07
15630.	6.6	151.98	20.00
15970.	6.8	87.04	15.83
16200.	7.0	28.68	3.14
16320.	7.1	31.31	3.91
16450.	7.2	14.97	2.34

TABLE V

Resonance Parameters W^{186}

E(ev)	ΔE	Γ_n^o	$\Delta\Gamma_n^o$
18.76	.06	73.88	6.93
170.7	.12	2.07	.31
217.5	.18	32.55	3.39
286.7	.27	1.89	.41
405.7	.45	4.47	.40
509.6	.32	4.08	.44
541.3	.35	21.06	1.72
663.1	.47	23.88	1.36
719.8	.53	76.41	5.59
831.0	.33	1.11	.14
963.4	.41	33.19	3.22
1071.	.48	15.74	1.83
1121.	.52	11.50	1.20
1187.	.56	25.54	2.32
1418.	0.7	2.34	.27
1500.	0.8	32.53	2.58
1795.	0.5	.64	.19
1933.	0.6	17.74	1.82
2025.	0.6	12.56	1.44
2105.	0.7	3.81	.76
2349.	0.8	4.95	.62
2515.	0.9	14.96	1.50
2590.	0.9	20.24	1.97
2659.	1.0	94.06	5.82
2779.	1.0	8.16	1.33
2876.	1.1	18.65	1.87
2976.	1.1	2.09	.55
3039.	1.6	202.26	21.77
3158.	1.2	42.71	3.56
3312.	1.3	13.55	1.56
3423.	1.4	59.82	5.13
3541.	1.5	8.40	1.01
3713.	1.5	2.71	.82
3768.	1.6	25.41	2.44
3871.	1.6	52.24	4.82
3963.	1.7	11.12	1.11
4165.	1.8	23.71	2.32
4221.	1.9	42.48	3.85
4395.	2.0	28.66	3.02
4540.	2.1	33.25	2.97
4805.	2.3	87.28	4.33
4976.	2.4	6.38	1.70
5158.	2.5	37.59	3.48
5282.	2.7	5.71	.83
5383.	2.7	14.45	2.04
5402.	2.7	7.35	.82
5667.	2.9	70.40	5.31
5777.	3.0	68.42	5.26
6293.	3.4	17.02	1.89
6386.	3.5	21.90	2.50
6489.	3.6	63.00	4.97
6698.	3.8	2.99	.73
6754.	3.8	49.89	4.26
6949.	4.0	13.20	1.80
6968.	4.0	21.30	2.16
7114.	4.1	6.88	1.07
7176.	4.1	16.53	1.77
7324.	4.3	7.95	1.17
7472.	4.4	63.63	5.78
7634.	4.6	19.92	2.29
7712.	4.7	26.87	2.85
7844.	4.8	11.29	2.26
7978.	4.9	11.76	1.68
8132.	5.0	8.65	1.11
8295.	5.2	28.55	3.29
8347.	5.2	9.63	2.19
8625.	5.5	9.42	1.88
8669.	5.6	6.87	1.72
9177.	6.0	42.80	4.18
9201.	6.0	2.82	1.04
9286.	6.1	88.21	9.34
9410.	6.2	93.81	9.28
9542.	6.3	30.71	6.14
9587.	6.3	278.82	30.64
9843.	6.6	23.69	2.52
10270.	7.2	20.53	2.96
10350.	7.2	81.59	8.85
10580.	7.4	10.31	2.43
10630.	7.5	28.81	3.88
10770.	7.6	33.73	3.85
10850.	7.7	105.60	14.40
11750.	8.6	33.21	3.69
11870.	8.7	10.46	3.67
12310.	9.4	72.10	13.52
12410.	9.5	100.09	17.95
12590.	9.6	37.43	8.91
12620.	9.6	71.21	15.13
13200.	10.4	26.98	3.92
13320.	10.5	17.76	4.33
13570.	5.4	50.65	7.73
14020.	5.6	30.40	5.07
15200.	6.4	66.11	9.73
15440.	6.6	49.09	12.07
15480.	6.6	47.02	12.06
15650.	6.7	151.88	23.98
15720.	6.7	22.13	4.79
16490.	7.2	67.75	11.68
16630.	7.3	75.22	11.63
16930.	7.4	61.48	9.22
17060.	7.5	11.48	4.59
17300.	7.7	44.86	7.60
17340.	7.7	9.49	3.04

DATA NOT FOR QUOTATION

neutron beam at the Brookhaven National Laboratory HFBR[1] gave an unreasonably high value for the efficiency. The high value was ascribed to direct detection of the pair-electron flux from the Pb-207 target because of an insufficiently thick first-stage converter on the detector. A new calibration was done using the entire array of eight detector units with the same thicker first-stage converter and in the same configuration as used during the Nevis run. This recent calibration confirms the linearity of detector efficiency from 0.5 to 4 MeV. While not yet final, results for the 7.367 MeV. point using the Pb-207 target, as well as for "total energy" points at 4.8 MeV. and 6.9 Mev., using U-238 and Au-197 targets indicate a linear response over the high energy range. As operated during the Nevis run, the detector array had a total efficiency (including geometry) of about 0.6%/MeV.

The results from this most recent run are in the process of being analyzed. The resonance parameters are first being obtained by means of the area method. The capture area is the sum of the counts under a capture peak, corrected for multiple scattering effects. This area can then be related to the resonance parameters through the "saturated open" count rate. Because the Moxon-Rae experiments are relatively low counting rate by nature, the data are combined with the transmission data, and self-indication data obtained by the NVS group where ever possible(see preceeding section). The NVS self-indication data has better statistics due to the higher counting rate obtainable, and the use of these data with the Moxon-Rae data, which are independent of the gamma ray cascade which occurs from resonance to resonance, leads to an accurate determination of the resonance parameters.

The first isotope to be analyzed was U^{238}, due to its importance in the fast breeder program, and in view of the recent uncertainty arising in its Γ_γ values. Results on Th^{232} are in the initial stages of preparation. The preliminary report of the U^{238} data up to 1.5 keV will be presented at the February 1971 meeting of the American Physical Society while the complete analysis to greater than 5 keV will be ready for the Knoxville meeting of the Neutron Cross Section and Technology Conference.

---

[1]Use of High Flux Beam Reactor facility courtesy of Dr. W. R. Kane, Physics Department, Brookhaven National Laboratory.

For the purpose of obtaining some preliminary information concerning the discrepancies in Γ_γ's between the Los Alamos and Geel groups, four large levels near 1000 eV were examined for the relative magnitudes of Γ_γ. The results showed considerably better agreement with the Geel values with respect to the relative variations in the values of Γ_γ's. The absolute values of Γ_γ were not determined in the initial investigation.

3. Gamma Ray Spectra from Radiative Capture in the Resonance Region (M. Derengowski, J. Felvinci, C. Ho, E. Melkonian, F. Rahn, and W. W. Havens, Jr.)

An experiment has been run at the Nevis cyclotron, in which a germanium detector was used to study the gamma rays between 1 and 8 MeV. emitted by a U^{235} target after capture of resonance energy neutrons. Preliminary analysis of the data has been done on the PDP-8 computer. Comparison of target-in and target-out data integrated over all neutron energies shows several weak transitions attributable to uranium. We are now analyzing the spectra at separate resonances, in an effort to reduce the effects of background, to separate the capture gamma rays from those associated with fission, and to look for differences in the capture gamma ray spectra from resonance to resonance.

4. Resonance Spin Determination in Fissioning Nuclei (J. P. Felvinci and E. Melkonian)

The planned experiment with the Nevis neutron beam took place in late Spring, 1970 and resulted in a large quanity of data. Due to the number of experiments run simultaneously and the complexity of data reduction, most of the elapsed time was spent in a preliminary survey of the data and in writing programs for analysis. It was decided to analyze the experiments sequentially, and thus, we report here on one of them (Th^{229}) in detail and summarize the others briefly.

The analysis of the U^{233} cross section continues with the additional data taken during this run. It is hoped that yield curves as a function of cuts in the single fragment kinetic energy spectrum will be available in the very near future.

The Np^{237} subthreshold fission cross section obtained is quite similar to that measured by Paya et al.[1] There is indication though,

---

[1]Paya et al., 1968 Dubna Conference.

that the 39.07 ev resonance, not seen in fission previously, has a fission width of approximately 1 MeV. (The 39.9 ev resonance has Γ_f = 6 MeV).

Preliminary analysis of the γ-γ coincidence technique applied to Np^{237} indicates differences in yield between resonances as a function of average γ-ray energy.

5. Slow Neutron Fission Cross Section of Th^{229} (J. P. Felvinci, J. R. Toraskar, and E. Melkonian)

Neutrons produced by the Columbia synchrocyclotron were used to measure the fission cross section of Th^{229} relative to U^{235}. Fission fragments from a thin, 21 $\mu g/cm^2$ Th^{229} target of high, 99.94% isotopic purity were detected by a solid state detector. The time-of-flight of the neutron causing the fission and the energy of the single fission fragment were recorded.

Table I gives the resonance energies and the calculated $\sigma_0\Gamma_f$ values for Th^{229}. At resonances where σ_0 is known. Γ_f was also calculated. Additional resonances to these reported by Bollinger et al[1] were found at 5.95, 10.8, 13.3, 23.3, 25.9, 29.7, 35.0, 39.3, 43.2, 46.5, 48.5, and 51.0 ev. The yield at 0.07 ev was directly compared with the yield of U^{235} and from this measurement the thermal (0.0253 ev) cross section was calculated assuming a 1/v dependence. The result, 7 barns is much lower than the presently accepted value of 30.5 barns.[2] From the $\sigma_0\Gamma_f$ values of the measured resonances, the obtained thermal cross section is only about 3 barns. This may indicate the presence of a negative level (It may be noted, that approximately 4% of U^{233} contamination could account for the 30 barn thermal cross section).

The three very low energy resonances reported by Konakhovich and Pevsner[3] were not observed in this experiment.

---

[1]L. M. Bollinger, H. Diamond and J. E. Gindler, BAPS 8 370 (1963)

[2]J.E. Gindler, R.F. Flynn and J. Gray, Jr., J. Inorg. Nuc. Chem. 15 1 (1960)

[3]Y. Y. Konakhovich and M. I. Pevsner. Atomic Energy 8 39 (1961)

Table 1
Th^{229} results

E_o(eV.)	$\sigma_o\Gamma_f$(eVb)	σ_o Barns†	Γ_fmV
0.610	2.61 ± 0.24	6000 ± 460	0.435
1.26	13.3 ± 0.71	4600 ± 1800	2.9
1.44	1.68 ± 0.26		
1.72	2.47 ± 0.35	1500 ± 950	1.65
1.96	5.41 ± 0.5	2150 ± 850	2.51
3.18	5.15 ± 0.6		
4.23*	49.58 ± 21.2	3200 ± 830	15.5
5.58	3.03 ± 0.6		
5.95	2.04 ± 0.5		
6.95	3.88 ± 0.7		
8.27	0.98 ± 0.4		
9.15	5.00 ± 0.9		
9.6	3.51 ± 0.8		
10.4	3.54 ± 0.8		
10.8	1.82 ± 0.6		
12.6	4.80 ± 1.0		
13.3	1.91 ± 0.7		
14.6	4.10 ± 1.0		
15.4	8.28 ± 1.5		
16.8	5.72 ± 1.3		
23.3	5.54 ± 1.4		
25.9	5.61 ± 1.5		
29.7	15.2 ± 2.6		
35.0	8.11 ± 2.0		
39.3	16.6 ± 3.0		
43.2	14.9 ± 3.0		
46.5	11.4 ± 2.7		
48.5	9.85 ± 2.5		
51.0	4.08 ± 1.6		

*Probably several levels.

†From BNL 325 2nd Ed. Supplement No. 2 (1965).

C. NEUTRON AND GAMMA RAYS

1. Sensitivity of Transport Calculations to Microscopic Cross Sections (E. Oblow, P. Soran, J. Ching, L. Lidofsky, and H. Goldstein)

The program for studying the importance of cross section features in deep neutron penetration has continued along the lines described in the previous report. Calculations on Be and BeO have been completed at least in so far as they concern the infinite medium spectrum and the age. Results have been reported at the November 1970 ANS meeting in a paper by Weisbin, Goldstein, and Lidofsky.[1] The most important cross section uncertainties in Be revealed by the calculations are in the keV. total cross section of Be (for age calculations) and in the energy distribution of neutrons from the (n,2n) reactions induced by neutrons of energy above 4 MeV. (for problems involving 14 Mev sources). Work on the carbon benchmarks problem has also been completed and is now being written up. The discrepancy at high energies mentioned in the previous report has been traced to incorrect treatment of the (n,n'3α) reaction in the GGA and ORNL calculations. This experience emphasizes the importance of apparently "exotic" reactions in specific transport problems.

Most of the effort in the interval has been concentrated on studies of neutron transport in iron. Considerable time was spent in cleaning up details of work previously reported. It appears that we were unduly optimistic about finding a suitable "weighting flux" for calculating multigroup cross sections in iron. It has not yet been possible to define a space-independent weighting flux suitable for coarse groups which suitably balances the emphasis on the region of the minima with adequate recognition of the flux of neutrons locally scattered out of the minima. It has been also found that the method of computing the scattering integral used in a discrete energy solution of the Boltzmann equation needs at least 5 to 10 closely spaced energy points in the immediate high-energy side of a deep cross section minimum. Preliminary calculations with synthetic iron cross sections (see following section) indicate that fluctuations in the inelastic cross section below 2 MeV. are not large enough to effect the penetration significantly. On the other hand, they suggest that resolution effects may be noticeable in the measured total cross sections even below 2 MeV. The actual cross section structure of iron may be even more strongly fluctuating than the GGA measurements indicate, with corresponding affects on the deep penetration of neutrons in this energy range.

---

[1] Trans ANS 13, 758.

2. Generation of Synthetic Fluctuating Neutron Cross Sections For Fe^{56} (E.S. Troubetzkoy)

High resolution measurements for Fe^{56} cross sections in the MeV range have been made only for the total cross section. To see what fluctuations might exist for other cross sections, particularly the inelastic and the differential elastic, synthetic iron cross section sets have been constructed. Statistical ensembles of R-matrix parameters have been generated by random selection from appropriate probability distributions. The required nuclear parameters (strength functions, level densities, etc.) have been deduced from whatever data are available. Some 500-1000 poles of the R-matrix have been taken into account. S-matrix components are calculated by numerical matrix inversion in channel space. On this basis sets of the total, elastic, differential elastic, and inelastic (0.85 MeV. level) cross sections have been calculated in the range 1.5-2.0 MeV., all exhibit a strongly fluctuating character. Energy-averages of these sets agree well with measured vlaues, and the statistical properties of the total cross section values (when folded into a resolution function) are reasonably similar to those measured for iron. It is therefore felt that the statistical properties predicted here for the cross sections not presently amenable to measurement correspond well enough to nature that their effect on neutron penetration can be studied adequately.

3. Effects of Truncating Representations of the Elastic Angular Distribution (J. Wagschal, E. Oblow, L.J. Lidofsky, and H. Goldstein)

Almost all methods of transport computation represent the angular distribution for elastic scattering by a suitable sum of Legendre polynomials. Several years ago, Ozer investigated the effect of arbitrarily truncating the representation at various order polynomials. Truncation to P_3 or even P_5 would greatly simplify the calculations and also reduce the complexity of the cross section measurements needed. He found that an expansion through P_3 was sufficient in all the instances he examined for predicting deep penetrations.[1] The problem has been re-examined with the more powerful calculational tools now available. Ozer's results have been verified for monoenergetic problems and analytic justifications have been obtained in their case. In the more realistic transport problems with slowing down, however, the angular distribution of elastic scattering affects not only the geometry of the particle transport but also the energy distribution of the scattered neutrons. There can be circumstances where

---

[1] cf WASH 1093, p. 36.

singly-scattered neutrons form a large part of the neutron flux, e.g. close to the energy of a monoenergetic source, either an actual source or a virtual source. In such cases truncation of the angular distribution representation at low orders may have significant effect on the spectrum at least locally. The effect on the overall spectrum still remains small.

4. Gamma Spectra Following the Capture of 14 MeV. Neutrons by Cu, Zr, and Sb (M. Stamatelatos, Bo Lawergren, L.J. Lidofsky)

The project is essentially complete and a paper is being prepared for publication. The spectra observed have particular features peaks which we have interpreted as being due to the position of the giant resonance and of single particle states in the mass region of the target nucleus. The magnitude of the capture cross sections are in reasonable agreement with those determined by activation measurements. As a consequence we may deduce that capture reactions induced by 14 MeV. neutrons are characterized by the emission of a first gamma ray with $E_\gamma > 14$ MeV. This is plausible since emission of a lower energy gamma would lead to the formation of an unbound state which with high probability would decay by particle emission i.e. $(n,\gamma n)$ and would constitute an inelastic rather than a capture reaction.

GULF RADIATION TECHNOLOGY
A Division of Gulf Energy and Environmental Systems Incorporated
San Diego, California

A. NEUTRON CROSS SECTIONS

1. Rhodium Resonance Parameters and Average Capture Cross Section (A. D. Carlson, M. P. Fricke and S. J. Friesenhahn)

The analysis of Rh capture and self-indication data for resonance parameters is continuing. The results obtained are shown in Table A-1. Area analysis has been employed for the determination of the width parameters. For the relatively strong levels, spin determinations are possible from a combined area and shape analysis. For strong resonances, the shape analysis is almost unnecessary since the radiation width obtained for the wrong spin value is quite different from the average radiation width for the other levels. The shape analysis in this case verifies the constancy of the radiation width from level to level. The spin assignments obtained agree with those of King,[1] Ribon[2] and except for the levels at 272.4 eV and 319.5 eV with those of Wang.[3]

Ribon has also obtained radiation widths from shape analysis of his transmission data. Though there is generally agreement within the sum of the error bars between these and the present results for each level, the average radiation width determined for the levels by Ribon, 171 meV, is more than 10% higher than that obtained in the investigation. Yet the estimated uncertainties in these average radiation widths are only 2-3% for both data sets.

In Fig. A-1 measurements of the capture cross section of Rh from about 1 to 1000 keV are shown. The smooth curve is that recommended by Poenitz at the Paris Conference in 1966. All data

---

[1] T. J. King and R. C. Block, Nucl. Phys. A138, 556 (1969).

[2] P. Ribon, J. Girard and J. Trochon, Nucl. Phys. A143, 130 (1970).

[3] Nai-yen Wang et al., Sov. Phys.-JETP 18, 1194 (1964).

TABLE A-1

Rhodium Resonance Parameters

E_o (eV)	$2g\,\Gamma_n$ (meV)	Γ_γ (meV)	J
1.259	0.774 ± 0.01	154 ± 3	-
34.4	0.024 ± 0.001	--	-
46.8	0.80 ± 0.05	143 ± 30	
68.4	0.30 ± 0.02	--	-
95.7	3.5 ± 0.2	155 ± 15	-
125.6	11.0 ± 0.5	141 ± 25	-
154.2	Γ_n = 211 ± 20	148 ± 10	0
187.0	Γ_n = 36 ± 3	133 ± 18	1
253.9	Γ_n = 31 ± 4	160 ± 14	1
263.2	2.1 ± 0.3	--	-
272.4	Γ_n = 61 ± 7	159 ± 9	1
319.5	Γ_n = 93 ± 15	148 ± 20	1
406.1	21.0 ± 3	165 ± 30	-
435.3	Γ_n = 190 ± 60	140 ± 20	1
555.1	Γ_n = 90 ± 20	150 ± 15	1
581.5	4.3 ± 0.5	--	-
620.5	Γ_n = 9.5 ± 1.5	--	-
741.2	4.5 ± 1.5	--	-
844.5	Γ_n = 186 ± 45	153 ± 13	1

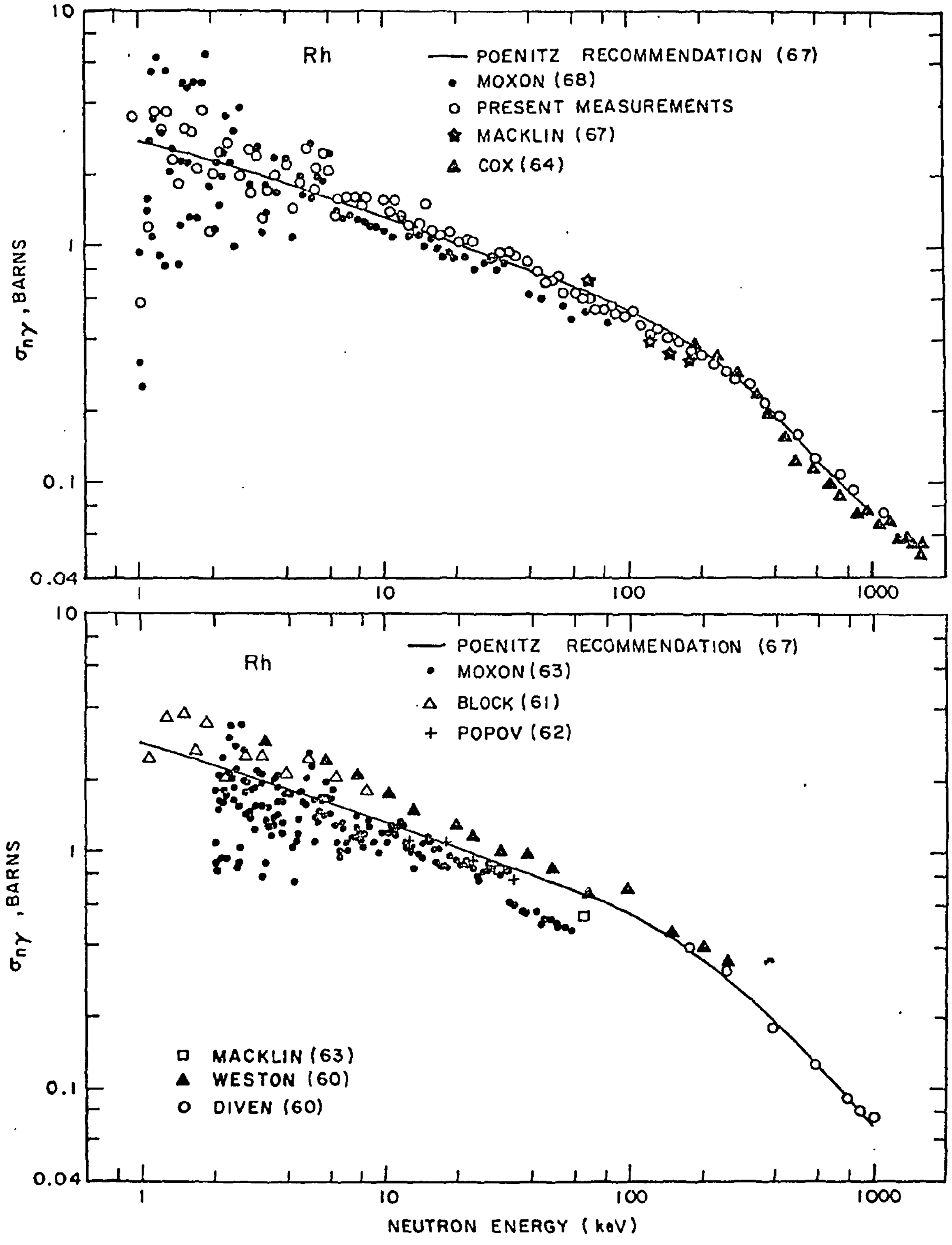

Figure A-1. Measurements of the Rh capture cross section from 1 keV to 1 MeV.

DATA NOT FOR QUOTATION

shown here are contained in the latest BNL-325 except those of Moxon (68),[4] Macklin (67)[5] and the present measurements. Some of the techniques employed in obtaining the present data are indicated in the following section.

Above 100 keV there is agreement with the present data within the uncertainties of the previous measurements. Below 100 keV there are differences in normalization. The data of Block and Weston are relative measurements with shapes which are similar to that of the present data and therefore represent no disagreement within the uncertainties. The data of Moxon however are absolute measurements which are as much as ≈ 20% lower than the present measurements. (This work is pertinent to request No. 228 in WASH-1144.)

2. Fast Neutron Radiative Capture (M. P. Fricke, S. J. Friesenhahn, A. D. Carlson)

A program supported in part by the NASA and the USAEC has recently been completed at GRT to develop the techniques necessary to measure radiative capture cross sections over a continuous neutron energy range spanning the full eight orders of magnitude of prime interest in reactor programs, thermal to 1 MeV. In particular, this capability allows (n, γ) measurements in the upper-keV region to be normalized directly to saturated resonances in the eV region. In many cases this self-calibration method results in a normalization accurate to 1-2%, and the method does not rely on the value of any standard cross section. The incident neutron flux spectrum (and hence the energy variation of the average capture cross section) is measured relative to the hydrogen scattering cross section above 80 keV and relative to $^{10}B(n, \alpha)$ at lower energies. The flux can be measured in this way with an overall uncertainty of ≤ 5% over the full energy range.

Two neutron flight paths of length 20 and 230 meters are used in a complementary fashion to optimize data accumulation. A 4000-liter liquid scintillator is used with the 20-meter flight path, and a newly constructed 2400-liter scintillator is used with the 230-

[4] M. C. Moxon, M. Sc. Thesis, London University (1968).

[5] R. L. Macklin and J. H. Gibbons, Phys. Rev. 159, 1007 (1967).

DATA NOT FOR QUOTATION

meter flight path. Data for eight elements have been obtained to date, and the average cross sections from ~ 1-1000 keV were reported at the Helsinki Conference.[6] These data have been forwarded to the National Neutron Cross Section Center and are illustrated and discussed briefly below. (This work is pertinent to request Nos. 223, 228, 274, 318, 331, 413 and 414 in WASH-1144.)

a. Au(n, γ)

The GRT data for this important standard cross section are shown together with the most recent results of other measurements in Fig. A-2. The solid curve in the figure is the recent evaluation of Vaughn and Grench,[7] and the broken curve is that obtained by Moxon[8] from a strength-function fit to his data. The GRT results are considered to establish the shape of the excitation function to ~± 5% above the region of strong fluctuations, say ⩾20 keV, and our data also agree within 4% and 1% with recent, high-accuracy results at 24 keV[10] and 30 keV,[9] respectively.

The average Au(n, γ) cross section can probably now be considered established to ⩽10% throughout the energy region illustrated, and more monoenergetic experiments of high accuracy in the region above 100 keV might permit an evaluation of the existing data which would produce a useful standard cross section known to about ± 5% everywhere in the region ~ 10-1000 keV.

b. ^{238}U(n, γ)

The ^{238}U capture cross section from 1 keV to 1 MeV is considered to be extremely important to fast reactor calculations, and knowledge of this cross section has been improved in the last year.

---

[6] M. P. Fricke et al., International Conference on Nuclear Data for Reactors, CN-26/43, Helsinki (1970).

[7] H. Grench, private communication (1970).

[8] M. C. Moxon, Thesis - London University (1968).

[9] W. P. Poenitz et al., J. Nucl. Energy 22, 505 (1968).

[10] F. H. Fröhner, International Conference on Nuclear Data for Reactors, CN-26/8, Helsinki (1970).

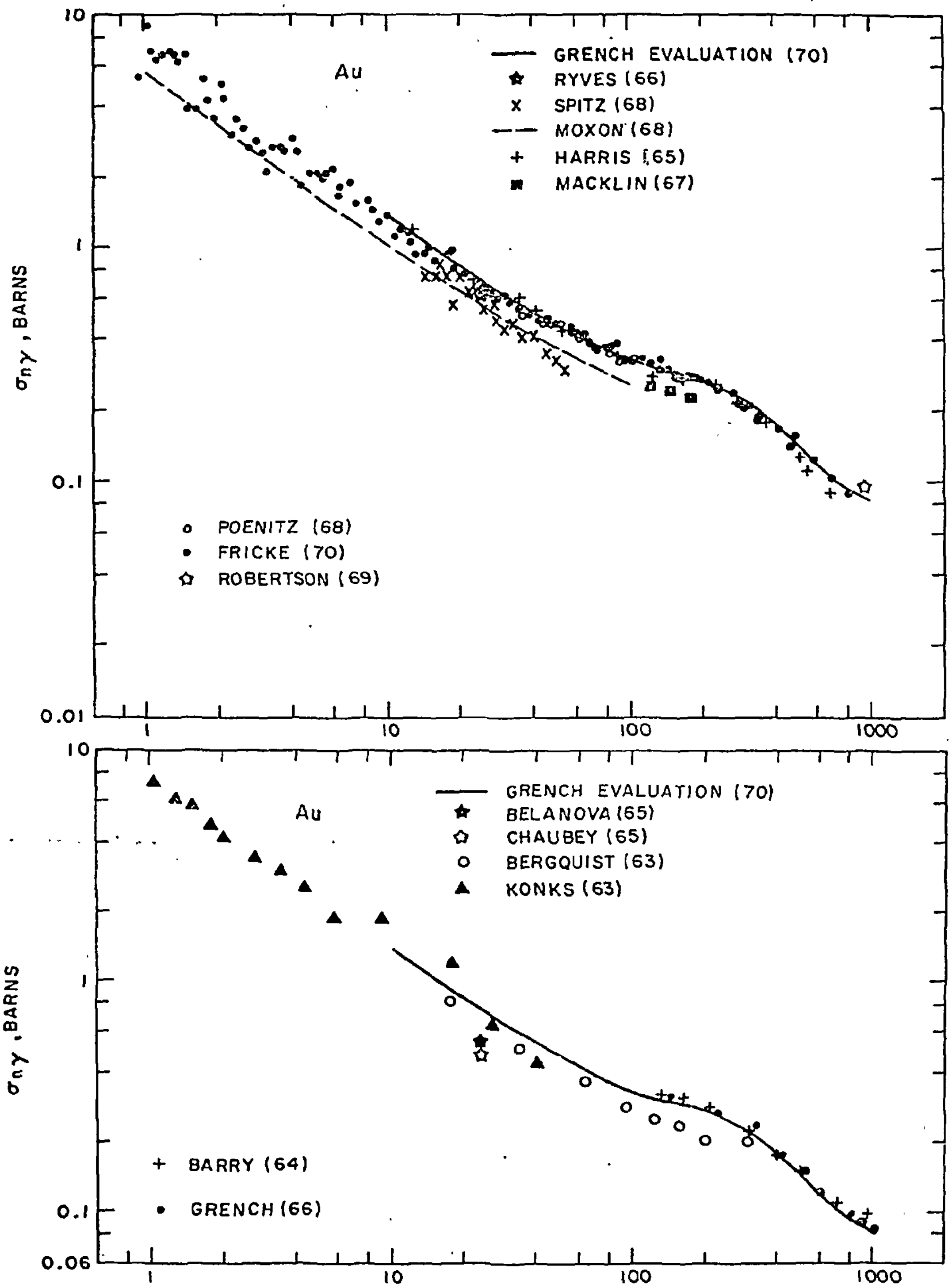

Figure A-2. Recent capture data for gold. The GRT results are shown by the darkened circles in the top figure.

DATA NOT FOR QUOTATION

Prior to this time three of the absolute cross-section sets widely considered "best" were discrepant at energies where they overlapped by amounts larger than their estimated uncertainties. The scintillator data of Menlove and Poenitz,[11] obtained with a grey (flat-response) neutron flux detector, spanned the energy region 25-500 keV. Between 25 and 100 keV these data were ~15% higher than those obtained by Moxon[8] using a Moxon-Rae detector and a flux measurement relative to $^{10}B(n, \alpha\gamma)$; and between 130 and 500 keV the data of Menlove and Poenitz were ~ 15% lower than the activation data of Barry et al.,[12] who measured the flux with a fission counter calibrated against n+p. The latter data extend to higher energies, and recent evaluations follow these data closely in the region ~ 100-1000 keV.

Two new absolute measurements made with large liquid scintillators have been reported in the last year. The results from this laboratory span the region ~ 1-800 keV and thus connect all three data sets discussed above. Our data are normalized to the saturated resonance at 6.7 eV, and the flux shape is relative to n+p and $^{10}B(n, \alpha)$ above and below 80 keV, respectively. The other new data are the preliminary results from 0.5 to 100 keV reported by deSaussure et al.[13] These are normalized to the resonance integral from 30-90 eV, and the flux shape is relative to $^{10}B(n, \alpha)$. The two new measurements use similar methods to detect the capture gamma rays and incident neutrons, and (except perhaps for normalization) one would expect the uncertainties in the cross-section values to be comparable.

The two new data sets and the three previous results are shown in Fig. A-3. The dotted curve shown above 100 keV in this figure is representative of recent evaluations. In the region 20-90 keV the two new data sets agree with each other and with the results of Menlove and Poenitz within ~5%; all three data sets are significantly higher at these energies than the results of Moxon. In the region ~100-500 keV, the GRT data agree excellently with the results of Menlove and Poenitz and do not support the older data of Barry et al. (nor the evaluations which follow these data). In the region below 20

[11] H. O. Menlove and W. P. Poenitz, Nucl. Sci. and Eng. 33, 24 (1968).

[12] J. F. Barry et al., J. Nucl. Energy 18, 481 (1964).

[13] G. deSaussure, private communication (1970).

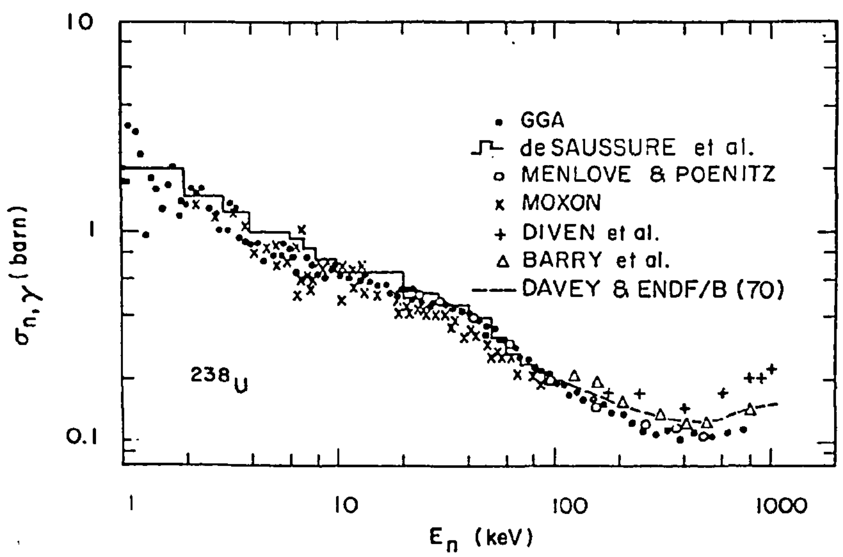

Figure A-3. Capture data for ^{238}U. The GRT data are shown by the darkened circles. The data of Moxon (Ref. 8) are reported at very small energy intervals; only a few typical points are shown in this figure.

keV the two new data sets disagree significantly, and by amounts as large as 20% near 6 keV. This difference lies well outside that which might be expected from uncertainties in the resonance self-protection correction at these energies.

Thus, from the standpoint of sheer numerical agreement, there is now good confirmation of the Menlove and Poenitz results from ~ 25-100 keV by both new measurements and from 100 keV to 500 keV by the one new measurement that spans this region. In the decade 10-100 keV the behavior of the cross section has often been discussed in regard to the existence of a "dip" due to competition from (n, n') to the 45-keV level of ^{238}U. However, this competition is a rather useless discriminant in resolving differences ~ 10% since, without it, the capture cross section near 100 keV would be approximately doubled (but one does not know the factor exactly).

The remaining discrepancies in the ^{238}U capture cross section are not confined to the large differences below 20 keV. When the four data sets discussed here with points below 100 keV are averaged over similar energy intervals, a dichotomy in the overall shape of the excitation function appears between 1 and 100 keV. Our data agree in this manner very well with those of Menlove and Poenitz, and the data of deSaussure et al. with those of Moxon. This is particularly curious since such a division cannot readily be made on the basis of either the method used to detect the capture events or that used to determine the neutron flux distribution. A similar disagreement in shape, but of varying degree, can be observed between the GRT results and those of Moxon for all the elements common to the two experiments (Rh, Ta, Au and ^{238}U), and the agreement between our data and those of Poenitz et al.[9] also exists for Au(n, γ).

c. Other Results

The six other elements studied include Gd, Rh (discussed above) and the four refractory metals Mo, Ta, W and Re. Our results for these elements are plotted together with other data in Fig. A-4. In addition to its applicability to high-temperature space reactor systems, Ta is also of interest as a possible capture cross-section standard. The various results for Ta(n, γ) are now thought[14] to establish this cross section to ~ 10% throughout the region 10-1000 keV.

[14] A. D. Carlson, Proceedings of the EANDC Symposium on Neutron Standards and Flux Normalization, Chicago (1970).

DATA NOT FOR QUOTATION

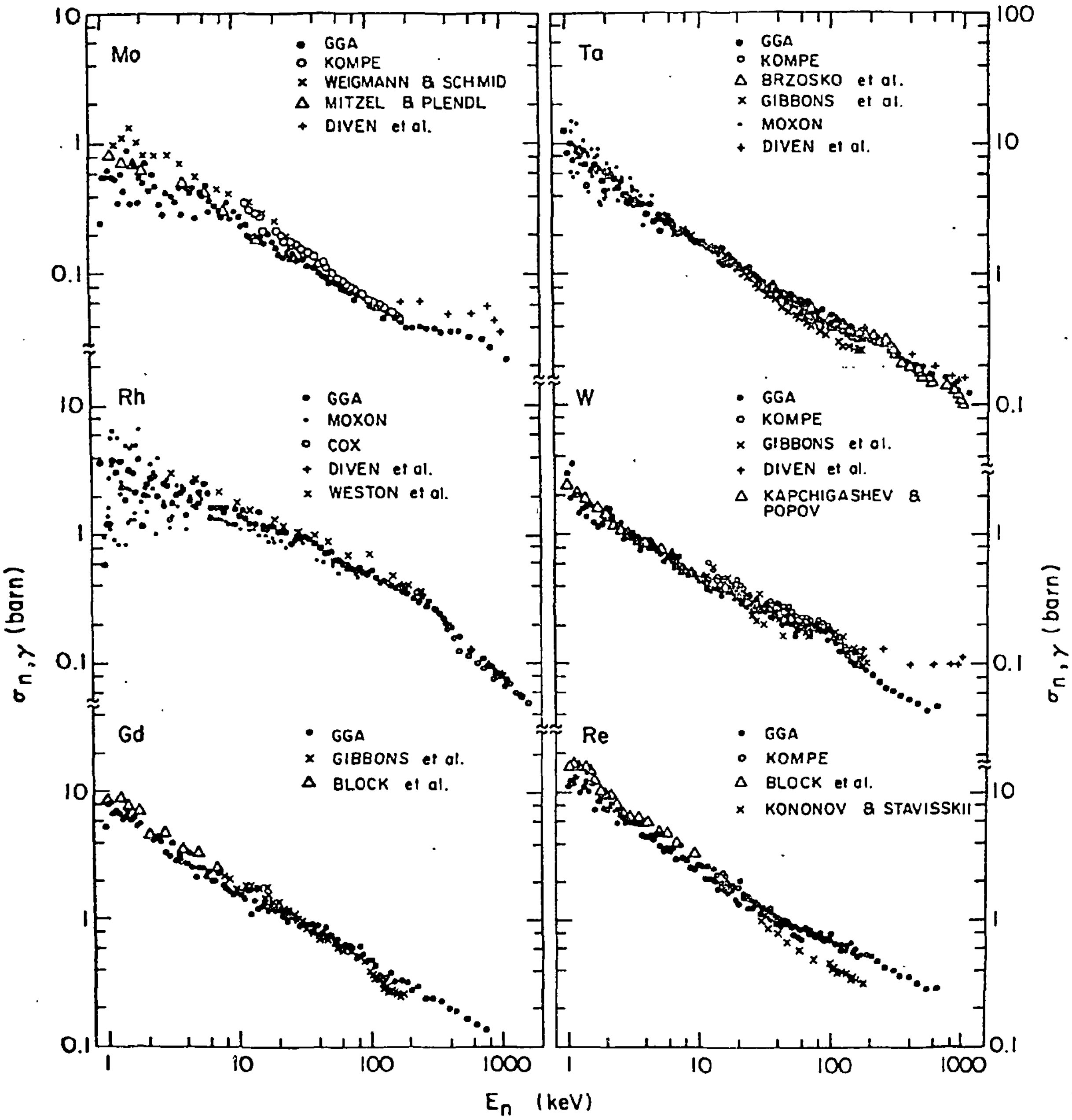

Figure A-4. Capture data for Mo, Rh, Gd, Ta, W, and Re. The GRT data are shown by the large darkened circles.

DATA NOT FOR QUOTATION

3. Gamma-Ray Production Cross Sections for Fe and Al
(V. J. Orphan, C. G. Hoot, and Joseph John)

Gamma-ray production cross sections have been measured for natural Fe and Al over the neutron energy range, 0.86 MeV $\leq E_n \leq$ 16 MeV. The GRT LINAC was used to produce a pulsed source of neutrons having a continuous distribution of energies. The gamma rays were detected with an 80-cm^3 Ge(Li) detector operated as a total absorption spectrometer. The corresponding neutron energies were determined by the time-of-flight (TOF) technique. The experimental apparatus and computerized two-parameter data acquisition system have been described elsewhere.[15] The Fe and Al data are currently being analyzed to determine average gamma-ray production cross sections for the discrete lines and continuum for about 20 neutron energy groups covering the above energy range.

Our two-parameter data have been sorted to obtain TOF spectra corresponding to gamma-ray energy intervals encompassing strong gamma-ray lines. High resolution gamma-ray production cross sections have been deduced from these data for several lines in Fe and Al. The neutron energy resolution was about 1% at 1 MeV using a 20-nsec burst width and a 50-meter neutron flight path. It should be possible to achieve about an order-of-magnitude better resolution by optimizing LINAC parameters and using a 200-meter flight path

Preliminary results are shown in Fig. A-5 for the gamma-ray production cross section for the 847-keV gamma ray produced by the $^{56}Fe(n, n'\gamma)$ reaction. The cross section displays considerable structure which is in reasonably good agreement with several high resolution studies[16,17] from threshold to 1500 keV neutron energy. The neutron energy resolution is indicated at selected neutron energies by the FWHM of the triangles shown in Fig. A-5. Previous data, measured with monoenergetic neutron sources, are shown for comparison. The agreement with the previous data is quite good in most cases; however, the present data are 20 to 25% lower than the values of

---

[15] V. J. Orphan, C. G. Hoot, A. D. Carlson, Joseph John, and J. R. Beyster, Nucl. Instr. and Meth. 73, 1 (1969).

[16] A. B. Tucker, J. T. Wells, and W. E. Meyerhof, Phys. Rev. 137, B1181 (1965).

[17] E. Barnard et al., Nucl. Phys. A118, 321 (1968).

DATA NOT FOR QUOTATION

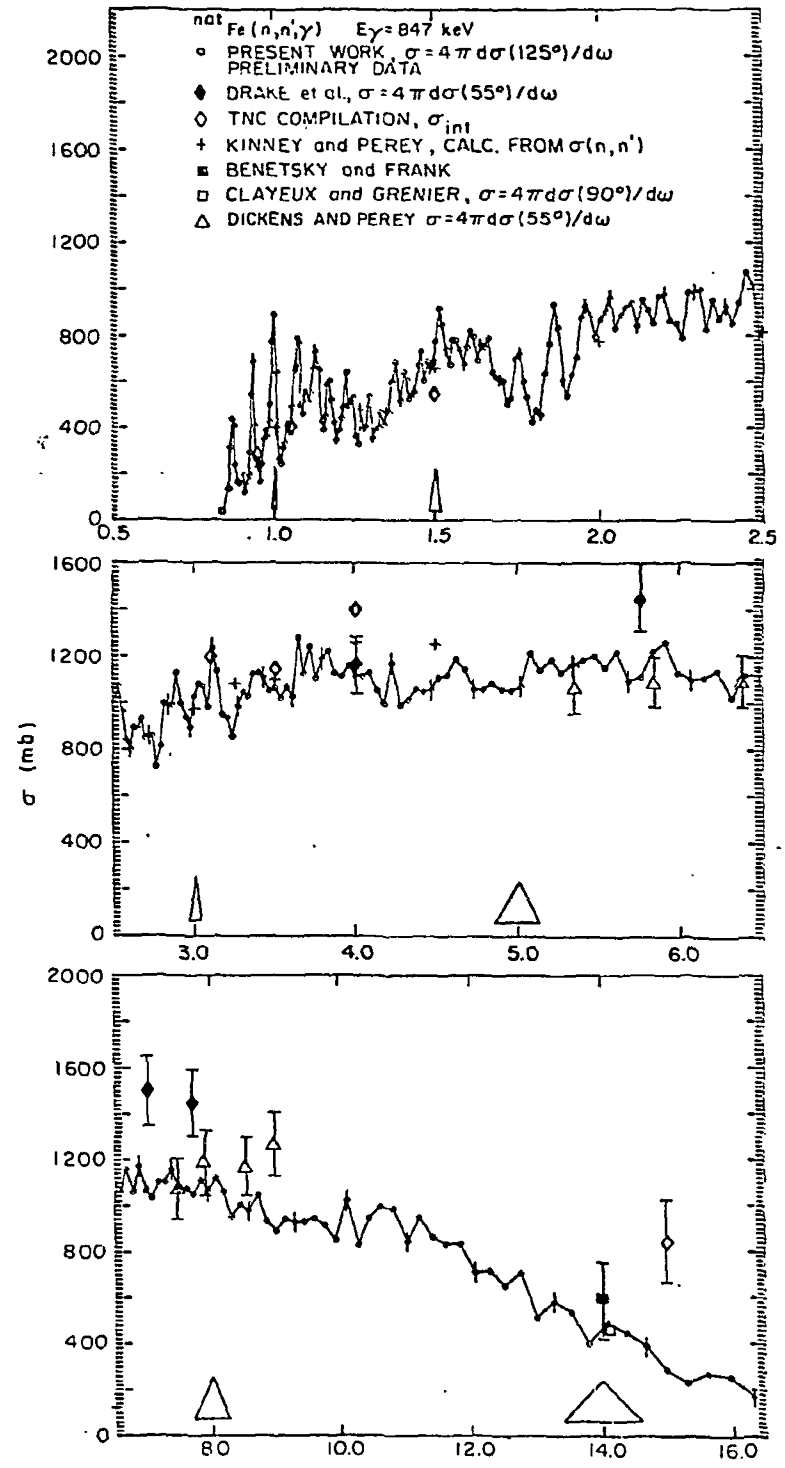

Figure A-5. Gamma-ray production cross section for the 847-keV gamma ray from the $^{56}Fe(n, n'\gamma)$ reaction for neutron energy range, 0.86 MeV to 16 MeV.

DATA NOT FOR QUOTATION

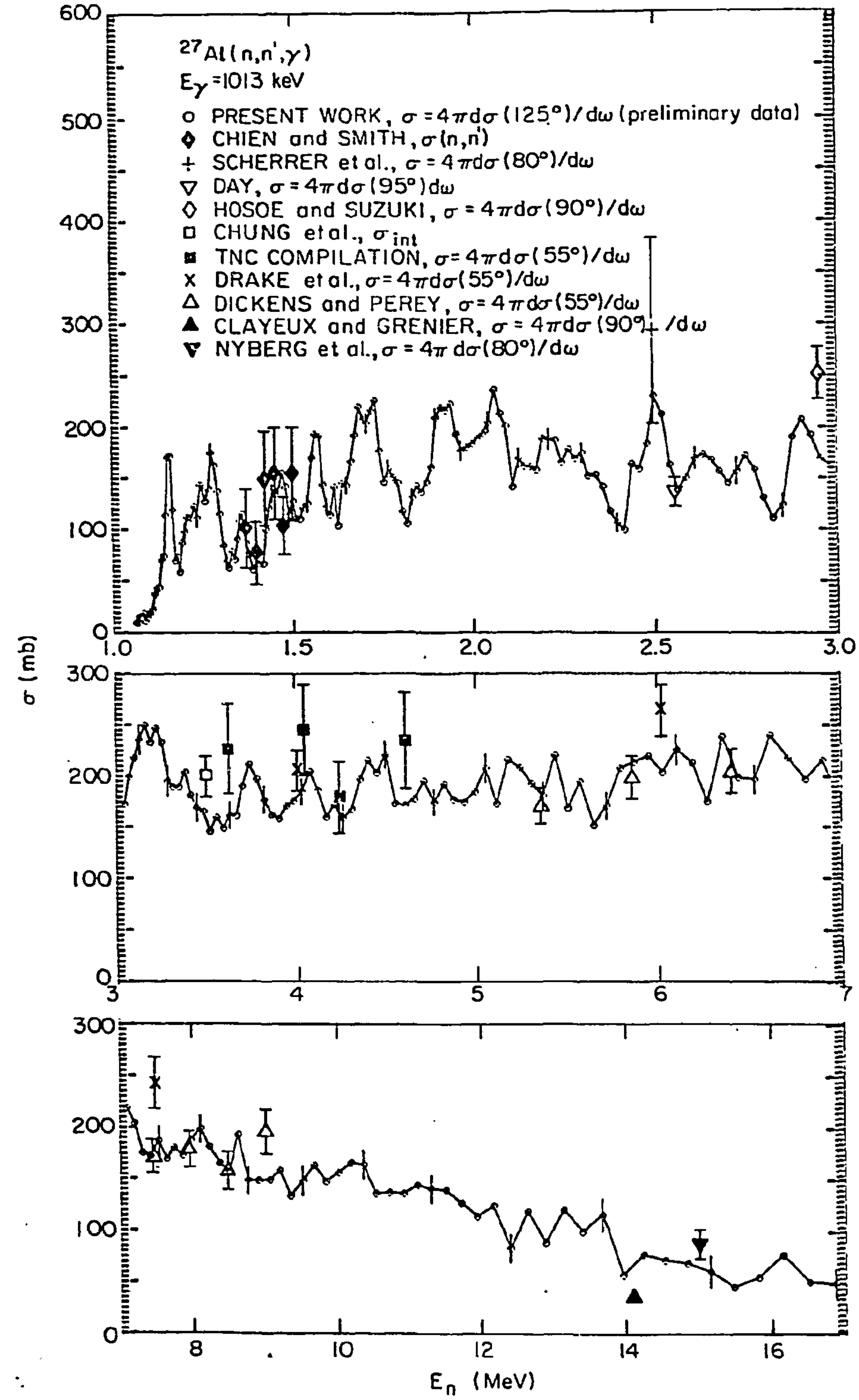

Figure A-6. Gamma-ray production cross section for the 1013-keV gamma ray from the ^{27}Al(n, n'γ) reaction for neutron energy range 1.01 MeV to 16 MeV.

DATA NOT FOR QUOTATION

Drake et al.[18] at 5.74, 7.2, and 7.67 MeV. Also, the present data are about 50% lower than the TNC measurement[19] at 14.8 MeV.

Figure A-6 shows preliminary data for the 1013-keV gamma ray from the $^{27}Al(n, n'\gamma)$ reaction compared to previous measurements. The agreement with most previous data is good. Consistent with the observation made for the Fe cross section in Fig. A-5, the present data are 20 to 25% lower than Drake's values at 6.0 and 7.5 MeV. However, as was true in the case of Fe, the present result agrees closely with that of Drake et al. at 4.0 MeV.

The data shown in Figs. A-5 and A-6 should be regarded as preliminary. Corrections have been applied for the background contribution of neutrons scattered from the sample into the detector, for gamma-ray self-absorption in the sample, and for neutron attenuation and multiple scattering in the sample. The latter corrections were made in an approximate manner and a more rigorous method of correcting the data will be applied in the near future. However, these refinements are expected to alter the cross sections by no more than 5%. (These measurements are pertinent to request Nos. 64, 104, 105 and 106 in WASH-1144.)

4. <u>$^3He(n, p)T$ Cross Section from 80 keV to 500 keV</u>
(D. G. Costello, M. P. Fricke, A. D. Carlson, and S. J. Friesenhahn)

In the past the usefulness of the $^3He(n, p)T$ reaction has been hampered by the lack of accurate direct experimental measurements between 10 keV and 1 MeV. To remedy this situation, new direct measurements of this reaction have been made at Gulf Radiation Technology in this energy range, and good agreement has been obtained with the indirect measurements by Gibbons and Macklin[20, 21] which were deduced by reciprocity from the $T(p, n)^3He$ reaction.

---

[18] D. M. Drake et al., Nucl. Sci. Eng. 40, 294 (1970).

[19] P. S. Buchanan, ORO 2791-28, Texas Nuclear Corporation (1969).

[20] J. H. Gibbons and R. L. Macklin, Phys. Rev. 114, 571 (1959).

[21] R. L. Macklin and J. H. Gibbons, International Conference on the Study of Nuclear Structure with Neutrons, Antwerp, 1965, EANDC-50-S, Vol. 1, Paper 13.

Four one-in. diameter by six in. long (active length) ^{3}He proportional counters were used in these measurements. Neutrons were obtained from a LINAC-pulsed neutron source, and time-of-flight techniques were used with a 220-meter neutron flight path. The neutron flux was determined by a CH_4 proportional counter. Further details of these flux measurements are given in Ref. 22. The wall effect corrections to the bias efficiency for the ^{3}He proportional counters were obtained by a Monte Carlo calculation.

Since the density of the ^{3}He gas in the proportional counters was not known accurately, it was necessary to normalize the present results to our previous measurements[23] which were obtained from pulse height spectra. The previous measurements were based on the total ^{3}He cross section and were independent of the ^{3}He gas density. The present data have been normalized at 515 keV to a cross-section value of 0.890 barn.

The preliminary results of the present measurements are given in Table A-2. The flux shape determined by the CH_4 proportional counter is estimated to be known to better than 5%, and the error introduced by the normalization is estimated to be 5%; thus the total error of the present cross-section measurements is approximately 10% and is so listed in Table A-2.

In Fig. A-7 our results are compared to previous data. The present data are in good agreement with the indirect measurements and generally support the evaluated cross section of Als-Nielson[24] who placed greater weight on the indirect results. (These measurements are pertinent to request No. 8 in WASH-1144.)

---

[22] W. M. Lopez, M. P. Fricke, D. G. Costello and S. J. Friesenhahn General Atomic Report GA-8835 (1968) (unpublished).

[23] D. G. Costello, S. J. Friesenhahn and W. M. Lopez, Nucl. Sci. Eng. 39, 409 (1970).

[24] J. Als-Nielsen, Newsletter No. 6, Neutron Data Compilation Centre, European Nuclear Agency (1967).

DATA NOT FOR QUOTATION

TABLE A-2

$^3He(n,p)T$ Cross Section

Incident Neutron Energy (keV)	Present Measured Cross Section (b)	Als-Nielsen Evaluated Cross Section (b)
84.7	2.35 ± 0.24	2.22
93.1	2.34 ± 0.22	2.09
103	1.99 ± 0.20	1.95
114	1.92 ± 0.19	1.82
127	1.78 ± 0.18	1.76
142	1.71 ± 0.17	1.62
161	1.58 ± 0.16	1.50
183	1.43 ± 0.14	1.41
210	1.34 ± 0.13	1.32
244	1.19 ± 0.12	1.21
288	1.10 ± 0.11	1.12
343	1.01 ± 0.10	1.04
416	0.93 ± 0.09	0.96
515	0.89	0.91

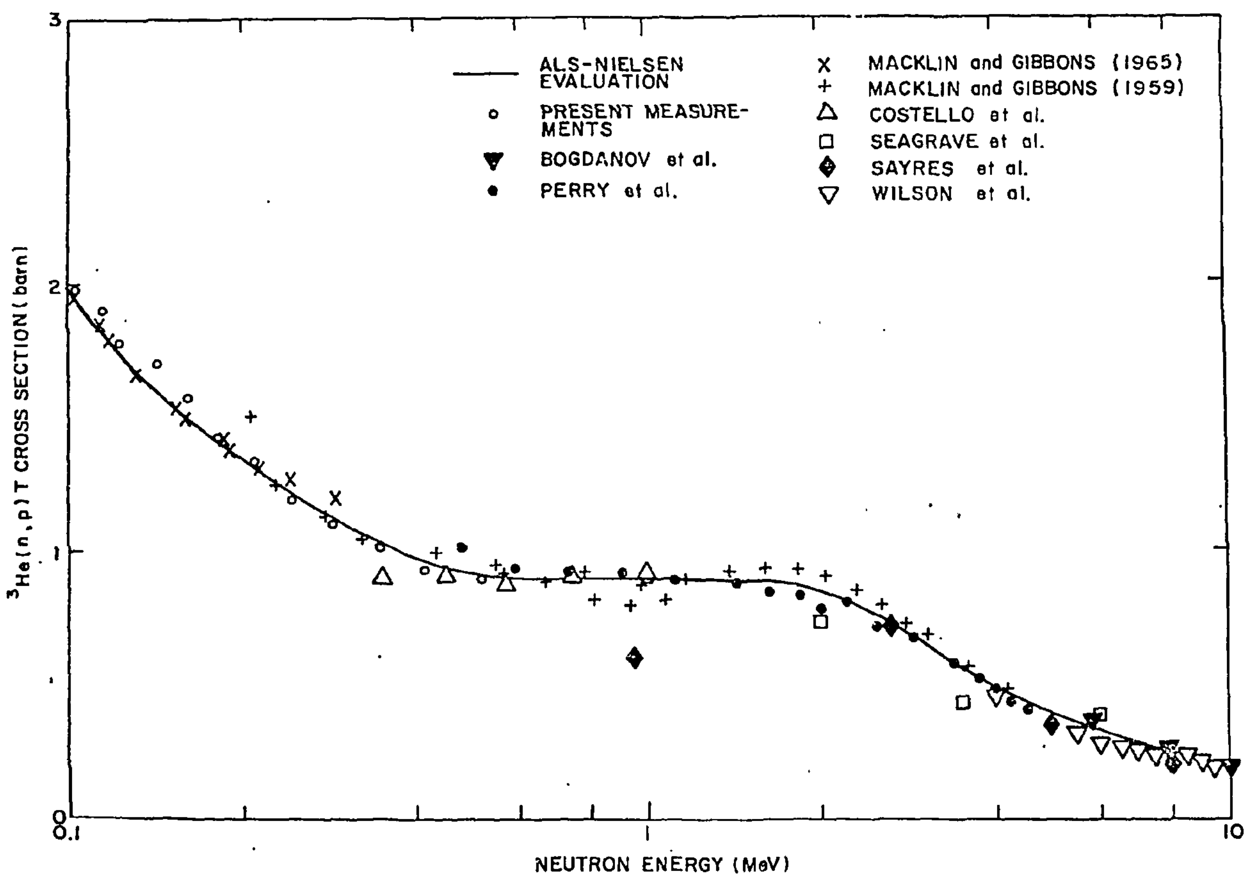

Figure A-7. Measurements of the ^{3}He(n,p)T reaction.

DATA NOT FOR QUOTATION

5. Epithermal Neutron Capture Gamma Rays from Shield Materials: Depleted Uranium (Joseph John, V. J. Orphan and C. G. Hoot)

Studies of thermal and epithermal neutron capture gamma rays in tungsten have been reported previously.[25] Measurements have now been made of gamma rays from resonant capture in ^{238}U of neutrons up to 100 keV using the capture gamma-ray facility.[26] An electron LINAC was used to produce a beam of pulsed neutrons from a cylindrical uranium target. The neutrons were moderated by an inch of polyethylene and were incident on a 6-in. diameter depleted uranium sample located at the end of a 16-meter flight path. The gamma rays were detected using a Ge(Li)-NaI(Tl) spectrometer operated simultaneously as a three-crystal pair spectrometer and an anti-Compton spectrometer. The energy of the captured neutrons was measured by the time-of-flight technique.

Gamma-ray pulse height spectra were generated from the two-parameter data for fifteen neutron energy groups which covered individual resonances wherever possible. The spectra were corrected for analyzer deadtime effects and background radiations. They have been unfolded to remove spectrometer responses and intensities of capture gamma rays have been deduced. These intensities are grouped into 0.25-MeV wide gamma-ray energy bins suitable for shielding calculations.

The intensities of gamma rays and the observed radiated energy are summarized in Figs. A-8 and A-9 for the fifteen neutron energy groups. The shaded regions in the histograms represent the calculated uncertainties. The total radiated energy in the resolved resonance region is within ±15% of the known neutron binding energy. Further details are given elsewhere.[27] (This work is pertinent to request no. 415 in WASH-1144.)

---

[25] V. J. Orphan and Joseph John, Gulf General Atomic Report GA-9121, December 31, 1968.

[26] V. J. Orphan, C. G. Hoot, A. D. Carlson, Joseph John and J. R. Beyster, Nucl. Instr. Meth. 72, 254 (1969).

[27] Joseph John and V. J. Orphan, Gulf General Atomic Report GA-10186, June 15, 1970.

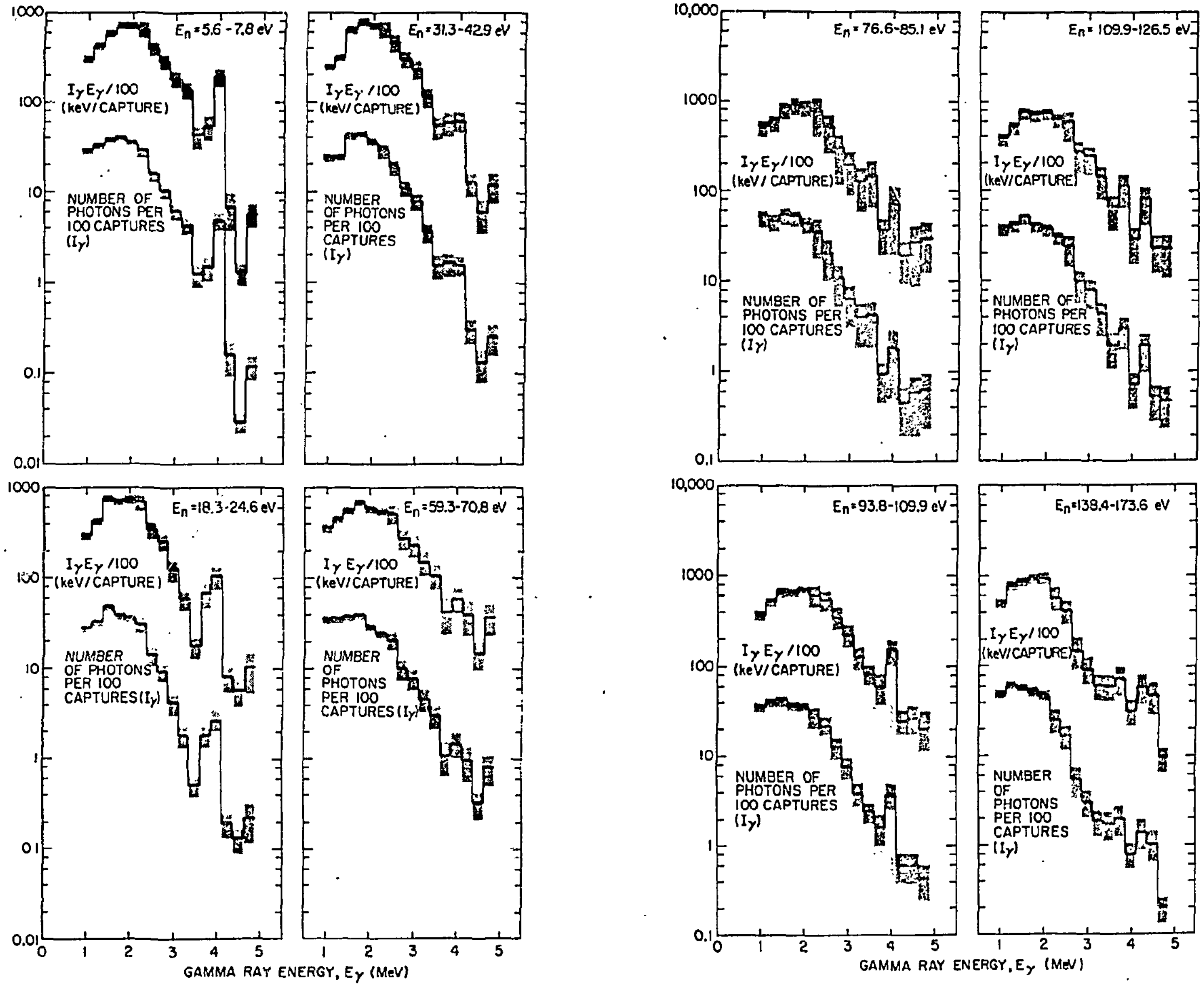

Figure A-8. Intensities of capture gamma rays grouped into 0.25-MeV bins. The fractional radiated energy are also shown. The shading represents the uncertainties in these quantities.

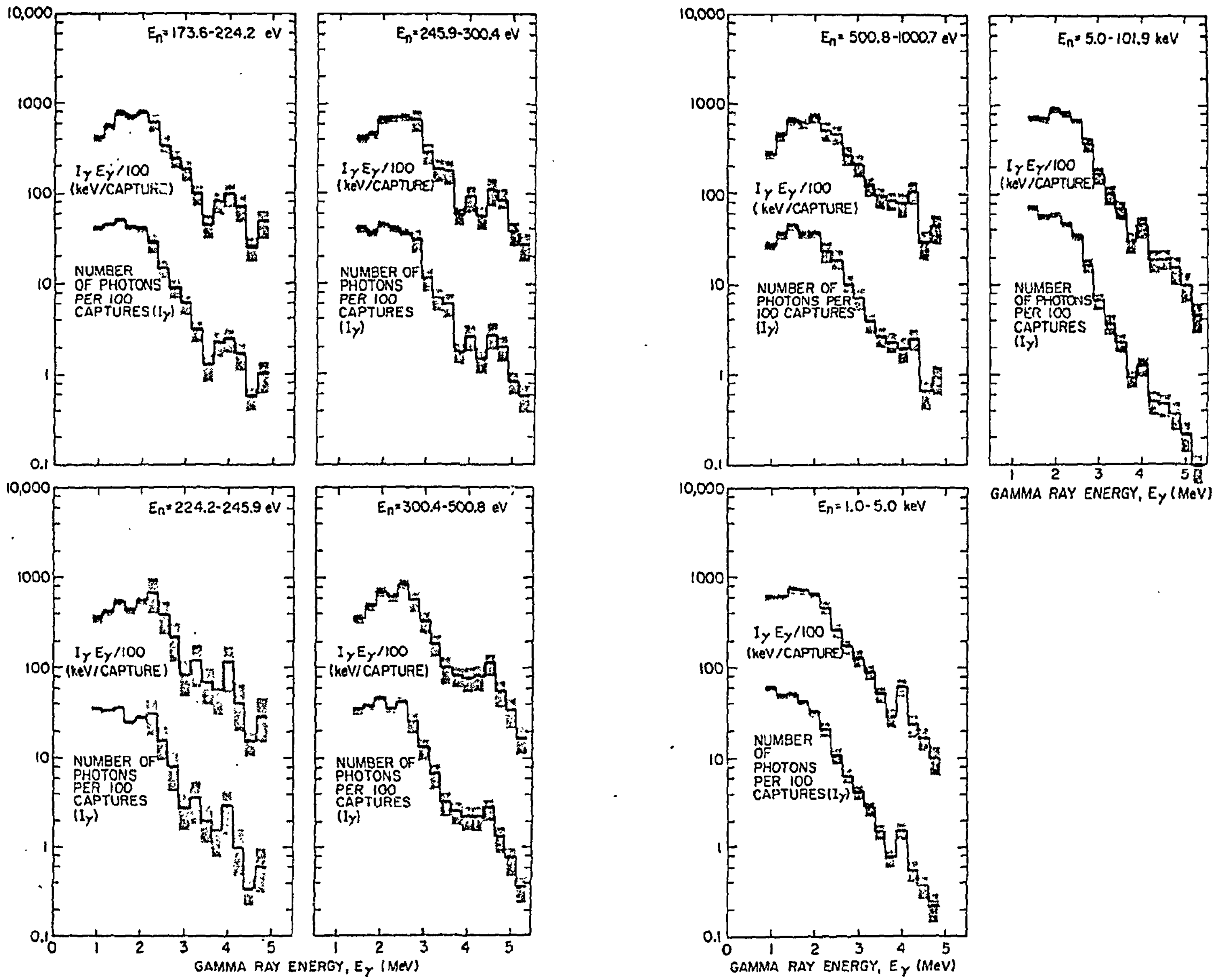

Figure A-9. Intensities of gamma rays and radiated energy for the high neutron energy groups.

6. Line and Continuum Gamma-Ray Yields from Thermal Neutron Capture in 75 Elements (V. J. Orphan, N. C. Rasmussen* and T. L. Harper*)

Thermal neutron capture gamma-ray spectral data for 75 natural elements obtained at the MIT thermal capture gamma-ray facility[28] using a Ge(Li)-NaI spectrometer have been analyzed to obtain the yield of continuum gamma rays. The results of a previous analysis of this data to determine the yield of discrete lines has been reported.[29] In the present analysis an unfolding technique[30] was applied to three-crystal pair spectrometer data to obtain the continuum yield for gamma-ray energies greater than ~ 1.5 MeV. For 27 elements (usually for Z less than ~ 30) 70% or more of the expected gamma-ray energy was observed in the resolved lines and the continuum contribution could be assumed negligible. For the remaining elements, the continuum contribution varied from 19% of the binding energy for cobalt to as much as 98% of the binding energy for europium. For over two-thirds of the elements studied, the percent of the total binding energy observed was within 100 ± 20%. The sum of the line and continuum yields were normalized to the known average binding energy for each element in order to produce a consistent set of data. The normalized yield data grouped into 250-keV bins, has been placed on magnetic tape and appropriately documented.[31]

7. Numerical and Experimental Studies of Spectral Unfolding (M. Sperling, L. Harris and H. Kendrick)

Theoretical studies of unfolding have yielded new approaches to (1) spectral estimates, (2) smoothing, and (3) errors. New numerical techniques have been developed to implement these approaches. A new unfolding code, MAZE1, has been written and tested with Monte

---

*Massachusetts Institute of Technology.

[28] V. J. Orphan and N. C. Rasmussen, Nucl. Instr. and Methods 48, 2 (1967).

[29] N. C. Rasmussen et al., Mass. Institute of Tech. Report MITNE-85, January 1969.

[30] T. L. Harper and N. C. Rasmussen, Mass. Institute of Tech. Report MITNE-104, July 1969.

[31] V. J. Orphan, N. C. Rasmussen and T. L. Harper, Gulf Radiation Technology Report GA-10248, July 1970.

Carlo data. This code is applicable to continuum unfolding in the approximate range of 4 to 200 channels. Running time for the Univac 1108 computer is about one minute for a hundred-dimensional spectrum. Positivity is strictly obeyed. Smoothing is adjusted automatically on the basis of the data error estimate. Upper and lower errors are computed separately and may be asymmetric about the spectrum. Lower error is strictly positive. The primary advance that MAZE1 represents is the ability to unfold spectral detail with higher resolution than was heretofore possible with a given detector. Experimental tests are now in progress to compare spectra unfolded with MAZE1 to spectra measured by time-of-flight. Neutrons are passed through uranium, concrete, and graphite filters and the resulting spectra are measured simultaneously by 2-in. and 5-in. NE-213 detectors in unfolding and time-of-flight modes.

IDAHO NUCLEAR CORPORATION

A. LOW ENERGY ETA MEASUREMENTS (J. R. Smith, S. D. Reeder)

The ^{233}U eta measurement at 0.26 eV, which was made with the Phoenix Core, showed much more scatter than was expected. Therefore, a set of four irradiations was performed, during the two-day Pheasant Core run of the MTR, to measure the relative value of eta for ^{233}U at 0.26 eV. The new irradiations included one run each with sample in and sample out, along with their corresponding backgrounds. Since no run was repeated, no check on reproducibility is possible, but the determination of eta agreed well with the average value from the Phoenix Core data.

The results of the measurements are shown in Table A-I. These data are the same as those shown in the previous NCSAC report, except that the ^{241}Pu data have been added. The ^{241}Pu data are being re-examined

TABLE A-I

Relative Values of Eta

Energy (eV)	$\eta(^{233}U)$	$\eta(^{235}U)$	$\eta(^{241}Pu)$
0.060	1.000	1.000	1.00
0.095	0.993 ± 0.005		
0.160	0.966 ± 0.005	0.997 ± 0.005	1.05
0.260	0.993 ± 0.013		0.91

to determine whether the rather astonishing change between 0.16 eV and 0.26 eV can be due to miscalculation of the effects of ^{241}Am in the samples. The ^{233}U points are also shown plotted along with previous measurements[1,2] in Figure A-1. In the figure the points have been normalized to the ENDF/B value of 2.293 at 0.06 eV. The latter value is probably a little high; 2.288 is a more likely number. The current set of measurements agree surprisingly well with the evaluated curve. (Pertinent to requests 358, 385 and 446, WASH 1144.)

1. J. R. Smith and E. Fast, "Conference on Neutron Cross Sections Technology", Vol. 2, p. 919, CONF 660303, USAEC (1966).

2. L. W. Weston, et al., "Neutron Fission and Capture Cross-Section Measurements for ^{233}U in the Energy Region 0.02 to 1 eV", ORNL-TM-2353, (Feb. 1, 1969).

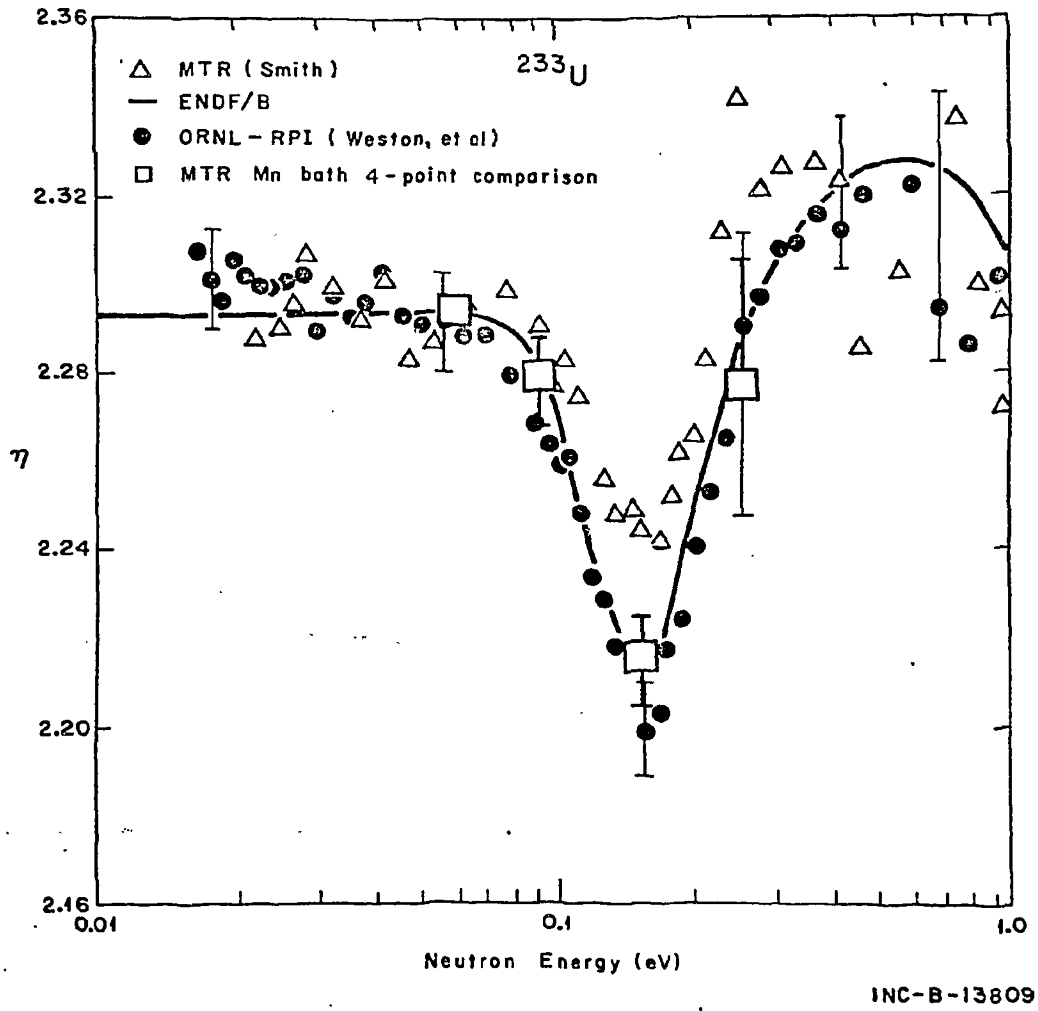

Figure A-1 The low-energy variation of eta for ^{233}U. The large squares represent relative measurements by the manganese bath technique, normalized to the ENDF/B evaluated curve at 0.06 eV.

DATA NOT FOR QUOTATION

B. NEUTRON TOTAL CROSS SECTION OF ^{175}Lu, ^{176}Lu AND NATURAL Lu (T. E. Young)

Analysis of MTR fast chopper neutron transmission measurements of natural lutetium samples and samples enriched in ^{175}Lu and ^{176}Lu have yielded values of the ^{175}Lu and natural Lu cross sections which are significantly different from those previously reported. A comparison of values obtained in this measurement and those shown in BNL-325 (August 1966) is given in Table B-I. These values were determined by assuming potential scattering cross sections of 8.26 barns for both ^{175}Lu and ^{176}Lu. Corrections for water contamination and scattering by particles of the oxide samples were used to fit the data near 1.0 eV

TABLE B-I

Thermal Cross Section Values for Lu

	σ_{nT}(b)		$\sigma_{n\gamma}$(b)	
	MTR	BNL-325	MTR	BNL-325
Lu (natural)	71 $^{+6}_{-2}$	118 ± 1	65 $^{+6}_{-2}$	108 ± 5
^{175}Lu	21.5 $^{+4.0}_{-1.0}$	~31 (graph)	15.5 $^{+4.0}_{-1.0}$	23 ± 3
^{176}Lu	2134 ±60		2129 ±60	2100 ± 150

and 0.01 eV, respectively. A discussion of corrections of this type has been given in Nucl. Sci. and Engr., 40, 389 (1970). Metal samples are needed to determine if the corrections made are valid in this case.

C. SEARCH FOR THE PROPOSED 0.3-y ISOMER IN ^{241}Pu (L. A. Kroger, C. W. Reich, L. D. McIsaac, S. D. Reeder, D. K. Oestreich, J. R. Berreth, O. D. Simpson, F. B. Simpson)

The search for the proposed 0.3-y isomeric state in ^{241}Pu continues. Conclusive proof that the reactivity effect observed by Nisle and Stepan[1] (if indeed it is a real one) does not arise from spontaneous fission has been provided by a radiochemical analysis. If the reactivity effect is indeed due to spontaneous fission, long-lived fission products should be present in the sample. Fortunately, several samples of the shavings produced during the fabrication of the original sample of Nisle and Stepan (and hence not irradiated during their measurements) were available. Radiochemical analysis of these shavings for ^{137}Cs and ^{144}Ce-^{144}Pr was performed. In two of the samples ^{137}Cs in approximately the expected amount ($\approx 10^{10}$ atoms) was detected

1. R. G. Nisle and I. E. Stepan, Nucl. Sci. and Engr. 39, 257 (1970).

DATA NOT FOR QUOTATION

but no evidence was found for the expected ^{144}Pr (from the decay of 285-d ^{144}Ce). Analysis of a third sample, however, carried out under special conditions to avoid possible ^{137}Cs contamination from external sources, revealed no detectable ^{137}Cs (<1/100 the concentration expected from the magnitude of the reactivity effect). Consequently, it must be concluded that the effect, if real, observed by Nisle and Stepan does not arise from spontaneous fission.

In order to investigate the remaining possible explanation for the effect (i.e. the existence of a sample component with a large thermal-neutron cross section) measurements of the low-energy (0.01-0.3 eV) total cross section of a 0.4-g portion of a "freshly" irradiated sample of ^{240}Pu were carried out. The ^{240}Pu sample enclosed in a thick (0.2") Cd covering, had been irradiated for $\approx$6 weeks in the core of the ETR. After irradiation, the sample was chemically purified and an isotopic analysis was performed. The isotopic composition of the Pu in the sample is as follows: ^{239}Pu (0.74%); ^{240}Pu (96.15%); ^{241}Pu (2.93%); and ^{242}Pu (0.19%). Two cross-section measurements were made approximately four months apart using the MTR fast chopper, beginning roughly six months after the irradiation. The analysis of these data is currently in progress, and the results may shed some light on the question of the existence of an isomer with a large slow-neutron cross section. (Pertinent to request 470, WASH 1144.)

C. CROSS SECTIONS FITTING TECHNIQUES (O. D. Simpson, N. H. Marshall, J. R. Smith)

The Automated Cross Sections Analysis Program (ACSAP) has been modified to increase its speed and to improve its versatility in the analysis of different types of data. A movie was produced to illustrate the operation of ACSAP in conjunction with the graphic display system SCØRE.

D. INTEGRAL CROSS SECTION MEASUREMENTS IN THE CFRMF (J. J. Scoville, Y. D. Harker, D. A. Millsap, R. G. Nisle, D. A. Pearson, J. W. Rogers)

The Coupled Fast Reactivity Measurement Facility (CFRMF) was designed and built for the purpose of measuring integral cross sections in an energy region important to fast reactor designs. The spectrum in the facility has been extensively studied by proton-recoil spectrometry, multiple foil techniques and calculations employing both transport and diffusion theory reactor codes. The results of these studies are plotted in Figure D-1. It should also be noted that the proton-recoil data above 1 MeV are subject to wall and edge effects in the proportional counter which have not as yet been corrected for. With these two considerations in mind, it is possible to say that the calculated spectrum is in quite good agreement with that determined by experiment.

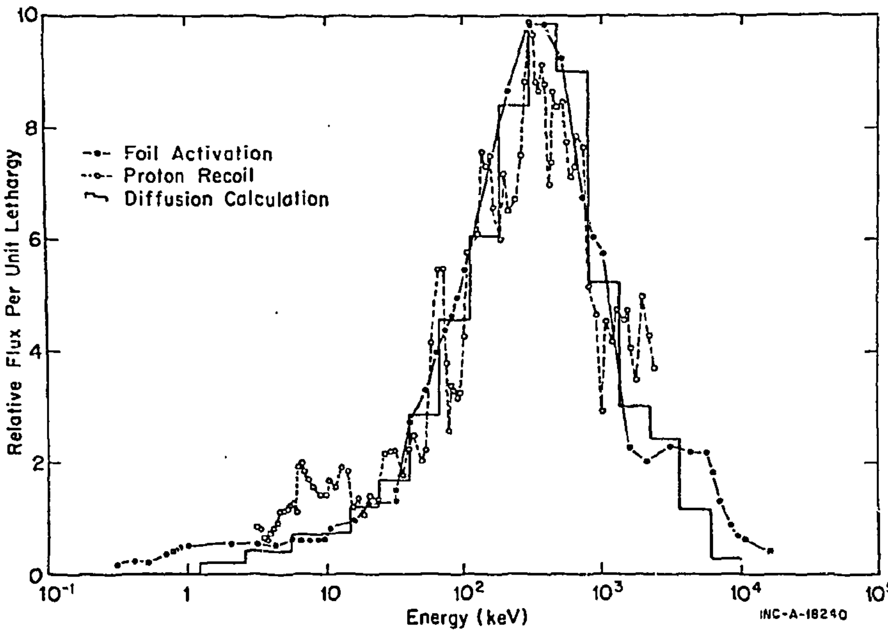

Figure D-1 CFRMF neutron spectrum as determined by foil activation, proton-recoil and diffusion calculations.

Relative reaction rates, considering gold as a standard, have been measured by activation analysis in this facility. These same reaction integrals may be calculated by numerically integrating the materials capture cross section over the CFRMF spectrum. Results and comparisons are given in Table D-I. The materials chosen for this initial series of measurements are either fission products or reactor structural materials that are readily activated and analyzed by gamma spectroscopy techniques. The calculated values listed under the column heading, CCDN-NW/10 are determined from the work of Benzi, et al. reported through the EANDC consisting of capture cross sections as predicted by nuclear model considerations.

Reactivity measurements on an assortment of materials were made as a test of both the ENDF/B data available for these materials, and the mathematical model used in the CFRMF analysis. Table D-II lists these results. The calculated values were determined by the eigenvalue difference technique. Because of the complexity of the reactivity calculation, it is difficult to relate discrepancies between measured and calculated values to specific cross section errors. However, the

TABLE D-I

Reaction	Relative Reaction Integrals			Comments
	Measured	BNL-325	CCDN-NW/10	
$^{63}Cu(n,\gamma)^{64}Cu$	0.085			Secondary Standard
$^{89}Y(n,\gamma)^{90m}Y$	8.8×10^{-4}		0.034	Metal Chips
$^{93}Nb(n,\gamma)^{94}Nb$	0.42	0.36	0.33	Metal Powder
	0.46			5 mil Foil
$^{98}Mo(n,\gamma)^{99}Mo$	0.137	0.18	0.14	Metal Powder
$^{103}Rh(n,\gamma)^{104m}Rh$	0.081	0.84	0.89	10 mil Wire
$^{103}Rh(n,\gamma)^{104g}Rh$	0.86			10 mil Wire
$^{139}La(n,\gamma)^{140}La$	0.046	0.061	0.055	Oxide Powder
$^{140}Ce(n,\gamma)^{141}Ce$	2.2×10^{-3}		0.047	Oxide Powder
$^{141}Pr(n,\gamma)^{142}Pr$	0.19	0.16	0.14	Oxide Powder
$^{142}Ce(n,\gamma)^{143}Ce$	0.046		0.074	Oxide Powder
$^{158}Gd(n,\gamma)^{159}Gd$	0.45	0.53	0.56	2 mil Foil
$^{159}Tb(n,\gamma)^{160}Tb$	2.22		2.27	Oxide Powder
$^{160}Gd(n,\gamma)^{161}Gd$	0.23		0.35	2 mil Foil
$^{165}Ho(n,\gamma)^{166g}Ho$	1.50	2.04		Oxide Powder
$^{181}Ta(n,\gamma)^{182}Ta$	1.23	1.00		Metal Powder
$^{186}W(n,\gamma)^{186}W$	0.36	0.23		5 mil Foil

TABLE D-II

SAMPLE	SAMPLE REACTIVITY, $\frac{\Delta K}{K} \times 10^{-6}$	
	Calculated	Measured
Be	-103.2	-103.0
C	- 54.7	- 49.3
Mg	- 42.2	- 20.3
Al	- 20.2	- 19.1
Mo	- 33.6	- 35.3
Pb	- 9.6	- 11.8
Bi	- 9.9	- 9.2
Au	- 18.79	- 18.85

importance of this kind of measurement is illustrated in the fact that seven of the eight materials are predicted quite well. An obvious, though still preliminary conclusion is that there is an error in the magnesium data included in ENDF/B. A more general conclusion is that the CFRMF offers a new and inexpensive method of data testing in a well-known FBR-type reactor spectrum, through the use of both activation and reactivity measurements.

E. ELECTROMAGNETIC MASS SEPARATOR (J. J. Scoville, Y. D. Harker)

The electromagnetic mass separator for the Fast Reactor Constants program has been ordered. In September 1970, Nucletec, S.A. of Geneva, Switzerland was awarded the contract to construct two mass separators, one for LASL and one for Idaho Nuclear Corporation. Our share of the purchase price is approximately $85,000.00 excluding shipping and installation charges.

Our separator is a 90° sector magnet, line focusing machine capable of beam currents in the hundreds of microamps. At these currents the resolving power will be at least 2000. Recent developments at CERN are being incorporated into the design; these improvements will eliminate aberrations in the ion lens systems and the need for continual alignment adjustments.

The machine will be used primarily to separate radioactive isotopes of the fission products. The separated samples will then be used to measure the integral absorption cross sections of the isotopes in the fast neutron spectrum of the Coupled Fast Reactivity Measurement Facility. These integral cross sections will be used to check the experimental differential neutron cross section data and theoretical calculations in the 100 keV neutron energy region.

F. CROSS SECTIONS OF THE $^{204}Pb(n,\gamma)$ AND $^{207}Pb(n,\gamma)$ REACTIONS FOR 2-keV NEUTRONS (R. C. Greenwood, C. W. Reich)

Analysis of the 2-keV neutron capture gamma-ray spectrum obtained with a natural lead target has been completed.

In order to obtain absolute capture cross sections for lead we had used ^{10}B and ^{197}Au monitor foils in the experiments. However, using a cross section value of 13.8 barns for the $^{10}B(n,\alpha)$ reaction, and a value of 4.8 barns for the $^{197}Au(n,\gamma)$ reaction, we found that the neutron flux values obtained from the two monitors were in serious disagreement. Since there are significant discrepancies between the keV neutron capture cross sections measured at various laboratories for ^{197}Au, and since recent neutron transmission measurements of ^{197}Au have shown definite resonance structure in this energy region, we have chosen the ^{10}B flux monitor as standard and used our experimental comparisons to provide a measurement of the $^{197}Au(n,\gamma)$ reaction cross section in the 2-keV MTR beam facility. From these data we obtain a value of (3.2 ± 0.5) barns for 2-keV neutron capture in a 5-mil thick gold foil.

The isotopic ratios of $^{204}Pb/^{206}Pb/^{207}Pb/^{208}Pb$ in the target were measured by mass spectroscopy to be 1.34/24.8/21.2/52.7 weight percent; and emission spectroscopic analysis showed that the sample contained no significant impurities (>0.1%). Both $^{204}Pb(n,\gamma)$ and $^{207}Pb(n,\gamma)$ prompt gamma-ray lines are observed in the 2-keV neutron-capture spectrum. The capture cross section for the $^{207}Pb(n,\gamma)$ reaction is simply obtained from this prompt gamma-ray spectrum because the 7.37-MeV ground-state transition is the only E1 transition which can occur as a result of s-wave capture in ^{207}Pb. Consequently the 7.37-MeV ground-state transition is emitted in essentially all of the thermal-neutron captures and captures into the 42-keV resonance. From these measurements, a cross-section value of (3.4 ± 1.2) mb was obtained for 2-keV neutron capture in ^{207}Pb.

Detailed studies of the thermal-neutron capture gamma rays from ^{204}Pb have been reported by Jurney et al.[1] Comparison of our 2-keV and these thermal-neutron capture data show gross differences in the features of the spectra. Although many of the same primary gamma-ray transitions are seen in both spectra their relative intensities are quite different. For example, a 6157-keV transition populating the 576-keV level in ^{205}Pb is one of the strongest transitions observed with 2-keV capture but is absent in the thermal-neutron capture spectrum. The prompt gamma rays resulting from 2-keV neutron capture in ^{204}Pb are shown in Table F-I together with their partial production cross sections, $\sigma_{\gamma i}$. Since the transitions shown probably represent the majority of the primary transitions we can estimate the 2-keV neutron capture cross section in ^{204}Pb as (1.6 ± 0.4) b. Such a large cross-section value is reasonable since the 2-keV neutron energy distribution (700 eV FWHM) overlaps two strong resonances in ^{204}Pb at 1.68 keV and 2.48 keV.

1. E. T. Jurney, H. T. Motz and S. H. Vegors, Jr., Nucl. Phys. A94, 351 (1967).

TABLE F-I

High Energy Prompt Gamma Rays Resulting From 2-keV Neutron Capture in ^{204}Pb

Gamma-Ray Transition Energy (keV)[a]	Gamma-Ray Intensity[a]	Partial Production Cross Section (barns)[a]	Level Energy (keV)[a]
6731.2 (7)	100 (3)	0.40 (8)	2.3
6471.6 (10)	9 (2)	0.04 (1)	261.9 (8)
6157.2 (8)	58 (5)	0.23 (5)	576.3 (3)
5929.2 (12)	28 (4)	0.11 (2)	804.3 (10)
(5361)[b]	<13	<0.05	
5115.8 (8)	34 (4)	0.14 (2)	1617.7 (4)
4985.3 (8) (?)	45 (5)	0.18 (2)	1748.2 (4) (?)
(4922)[b]	<13	<0.05	
4815.1 (9)	22 (3)	0.09 (1)	1918.4 (6)
(4647)[b]	<13	<0.05	
4615.8 (11)	15 (3)	0.06 (1)	2117.7 (9)
(4382)[b]	<13	<0.05	
(4372)[b]	<13	<0.05	
(4247)[b]	<16	<0.06	
(4180)[b]	<16	<0.06	
(4168)[b]	<16	<0.06	
(4101)[b]	<23	<0.09	
(3574)[b]	<23	<0.09	

[a] Uncertainties in the last digit (or digits) are shown in parentheses after each value.

[b] These transitions were observed in thermal-neutron capture (ref. 1). However, here we are only able to assign upper limits on their intensities.

G. NEUTRON CAPTURE GAMMA-RAY STUDIES USING THE 2-keV NEUTRON BEAM FACILITY (R. C. Greenwood, C. W. Reich)

The measurement of neutron capture gamma-ray spectra to obtain data relevant to problems of fast reactor shielding is continuing. The primary tool thus far used in these studies has been the 2-keV neutron beam facility of the Materials Testing Reactor.

The 2-keV neutron capture gamma-ray spectrum of manganese has been shown in a previous report[1]. As shown in Table G-I absolute prompt gamma-ray intensities have now been determined by using the 846-keV gamma ray emitted in the β^- decay of 2.58-hr ^{56}Mn as an intensity standard. The thermal neutron capture gamma-ray intensities shown in Table G-I are in generally good agreement with earlier measurements. In all cases where the thermal and 2-keV capture lines are both seen, it was observed that the 2-keV capture line had an energy which was approximately 2-keV higher than that of the thermal capture line, confirming that these lines are indeed primary transitions. From summing these primary gamma-ray intensities we find that 87% of the thermal and 70% of the 2-keV primary transition strength is accounted for by the transitions listed in Table G-I. These are the primary transitions that generally constitute the hard gamma-ray component and are therefore most difficult to shield against. Another method of quantitatively identifying the fraction of capture gamma-ray intensity which has been measured in a spectrum is to define

$$\text{Percentage of total transition intensity} = \frac{1}{E_B} \sum I_\gamma E_\gamma$$

where E_B is the capturing state energy and I_γ and E_γ are the absolute intensity and energy of a prompt gamma ray. Using this definition, one finds that the percentage of total transition intensity, from Table G-I, for thermal and 2-keV neutron capture are 70% and 60%, respectively.

The 2-keV and thermal neutron capture gamma-ray data from copper have now been analyzed. Figure G-1 shows a comparison of these spectra. In Table G-II their relative prompt gamma-ray intensities are compared. In this table the relative prompt gamma-ray intensities have been normalized in the following two ways:

1. such that $I_\gamma = 100$ for the same gamma-ray transition in both thermal and 2-keV neutron capture,

---

1. R. C. Greenwood, R. A. Harlan, C. W. Reich, IN-1317, p. 116 (1970).

TABLE G-I

Comparison of Prompt Gamma-Ray Intensities Resulting From 2-keV and Thermal Neutron Capture in Manganese

Gamma-Ray Energy (keV)[a]	I_γ (γ's per 100 Neutrons Captured) Thermal Neutron Capture	2-keV Neutron Capture	Gamma-Ray Energy (keV)[a]	I_γ (γ's per 100 Neutrons Captured) Thermal Neutron Capture	2-keV Neutron Capture
7270.3	3.6	1.4	4949.6	1.7	
7243.6	11.9	0.4	4907.6	0.8	0.6
7159.7	5.6		4875.0	0.6	
7057.9	10.8	21.8	4841.4	0.6	
6929.0	2.3	3.0	4833.8	0.8	
6817.9[b]		5.1	4827.8	0.9	
6784.0	3.1	3.9	4725.0	2.5	0.7
6731.6[b]		0.7	4689.4	0.9	1.1
6554[b]		0.6	4643.7	0.8	
6430.2	0.7	3.1	4588.7	0.4	
6276[b] (?)		0.2	4566.7	1.8	
6104.4	1.8		4550.3	0.6	1.0
6031.1	0.6	1.4	4445.5	0.5	1.7
5921.0	0.8	0.6	4440.5[b]		0.6
5761.4	1.8	1.9	4267.8	0.5	
5527.1	6.3	7.6	4253.6		0.7
5437.6	1.0		4230.0	0.3	
5432.6	0.9	1.4	4222.8	0.6	
5404.0	0.4	0.7	3927.4	0.4	1.2
5254.0	1.2	2.6	3920.1	0.3	
5198.6	0.8		3820.3	0.4	
5192.2[b]		1.1	3814.1	0.8	
5181.1	3.5	0.9	3685.6	0.9	
5111.4	0.3	1.4	3408.5	2.7	
5067.7	2.7		3002.3	0.6	
5034.6	0.9	0.9			
5014.6	5.5	1.6			

a. The thermal neutron capture gamma-ray energies are listed here, the corresponding 2-keV neutron capture gamma rays have energies which are 2 keV higher than these.

b. These energies are those determined from the 2-keV capture gamma-ray data only.

TABLE G-II

Comparison of Prompt Gamma-Ray Intensities Resulting From 2-keV and Thermal Neutron Capture in Copper

Gamma-Ray Energy (keV)[a]	Relative Intensities: Thermal Neutron Capture	Relative Intensities: 2-keV Neutron Capture $I_\gamma(1)$	Relative Intensities: 2-keV Neutron Capture $I_\gamma(2)$[b]	Gamma-Ray Energy (keV)[a]	Relative Intensities: Thermal Neutron Capture	Relative Intensities: 2-keV Neutron Capture $I_\gamma(1)$	Relative Intensities: 2-keV Neutron Capture $I_\gamma(2)$[b]
7916.8	100	100	17.6	5259.6	3.0		
7757.7	5.5			5246.8	4.0		
7638.8	50	115	20.3	5190.4	2.3		
7573.1	5.8	17	3.0	5045.0(D)	4.2		
7308.3	28.0	130	22.9	5021.9[c]		29	5.1
7254.2	12.7			4986.4[c]		19	3.3
7188.5[c]		19	3.3	4902.1	1.4	64	11.3
7177.7	7.7	88	15.5	4794.4[c]		78	13.8
7041.0[c]		90	15.9	4731.4[c]		27	4.8
6990.0	10.3			4659.6	2.5	25	4.4
6792.6	1.3			4477.6	1.7	62	10.9
6681.6	7.3	11	1.9	4444.9[c]		18	3.2
6676.4	5.9	114	20.1	4386.2	2.1		
6619.2	3.2	70	12.3	4327.5	1.3	13	2.3
{6599.0[c]		177	31.2	4321.4	4.5	30	5.3
{6601.7(D)	8.2			4314.1	1.3		
6481.3[c]		26	4.6	4207.1[c]		19	3.3
6419.9[c]		115	20.3	3712.0[c]		37	6.5
6396.1	4.4	41	7.2	3616.0	1.1		
6322.5	1.2			3590.7	1.6		
6244.6	1.4			1559.7	3.4		
6064.9	1.9	23	4.1	1320.4	3.3	137	24.2
6012.4	4.9	53	9.3	1159.5	3.0		
5855.6	1.2			1039.4	6.3		
5772.9	1.8	22	3.9	878.4	4.2	91	16.0
5731.4[c]		44	7.8	822.4	2.7		
5637.2	1.3	12	2.1	767.8	2.6		
5616.6	1.4	8	1.4	663.0	7.2		
5531.0[c]		22	3.9	648.9	8.9	64	11.3
5419.6	5.7			608.9	23.8	266	47
5414.0[c]		15	2.6	579.9	7.4	103	18.2
5321.5	3.4						

a. Thermal neutron capture gamma-ray energies are listed here for $E_\gamma > 3.5$ MeV the corresponding 2-keV neutron capture gamma rays have energies which are 2 keV higher than these, while for $E_\gamma < 3.5$ MeV the energies are all identical.

b. Normalized so that $\Sigma I_\gamma(2)$ for $E_\gamma > 3.5$ MeV is identical to the corresponding intensity sum for thermal neutron capture.

c. Energy value determined from the 2-keV capture gamma-ray data only.

DATA NOT FOR QUOTATION

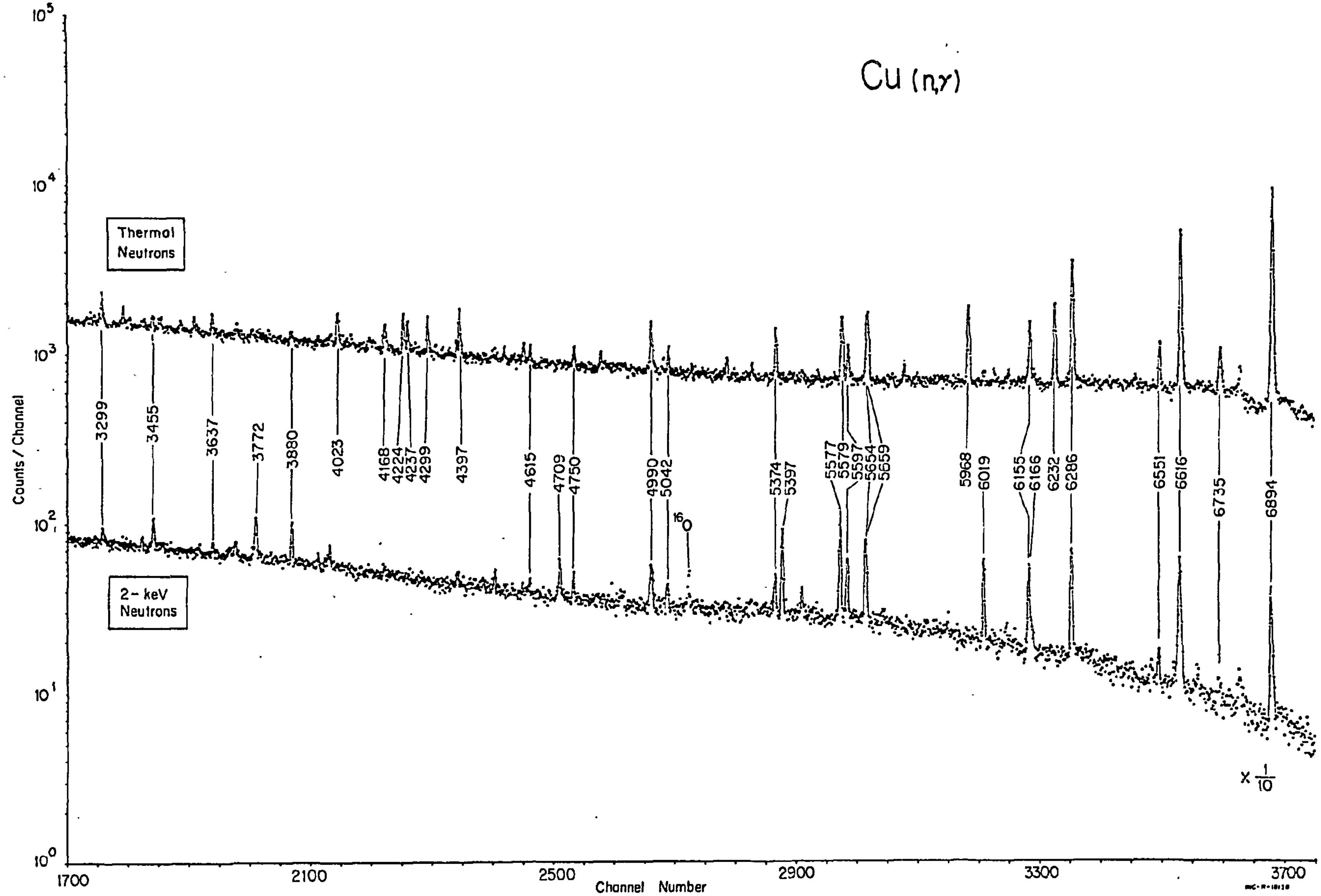

Figure G-1 A comparison of the high energy portions of the prompt gamma-ray spectra resulting from 2-keV and thermal neutron capture in copper. The energies shown for the peaks in this spectrum are the double-escape peak energies obtained for the thermal neutron capture data, except for those lines which are seen only in the 2-keV spectrum.

2. such that ΣI_γ for E_γ > 3.5 MeV is identical in both thermal and 2-keV neutron capture data.

Since, in this case, the prompt gamma-ray transitions shown in Table G-II with E_γ >3.5 MeV are probably all (or nearly all) primary transitions and should represent most of the total primary capture gamma-ray intensity, this second comparison of relative intensities should provide a more realistic comparison of the prompt gamma-ray intensity distributions. This comparison shows that the gamma-ray intensity distributions in the thermal and 2-keV neutron capture gamma-ray spectra are significantly different. In the former case much of the gamma-ray intensity (approximately 60%) is concentrated in a few gamma-ray transitions with E_γ > 7.0 MeV while in the latter case the gamma-ray spectrum is somewhat softer. It is interesting to note that the 2-keV neutron capture gamma-ray spectrum in Figure G-1 appears to result almost entirely from the $^{63}Cu(n,\gamma)$ reaction. No lines have been identified in this spectrum which can positively be associated with the $^{65}Cu(n,\gamma)$ reaction. This dominance of the $^{63}Cu(n,\gamma)$ reaction is probably quite reasonable because there is a major $^{63}Cu(n,\gamma)$ resonance at 2.06 keV while the closest $^{65}Cu(n,\gamma)$ resonance is at 2.55 keV, that is just outside the range of the neutron energy distribution in the 2-keV beam.

H. FILTERED BEAMS AS STANDARD SOURCES OF keV NEUTRONS (O. D. Simpson, J. R. Smith)

The important properties of the scandium, iron and silicon filtered beams are summarized in Table H-1. Beam intensities listed are for installation in a high-flux beam hole of the Materials Testing Reactor with reactor power at 40 MW. Some departures from the listed values may be expected when final optimization of the filters is realized.

TABLE H-1 - Preliminary Values

	Scandium	Iron	Silicon
Energy (keV)	2	24.5	144
FWHM (keV)	0.7	1.8	30-50
Beam Diameter (in.)	1/8 to 1	1/4 to 4	1/4 to 4
Maximum Intensity (neut/sec)	1×10^7	4×10^7	$\sim 10^9$
Flux (neut/sec/cm^2)	5×10^6	6×10^5	$\sim 10^7$
Gamma Intensity (mR/hr)	<1	<2	~500
Filter Thickness (in.)	42 Sc (99.9%) 9/16 Ti	26.84 Fe (99.7%) 8.22 Al 2.31 S	40 Si (99.999%) 4 Pb 1/8 $^{10}B_4C$

These filtered beams constitute a distinctive set of sources for the keV neutron region. They offer constant, collimated neutron beams of high intensity for their energy region. They comprise a matched set of sources for internormalization of measurements in three important sectors of the keV energy ranges, 2, 24.5 and 144 keV. This means that effects of temperature changes and sample thickness variations can be studied with excellent statistical precision. While the energy resolution is wider than that of some facilities, there is no instrument capable of resolving all the detailed structure encountered in the keV region. The filtered beams really represent an intermediate case between differential and integral measurements, and will be of great help in resolving discrepancies between these two types of measurements.

A high intensity neutron radiography and rabbit irradiation facility is under construction for the Advanced Testing Reactor (ATR). This facility will also be available for filtered beam experiments. Neutron beam intensities should be similar to those given in Table I-1. With the availability of the ATR we will soon be in a position to offer the facilities as true standards for the keV energy region.

I. ACTIVATION CROSS SECTION MEASUREMENTS FOR Au AT 25 keV
(R. L. Tromp)

Activation cross section measurements for Au have been made in the MTR 25 keV neutron filtered beam. Stacks of gold foils were activated in the beam and then the individual foils were gamma-counted to obtain specific activity as a function of sample thickness. These results showed appreciable resonance self-shielding. The purpose of these measurements was to see if theoretical predictions could describe the resonance self-shielding effects. Figure I-1 shows the comparison of the experimental data with the theoretical predictions of the FACE[1] code. Good agreement was obtained. It would also be interesting to do similar measurements as a function of temperature.

1. W. R. Bohl and W. K. Foell, Integral-Transport Analysis of Resonance Absorption Measurements in Neutron Beams, presented at the ANS November 1970 Meeting.

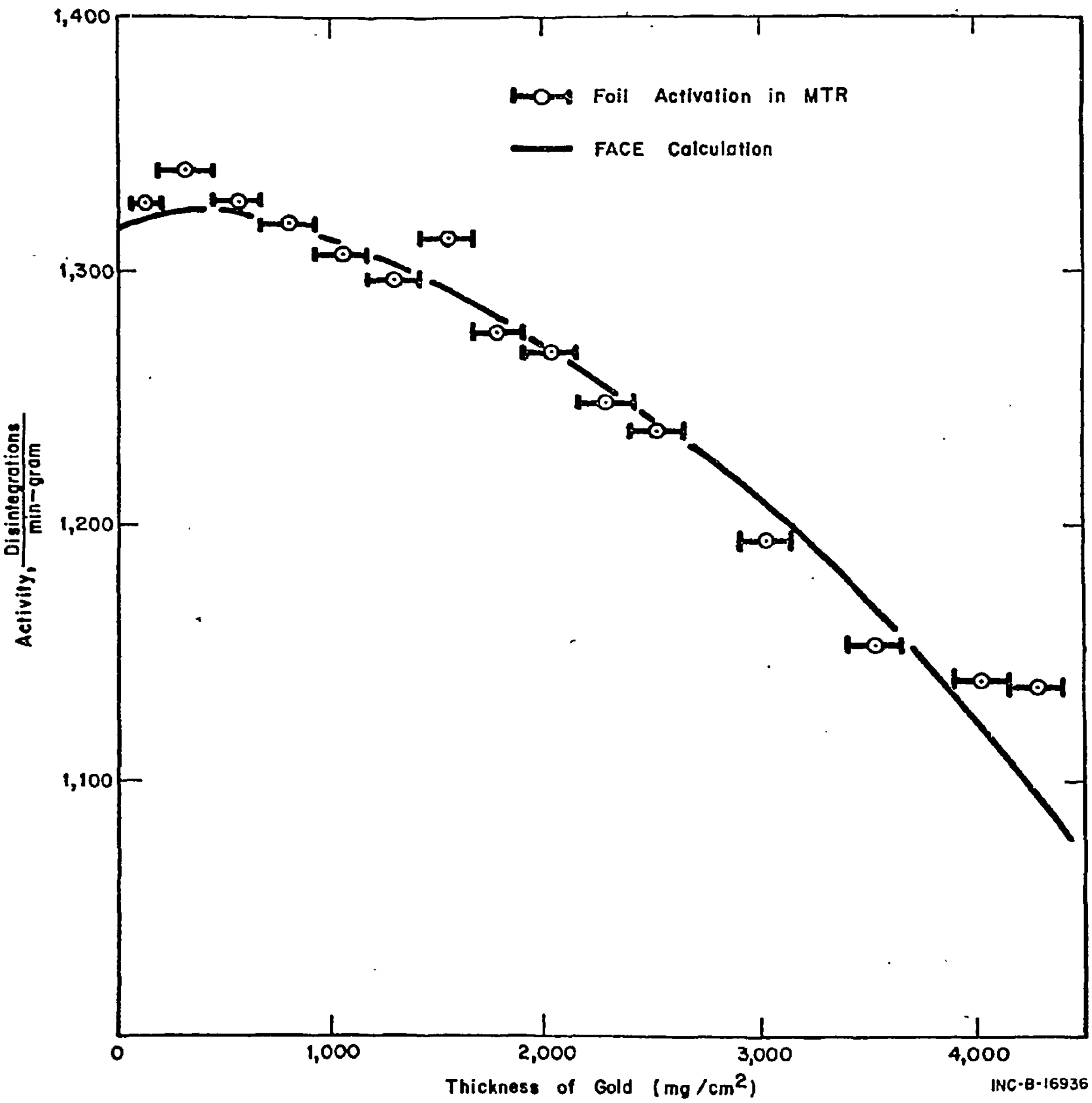

Figure I-1 Activation of stacked gold foils as a function of sample thickness vs. "FACE" code theoretical prediction.

DATA NOT FOR QUOTATION

LAWRENCE RADIATION LABORATORY

A. NEW FACILITIES

1. 100 MeV Livermore Electron Accelerator Facility

The Livermore linear accelerator has met or exceeded all specifications with the exception of performance as a positron accelerator. The tests for positron performance have not yet begun. Full power (45 kW) electron beams are available for production of neutrons for both the below-ground and the above-ground paths. More than 95% of the beam can be transported to the above-ground neutron cell and focused to a 8mm diameter spot. The 66 and 256 M flight paths above ground and the 4-20 meter stations below ground are now operational and neutron experiments have begun.

The electron-positron beam transport system for the photonuclear system is now being tested and alighned. Electron beam has been obtained in both photonuclear experimental caves. Photonuclear experiments will begin in January 1971.

The "rabbit" facility, for isotope production and activation analysis by the (γ,n) process, is installed and experiments with it are planned for December 1970.

The accelerator is now operated from 4 P.M. to 8 A.M. for experiments five days a week. The time from 8 A.M. to 4 P.M. is devoted primarily to set-up of experiments and maintenance.

2. Cyclograaff Facility

The LRL Cyclograaff is in the final stage of assembly and beam injection from the cyclotron through the tandem accelerator is planned for March, 1971. The LRL Cyclograaff, the second to be operational within the U.S., differs from the Triangle Universities Nuclear Laboratory accelerator slightly in that the tandem accelerator is a type E-N High Voltage Engineering Corporation accelerator. This will assure proton beam energies up to 27 MeV. The present 90" cyclotron will cease operations in January, 1971, and its removal will make space available for a split pole spectrograph and other experimental apparatus. The present general purpose experimental pit associated with the 90" cyclotron will continue in use, primarily for neutron time-of-flight experiments. The Cyclograaff is installed at ground level. The beam will be transported to a horizontal center line 18 feet below the

Cyclograaff center line, which passes through the adjoining experimental cells. Initial operation of the facility is planned for the fourth quarter of FY 1971. The cyclotron injector is expected to play a dual role -- that of Cyclograaff ion source, and also a general purpose activation facility for Laboratory users who have employed the 90" cyclotron for such purposes in the past.

B. NEUTRON PHYSICS

1. Detection of Symmetric Division in Spontaneous and Thermal Neutron Induced Fission of ^{257}Fm (W. John, K. Hulet, R. W. Lougheed and J. J. Wesolowski)

Energy measurements have been made on the coincident fission fragments from the spontaneous and neutron-induced fission of ^{257}Fm. 5.10^8 atoms of ^{257}Fm obtained from an underground nuclear explosion were placed on a thin foil located between two silicon detectors. The assembly was operated in the thermal column of the Livermore reactor. The mass and energy distributions for 15,000 spontaneous fissions of ^{257}Fm show peaks in agreement with extrapolation of asymmetric fission of lighter elements. However, there are also symmetric fissions (Fig. B1) with total kinetic energies extending up to 250 MeV. The distributions for 90,000 thermal neutron-induced fissions of ^{257}Fm show a symmetric peak at 220 MeV extending up to 260 MeV. Asymmetric peaks are also observed, but some interference from ^{235}U contamination is present. The high kinetic energy of the symmetric fissions indicate that the fragments are formed with little excitation, probably as a consequence of the proximity to proton number 50 and neutron number 82. (Pertinent to request #534 of WASH-1144.)

2. Thermal-Neutron Fission Cross-Section of ^{257}Fm (J. F. Wild)

We have measured the thermal-neutron fission cross-section of 102-d ^{257}Fm by counting the fissions induced by irradiations of this isotope with thermal neutrons. The absorption of thermal neutrons by ^{257}Fm results in either fission of the excited compound nucleus, ^{258}Fm, or in radiative capture to the ground state of ^{258}Fm followed by spontaneous fission decay with a half-life of 0.4 msec. In either case, the result is the occurrence of one fission event per neutron absorbed.

We assembled a sandwich between two pieces of 1/2"-thick polystyrene of $\sim 5 \times 10^8$ atoms of ^{257}Fm, electroplated on a thin beryllium foil, and a 3-mil-thick sheet of muscovite mica to detect the emitted fission fragments. We also included a weighed piece of gold foil to serve as a flux monitor. After each irradiation, the target was quickly disassembled to reduce the background exposure of the mica to

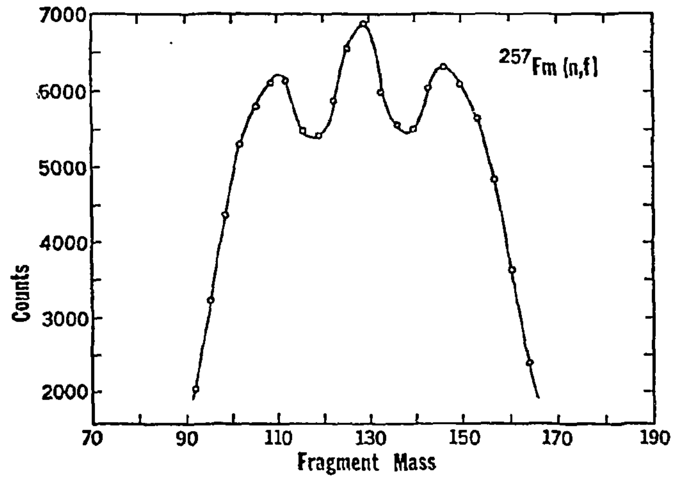

Fig. B1

DATA NOT FOR QUOTATION

fragments from the spontaneous fission decay of ^{257}Fm.

Preliminary calculations using the data obtained from five irradiations, which possibly do not include all systematic errors, indicate a value of 3080 ± 200 barns for the thermal-neutron fission cross-section of ^{257}Fm. In our experiments, it was impossible to separate those fissions occurring in the ground state of ^{258}Fm from those occurring in the excited state. Nevertheless, we have supposed from fission systematics that only a few percent result from SF following neutron capture and, therefore, the measured cross-section most likely results from direct neutron-fission reactions. Our results disagree with a value of ≥ 5600 ± 600 barns obtained by Dr. Curtis E. Bemis (private communication, August, 1970) at ORNL. (Pertinent to Request #534 of WASH-1144)

3. The Transport of 14-MeV Neutrons Through Iron (L. F. Hansen, M. Gregory, J. Kammerdiener and C. Wong)

Using the sphere transmission and time-of-flight techniques, through the neutron spectra 0.95, 2.74, and 4.72 mfp of iron have been measured. The targets were solid iron spheres of 4.46-, 12.94-, and 25.52-cm radius and the neutron source was a nominal 14-MeV neutron beam generated by the T(d,n)α reaction. The deuteron beam of 0.40 MeV energy was supplied by the ICT* accelerator facilities at Livermore and impinged on a tritium target centered at the spherical targets.

The measured neutron spectra covered the energy range from about 75 eV to 14.8 MeV. This was accomplished by using high and low energy detectors as described below. The low energy measurements covered the range from 75 eV to 1.0 MeV, while the high energy measurements went from 1.6 to 14.8 MeV. Since the experimental techniques using these two detectors were different, they will be discussed separately.

Low Energy Measurements

Neutrons with energies between 75 eV and 1 MeV were detected using a ^{6}Li loaded glass scintillator detector. The corrections for γ background in the measured neutron spectra were accurately determined using an identical ^{7}Li loaded glass scintillator. The efficiency of the ^{6}Li detector as a function of neutron energy was experimentally measured by calibrating it against a low-efficiency fission chamber.

---

*High Voltage Engineering Corp. 500-keV Insulated Core Transformer

DATA NOT FOR QUOTATION

The ^{6}Li detector was located at 769.6 cm from the center of the iron spheres and at 30° with respect to the deuteron beam line. The neutron spectra were stored in the PDP-8 computer using 512 channels. The neutron spectrum measured with a channel width of 25 nsec and which covers the energy region between 1 MeV and 14. keV is shown in Fig. B2. The peak at 3.75 μsec corresponds to the window in the iron total cross section at 24 keV.

High Energy Measurements

The energy range covered in these measurements is from 14.8- to 1.6-MeV neutrons. The neutron detectors were NE213 scintillators located at 30° and 120° with respect to the deuteron beam line. The gamma background was reduced by using the pulse shape discrimination properties of NE213. The time resolution in these measurements was around 2ns and the flight path for the emitted neutrons was 7.66 meters at 30° and 9.75 meters at 120°.

Figure B3 shows the measured neutron time-of-flight spectra at 120° plotted as function of neutron energy.

The low lying levels in iron below 2-MeV excitation energy are not resolved, because they fall under the tail of the elastic scattering peak which results from large-angle scattering. The peak at around 10-MeV neutron energy corresponds to two levels at 2.66- and 3.119-MeV excitation energy. The peak at around 8.5 MeV corresponds to the 4.50-MeV level in ^{56}Fe. This 4.5-MeV level has the largest cross section of all the inelastic levels, except the 0.845-MeV level, and it would be reasonable to assume that it is the first 3^- level in ^{56}Fe.

The analysis of these data is continuing and in the near future we hope to have a comparison of these data with calculated spectra using the Livermore Monte Carlo Neutron Transport Program, SORS. Preliminary design work for concrete spheres is finished and a pilot sphere is being fabricated. (Pertinent to Requests 99-103 of WASH-1144.)

4. Threshold Photoneutron Cross-Section Measurements (R. J. Baglan, C. D. Bowman and B. L. Berman

Measurements have been carried out for ^{52}Cr, $^{56,57}Fe$, and ^{206}Pb. Figure B4 shows the data for ^{56}Fe. The data for these and other nuclei have been analyzed for resonance parameters (for over 200 resonances) as well as other features of interest.

Evidence for doorway states in the photon channel has been obtained for ^{57}Fe at 50 and 250 keV above threshold in addition to the

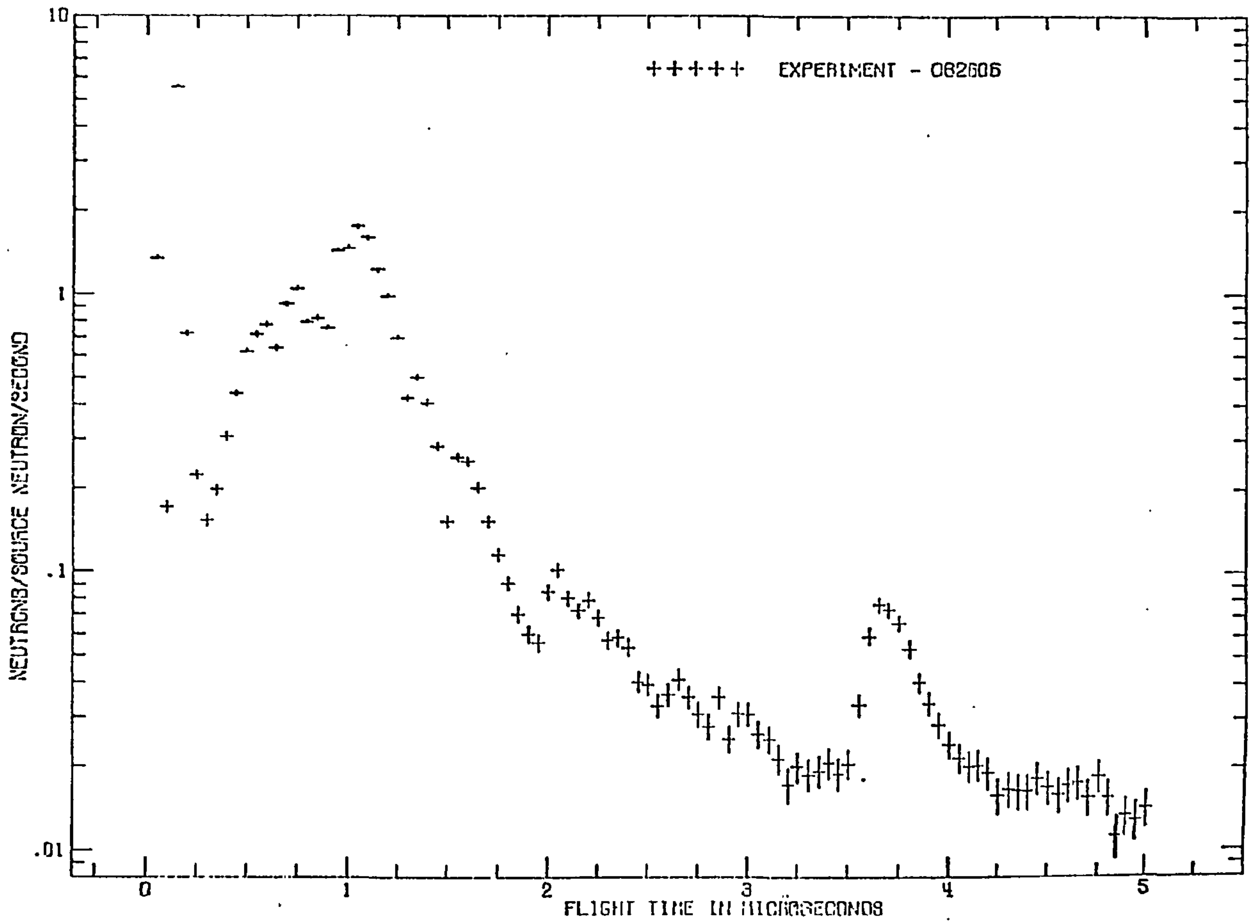

IRON -- ID-.95 CM -- OD-25.87 CM -- LO ENERGY (30 DEG) Fig. B2

DATA NOT FOR QUOTATION

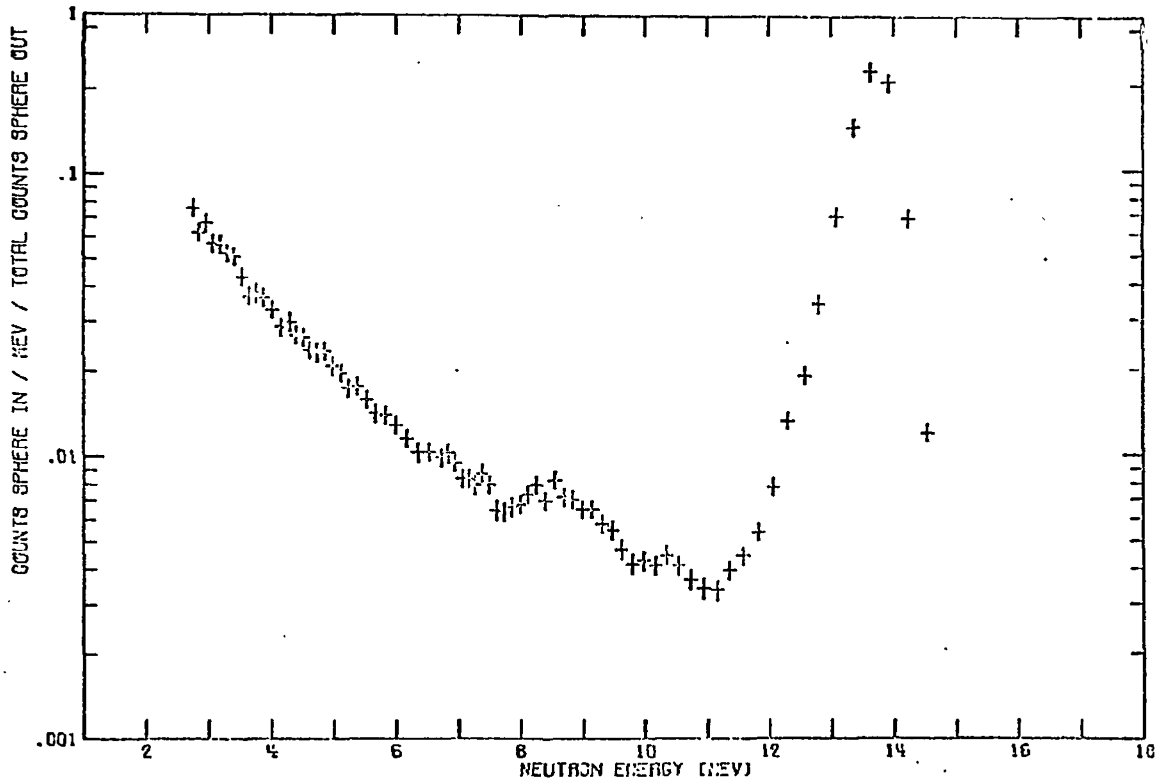

IRON -- ID-.95 CM -- OD-25.87 CM -- 120 DEG Fig. B3

DATA NOT FOR QUOTATION

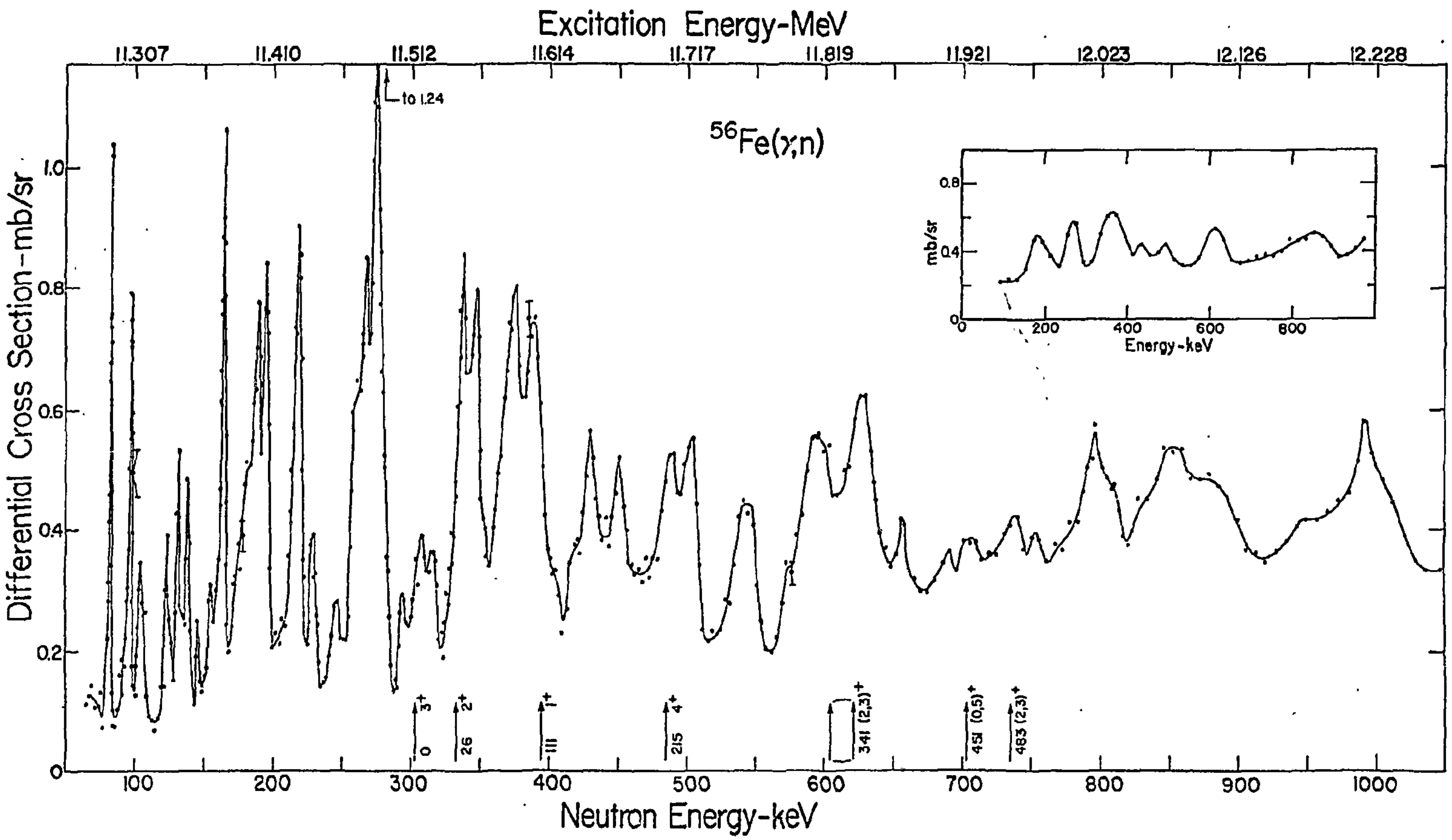

The 135° differential threshold photoneutron cross section for ^{56}Fe as a function of the laboratory energy of the emitted neutron (lower scale) and the excitation energy (upper scale). The locations, energies, and J^{π} values of isobaric analogs of low-lying states in ^{56}Mn are indicated by the arrows below the data. The inset shows the cross section averaged with a square, 40-keV wide smoothing function.

Fig. B4

previously reported cases of ^{207}Pb at 125 and 400 keV (the latter also seen in the neutron channel) and ^{208}Pb at 500 keV; the ^{208}Pb case represents the M1 giant resonance.

An attempt was made to detect the channel-resonance effect in ^{53}Cr and ^{57}Fe, which is expected to produce a correlation between neutron and γ-ray widths; no significant correlation was observed for these nuclei.[2]

An attempt was made to identify analog states in ^{52}Cr and ^{56}Fe, in addition to the previously reported case of ^{25}Mg.[5] The only successful candidate is the analog, at an excitation energy of 11.602 ± 0.005 MeV in ^{56}Fe, of the second excited state of ^{56}Mn (see Figure B4). This state has $J^{\pi} = 1^+$, is excited by an M1 transition whose strength is about 10 eV, about 1/3 of a Weisskopf unit.

A state at 7.3 keV above threshold in ^{206}Pb has a peak height of nearly 3b, which is the largest measured (γ,n) cross section in any nucleus. This resonance is fairly well isolated and possibly could be used to produce a useful source of monoenergetic 7.3-keV neutrons.

Electric-dipole strength functions $\langle\Gamma_{\gamma 0}/D\rangle_{E1}$ have been obtained for several nuclei and are given in the table. With the exception of ^{207}Pb, for which $\langle\Gamma_{\gamma 0}/D\rangle_{E1}$ is anomalously large owing to the presence of the doorway state, the values of C_1 (defined in the Table), which is proportional to the single-particle estimate of $\langle\Gamma_{\gamma 0}/D\rangle_{E1}$, are essentially constant. The values for C_2 (defined in the Table) however, which is proportional to the extrapolated-giant-resonance estimate, systematically decrease with increasing A. Hence, these data indicate a preference for the single-particle estimate of the E1 strength function. (Pertinent to Requests 92, 108, 335, 336.)

E1 strength functions.

Nucleus	$\langle\Gamma_{\gamma 0}/D\rangle \times 10^5$	$C_1{}^a \times 10^5$	$C_2{}^b \times 10^5$
^{26}Mg	3.1 ± 2.0	1.6 ± 1.0	8.8 ± 5.7
^{53}Cr	1.6 ± 0.8	1.6 ± 0.8	4.0 ± 2.1
^{57}Fe	1.1 ± 0.6	1.1 ± 0.6	2.8 ± 1.3
^{207}Pb	13 ± 7	8.1 ± 4.1	1.9 ± 0.9
^{208}Pb	4.0 ± 3.6	1.9 ± 1.7	0.4 ± 0.4

[a]Computed from the relation $\langle\Gamma_{\gamma 0}/D\rangle = C_1[E_\gamma(\mathrm{MeV})/7]^3 \ (A/100)^{2/3}$

[b]Computed from the relation $\langle\Gamma_{\gamma 0}/D\rangle = C_2[E_\gamma(\mathrm{MeV})/7]^5 \ (A/100)^{8/3}$

DATA NOT FOR QUOTATION

5. Evaluations (R. Howerton)

During the past six months, neutron cross section evaluations from 10^{-10} to 20 MeV were performed for the following materials:

Total Evaluation: Li, ^{6}Li, ^{10}B, ^{12}C, ^{14}n: Partial Evaluation: ^{1}H, B, ^{16}O, ^{27}Al, ^{55}Mn, Fe, Eu, ^{165}Ho, ^{181}Ta, W, ^{233}U, ^{235}U, ^{239}Pu; New Evaluation (single reaction): ^{54}Fe, ^{56}Fe, ^{58}Fe, ^{237}Np

A recently completed processing code (CLYDE) produces group cross sections, transfer matrices, energy depositions, isotope production cross sections and isotope destruction cross sections, for neutronic codes. No limit is placed on number of groups, order of transfer matrices, or number of input energy-cross section pairs.

Experimental neutron cross section data are routinely received from NNCSC and by private communication and incorporated into the ECSIL library. At the present time, there are about 750,000 data points in the system. This information is used for producing evaluations and to investigate systematics of neutron induced reactions.

One such study uses the 35,000 resolved resonance parameters in the ECSIL library. These data are being computer analyzed to: 1) select an evaluated set of resolved resonance parameters for an isotope; 2) determine in a consistent manner average resonance parameters, e.g., strength functions, level spacings, average resonance widths, etc., for all available isotopes; 3) investigate systematics of the averaged resonance parameters. At the current time, the study is in the second phase.

Evaluated neutron cross sections are tested by calculations, both S_n and Monte Carlo, of simple spherical critical assemblies, reflected by single materials of varying thicknesses. A computerized library of integral experiments, currently containing about 1500 references, abstracts and comments, has been developed. From this library, about 180 critical assemblies have been evaluated for use in the cross-section-checking program. As new evaluations are produced for materials used either for cores or reflectors in any of the evaluated critical assemblies, k-eff values are calculated for the appropriate assemblies. The results of these calculations are not used to adjust evaluated cross sections in order to obtain a better k-eff value but, rather to form a basis for estimating the validity of the evaluated cross sections in appropriate energy regimes and for appropriate reactions.

C. ACTIVATION ANALYSIS

1. Detection of Pb (γ,n) by Activation Analysis (M. L. Stelts and C. D. Bowman

Lead pollution of the environment is a subject of much current interest. The commonly used techniques for detection involve wet chemistry which makes the analysis both time consuming and expensive. Reactor activation analysis with thermal neutrons is a much faster and less costly technique for many elements, but it cannot be applied to lead. Preliminary experiments at the linac indicate that Pb can be detected via the ^{204}Pb (γ,n) reaction with a sensitivity of less than 100 ng of natural Pb. The experiments carried out to date are summarized below.

A sample was prepared by passing a known amount of Livermore air through a cellulose filter paper. A 1 cm^2 portion of this paper, through which 7m^3 of air had passed, was exposed to the linac bremsstrahlung beam along with a 22 mg natural lead standard sample. The bremsstrahlung was produced by a 190 μa average electron current with an energy of about 100 MeV incident on a 5 cm thick assembly of water cooled Ta plates. The irradiation of one hour can be compared with the ^{203}Pb half-life of 52 hours.

The filter paper was counted with a 20 cc coaxial Ge(Li) detector 72 hours after the end of the activation. A counting rate of 0.336 cpm for the 279.2 keV γ-ray was measured. By comparison with the 22 mg reference this activity was found to correspond to 8.7 $\pm$ .8 μg of Pb in the filter or a concentration of 1.2 $\pm$ 0.1 $\mu g/m^3$ in the air in Livermore. The national average is in the 0.5 to 2 $\mu g/m^3$ range.

Under these conditions of analysis, the estimated maximum sensitivity is about 1 μg of natural Pb. However by bombarding 10 times as long, counting one half-life earlier, using twice the beam amount and a larger Ge(Li) detector in a more efficient geometry, the sensitivity probably could be increased into the 20 to 100 ng range. However the present sensitivity is adequate for most environmental problems.

LOCKHEED PALO ALTO RESEARCH LABORATORY

A. NEUTRON PHYSICS

1. "Best-fit" $^{197}Au(n,\gamma)^{198}Au$ Cross Section for Neutron Energies from 10 to 5400 keV (F. J. Vaughn and H. A. Grench)

The basic procedure adopted in arriving at the "best-fit" cross-section curve was similar to that described in detail in WASH-1068 (hereafter referred to as WASH). Namely, only sets of data which cover a significant range of neutron energies, and therefore give information on the shape of the cross section vs. energy, were used in the analysis. These sets of data were, in general, systematically adjusted in the process of arriving at the "best-fit" curve. We define "adjustment" as the multiplication of all the cross-section data of a particular experiment by a constant factor; thus adjustment affects the magnitudes of the cross sections but not the shape of the curve of cross section vs. energy.

However, three additional extensive sets of data have become available since the former work, and these were employed in the present reduction. Another difference was that the procedure followed in WASH relied on hand calculations; the present work employed computer calculations as far as possible. The third, and major, difference between the two procedures is that different assumptions were made in arriving at the initial "standard" portion of the cross-section vs. energy curve. This writeup will give only a brief outline of the steps followed in arriving at our new "best-fit" curve.

Fourteen sets of data were used as input information; they were chosen according to the criterion referred to above, which requires that a particular set of results extend over a significant range of neutron energy. The names of the first author of the articles in which these results are presented are listed below (complete references are given later on a figure). Fricke, Poenitz, Barry, Harris, Cox, Grench (WASH), Johnsrud, Diven, Miskel, Bergqvist, Bilpuch, Gibbons, Moxon, Spitz.

Reference to a particular set of data in the following discussion will be made by giving the appropriate name from this list (except WASH).

The data in these various sets were first renormalized to take into account information which became available after publication, for example newer ^{235}U fission cross sections. The sets affected were Harris, Cox, Johnsrud, Diven, Miskel, and Gibbons. It should perhaps be noted that what we refer to as renormalization is quite different from the process of adjustment described above. Renormalization refers merely to updating results in accordance with real physical information, and renormalization factors may, of course, differ with energy. Adjustment, however, is done not on the basis of physical evidence, but as part of the mathematical procedure of arriving at the best-fit curve; as stated above, adjustment factors are not energy dependent but are constant for all the cross-section data of a particular experiment. The renormalizations for all sets except Harris are described in WASH; a description of the procedure followed for the data of Harris is given in Ref. 1.

The so-called "standard" portion of the best-fit curve in WASH was obtained by assuming that the cross sections measured relative to that for ^{235}U fission (and also the data of Barry) are correct in the energy region from 200-1000 keV. This assumption was abandoned in the present work. Various alternative procedures were tried, but the one finally adopted was based on the assumption that the results of five different methods of measurement should all have equal weight in an energy region where good data are available from all methods, and in which the cross section has a simple shape (namely, is well fit by a low-order polynomial). This "standard" energy region was chosen to be 123-560 keV. The five methods were those employed by Fricke, Poenitz, Barry, Harris, and measurement relative to the ^{235}U fission cross section as made by Cox, WASH, and Johnsrud.

An iterative procedure using a least-squares polynomial computer code was followed in arriving at the best-fit curve in the standard energy region. The reported cross-section uncertainties were first adjusted to make the total weight of the data using each of the five methods identical. Specifically, the total weights of the results of Fricke, Poenitz, Barry, and Harris were made equal, while the weights attached to the data of Cox, WASH, and Johnsrud were adjusted so each had one-third the weight of the first four sets.

Best least-squares polynomial fits to the data from these seven sets were then obtained using the code referred to above. Fits of orders 1-8 were obtained. Examination of the results indicated that the best fits were obtained with polynomials of degree two and three, so only these were employed in the iterations. The second step of the first iteration consisted of obtaining adjustment factors for each set of data to the least-squares polynomials. These adjustment factors are the constants

---

[1] Reports to the AEC Nuclear Cross Sections Advisory Committee, NCSAC-31.

DATA NOT FOR QUOTATION

by which the results of a particular set must be multiplied to give the best least-squares fit to the second- and third-degree polynomials obtained using all seven data sets. In accordance with the criterion that each method have equal weight, the set of seven adjustment factors was required to have a weighted average equal to unity. These requirements of equal weight for the various methods and a weighted-average adjustment factor equal to unity insured that the final cross-section curve in the standard region would essentially "split" the original unadjusted data, i.e., about the same number of points would be below the final curve as above.

The iterative procedure then was continued by obtaining new least-squares polynomial fits using data adjusted by the factors found in the first iteration, and then finding new adjustment factors to these polynomials. The iterations were continued until the results converged, i.e., no further changes (greater than the convergence criteria) occurred in either the polynomials or the adjustment factors. This procedure thus led to both the least-squares-fit cross-section curve (second and third degree) and to final adjustment factors necessary to make the cross sections of the seven sets lie (as well as possible) on these final curves.

The best-fit curve was then extended to energy regions above and below the 123-560 keV "standard" region. This was done using iterative procedures similar to those described above. In the energy region from 400-1800 keV (note overlapping with "standard" region), the data from the seven sets used in the 123-560 keV region, adjusted by the final factors obtained as described above, were first fit to polynomials of various degrees, using the same least-squares computer code. It was found that third- and fourth-degree polynomials gave the best fits in the 400-1800 keV region. Adjustment factors for the data of Diven and Miskel were then obtained. The iterative procedure was continued by obtaining new polynomial fits to the 9 sets of data--the 7 original with adjustment factors fixed from the "standard" region results, plus the adjusted Diven and Miskel results. The iterations were continued until the adjustment factors for Diven and Miskel converged and the final polynomials were obtained.

The best-fit curve in the 10-150 keV region (again note overlap) was obtained using a procedure similar to that employed from 400-1800 keV. In the low-energy region, however, it was found that best fits were obtained using a power law multiplied by a first- or second-degree polynomial. Again the initial fits were found by using the original data sets--adjusted by their appropriate factors from the "standard" region. One minor point should be noted; namely the data of Cox for energies in the 10-150 keV region was treated as a separate set of data from that in the region extending upward from 200 keV. This was done because Cox's measurements in the lower-energy region were relative only, and were normalized to his result relative to the ^{235}U fission cross section at 200 keV.

Adjustment factors for the data of Cox, Bergqvist, Bilpuch, Gibbons, Moxon, and Spitz were then found, using the power law times polynomial fits obtained with the data from the sets used in the "standard" region. The usual iterative technique was then followed until the adjustment factors for Cox etc. converged and final fits were attained.

A minor point which should perhaps be mentioned is that the results from three sets of data which were not used in the "standard" region extend over more than one of the three separate energy regions used in the analysis. These three sets of data are those of Diven, Miskel, and Bergqvist. For these sets, weighted-average adjustment factors were found using the factors obtained in the pertinent separate regions. It should also be noted that one result of Bilpuch and 5 of Gibbons lie in the 123-560 keV region; this was ignored since most of the data in these two sets lies in the 10-150 keV region. Adjustment factors were found from the low-energy region results only for these two sets.

Use of the techniques described above led to final adjustment factors for all fourteen sets of data. The final portion of the cross-section vs. energy curve, namely that extending above 1800 keV, was found by fitting all adjusted data to polynomials in the 1200-5400 keV region (note overlap of energy regions.) It was found that third- and fourth-degree polynomials gave the best fit.

The final best-fit cross-section curve was then obtained by combining the portions covering the separate energy regions. A small amount of hand adjustment was found necessary in order that the separate segments join smoothly. It was found necessary to use a hand fit in the region above 2500 keV because the highest-energy result of Johnsrud at 5400 keV is somewhat larger than his cross section at 4780 keV. Since these are the only two reported results in this energy region, the computer polynomial fits showed a rising cross section with increasing energy. Although this behavior of the cross section with energy may be real, it seems less probable than a monotonically decreasing behavior, and the hand fit was therefore used.

The final cross-section curve is composed of the following segments:

Energy Region (keV)	Type of Fit
10-120	Power law times 1st deg. polynomial
120-290	Hand transition
290-560	Second deg. polynomial
560-600	Hand transition
600-800	Fourth-deg. polynomial
800-1200	Hand transition
1200-2500	Fourth-deg. polynomial
2500-5400	Hand fit

It should be noted that all the hand adjustments consisted of very minor deviations from the computer-calculated fits.

The final cross-section curve is shown on Figure A-1. Figure A-2 includes all the adjusted data in addition to the best-fit curve. Table A-1 lists the final adjustment factors for the 14 sets of data employed in the analysis, while Table A-2 gives numerical values for the best-fit cross-section vs. energy curve.

A final important problem which will now be briefly discussed is that of obtaining the uncertainty of the best-fit cross-section curve. It was noted above that the iterative calculations in the various energy regions were carried out using more than one type of fit. Specifically, an attempt was made to determine the range of reasonable fits in the various regions. For example, in the "standard" energy region, 123-560 keV, fits were obtained for both 2nd- and 3rd-degree polynomials. These fits were obtained not only with the uncertainties of the individual data points adjusted so each method would have equal weight, but also using the uncertainties as reported by the various authors. In other energy regions likewise, calculations were made using various assumptions regarding the uncertainties and for more than one type of polynomial (or power law X polynomial) fit.

The results of these various types of calculations were then compared to determine the uncertainty arising from the range of reasonable fits. This uncertainty was then combined quadratically with the uncertainty of the final polynomial (or other) fit to give the relative uncertainty at a particular energy. The uncertainty of the final polynomial fit (width of the uncertainty band) was automatically calculated by the same computer code used in the iterative procedures described above. A final curve of relative uncertainty vs. energy was then obtained by drawing a smooth hand fit through the points obtained as described above; Figure A-3 shows this curve.

In order to obtain the absolute uncertainty of the best-fit curve, one must include the uncertainty in the normalization. This was obtained by examining the adjustment factors obtained in the "standard" region for the seven sets of data employed therein. It was found that the adjustment factors for 5 of these 7 sets are within 7% of unity (only that for Cox, namely .84796, exhibits a deviation significantly greater than 7%). Therefore the absolute uncertainty of the best-fit cross-section curve (in percent) at a particular energy can be obtained by a quadratic combination of 7% and the value on the relative-uncertainty curve at the appropriate energy.

Another "best fit" cross-section curve for the $^{197}Au(n,\gamma)^{198}Au$ reaction has recently been obtained by W. D. Poenitz (private communication). The techniques employed and the results obtained by Poenitz differ considerably from those we used; we plan to make a detailed examination of these differences.

DATA NOT FOR QUOTATION

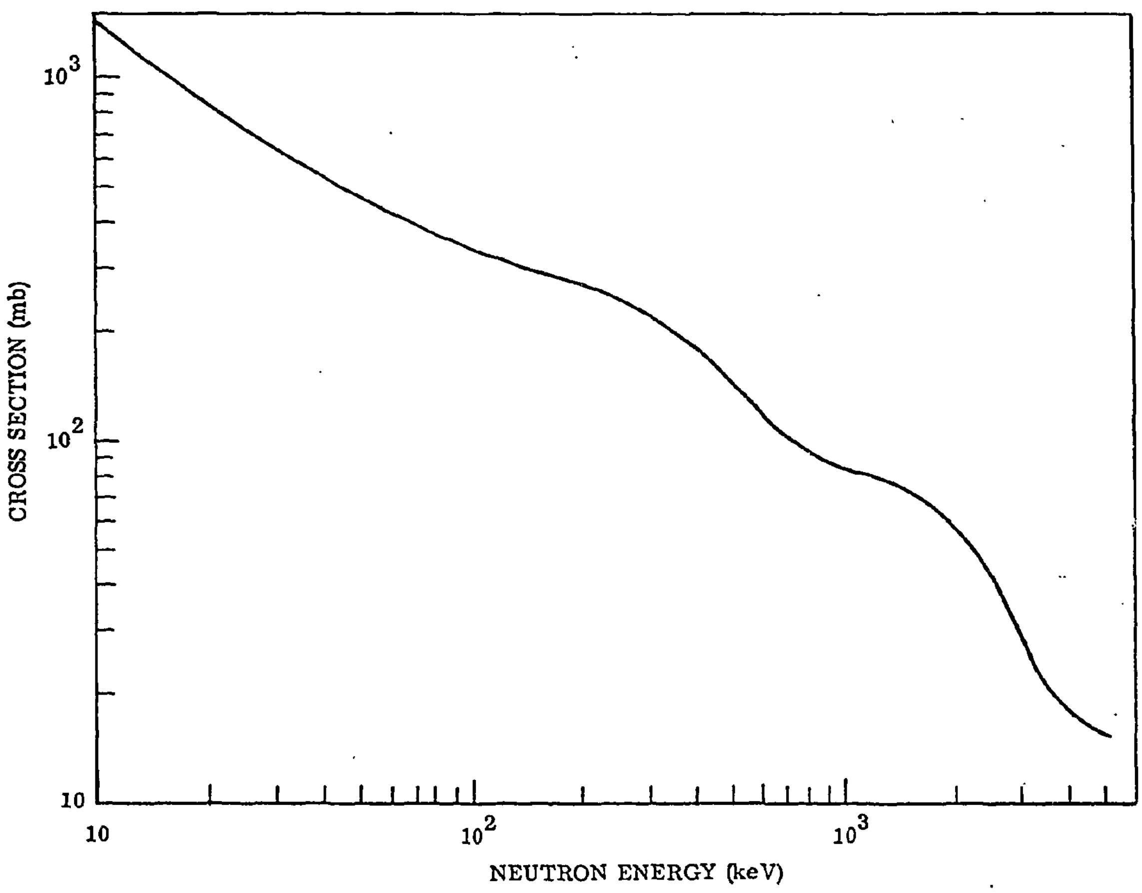

Figure A-1. "Best-fit" $^{197}Au(n,\gamma)^{198}Au$ cross-section curve.

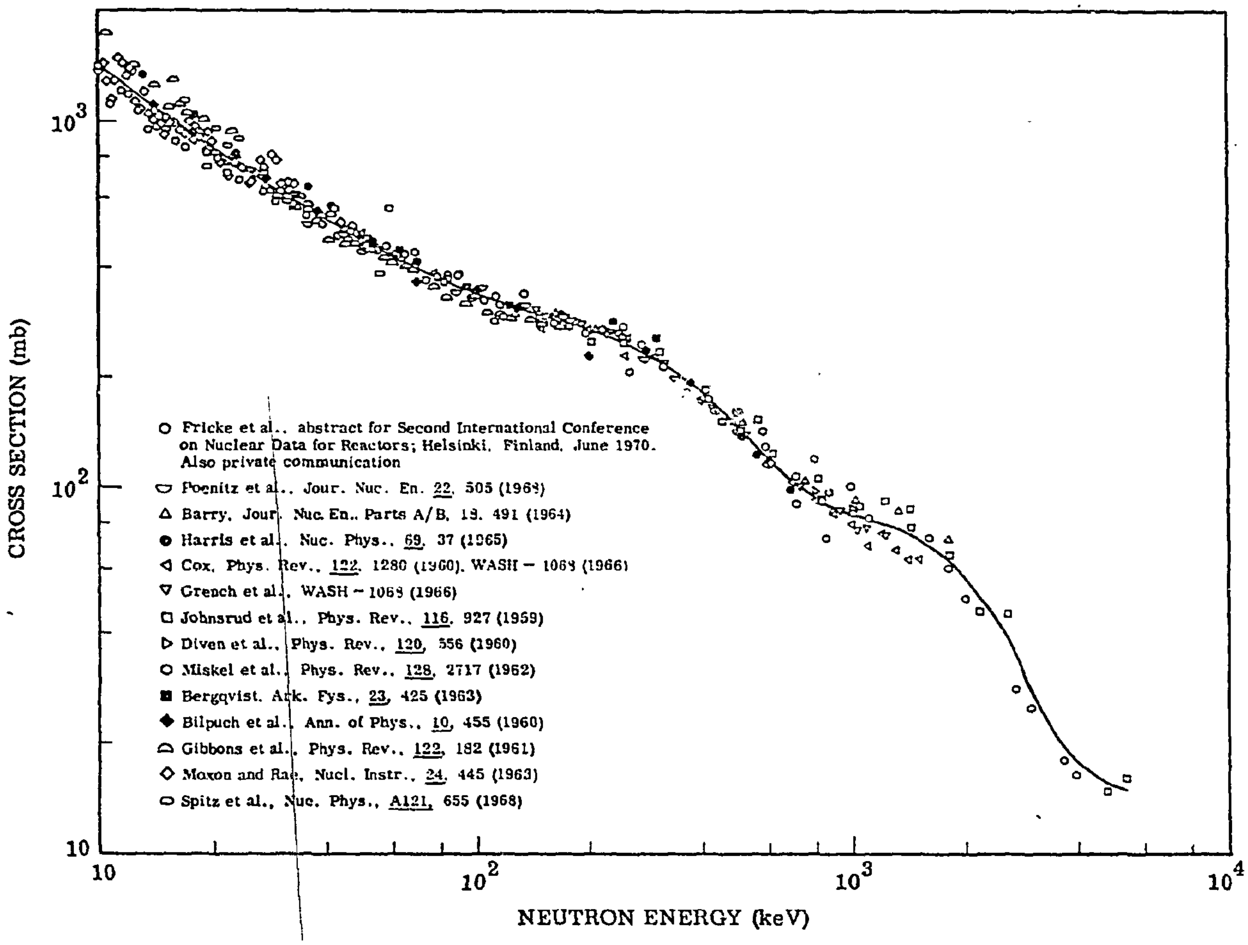

Figure A-2. "Best-fit" $^{197}Au(n,\gamma)^{198}Au$ cross-section curve with adjusted data used in obtaining curve.

DATA NOT FOR QUOTATION

Table A-1. Adjustment factors for sets of data used in obtaining "best-fit" $^{197}Au(n,\gamma)^{198}Au$ cross-section curve.

Experiment	Adjustment Factor
Fricke	1.01567
Poenitz	1.07871
Barry	0.93771
Harris	1.06969
Cox	0.82853 for $E < 200$ keV
	0.84796 for $E \geq 200$ keV
Grench	0.93168
Johnsrud	0.99136
Diven	0.88967
Miskel	0.80486
Bergqvist	1.21143
Bilpuch	0.85055
Gibbons	1.22366
Moxon	1.20556
Spitz	1.28708

Table A-2. "Best fit" $^{197}Au(n,\gamma)^{198}Au$ cross section.

E (keV)	σ (mb)	E (keV)	σ (mb)	E (keV)	σ (mb)	E (keV)	σ (mb)	E (keV)	σ (mb)
10	1410	42	527.4	190	275.7	600	119.9	2800	33.1
11	1313	44	513.2	200	270.8	650	111.0	2900	30.7
12	1230	46	500.2	210	266.1	700	103.8	3000	28.4
13	1160	48	488.3	220	261.5	750	98.16	3200	24.6
14	1099	50	477.2	230	256.8	800	93.71	3400	21.9
15	1045	52	466.9	240	252.2	850	90.27	3600	19.9
16	997.6	54	457.4	250	247.6	900	88.05	3800	18.7
17	955.3	56	448.5	260	243.0	950	86.08	4000	17.8
18	917.4	58	440.3	270	238.5	1000	84.45	4200	17.1
19	883.1	60	432.5	280	233.8	1100	81.73	4400	16.6
20	852.1	65	415.1	290	229.4	1200	79.53	4600	16.1
21	823.8	70	400.1	300	224.7	1300	77.53	4800	15.7
22	797.9	75	387.1	320	215.5	1400	75.20	5000	15.4
23	774.1	80	375.7	340	206.7	1500	72.61	5200	15.2
24	752.1	85	365.5	360	198.1	1600	69.80	5400	14.9
25	731.8	90	356.5	380	189.8	1700	66.81		
26	712.9	95	348.5	400	181.9	1800	63.68		
27	695.4	100	341.2	420	174.2	1900	60.46		
28	679.0	110	328.6	440	166.9	2000	57.17		
29	663.6	120	318.2	460	159.9	2100	53.86		
30	649.3	130	309.6	480	153.1	2200	50.56		
32	623.0	140	302.6	500	146.7	2300	47.30		
34	599.7	150	296.5	520	140.6	2400	44.09		
36	578.8	160	290.9	540	134.8	2500	40.98		
38	560.0	170	285.5	560	129.3	2600	38.0		
40	542.9	180	280.6	580	124.3	2700	35.5		

DATA NOT FOR QUOTATION

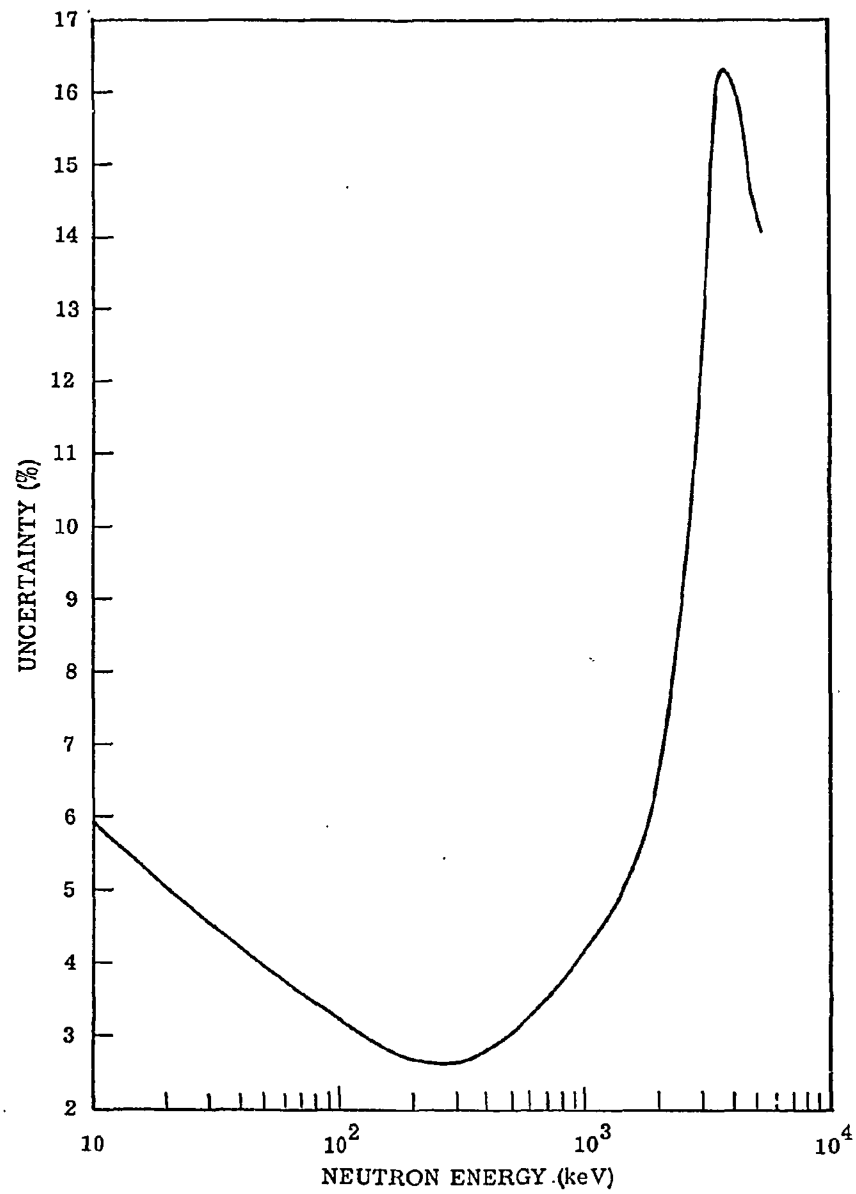

Figure A-3. Relative uncertainty of "best-fit" $^{197}Au(n,\gamma)^{198}Au$ cross-section curve.

DATA NOT FOR QUOTATION

2. Gross-Fission-Product Gamma-Ray Spectroscopy (W. L. Imhof, L. F. Chase, Jr., R. A. Chalmers, and F. J. Vaughn)

The products of the neutron-induced fission of ^{235}U and ^{239}Pu have been observed using high-resolution Ge(Li) γ-ray spectroscopy. The irradiated samples were counted using an 8000-channel ADC for a vairety of bombardment and delay times in the range from ~5 minutes to ~5 days. The yields of various product isotopes from ^{235}U fission have been studied for neutron bombardments at thermal and at 0.05, 0.42, 0.52, 0.62, 0.71, 0.81, 0.90, 1.00, 4.5,and 15 MeV.

The yields of fission products located on the sides of the two mass-distribution peaks show large variations over the full range of neutron energies covered. However, from 0.42 MeV to 1.0 MeV relatively little structure is observed.

3. Spin-Spin Effect in the Neutron Total Cross Section of ^{59}Co (T. R. Fisher, H. A. Grench, D. C. Healey,* J. McCarthy,* and D. Parks*)

In the last report,[1] data on the "spin-spin" effect in the neutron total cross section of ^{59}Co were presented. The data were obtained with a polarized ^{59}Co target and covered the energy region from 0.3 to 8.0 MeV. These results have been published[2] and a detailed optical-model calculation is nearing completion.

Suitable optical parameters for ^{59}Co were determined by fitting the total cross section for energies from 0.3 to 16 MeV and by fitting angular distributions at 1.0, 4.0,and 14.0 MeV. The parameters of Moldauer,[3] with a reduced radius of 4.87 f for the real potential, were adopted. A generalized spin-spin potential of the form

$$-\frac{V_{SS}}{I} F(r) \left[\underset{\sim}{I} \cdot \underset{\sim}{\sigma} + \beta_{SS} \sum_{m\mu} \sqrt{\frac{6\pi}{5}} (11\mu\, m{-}\mu | 2m)\, I^{\mu}\, \sigma^{m-\mu}\, Y_2^{-m}(\theta,\varphi) \right]$$

was used in the calculations. If F(r) is chosen to have a Woods-Saxon shape, best fits to the data are obtained with $V_{SS} = -1.7$ MeV and $\beta_{SS} = 2$. The strength of the spin-spin potential, V_{SS}, is about a factor of 10 greater than would be expected from the interaction of the incoming neutron with a single proton hole in the $f_{7/2}$ shell.

* Stanford University, Stanford, California.

2 D. C. Healey et al., Phys. Rev. Letters 25, 117 (1970).

3 P. A. Moldauer, Nucl. Phys. 47, 65 (1963).

DATA NOT FOR QUOTATION

4. Deformation Effect in the Neutron Total Cross Section of ^{59}Co
(T. R. Fisher, D. C. Healey,* J. S. McCarthy,* and D. Parks*)

If a nucleus has a quadrupole moment, a deformation effect can be observed when the neutron total cross section is measured with an aligned target. This effect is defined as $\Delta\sigma_{Def} = \sigma_{oriented} - \sigma_{unoriented}$ and has been observed for the strongly deformed rotational nucleus ^{165}Ho.[4] We have now observed a similar effect for the vibrational nucleus ^{59}Co. The data are shown in Fig. A-4. The classical black-nucleus estimate shown in the figure is just the change in geometrical cross section resulting from nuclear alignment. A DWBA calculation is in progress in an attempt to obtain a better understanding of the results.

5. Studies of the Decay of ^{30}Al Produced by the $^{30}Si(n,p)^{30}Al$ Reaction
(H. A. Grench, A. D. W. Jones, and R. W. Nightingale)

The level structure of ^{30}Si has been investigated by observing the γ rays associated with both the β-ray decay of ^{30}Al and with the $^{30}Si(p,p'\gamma)^{30}Si$ reaction. Previously unreported β-ray branches were found to the 4.81- and 4.83-MeV states in ^{30}Si. The γ-ray decay of these states, as well as that of the lower-lying excited states, was measured in both the β-ray decay and $(p,p'\gamma)$ experiments. It was found that the 4.81-MeV level decays to the ground, 2.23- and 3.50-MeV states, whereas the 4.83-MeV level decays only to the 2.23- and 3.50-MeV states. A search was made for a reported $T_{1/2}$ = 72.5 sec ^{30m}Al activity.[5] No evidence was found for such activity; an upper limit for the $^{30}Si(n,p)^{30m}Al$ cross section induced by 15-MeV neutrons was found to be less than 0.1% of the value previously quoted.[5]

6. Studies of the Decay of ^{26}Na Produced by the $^{26}Mg(n,p)^{26}Na$ Reaction
(H. A. Grench and R. Hirko*)

The 1-sec ^{26}Na activity is being studied using high-resolution γ-ray spectroscopy. Several γ-ray transitions in ^{26}Mg not previously reported in the β-ray decay of ^{26}Na have been found.

---

* Stanford University, Stanford, California.

[4] T. R. Fisher et al., Phys. Rev. 157, 1149 (1967).

[5] E. Peeters, Phys. Lett. 7, 142 (1963).

DATA NOT FOR QUOTATION

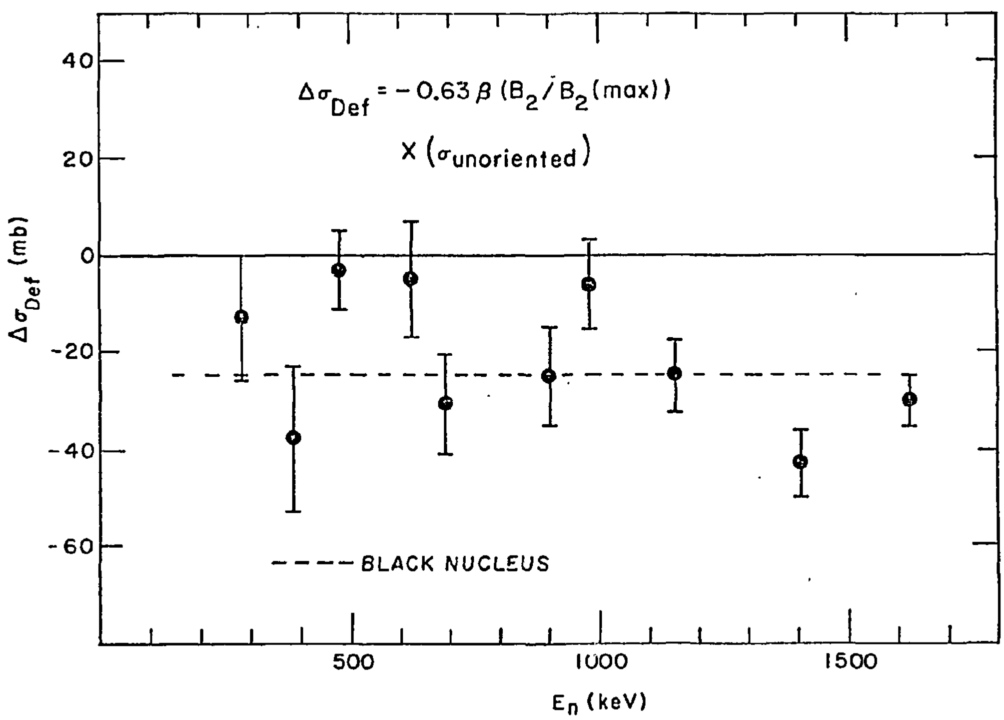

Figure A-4. Deformation effect in the ^{59}Co neutron total cross section as a function of neutron energy.

DATA NOT FOR QUOTATION

LOS ALAMOS SCIENTIFIC LABORATORY

A. TIME OF FLIGHT WITH NUCLEAR EXPLOSIONS

1. Neutron Capture Gamma-Ray Yield of ^{93}Nb (M. V. Harlow, Jr., A. D. Schelberg, J. H. Warren, A. Phillips, and N. W. Glass) Relevant to WASH-1144, Requests 208, 210.

The neutron capture gamma-ray yield of ^{93}Nb was measured on Physics 8 for two sample thicknesses, 0.6543×10^{-3} and 0.24519×10^{-1} atoms/barn, respectively. Gamma rays were observed by Moxon-Rae detectors, and the neutron intensity was measured by ^{6}Li(n,α)T beam monitors. Neutron energy was determined from the time-of-flight over a 250 m flight path. Linear electronics and high resolution drum cameras were employed for the primary data recording channels. Normalized gamma-ray yields from the thin sample exhibit clearly resolved resonances over the entire neutron energy range of 34 eV to 10 keV. Comparison of resonance energies with those of the Columbia total cross section data below 2200 eV shows good agreement. Areas of individual resonances in data below 1000 eV compare well with those obtained from calculations done with published resonance parameters. Further analysis of the thin sample data and the reduction and analysis of the thick sample data are being carried out.

2. Radiative Capture by ^{232}Th (L. Forman, A. D. Schelberg, J. H. Warren, M. V. Harlow, and N. W. Glass) Relevant to WASH-1144, Request 343.

Neutron capture in ^{232}Th has been investigated utilizing time-of-flight techniques with modified Moxon-Rae detectors on a neutron beam of the Physics-8 underground nuclear detonation. Area analysis of resonance data was possible between 20 eV and 2000 eV. For larger resonances, the capture areas are primarily sensitive to the radiation width, Γ_γ; preliminary values for 66 $\ell = 0$ levels are given in Table A-I. In the case of smaller levels ($g\Gamma_n \ll \Gamma_\gamma$) capture areas are almost directly proportional to $g\Gamma_n$; approximately 130 of these levels are now being analyzed. It further appears feasible to determine average cross sections from 2 keV to 30 keV.

3. Fission, Capture, and Scattering Cross Sections of ^{239}Pu (J. A. Farrell, G. F. Auchampaugh, and P. A. Seeger) Relevant to WASH-1144, Requests 442, 447, 449.

Preliminary results of the Physics-8 simultaneous measurement of the fission, capture, and scattering cross sections of ^{239}Pu were reported at the Helsinki conference on Nuclear Data for Reactors. The quality of the data obtained is illustrated in Fig. A-1. From these data, it was possible to obtain alpha, the capture-to-fission ratio, in the keV region

TABLE A-I

Thorium-232 Radiation Widths (Preliminary)

E_o Volts	Γ_γ MeV	Γ_γ Asghar* MeV	E_o Volts	Γ_γ MeV	Γ_γ Asghar* MeV
59.5	22.7 ± 6	23.2 ± 2	943.4	29.6 ± 4.3	
69.1	21.9 ± 2.8	21.2 ± 1.1	982.9	20.6 ± 3.5	
112.9	21.0 ± 4	20.1 ± 1.1	990.5	18.4 ± 2	
120.8	21.0 ± 5.8	20.7 ± .9	1010.5	20.2 ± 3.2	
170.2	22.3 ± 2.5	22.2 ± 1.0	1110.0	31.3 ± 11	
192.6	30.3 ± 7.2	19.6 ± 1.6	1139.0	23.0 ± 7	
221.1	21.9 ± 3.4	20.3 ± 1.2	1227.8	16.1 ± 3.9	
251.4	22.2 ± 3.0	21.1 ± 1.4	1248.7	22.8 ± 3.9	
263.1	17.3 ± 3.1	17.8 ± 1.6	1292.1	24.1 ± 4.7	
285.7	18.8 ± 2.4	21.8 ± 1.6	1301.6	15.6 ± 3.7	
305.4	18.3 ± 3.2	24.2 ± 1.9	1354.8	18.5 ± 3.6	
328.9	21.8 ± 2.3	22.9 ± 1.2	1377.9	21.5 ± 5	
341.8	20.6 ± 3.4	20.5 ± 1.2	1397.7	19.7 ± 3.8	
365.1	21.8 ± 5.7		1426.6	21.2 ± 3.7	
369.3	21.2 ± 5.8		1433.7	26.8 ± 5	
400.9	19.3 ± 10		1518.4	19.8 ± 3	
462.5	19.3 ± 3.5	21.5 ± 1.3	1524.1	25.2 ± 4	
488.7	17.2 ± 3.8	19.2 ± 1.3	1581.0	26.4 ± 8.5	
528.5	17.4 ± 3.8		1589.1	23.1 ± 3.5	
569.8	30.2 ± 10.5	19.3 ± 2.4	1602.7	27.1 ± 6	
598.2	38 ± 20		1630.6	19.2 ± 3.6	
656.5	16.7 ± 3		1640.6	19.8 ± 3.9	
665.2	14.6 ± 2.5		1661.0	24.4 ± 3.9	
675.2	18.4 ± 2.5		1677.8	18.4 ± 7	
687.3	18.1 ± 3		1746.5	19.7 ± 3.7	
701.1	28 ± 7		1762.7	24.6 ± 4.5	
712.9	13.1 ± 4		1803.2	18.0 ± 3	
740.9	19.8 ± 2	21.6 ± 1.5	1811.8	28 ± 6	
778.7	24.2 ± 4.5		1824.4	20.2 ± 4.5	
804.3	19.5 ± 2.3	20.5 ± 2.1	1853.9	24.3 ± 8	
842.5	20.8 ± 4.2	23.2 ± 5.0	1861.5	29.6 ± 8	
866.5	26 ± 7		1951.2	18.9 ± 3.7	
890.2	24.4 ± 3.4		1971.2	19.0 ± 4.5	

*M. Asghar, C. M. Chaffey, M. C. Moxon, N. J. Pattenden, E. R. Rae, and C. A. Uttley, Nucl. Phys. 76, 196 (1966).

DATA NOT FOR QUOTATION

with an overall accuracy comparable to other recent measurements, as shown in Fig. A-2. Tables A-II and A-III give average values of alpha and of the fission cross section of ^{239}Pu, respectively, compared to other measurements.

TABLE A-II

^{239}Pu Alpha

Neutron Energy Interval (keV)	Physics 8[1]	ORNL[2]	LRL[3]	Harwell[4]	IETP[5]
9.0-10.0	0.74	0.64	0.56	0.64	
8.0- 9.0	0.58	0.58	0.56	0.56	
7.0- 8.0	0.68	0.71	0.63	0.59	
6.0- 7.0	0.86	0.88	0.86	0.69	
5.0- 6.0	0.93	0.91	0.82	0.80	
4.0- 5.0	0.90	0.98	0.81	0.72	0.83
3.0- 4.0	0.95	1.26	0.90	0.73	0.96
2.0- 3.0	1.31	1.38	1.02	0.92	1.23
1.0- 2.0	1.17	0.97	0.89	0.69	1.02
0.9- 1.0	0.70	0.81	0.65	0.55	0.71
0.8- 0.9	0.79	1.07	0.66	0.53	0.78
0.7- 0.8	0.85	1.05	1.03	0.94	0.94
0.6- 0.7	1.68	1.89	1.47	1.44	1.72
0.5- 0.6	0.64	0.78	0.70	0.63	0.75
0.4- 0.5	0.57	0.50	0.53	0.44	0.45
0.3- 0.4	0.94	1.31	0.84	1.13	1.23
0.2- 0.3	0.67	1.06	1.01	0.79	1.07
0.1- 0.2	0.67	0.98	0.76	0.96	0.88

[1] J. A. Farrell, G. F. Auchampaugh, M. S. Moore, and P. A. Seeger, The Second IAEA International Conference on Nuclear Data for Reactors. Helsinki, June 15-19, 1970, Paper CN-26/46.

[2] R. Gwin, L. W. Weston, G. de Saussure, R. W. Ingle, J. H. Todd, and F. E. Gillespie, Nucl. Sci. Eng. 40, 306 (1970) and private communication, R. Gwin, June, 1970.

[3] J. B. Czirr and J. S. Lindsey, The Second IAEA International Conference on Nuclear Data for Reactors. Helsinki, June 15-19, 1970, Paper CN-26/47.

[4] M. G. Schomberg, M. G. Sowerby, D. A. Boyce, K. J. Murray, and Miss D. L. Sutton, The Second IAEA International Conference on Nuclear Data for Reactors. Helsinki, June 15-19, 1970, CN-26/33.

[5] F. N. Belyaev, K. G. Ignat'ev, S. I. Sukhoruchkin, S. P. Borovlev, V. V. Pavlov, M. V. Polozov, and A. N. Soldatov, The Second IAEA International Conference on Nuclear Data for Reactors. Helsinki, June 15-19, 1970, Paper CN-26/89.

TABLE A-III

Average Fission Cross Sections of ^{239}Pu

Neutron Energy Interval	Physics 8	ORNL[1]	Saclay[2]
20.0-30.0 keV	1.85	1.80	1.86
10.0-20.0	1.94	1.90	1.89
9.0-10.0	2.11	1.97	1.96
8.0- 9.0	2.48	2.33	2.48
7.0- 8.0	2.44	2.22	2.00
6.0- 7.0	2.23	2.23	2.00
5.0- 6.0	2.59	2.35	2.22
4.0- 5.0	2.59	2.48	2.37
3.0- 4.0	3.28	3.25	3.09
2.0- 3.0	3.47	3.40	3.35
1.0- 2.0	4.47	4.59	4.53
0.9- 1.0	8.67	8.75	8.71
0.8- 0.9	5.43	5.10	5.18
0.7- 0.8	6.11	5.60	6.05
0.6- 0.7	4.50	4.25	4.77
0.5- 0.6	16.2	16.2	15.7
0.4- 0.5	10.3	9.70	9.91
0.3- 0.4	9.43	8.35	9.04
0.2- 0.3	20.6	18.0	18.0
0.1- 0.2	21.1	18.4	19.2
90-100 eV	33.4		31.7
80-90	75.4		69.0
70-80	69.7		65.6
60-70	60.2		57.1
50-60	80.6		77.7
40-50	31.7		29.4
30-40	30.5		
20-30	35.2		

[1] R. Gwin, L. W. Weston, G. de Saussure, R. W. Ingle, J. H. Todd, and F. E. Gillespie, Nucl. Sci. Eng., 40, 306 (1970), and private communication, R. Gwin, June, 1970.

[2] J. Blons, H. Derrien, and A. Michaudon, The Second IAEA International Conference on Nuclear Data for Reactors. Helsinki, June 15-19, 1970, Paper CN-26/63.

DATA NOT FOR QUOTATION

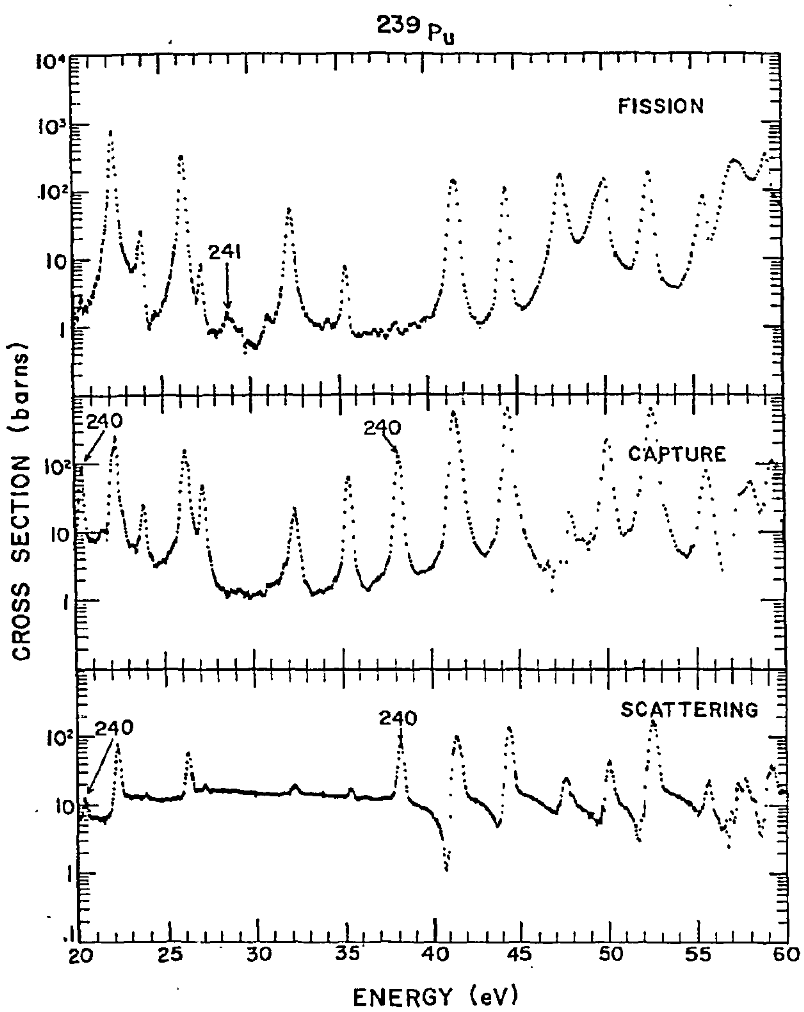

Fig. A-1. The fission, capture, and scattering cross sections of ^{239}Pu from 20 to 60 eV. Resonances in ^{240}Pu and ^{241}Pu are identified. The apparent drop in the scattering cross section below 22 eV is spurious and is due to a rapidly decreasing neutron flux.

DATA NOT FOR QUOTATION

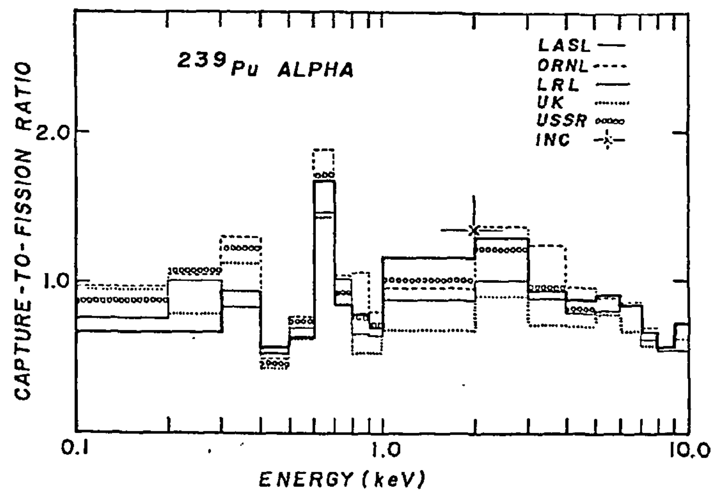

Fig. A-2. Alpha for ^{239}Pu as determined from the Physics-8 event, compared with other recent measurements. References are given in Table A-II.

DATA NOT FOR QUOTATION

4. Subthreshold Fission in ^{242}Pu and ^{244}Pu (G. F. Auchampaugh, J. A. Farrell, D. W. Bergen)

The subthreshold fission cross sections of ^{242}Pu and ^{244}Pu were measured in the Physics-8 event from 20 eV to 8 MeV. A preliminary analysis of these data has been completed. The threshold regions of ^{242}Pu and ^{244}Pu are plotted in Figs. A-3 and A-4. The ^{242}Pu sample was viewed by two solid-state detectors positioned at 55° and 90° to the neutron beam direction, and the ^{244}Pu sample by two detectors at 55°. The data from the ^{242}Pu 55° signal above 4 MeV has not been plotted because of nonlinear effects in the 55° amplifier. The 12% difference between the 55° and 90° ^{242}Pu data below 4 MeV can be explained by an anisotropy in the fission fragment distribution. Similar values for the 55°/90° ratio have been observed by Simmons and Henkel[1] for even-even targets in this mass region. In the case of ^{244}Pu the agreement between the two 55° sets of data was better than 5% in the MeV region.

Intermediate structure was observed in both elements with the following observed D_I and D_{II} level spacings:

	ΔE (keV)	D_I (eV)	D_{II} (keV)
^{242}Pu	0 to 50		0.93
	0 to .9	18.7	
^{244}Pu	0 to 18		1.8
	0 to .1	14	

Fission components in the class I resonances are observed in energy regions where the average class I fission strength is enhanced by the coupling to a class II resonance, and only above about 300 eV. Below 300 eV the fission strength is so weak that even with a $\epsilon_\gamma/\epsilon_f$ of 10^{-3} it is not possible to observe fission fragments in the presence of the large γ-ray background in the resonances. The areas of those resonances in $^{242,244}Pu$ which have an observable fission component are given in Tables A-IV and A-V.

---

[1] J. E. Simmons and R. L. Henkel, Phys. Rev. 120, 198 (1960).

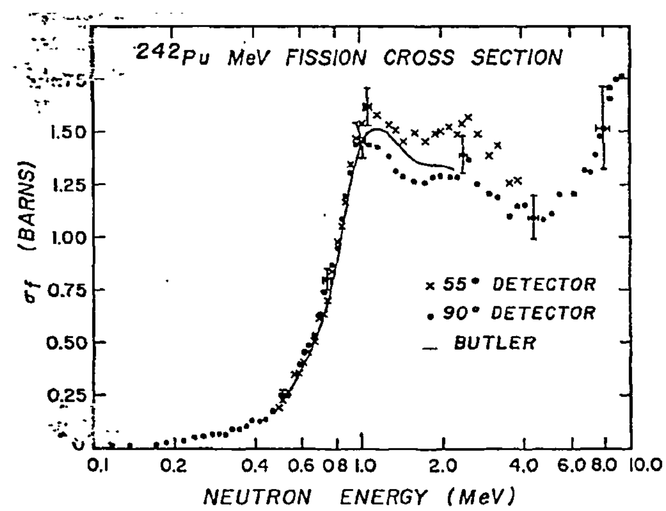

Fig. A-3. Threshold fission cross section of ^{242}Pu. The vertical error bars represent statistical errors only. The horizontal error bars indicate a 0.2-μsec uncertainty in the zero time. The data of Butler (Phys. Rev. 117, 1305 (1960)) are plotted as a smooth curve.

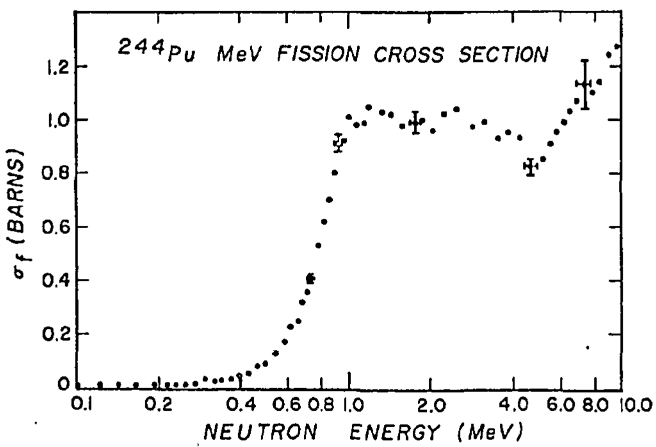

Fig. A-4. Threshold fission cross section of ^{244}Pu. The vertical error bars represent statistical errors only. The horizontal error bars indicate a 0.2-μsec uncertainty in the zero time.

DATA NOT FOR QUOTATION

TABLE A-IV

Below 1 keV, isolated ^{242}Pu class I fission areas. Above 1 keV, either isolated class I fission areas or a sum of class I areas over a class II resonance. The number in parentheses indicates the number of distinct resonances within the group.

E (keV)	A^I, $\int_{II} A^I dE$ (b-eV)	E (keV)	A^I, $\int_{II} A^I dE$ (b-eV)	E (keV)	A^I, $\int_{II} A^I dE$ (b-eV)
0.374	0.07 ± 0.02	1.862	0.09 ± 0.03	15.00 (2)	2.45 ± 0.45
0.382	0.16 ± 0.03	1.892 (2)	0.34 ± 0.05	16.03 (2)	6.02 ± 0.62
0.410	0.05 ± 0.02	2.748 (3)	0.50 ± 0.11	16.88	4.14 ± 0.48
0.424	0.09 ± 0.02	3.119	0.22 ± 0.14	17.23	1.35 ± 0.38
0.474	0.14 ± 0.03	3.145 (3)	0.14 ± 0.07	18.46	1.42 ± 0.50
0.483	1.29 ± 0.22	3.459 (2)	0.30 ± 0.09	18.74	0.98 ± 0.33
0.505	0.29 ± 0.04	3.490	0.39 ± 0.08	19.40	1.91 ± 0.48
0.537	0.46 ± 0.09	3.514	0.50 ± 0.08	20.68 (2)	2.30 ± 0.59
0.549	0.53 ± 0.08	3.539	0.38 ± 0.06	22.25 (3)	7.62 ± 1.04
0.577	0.17 ± 0.04	3.575 (2)	1.71 ± 0.14	23.47	5.58 ± 0.65
0.596	0.16 ± 0.04	3.660	1.18 ± 0.13	23.90	2.31 ± 0.38
0.600	0.22 ± 0.06	3.677	1.53 ± 0.14	24.36	2.18 ± 0.51
0.612	0.18 ± 0.05	3.716	0.36 ± 0.08	24.74	0.97 ± 0.40
0.671	0.23 ± 0.07	3.778	0.26 ± 0.09	26.18 (2)	4.50 ± 0.83
0.694	0.90 ± 0.16	3.828 (2)	0.15 ± 0.08	27.15 (2)	11.74 ± 1.06
0.713	0.30 ± 0.09	4.861 (4)	5.04 ± 0.27	28.26 (3)	19.30 ± 1.50
0.738	2.70 ± 0.39	4.904	5.32 ± 0.34	29.34 (2)	10.20 ± 1.07
0.757	6.96 ± 0.80	5.926 (3)	1.30 ± 0.28	31.16 (2)	7.40 ± 1.60
0.763	22.97 ± 2.57	6.461	0.70 ± 0.16	32.46 (2)	5.70 ± 1.20
0.790	4.85 ± 0.58	6.659 (2)	0.70 ± 0.16	33.31	3.90 ± 1.00
0.795	0.30 ± 0.04	6.943 (2)	2.09 ± 0.26	34.05	7.30 ± 1.50
0.825	0.18 ± 0.05	7.740	0.32 ± 0.15	35.02	6.00 ± 2.20
0.838	0.19 ± 0.06	8.164	0.97 ± 0.22	35.64	2.90 ± 1.00
0.857	0.45 ± 0.10	8.492 (2)	1.54 ± 0.28	37.11	2.50 ± 1.00
0.867	0.09 ± 0.03	9.547	2.01 ± 0.31	37.79	4.30 ± 1.00
0.879	0.16 ± 0.06	9.995	0.84 ± 0.21	39.09	6.80 ± 1.20
0.887	0.08 ± 0.03	10.30 (2)	3.59 ± 0.39	40.05	8.10 ± 1.40
0.923	0.16 ± 0.05	10.85 (2)	2.75 ± 0.45	41.02	17.90 ± 3.10
1.308	0.51 ± 0.04	11.64 (5)	3.44 ± 0.61	42.02	11.10 ± 2.40
1.698	0.16 ± 0.03	12.96 (3)	4.69 ± 0.61	42.99	4.20 ± 2.00
1.751 (3)	0.45 ± 0.06	13.81	7.45 ± 0.75	45.41	24.20 ± 4.30
1.792 (3)	0.68 ± 0.07	14.65	2.60 ± 0.37	46.41	5.20 ± 1.70
1.839 (3)	2.58 ± 0.31				

TABLE A-V

Sum of ^{244}Pu class I fission areas over a class II resonance. The resonances at 1.16 and 2.33 keV are questionable. The resonance at 18.2 keV appears to be a doublet.

E (keV)	$\int_{II} A^I dE$ (b-eV)	E (keV)	$\int_{II} A^I dE$ (b-eV)
1.16 (?)	0.9 ± 0.3	7.63	13.7 ± 3.2
1.65	6.6 ± 1.0	11.4	13.8 ± 3.7
2.33 (?)	1.4 ± 0.6	12.2	11.2 ± 3.4
3.74	9.8 ± 2.0	14.6	19.8 ± 5.0
5.46	9.8 ± 2.3	18.2 (2)	17.5 ± 5.1

5. Analysis of the Fission and Capture Cross Sections of Cm (G. A. Keyworth and M. S. Moore) Relevant to WASH-1144, Requests 499, 503-518.

Analysis of the Physics-8 measurement of the fission and capture cross sections of ^{244}Cm, ^{245}Cm, ^{246}Cm, ^{247}Cm, and ^{248}Cm has been completed. Final resonance parameters are given in Tables A-VI-A-X. The analysis of resonances in ^{244}Cm is suggestive of intermediate structure in fission near 820 eV. This structure also persists to higher energies, as shown in Fig. A-5. A paper describing these results in detail is in the final stage of preparation.

6. Fission Cross Section of ^{249}Cf (M. G. Silbert, W. Ogle; R. W. Lougheed, J. E. Evans, and R. W. Hoff, LRL, Livermore) Relevant to WASH-1144, Request 521.

The neutron-induced fission cross section of ^{249}Cf has been measured from 15 eV to 3 MeV on the Physics-8 event. The preliminary cross section, measured by a detector at 90° to the neutron beam, is illustrated in Fig. A-6 and selected integrals are listed in Table A-XI. In addition to the errors plotted, the systematic uncertainty in the cross section is estimated to be ±10%.

Preliminary theoretical fits to the cross section were carried out between 15 and 60 eV with the multilevel search routine of G. Auchampaugh. For the 32 resonances observed in this region the average level spacing is 1.4 eV. Assuming Γ_γ = 40 meV, the theoretical fit yielded values of $\langle \Gamma_n{}^o \rangle$ = 0.45 meV and $\langle \Gamma_f \rangle \approx$ 150 meV. The s-wave neutron strength function $\langle \Gamma_n{}^o \rangle / \langle D \rangle$ is then $(1.6 \pm 0.4) \times 10^{-4}$ for each of the two spin states (4^-, 5^-) involved.

This even-odd, spin-parity $9/2^-$ target is known to have a thermal fission cross section of 1700 b. The present results show abundant fission

TABLE A-VI

Resonance parameters for ^{244}Cm + n with Γ_γ = 37 mV assumed

E_o (eV)	$\frac{\pi}{2}\sigma_o\Gamma_\gamma$ (b-eV)	$\frac{\pi}{2}\sigma_o\Gamma_f$ (b-eV)	Γ_n (mV)	Γ_f (mV)
22.85	140 ± 10	14.0 ± 0.6	0.88 ± 0.09	3.7 ± 0.3
34.99	350 ± 9	23.7 ± 0.3	3.5 ± 0.3	2.51 ± 0.07
52.78	41 ± 5	1.9 ± 0.1	0.56 ± 0.08	1.7 ± 0.2
67.99	36 ± 3	2.9 ± 0.1	0.67 ± 0.07	3.0 ± 0.3
85.96	710 ± 20	12.5 ± 0.2	24.5 ± 2.3	0.65 ± 0.02
96.12	252 ± 6	10.5 ± 0.2	7.3 ± 0.6	1.54 ± 0.05
132.8	320 ± 11	10.2 ± 0.2	15.5 ± 2	1.17 ± 0.04
139.1	65 ± 6	5.0 ± 0.2	2.5 ± 0.3	2.8 ± 0.3
171.2	70 ± 8	2.4 ± 0.1	3.3 ± 0.5	1.3 ± 0.2
181.6	170 ± 9	9.7 ± 0.3	10 ± 0.9	2.1 ± 0.1
197.0	410 ± 17	11.1 ± 0.5	43 ± 5	1.00 ± 0.06
209.8	380 ± 17	5.3 ± 0.4	42 ± 5	0.52 ± 0.04
220.1	398 ± 48	13.6 ± 0.6	54 ± 16	1.25 ± 0.16
230.5	289 ± 41	3.1 ± 0.3	30 ± 7	0.40 ± 0.07
234.9	60 ± 17	1.5 ± 0.3	3.8 ± 1.2	0.9 ± 0.3
242.7	20 ± 19	2.1 ± 0.3	1.3 ± 1.2	> 2.2
264.9	124 ± 48	3.1 ± 0.4	10 ± 5	0.9 ± 0.4
274.1	164 ± 50	2.8 ± 0.4	16 ± 7	0.6 ± 0.2
316.8	62 ± 6	0.5 ± 0.1	5.5 ± 0.7	0.3 ± 0.07
329.5	294 ± 21	2.3 ± 0.2	6.6 ± 1.4	0.29 ± 0.03
343.6	177 ± 22	5.6 ± 0.4	26 ± 5	1.16 ± 0.16
353.1	309 ± 19	10.8 ± 0.6	101 ± 23	1.28 ± 0.11
361.7	196 ± 25	5.5 ± 0.4	34 ± 8	1.03 ± 0.16
364.4	85 ± 17	4.8 ± 0.3	10 ± 2	2.1 ± 0.4
386.2	158 ± 8	4.8 ± 0.3	26 ± 3	1.11 ± 0.09
397.6[a]	145 ± 8	2.6 ± 0.3	23 ± 3	0.66 ± 0.08
415.0	122 ± 9	0.9 ± 0.2	19 ± 2	0.27 ± 0.06
420.6[a]	254 ± 11	6.2 ± 0.5	93 ± 16	0.89 ± 0.08
426.9	94 ± 7	0.9 ± 0.3	13 ± 2	0.35 ± 0.12
443.4	236 ± 15	5.3 ± 0.6	86 ± 19	0.82 ± 0.11
470.9	260 ± 17	13.0 ± 0.7	167 ± 58	1.84 ± 0.16
488.9	88 ± 7	1.2 ± 0.3	15 ± 2	0.50 ± 0.13
491.9	180 ± 7	2.3 ± 0.5	54 ± 6	0.47 ± 0.10
512.4	290 ± 14	1.6 ± 0.3	Large	1.6 ± 0.3
520.5	116 ± 7	8.0 ± 0.6	26 ± 4	2.55 ± 0.26
596.4[a]	79 ± 39	2.1 ± 0.5	17 ± 12	1.0 ± 0.5
612.4	109 ± 45	3.0 ± 0.5	30 ± 22	1.0 ± 0.5
620.0	103 ± 23	2.2 ± 0.3	27 ± 10	0.8 ± 0.2
627.8	36 ± 21	0.2 ± 0.2	7 ± 4	< 0.5
637.9[a]	49 ± 21	0.9 ± 0.3	10 ± 5	0.7 ± 0.4
646.9[a]	321 ± 31	5.9 ± 0.6	Large	0.68 ± 0.10
652.4	160 ± 16	0.2 ± 0.2	81 ± 27	< 0.1
691.3	57 ± 17	1.2 ± 0.3	13 ± 5	0.8 ± 0.3

DATA NOT FOR QUOTATION

TABLE A-VI (Continued)

E_o (eV)	$\frac{\pi}{2}\sigma_o\Gamma_\gamma$ (b-eV)	$\frac{\pi}{2}\sigma_o\Gamma_f$ (b-eV)	Γ_n (mV)	Γ_f (mV)
695.3	64 ± 16	1.2 ± 0.3	16 ± 5	0.7 ± 0.3
704.5	135 ± 22	5.5 ± 0.7	64 ± 28	1.5 ± 0.3
712.8	75 ± 16	0.1 ± 0.1	20 ± 7	< 0.2
731.6[a]	128 ± 15	0.6 ± 0.3	60 ± 19	0.17 ± 0.09
746.0	18 ± 9	0.8 ± 0.3	4 ± 2	1.6 ± 1.0
759.7[a]	193 ± 14	0.9 ± 0.5	Large	0.17 ± 0.10
778.6	127 ± 9	6.0 ± 0.7	72 ± 15	1.7 ± 0.2
790.1	17 ± 8	0.8 ± 0.3	4 ± 2	1.7 ± 1.0
797.5	7 ± 7	1.8 ± 0.5	2 ± 2	> 3.7
802.5[a]	29 ± 9	2.4 ± 0.6	7 ± 2	3.1 ± 1.2
815.8	41 ± 7	3.3 ± 0.7	11 ± 2	3.0 ± 0.8
823.0	69 ± 13	17.4 ± 1.5	28 ± 7	9.3 ± 1.9
846.3	24 ± 14	1.1 ± 0.4	6 ± 4	1.7 ± 1.2
857.9	82 ± 19	3.2 ± 0.5	33 ± 14	1.4 ± 0.4
865.6	47 ± 22	5.2 ± 0.7	15 ± 9	4.1 ± 2.0
872.0	66 ± 16	1.8 ± 0.6	23 ± 9	1.0 ± 0.4
884.9	107 ± 19	0.7 ± 0.4	62 ± 29	0.2 ± 0.1
899.7	131 ± 14	0.5 ± 0.3	128 ± 62	0.14 ± 0.09
914.0	146 ± 20	2.3 ± 0.7	Large	0.6 ± 0.2
926.3	56 ± 13	0.4 ± 0.4	19 ± 7	< 0.5
946.9	76 ± 13	0.9 ± 0.6	34 ± 11	0.4 ± 0.3
971.5	139 ± 14	1.3 ± 0.4	Large	0.35 ± 0.11

[a]Resonances marked with an "a" are probably unresolved doublets, which were analyzed as single resonances. The neutron widths are thus upper limits, and the fission widths are a weighted average, the weighting factors being unknown.

TABLE A-VII

Resonance parameters for $^{246}Cm + n$ with Γ_γ = 37 mV assumed

E_o (eV)	$\frac{\pi}{2}\sigma_o\Gamma_\gamma$ (b-eV)	$\frac{\pi}{2}\sigma_o\Gamma_f$ (b-eV)	Γ_n (mV)	Γ_f (mV)
84.43	661 ± 100	12.5 ± 0.4	22 ± 5	0.70 ± 0.10
91.84	560 ± 30	2.6 ± 0.4	19 ± 2	0.17 ± 0.03
158.4	414 ± 40	8.2 ± 0.8	29 ± 5	0.73 ± 0.11
250.7	116 ± 60	1.2 ± 0.5	9 ± 6	0.38 ± 0.3
278.3	80 ± 60	2.9 ± 0.9	7 ± 6	1.3 ± 1.2
288.2	323 ± 80	2.7 ± 0.9	59 ± 38	0.31 ± 0.14
313.4	197 ± 35	0.8 ± 0.3	25 ± 8	0.15 ± 0.10
361.0[a]	--	3.5 ± 0.7	--	--
381.1	303 ± 35	1.5 ± 0.6	118 ± 57	0.18 ± 0.09

[a]The resonance at 361 eV is probably an unresolved doublet.

DATA NOT FOR QUOTATION

TABLE A-VIII

Resonance parameters for $^{248}Cm + n$ with $\Gamma_\gamma = 37$ mV assumed

E_o (eV)	$\frac{\pi}{2}\sigma_o\Gamma_\gamma$ (b-eV)	$\frac{\pi}{2}\sigma_o\Gamma_f$ (b-eV)	Γ_n (mV)	Γ_f (mV)
26.84	2270 ± 160	5.1 ± 0.4	25 ± 3	0.08 ± 0.01
76.08	1830 ± 200	162.0 ± 10.0	Large	3.3 ± 0.4
98.79	1640 ± 90	21.0 ± 1.3	Large	0.47 ± 0.04
140.0	--	5.9 ± 0.4	--	--
186.0	--	7.1 ± 0.5	--	--
232.5	--	2.3 ± 1.1	--	--
237.0	--	8.8 ± 1.1	--	--
415.2	--	2.8 ± 0.8	--	--

TABLE A-IX

Resonance parameters for resonances in (^{245}Cm + n) between 20 and 60 eV. Phase angles refer to the fission-width-vector orientation in a two-fission-channel, single-spin-state analysis.

E_o (eV)	$2g\Gamma_n^o$ (mV)	Γ_γ (mV)	Γ_f (mV)	θ (degrees)
21.36	0.457	(40)	485	-16
24.90	0.521	(40)	226	99
25.84	0.007	(40)	549	89
26.83	0.147	(40)	131	160
27.63	0.114	(40)	165	90
29.42	0.638	(40)	328	-171
31.71	0.088	(40)	691	-69[a]
32.99	0.064	(40)	4	-61
34.59	0.039	(40)	61	113
35.31	1.276	(40)	4195	54
36.32	0.256	(40)	189	177
39.45	0.104	(40)	102	-126[a]
40.44	0.705	(40)	585	128
42.45	0.824	(40)	10	56
43.10	0.264	(40)	537	-55
44.57	0.391	(40)	694	-67
45.74	0.087	(40)	901	-9
47.51	0.516	(40)	28	28
49.20	0.718	(40)	1399	58
50.48	0.252	(40)	751	92
51.64	0.087	(40)	207	106
53.63	1.687	(40)	896	-173
54.63	0.045	(40)	1057	174
56.32	0.186	(40)	505	54
58.54	1.811	(40)	393	162
59.99	0.079	(40)	518	-39

[a]Best fits were obtained by placing those resonances marked with an a in a different spin group.

DATA NOT FOR QUOTATION

TABLE A-X

Resonance parameters for resonances in (^{247}Cm + n) between 20 and 60 eV. Phase angles refer to the fission-width-vector orientation in a two-fission-channel, single-spin-state analysis.

E_o (eV)	$2g\Gamma_n^o$ (mV)	Γ_γ (mV)	Γ_f (mV)	θ (degrees)
21.30	0.027	(40)	404	-61
24.03	0.009	(40)	134	-153
25.35	0.002	(40)	26	-103
26.19	0.003	(40)	220	-129
28.04	0.011	(40)	53	35
30.25	0.627	(40)	4	-94
30.62	0.034	(40)	52	-30
32.23	0.089	(40)	26	-92
36.36	0.270	(40)	61	-38
37.74	0.004	(40)	555	-153
37.76	0.217	(40)	13	-178
39.52	0.001	(40)	705	-163
39.95	0.015	(40)	167	19
40.61	0.005	(40)	48	-134
41.25	0.103	(40)	20	105
41.76	0.008	(40)	546	-11
43.39	0.029	(40)	4	117
44.87	0.313	(40)	32	11
45.21	0.086	(40)	60	-119
47.92	0.169	(40)	164	-75
48.85	0.973	(40)	82	25
50.08	0.334	(40)	55	-127
50.69	0.447	(40)	52	22
51.78	0.231	(40)	14	-154
52.19	0.175	(40)	4	-48
53.63	0.062	(40)	324	121
55.10	0.072	(40)	38	88
56.18	0.088	(40)	69	63
59.66	2.037	(40)	114	-68

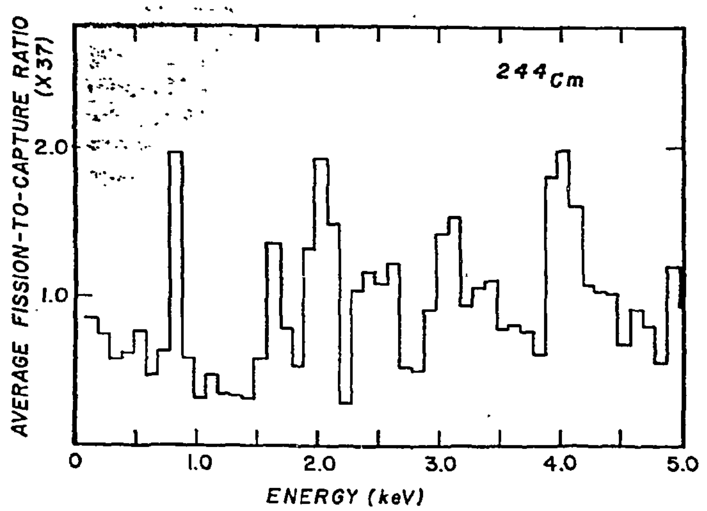

Fig. A-5. The fission-to-capture ratio of (^{244}Cm + n) below 5 keV. The ordinate has been multiplied by 37, the value in meV assumed for the average capture width, so that the scale is appropriate for the average fission width in meV.

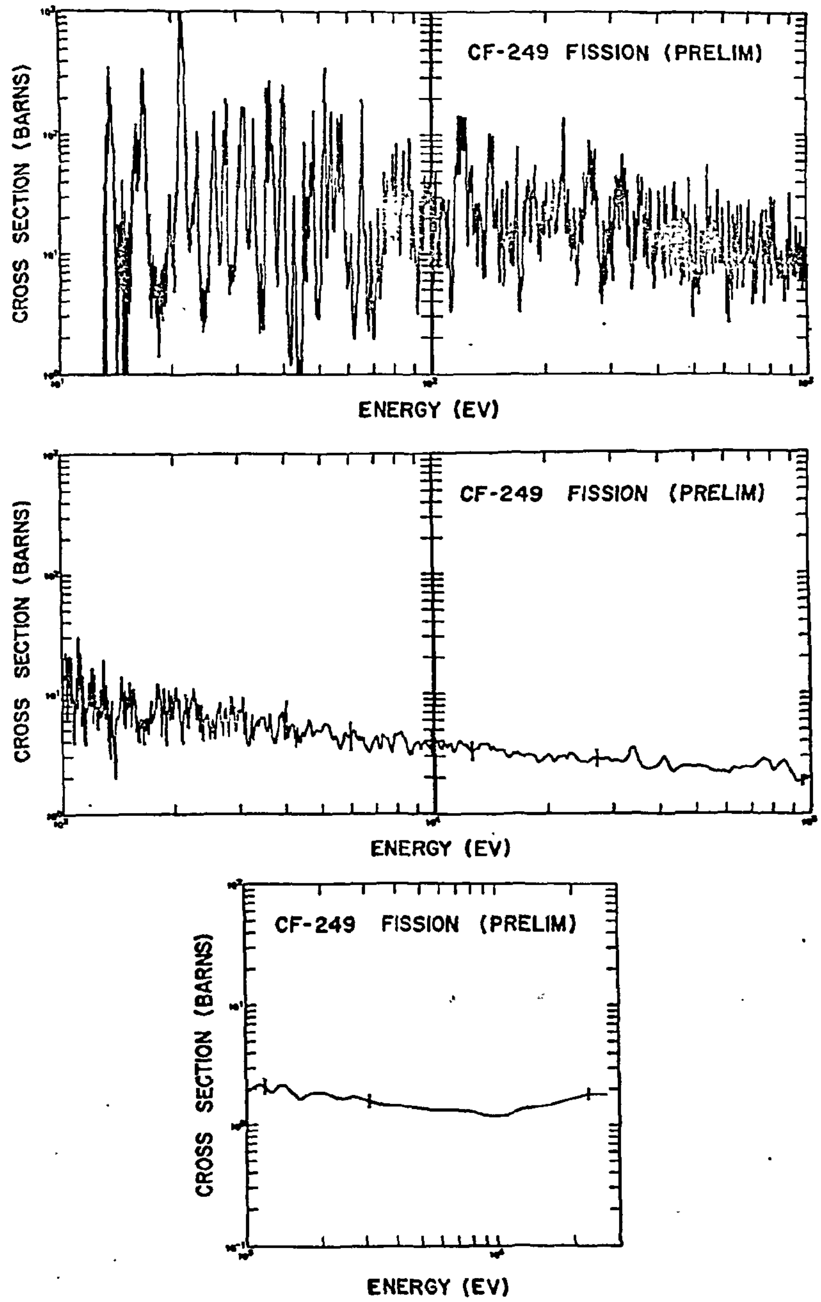

Fig. A-6. Preliminary fission cross section of ^{249}Cf measured on the Physics-8 nuclear explosion. 90° detector.

DATA NOT FOR QUOTATION

in the region studied, comparable to ^{235}U, although it is of interest to note that the several-MeV plateau is significantly lower than predicted by systematic formulae which are adequate in the U-Pu region.

TABLE A-XI

Preliminary ^{249}Cf fission cross section integrals (90° detector)

E_1 (eV)	E_2 (eV)	$\int_{E_1}^{E_2} \sigma_f dE$ (b-eV)	$\int_{E_1}^{E_2} \sigma_f \frac{dE}{E}$ (b)	$\bar{\sigma}_f$ (b)
2×10^1	10^2	3.3×10^3	86.2	41.7
10^2	3×10^2	5.3×10^3	30.3	26.5
3×10^2	10^3	9.3×10^3	17.5	13.3
10^3	3×10^3	1.4×10^4	8.4	7.2
3×10^3	10^4	2.9×10^4	5.2	4.1
10^4	3×10^4	5.8×10^4	3.3	2.9
3×10^4	10^5	1.6×10^5	2.8	2.3
10^5	3×10^5	3.9×10^5	2.2	1.9
3×10^5	10^6	1.0×10^6	1.8	1.4
10^6	3×10^6	3.2×10^6	1.7	1.6

B. VAN DE GRAAFF NEUTRON STUDIES

1. Neutron-Proton Scattering as a Nuclear Standard (J. C. Hopkins; G. Breit, SUNY, Buffalo) Relevant to WASH-1144, Requests 1-2.

A paper was accepted for publication in Nuclear Data on the $^1H(n,n)^1H$ scattering observables required for high precision fast-neutron measurements. Table B-I shows the most important results. The abstract is as follows:

The purpose of this paper is to provide the best possible values of the free n-p scattering total cross sections, differential cross sections, and polarization, for neutron energies between 100 keV and 30 MeV. These are extremely important numbers because they are used as standards for most fast-neutron cross-section measurements above 2 MeV and are frequently used at much lower energies. The relevant data will be defined, much of which has not been used in previous evaluations of the n-p cross sections. It is shown that the differential cross sections below 10 MeV

DATA NOT FOR QUOTATION

TABLE B-I. Representation of the c.m. $^1H(n,n)^1H$ Differential Cross Section in Terms of Legendre Polynomials Using Yale Phase Shifts. $\sigma(\theta) = C_o + C_1P_1 + C_2P_2 + C_3P_3 + C_4P_4$ mb/sr.

Lab Neutron Energy (MeV)	C_o	C_1	C_2	C_3	C_4	σ_T Calculated mb	σ_{TOTAL} (Gammel) mb
0.1	1.017×10^{3}	-5.691×10^{-1}	1.483×10^{-4}	1.067×10^{-8}	$-6.368\times10^{-[illegible]}$	12775	12790
0.2	7.696×10^{2}	-8.016×10^{-1}	5.992×10^{-4}	1.890×10^{-11}	$-5.520\times10^{-[illegible]}$	9671	9700
0.4	5.489×10^{2}	-1.052	-4.551×10^{-3}	4.872×10^{-6}	$5.029\times10^{-[illegible]}$	6897	6919
0.6	4.444×10^{2}	-1.226	9.922×10^{-3}	-7.035×10^{-5}	1.821×10^{-6}	5584	5596
0.8	3.817×10^{2}	-1.374	-7.720×10^{-3}	-1.130×10^{-4}	5.016×10^{-6}	4797	4801
1.0	3.390×10^{2}	-1.489	-7.403×10^{-3}	-3.249×10^{-4}	1.866×10^{-5}	4261	4259
2.0	2.320×10^{2}	-1.822	-3.466×10^{-2}	-7.535×10^{-3}	3.119×10^{-4}	2915	2903
3.0	1.825×10^{2}	-1.979	-4.865×10^{-2}	-1.446×10^{-2}	1.702×10^{-3}	2293	2279
4.0	1.517×10^{2}	-2.085	-5.991×10^{-2}	-2.821×10^{-2}	2.433×10^{-3}	1907	1893
5.0	1.301×10^{2}	-2.148	-2.520×10^{-2}	-4.613×10^{-2}	3.117×10^{-3}	1635	1623
6.0	1.138×10^{2}	-2.163	4.013×10^{-2}	-6.596×10^{-2}	5.142×10^{-3}	1430	1421
7.0	1.010×10^{2}	-2.150	7.064×10^{-2}	-8.682×10^{-2}	1.198×10^{-2}	1269	1262
8.0	9.065×10^{1}	-2.123	6.830×10^{-2}	-1.080×10^{-1}	2.455×10^{-2}	1139	1135
9.0	8.215×10^{1}	-2.100	1.446×10^{-1}	-1.320×10^{-1}	3.069×10^{-2}	1032	1029
10.0	7.506×10^{1}	-2.088	2.957×10^{-1}	-1.599×10^{-1}	3.194×10^{-2}	943.2	940.8
12.0	6.371×10^{1}	-2.065	4.999×10^{-1}	-2.131×10^{-1}	7.742×10^{-2}	800.5	800.0
14.0	5.514×10^{1}	-1.981	7.113×10^{-1}	-2.557×10^{-1}	1.078×10^{-1}	692.9	692.9
16.0	4.837×10^{1}	-1.871	9.248×10^{-1}	-2.934×10^{-1}	1.518×10^{-1}	607.8	608.8
18.0	4.289×10^{1}	-1.741	1.138	-3.233×10^{-1}	2.015×10^{-1}	539.0	540.9
20.0	3.838×10^{1}	-1.603	1.349	-3.423×10^{-1}	2.528×10^{-1}	482.3	485.1
22.0	3.462×10^{1}	-1.469	1.559	-3.544×10^{-1}	3.059×10^{-1}	435.0	438.4
24.0	3.143×10^{1}	-1.340	1.778	-3.611×10^{-1}	3.617×10^{-1}	394.9	398.8
26.0	2.869×10^{1}	-1.214	2.018	-3.604×10^{-1}	4.211×10^{-1}	360.5	364.8
28.0	2.632×10^{1}	-1.089	2.259	-3.531×10^{-1}	4.822×10^{-1}	330.7	335.4
30.0	2.426×10^{1}	-9.681×10^{-1}	2.489	-3.368×10^{-1}	5.406×10^{-1}	304.7	309.6

differ substantially from the isotropy that has frequently been assumed. In fact, the $\sigma(180^o)/\sigma(90^o)$ cross section ratios are approximately 1.023 at 7 MeV, 1.011 at 3 MeV, and 1.004 at 1 MeV. These anisotropies, minus 1.000, are higher than those predicted by the Gammel formula by factors of about 2 at 7 MeV, 5 at 3 MeV, 8 at 2 MeV, and 18 at 1 MeV. In addition, it will be shown that the shape of the differential cross section is far from symmetric about 90^o, the zero degree cross section, in fact, being less than the 180^o cross section for all energies below 30 MeV.

The cross sections given here differ significantly from previous estimates based only upon n-p data up to 30 MeV. The present results are derived from calculations using phase shifts obtained by the Yale N-N Interaction Group. Comparisons have been made with the results obtained from calculations employing the LRL and Dubna phase shifts. In all cases, the general features of large anisotropy and asymmetry are verified.

2. <u>n-^{4}He Angular Distribution Measurements Near E_n = 20 MeV</u> (A. Niiler*, M. Drosg, J. C. Hopkins, J. T. Martin, J. D. Seagrave, E. C. Kerr, and R. H. Sherman).

At the 3rd International Symposium on Polarization Phenomena, in Madison, Wisconsin, a talk was given by Niiler with the title "Phase Shifts from n-^{4}He Elastic Scattering Experiments Near 20 MeV," a shorter version reported in LA-4465-MS.

The n-^{4}He differential cross sections have been measured at 17.6, 20.9, and 23.7 MeV with a neutron time-of-flight technique using a 1-mole sample of liquid ^{4}He as a scatterer. The energies of 17.6 MeV and 23.7 MeV were chosen to match Broste and Simmons' polarization measurements. Using the measured data and the polarization data, phase shift searches with Dodder's general reaction matrix code EIA2 were carried out. The results are given in Table B-II. These measurements have made a substantial contribution to the single energy phase shift analyses and also the energy dependent analyses. This is important because the n-^{4}He polarization is used as a standard, and the polarization is calculated from the phase shifts.

The most significant differences between our set of phase shifts and that of Ref. 2 in Table B-II are smaller values for the $S_{1/2}$ and $P_{1/2}$ phase the somewhat larger values for the D- and F-waves, and the need for small amounts of G-waves.

The final paper on this experiment is being prepared.

---

*Now at Edgewood Arsenal, Maryland 21010.

DATA NOT FOR QUOTATION

TABLE B-II

n-^{4}He Phase Shifts in Degrees

	E_n (MeV)	$S_{1/2}$	$P_{3/2}$	$P_{1/2}$	$D_{5/2}$	$D_{3/2}$	$F_{7/2}$	$F_{5/2}$	$G_{9/2}$	$G_{7/2}$
Ref. 2	17.6	93	95	56	6	3	1	1		
	20.9	90	92	53	9	6	3	3		
	23.7	86	89	52	12	6	4	4		
Ref. 1	17.6	89	93	52	7.2	3.2	0.4	0.2		
	20.9	84	88	47	9.4	4.0				
Present Values Smooth Set	17.6	87	95	53.5	8	7.2	2.1	1.5	1.5	0.2
	20.9	79	92.5	48.5	11	10	3	3	3	0.8
	23.7	73	89	45.5	18.5	10.8	6.5	5.2	3.8	2.0
Present Values Single Energy	17.6	84	95	52.5	9.1	7.9	2.1	1.8	2.2	0.6
	20.9	83.7	97.7	45.7	8.5	15.7	1.2	4.6	6.5	-0.3
	23.7	71.2	88.3	45.6	19.7	10.8	6.8	5.7	3.3	1.9

1. G. R. Satchler, L. W. Owen, A. J. Elwyn, G. L. Morgan, and R. L. Walter, Nucl. Phys. A112, 1 (1968).

2. B. Hoop, Jr., and H. H. Barschall, Nucl. Phys. 83, 65 (1966).

3. <u>Elastic Scattering and Polarization of Fast Neutrons by Liquid Deuterium and Tritium</u> (J. D. Seagrave, J. C. Hopkins, A. Niiler (Edgewood Arsenal), R. K. Walter (EG&G), R. H. Sherman, and E. C. Kerr) Relevant to WASH-1144, Request 4.

Final cross section results are given in Tables B-III and B-IV. Model calculations were carried out by Lucke (SGS) this summer for some of the n-T cross sections which showed good fits but poor consistency of parameters as a function of energy. Arvieux (now at Grenoble) has corrected an error in his code for nucleon-deuteron phase shift analysis, and we will accept his offer to run it with our n-D data.

4. <u>Fast Neutron Fission of ^{244}Cm, ^{245}Cm, ^{246}Cm, ^{248}Cm, and ^{249}Cf (D. M. Barton and P. G. Koontz)</u>

Data for calculation of the (n,f) cross section of ^{248}Cm are now being gathered and will be included in a report listing the (n,f) cross section of ^{244}Cm at 1.0, 1.5, 3.0, and 14.9 MeV.

Requests for material for a similar measurement on ^{245}Cm, ^{246}Cm, and ^{249}Cf have been made to the Transplutonium Program Committee.

C. THERMAL NEUTRON CAPTURE GAMMA RAYS

1. <u>The $^{40}K(n,\gamma)^{41}K$ Reaction and the Level Structure of ^{41}K</u> (E. B. Shera and D. F. Beckstrand)

The low-lying level structure of ^{41}K has been studied using the thermal-neutron capture reaction, $^{40}K(n,\gamma)^{41}K$, on an isotopically separated target of ^{40}K. The γ-ray spectrum from this reaction has been investigated in the energy range from 0.1 MeV to 10.1 MeV using a Li-drifted Ge spectrometer system. γ-γ coincidence measurements using Ge(Li) detectors have also been made. Spin and parity assignments for the excited states below 2450 keV are proposed, primarily on the basis of γ-ray branching to levels with established spin and parity values. The proposed level energy (I^π) values are 0($3/2^+$), 980.4($1/2^+$), 1293.4($7/2^-$), 1559.9($1/2^+$), 1582.0($5/2^+$), 1677.5($5/2^+,7/2^+$), 1698.1($5/2^\pm,7/2^+$), 2144.1($5/2^+$), 2166.0($1/2^\pm,3/2^\pm$), 2316.5($5/2^+,7/2^+$), 2447.9($1/2^\pm,3/2^\pm$). Additional levels have been observed at 2494.7, 2507.9, 2527.9, 2599.8, 2681.5, 2712.2, 2756.5, 2760.7, 3042.1, 3142.1, 3164.5, 3213.4, 3235.6, and 3281.1 keV. The experimental findings are summarized in Fig. C-1. The low-lying excited states of ^{41}K are interpreted in terms of two-particle, one hole configurations of the form $p(d_{3/2})^{-1}n(f_{7/2})^2$.

DATA NOT FOR QUOTATION

TABLE B-III

Differential Cross Sections for Elastic Scattering of Fast Neutrons by Deuterium

E_n=5.55 MeV

cosθ'	σ	Δσ
0.695	184.0	12.9
0.600	163.0	11.4
0.411	141.0	9.9
0.120	99.5	7.0
-0.140	60.7	4.3
-0.240	55.8	3.9
-0.396	47.9	3.4
-0.566	57.2	4.0
-0.704	89.1	6.2
-0.826	104.6	7.3

E_n=9.0 MeV

cosθ'	σ	Δσ
0.695	123.0	8.6
0.266	80.3	5.6
0.064	54.8	3.8
-0.099	44.7	3.1
-0.241	34.7	2.4
-0.430	25.0	1.8
-0.559	22.8	1.6
-0.688	34.6	2.4
-0.912	107.0	7.5

E_n=20.5 MeV

cosθ'	σ	Δσ
0.7132	82.9	6.8
0.6951	73.5	6.1
0.6950	76.2	6.3
0.6000	64.2	5.5
0.4540	39.5	3.8
0.3889	35.7	3.5
0.3888	28.7	3.0
0.2430	26.6	2.9
0.0970	18.3	2.3
0.0749	17.8	2.3
0.0420	19.2	2.3
-0.1710	12.6	1.9
-0.2010	9.8	1.7
-0.3960	5.6	1.4
-0.3961	5.3	1.4
-0.5860	3.2	1.2
-0.5861	3.1	1.2
-0.7440	5.7	1.4
-0.7530	4.3	1.3
-0.8650	19.5	2.4
-0.9070	22.6	2.6
-0.9071	29.0	3.0

E_n=7.0 MeV

cosθ'	σ	Δσ
0.695	169.0	11.8
0.444	126.0	8.8
0.232	101.0	7.1
0.064	76.5	5.4
-0.161	47.2	3.3
-0.388	38.4	2.7
-0.523	36.6	2.6
-0.704	56.9	4.0
-0.815	99.3	7.0
-0.912	103.0	7.2

E_n=18.55 MeV

cosθ'	σ	Δσ
0.7478	88.2	6.8
0.7132	87.9	7.1
0.6199	68.3	5.8
0.5902	63.9	5.5
0.5183	53.8	4.8
0.3889	40.8	3.9
0.3556	39.2	3.7
0.2209	26.1	2.8
0.1870	27.2	2.9
0.1420	22.6	2.6
-0.0131	15.3	2.1
-0.0776	13.1	1.9
-0.1404	14.6	2.0
-0.2407	7.8	1.5
-0.2408	9.5	1.7
-0.4297	5.1	1.4
-0.4932	3.8	1.3
-0.6245	5.0	1.3
-0.6718	3.4	1.2
-0.7754	9.7	1.7
-0.8115	10.6	1.7
-0.8976	26.0	2.8
-0.9117	35.3	3.5

E_n=8.0 MeV

cosθ'	σ	Δσ
0.695	156.0	10.9
0.053	58.9	4.1
-0.120	44.1	3.1
-0.201	33.0	2.3
-0.241	33.5	2.3
-0.388	27.2	1.9
-0.470	28.0	2.0
-0.501	23.4	1.6
-0.612	28.2	2.0
-0.771	60.2	4.2
-0.871	95.5	6.7

E_n=23.0 MeV

cosθ'	σ	Δσ
0.7130	81.1	6.7
0.6490	56.5	5.0
0.5180	45.8	4.2
0.4870	46.1	4.2
0.3890	32.8	3.3
0.2660	17.5	2.2
0.1870	19.0	2.3
0.0749	13.6	2.0
0.0750	13.6	2.0
-0.0350	9.4	1.7
-0.0990	9.5	1.7
-0.2410	7.0	1.5
-0.4860	3.0	1.2
-0.6550	2.9	1.2
-0.7490	7.2	1.5
-0.8000	9.2	1.6
-0.9090	25.7	2.8

DATA NOT FOR QUOTATION

TABLE B-IV

Center-of-Mass Differential Cross Sections for Elastic Scattering of Fast Neutrons by Tritium

cosθ'	σ	Δσ	cosθ'	σ	Δσ	cosθ'	σ	Δσ
E_n=6.0 MeV			E_n=9.0 MeV			E_n=18.0 MeV		
0.850	427.9	21.4	0.856	276.2	13.8	0.850	182.5	9.4
0.669	337.4	16.9	0.644	206.3	10.3	0.710	135.2	7.3
0.376	180.4	9.0	0.386	127.6	6.4	0.627	116.4	6.4
0.098	88.2	4.4	0.128	73.4	3.7	0.501	85.0	5.0
-0.048	54.1	2.7	-0.086	37.4	1.9	0.337	52.2	3.4
-0.197	39.0	2.0	-0.301	17.8	0.9	0.198	40.9	2.6
-0.444	45.4	2.3	-0.481	18.6	0.9	0.078	26.6	1.9
-0.661	92.0	4.6	-0.655	39.7	2.0	-0.058	15.8	1.1
-0.854	183.1	9.2	-0.854	91.7	4.6	-0.206	7.8	0.7
						-0.406	2.3	0.5
						-0.510	1.9	0.5
						-0.644	5.4	0.7
						-0.767	13.7	1.2
						-0.847	22.9	1.7
E_n=19.5 MeV			E_n=21.0 MeV			E_n=23.0 MeV		
0.791	142.0	7.3	0.798	124.3	6.4	0.798	122.5	6.3
0.756	129.9	6.7	0.710	101.6	5.3	0.694	86.9	4.5
0.661	106.8	5.5	0.492	63.0	3.4	0.492	48.0	2.6
0.454	68.7	3.7	0.317	45.5	2.5	0.297	32.2	1.9
0.178	33.0	1.9	0.049	17.7	1.2	0.138	18.8	1.2
-0.058	13.4	1.0	-0.206	6.0	0.6	-0.086	9.7	0.8
-0.318	2.6	0.5	-0.414	1.3	0.4	-0.301	2.8	0.5
-0.503	1.7	0.5	-0.583	2.4	0.5	-0.523	1.7	0.5
-0.608	3.3	0.6	-0.672	5.0	0.7	-0.709	5.3	0.7
-0.719	8.5	0.9	-0.789	15.2	1.3	-0.758	8.0	0.9
-0.837	20.0	1.6	-0.854	19.2	1.5	-0.854	14.6	1.3

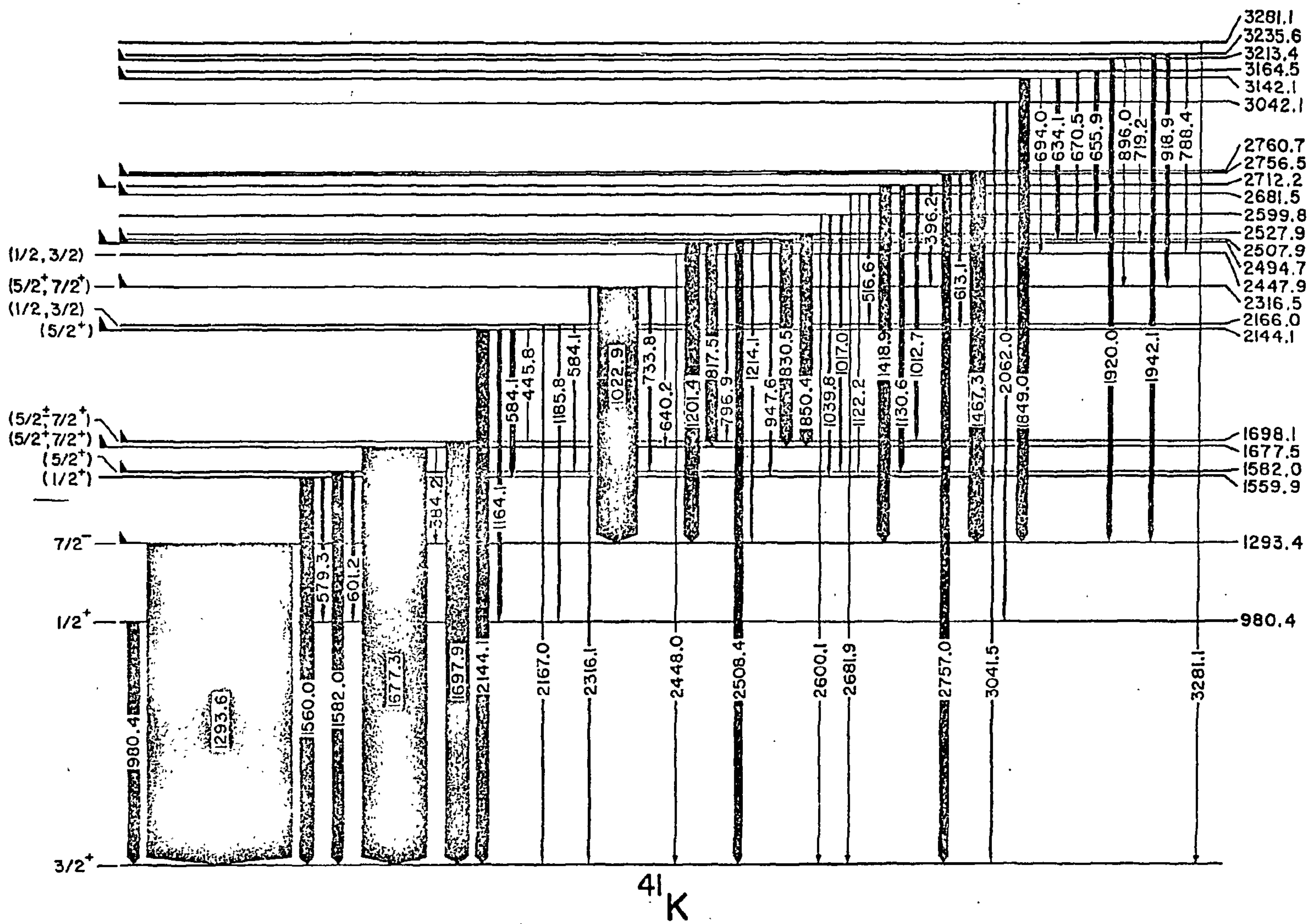

Fig. C-1. Level structure of ^{41}K, showing relative gamma-ray intensities.

2. High Energy Gamma Rays from Thermal Neutron Irradiation of ^{235}U and ^{239}Pu (E. T. Jurney)

The internal target thermal neutron capture gamma facility at the Omega West Reactor has been used to obtain preliminary gamma spectra between 4.4 and 6.8 MeV from targets of ^{235}U and ^{239}Pu. The measurements were made with a 26 cm^3 Ge(Li) detector inside a divided NaI annulus with the entire system operated as a double-escape pair spectrometer.

Table C-1 presents the observed spectra. Energies are in keV and intensities are expressed as barns of partial absorption cross section. Excitation energies and J^{π} values for the levels in the product nuclei have been assigned when it has been possible to identify gamma rays with neutron capture. Note that members of the ground-state multiplet are excited in both nuclei (2^+ and 4^+ in ^{236}U, 2^+ in ^{240}Pu). The neutron binding energy is 6544 ± 2 keV for ^{236}U and 6534 ± 2 keV for ^{240}Pu.

Of the 12 gammas which appear to be common to both spectra, 7 have about the same intensity and 5 are from 2 to 10 times more intense for Pu. Some of the difference might arise from the shift in the fission yield distribution. It is also possible that strong ^{240}Pu capture lines occur accidentally at energies coincident with lines in the U spectrum.

Work on these interesting nuclei will continue. In particular, the range of observation will be extended to both lower and higher energies.

D. FISSION ISOMER STUDIES (H. C. Britt, B. H. Erkkila, J. E. Lynn,* and W. E. Stein)

Excitation functions have been measured for the production of fission isomers in the reactions $^{237}Np(\alpha,2n)^{239m}Am$, $^{239}Pu(\alpha,2n)^{241}Cm$, $^{240}Pu(\alpha,2n)^{242m}Cm$, $^{242}Pu(\alpha,2n)^{244m}Cm$, $^{242}Pu(\alpha,3n)^{243m}Cm$, $^{244}Pu(\alpha,3n)^{245m}Cm$. The excitation energies of the fission isomers ^{241m}Cm, ^{243m}Cm and ^{245m}Cm appear to be 2.0 - 2.5 MeV above the ground state and have measured half-lives of 15±1 nsec, > 40 nsec and 23±5 nsec, respectively. The isomers ^{242m}Cm and ^{244m}Cm have half-lives > 80 nsec, are weakly excited and show apparent thresholds 3 - 4 MeV above the ground state. These isomers are believed to be examples of the decay of an excited state in the secondary minimum. For these even-even nuclei the lowest shape isomeric state was expected to have a half-life < 1 nsec which would be unobservable in the present experiment.

Excitation functions have been measured for isomer production from deuteron bombardment on targets of ^{235}U, ^{237}Np, ^{239}Pu, ^{240}Pu, ^{242}Pu, ^{244}Pu. The isomers from bombardment of ^{237}Np and the Pu targets are primarily from

*Consultant from AERE.

TABLE C-I

Gamma rays between 4.4 and 6.8 MeV from thermal neutron irradiation of ^{235}U and ^{239}Pu

E_γ (keV)	^{235}U Target dE_γ	$I_\gamma(b)$	$E_{ex}(J^\pi)$	E_γ (keV)	^{239}Pu Target dE_γ	$I_\gamma(b)$	$E_{ex}(J^\pi)$
				4432.5	0.3	3.5	
4453.4	0.3	1.9		4453.4	0.3	3.7	
4464.5	0.5	0.2		4464.6	0.4	3.1	
				4474.4	0.5	1.4	
4493.0	0.4	0.4		4493.7	0.4	1.5	
				4502.5	1.6	0.4	
				4555.7	0.4	1.1	
4563.2	0.5	0.3					
4573.8	0.8	0.1					
4611.8	0.5	0.1					
4638.0	1.0	0.07					
4646.8	0.3	0.7		4647.1	0.5	0.8	
				4654.3	0.3	1.9	
				4709.2	0.4	0.6	
4713.6	1.0	0.06					
4721.7	0.4	0.1					
4729.0	0.9	0.05					
4734.7	0.6	0.1	1810				
4748.3	0.5	0.1					
				4758.7	0.3	1.7	
4773.4	0.8	0.1					
4785.7	0.5	0.2					
4808.3	0.9	0.06					
4815.0	0.7	0.1					
4836.3	0.6	0.1					
4870.9	0.5	0.1					
4879.8	1.0	0.1					
4885.7	0.4	0.4					
4925.7	0.7	0.1		4926.9	0.4	0.7	
				4946.2	0.6	0.3	
4962.4	0.5	0.2					
4974.2	0.4	0.3					
4985.3	0.6	0.1					
				4994.7	0.4	0.8	
				5007.3	0.8	0.2	(1527)
5020.1	0.5	0.2					
				5046.1	0.4	0.7	
5119.9	0.6	0.1					
				5123.2	0.3	2.3	$1410(0^+)$
5146.0	0.5	0.2					
5163.8	0.9	0.1					
5187.4	0.4	0.4		5188.3	0.7	0.3	

TABLE C-I (Continued)

E_γ (keV)	^{235}U Target dE_γ	I_γ(b)	$E_{ex}(J^\pi)$	E_γ (keV)	^{239}Pu Target dE_γ	I_γ(b)	$E_{ex}(J^\pi)$
5197.2	0.4	0.2					
5203.0	0.7	0.05	1342				
5212.4	0.7	0.1					
5215.8	0.6	0.2					
				5289.5	0.9	0.2	
				5293.8	0.4	1.1	
5299.2	0.5	0.2					
				5311.4	0.6	0.3	
5323.8	0.5	0.08		5323.9	0.9	0.1	
				5397.3	0.6	0.3	1137(2^+)
5405.9	0.3	0.5		5405.4	0.5	0.6	
5456.7	0.6	0.08					
5517.8	0.3	0.3		5518.0	0.5	0.2	
5533.8	0.6	0.1		5534.3	0.6	0.2	
5544.6	0.7	0.07	1000(2^+)				
				5575.6	0.3	3.5	
5585.5	0.9	0.03	959(2^+)				
				5596.1	0.8	0.2	937(2^+)
5607.8	0.5	0.08					
				5630.7	1.0	0.1	902(2^+)
				5634.3	0.6	0.4	
				5673.4	0.8	0.2	860(0^+)
				5931.3	0.8	0.2	
				5937.3	0.5	0.4	597(1^-)
6211.4	0.5	0.06		6212.3	1.4	0.08	
6395.4	0.3	0.4	149(4^+)				
				6491.5	0.5	0.6	43(2^+)
6498.9	0.8	0.02	45(2^+)				
6780.0	0.4	0.1		6781.0	0.8	0.5	

DATA NOT FOR QUOTATION

(d,2n) reactions except for ^{239}Pu where for $E_d > 12$ MeV there is a significant contribution from the (d,pn) reaction. Using our measurements and results from Copenhagen it is possible to correct our results for contributions from (d,p) and (d,pn) reactions and obtain excitation functions for the (d,2n) reactions.

In many cases the data obtained from the (d,2n) reaction can be compared to data obtained from (α,2n), (p,2n), or (n,2n) reactions leading to the same final nucleus. Comparison of data from various reactions leading to fission isomers in ^{237}Pu, ^{239}Am and ^{240}Am show absolute measured ratios of the isomer to prompt fission cross sections agree to within ±20%. The agreement between results obtained with different reactions and the results obtained at two different laboratories with very different experimental systems is remarkable.

A model based on statistical considerations is being developed to try to fit the measured isomer excitation functions. For xn-evaporation reactions the calculations consider the competition between fission and neutron emission to the normal and isomeric deformation. For non-thermally fissioning nuclei the height of either the first peak, E_A, or the second, E_B, can be determined from the energy of the neutron fission threshold; the position of the secondary minimum, E_{II}, from the shape of the isomer excitation function; and the energy difference between the first and second peaks, $E_A - E_B$, from the absolute magnitude of the isomer cross sections. Then the curvatures of the two peaks A and B can be determined from measured spontaneous and isomer half-lives. Preliminary results give adequate fits to the isomer excitation functions and indicate for Pu, Am, and Cm isotopes that the first barrier is higher than the second fission barrier, $E_A > E_B$.

E. RESEARCH IN SUPPORT OF NUCLEAR SAFEGUARDS

1. Delayed-Neutron Yield from Fission as a Function of the Energy of the Neutron Causing Fission (M. S. Krick and A. E. Evans)

Measurements of total delayed-neutron yields as a function of the energy of the neutron inducing fission have been extended to neutron energies over the range from 4 to 7 MeV for ^{238}U, ^{235}U, and ^{233}U.

The experimental technique was as outlined previously.[2] The higher energy neutrons from the D(d,n)^{3}He reaction were produced by a 25-μamp deuteron beam from the LASL 3-MeV Van de Graaff accelerator impinging on a 1-mg/cm^2 TiD target. The accelerator beam was modulated to produce 40-millisec bursts of neutrons, followed by a 60-millisec "off" period. Delayed neutrons were counted during the final 50 millisec of the "off"

[2] M. S. Krick and A. E. Evans, Bull. Am. Phys. Soc. 15, 87 (1970); Report LA-4368-MS, pp. 11-12 (1969), and previous report to the NCSAC.

period, after bombarding the samples with the modulated beam long enough to allow the decay of all delayed-neutron groups to come into equilibrium with production. The fission rate of the sample materials was monitored by sandwiching the sample between two fission chambers containing some of the sample material. Delayed neutrons were counted using a calibrated ^{3}He-detector-polyethylene array described previously.[3]

The results are shown in Figs. E-1 to E-3. It is now established that, for the three isotopes measured, the delayed-neutron yield is independent of energy from 0 to 4 or 5 MeV; the yield then decreases rapidly over a ~ 2-MeV interval to near the yield value previously measured at 14.9 MeV.[4] This yield-vs-energy behavior strongly suggests that the energy dependence of the delayed-neutron yield is associated with the threshold for fission after inelastic neutron scattering. Since the fissioning nucleus has in this case one less neutron to distribute among fission products, it is reasonable to expect fewer neutron-rich precursors of delayed neutrons than in the case of conventional fission induced by capture of a neutron. These results are generally consistent with our understanding of the delayed neutron emission process and with known systematics of total delayed-neutron yields.[5]

F. FACILITIES AND TECHNIQUES

1. Time-of-Flight Neutron Resonance Radiography (L. Forman, C. U. Benton, D. A. Garrett, and A. D. Schelberg)

One possible application of cross-section data is the identification of elements by resonance structure. A technique has been developed at LASL whereby objects may be radiographed in a desired energy interval. Transmitted neutrons create light in a ^{6}Li-loaded fluor. The resulting image is recorded by a gated image intensified television camera tube in a time interval calculated by time of flight. In a feasibility study at the Sandia Pulsed Reactor Facility using a 13.2-meter flight path, radiographs were obtained about the 4.9-eV resonance of gold, the 1.45-eV resonance of indium, the 1.1-eV and 2.38-eV resonances of hafnium, and the 0.45-eV resonance of erbium. The samples were not imaged at energies that were off resonance. A more detailed description of this work should be published soon in Rev. Sci. Instr.

---

[3] L. V. East and R. B. Walton, Nucl. Inst. Meth. 72, 161 (1969).

[4] C. F. Masters, M. M. Thorpe, and D. B. Smith, Nucl. Sci. and Eng. 36, 202 (1969).

[5] G. R. Keepin, Physics of Nuclear Kinetics, Addison-Wesley, Reading, Mass. (1965), p. 101.

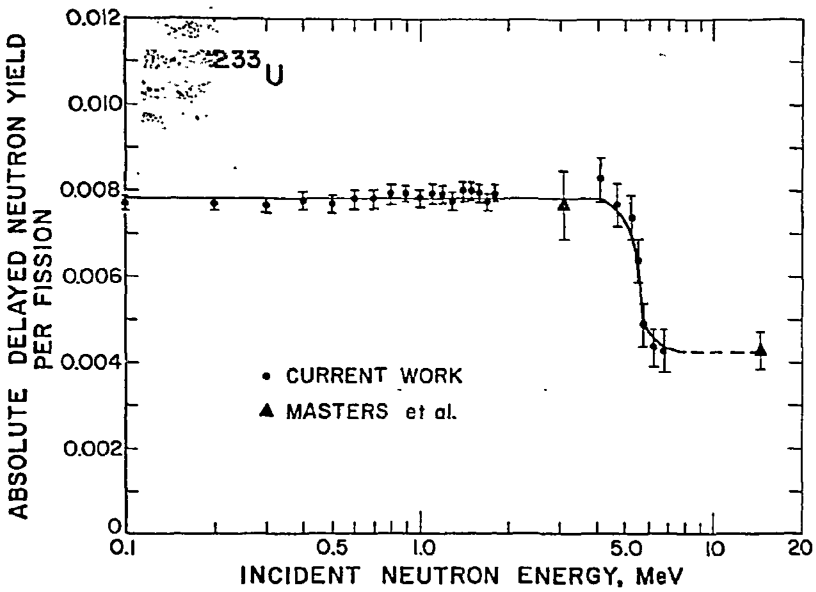

Fig. E-1. Delayed neutron yield per fission as a function of neutron energy for (^{233}U + n).

DATA NOT FOR QUOTATION

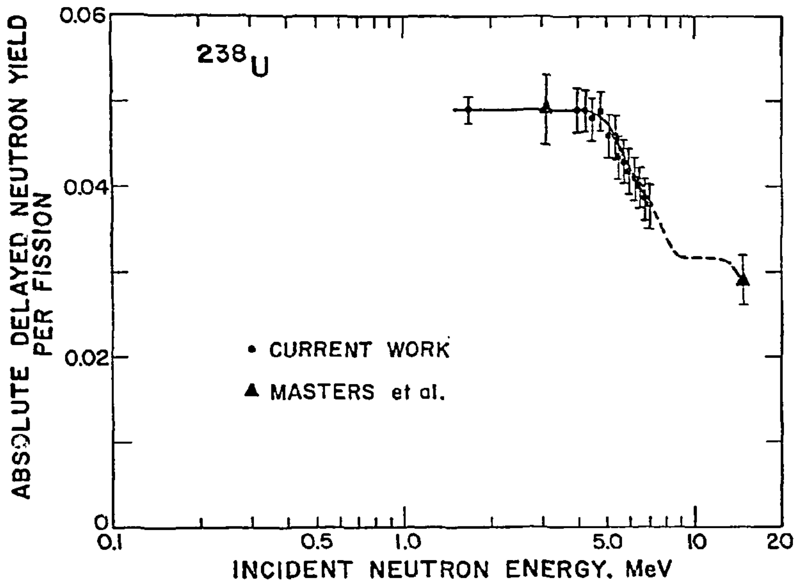

Fig. E-3. Delayed neutron yield per fission as a function of neutron energy for (^{238}U + n).

DATA NOT FOR QUOTATION

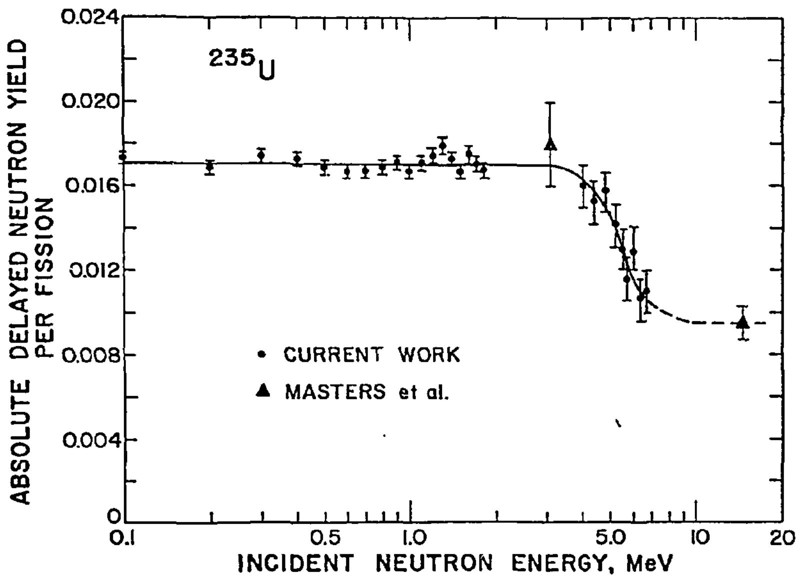

Fig. E-2. Delayed neutron yield per fission as a function of neutron energy for (^{235}U + n).

DATA NOT FOR QUOTATION

2. Energy Loss Codes (J. D. Seagrave)

Bichsel's program has been released from disc storage and is now on an Update tape. Some minor modifications are planned. The program MIXEL which uses dE/dx cards from Bichsel's program is available to prepare tables for binary mixtures. It has been used for various organic (and deuterated) scintillators and recently for NaI.

3. Liquid Fuel High Intensity Neutron Source (L. D. P. King)

Work is proceeding on the testing of the properties of 3.1 M uranyl sulfate fuel plus additives under simulated conditions expected in a full scale version of the Liquid Excursion Pulsed Reactor (LEPR) concept. A fuel capsule has been designed and pressure tested with explosives to hold a 0.1-cm^3 fuel sample in a 0.2-cm^3 cavity. The capsule and fuel have been shipped to the Livermore Super Kukla burst facility and await calibration runs and a maximum burst exposure.

Two special fuel capsules have been fabricated with two lens apertures for fuel tests in a neodymium doped laser pulse (1.06-μ wavelength). Two laser tests have been completed in which about 1 joule/μliter is believed to have been absorbed in a 1- and 5.3-μliter fuel sample. The physical and chemical composition of the fuel appears to have been maintained. Further laser fuel tests will be made as soon as higher pulse intensities become available without prelasing at Sandia and Los Alamos.

Slow progress continues on the Kinglet dynamic critical facility. This facility will be used as a proof test for the Kinetic Intense Neutron Generator (KING) concept. The equipment shown in Fig. F-1 has been completed. The following principal items remain before tests of the nuclear operating characteristics can begin. Complete system checkout; beryllium reflector stacking; final static critical check using an 85-gram ^{235}U/liter fuel solution; hydraulic checkout of all fuel handling components using water instead of fuel solution; and loading with ~500 liters of fuel solution.

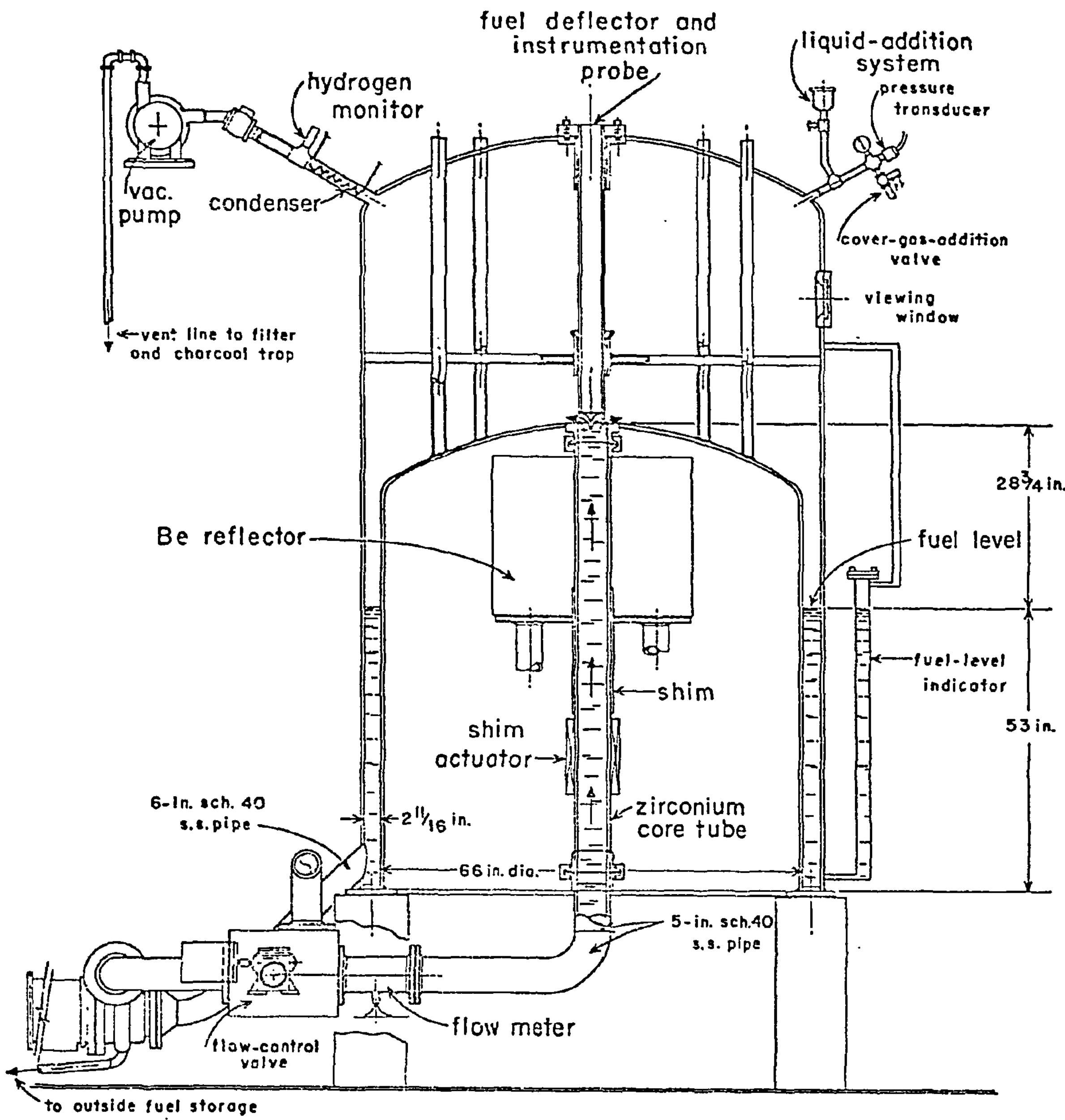

Fig. F-1. Experimental arrangement for the Kinglet dynamic critical facility.

DATA NOT FOR QUOTATION

NATIONAL BUREAU OF STANDARDS

A. NEUTRON PHYSICS

1. MeV Neutron Total Cross Sections (R. B. Schwartz, R. A. Schrack, and H. T. Heaton II)

We have completed measurements of the total neutron cross section of lead in the energy range 0.5 to 20 MeV, with results as shown in Figure A-1. The [illegible] is approximately 0.1 nsec/m, and the absolute accuracy is estimated to be close to 1%. In general, our results are in good agreement with other data, except that our results show more structure than most of the older work.

Preliminary results on the beryllium cross section also seem to be in good agreement with earlier data. We are continuing the beryllium measurements, primarily to check on the possibility of fine structure at the 2.7 MeV resonance.

We have measured the hydrogen-deuterium cross section difference by measuring the relative transmissions of heavy water and normal water. These results were compared with the results of the recent Wisconsin measurements of hydrogen and deuterium. Our directly measured differences are in good agreement with the differences calculated from the two separate Wisconsin measurements, except for a slight discrepancy at 4 MeV, where our results imply a slightly higher deuterium cross section. We plan to measure the deuterium cross section explicitly later this month using deuterated benzene samples.

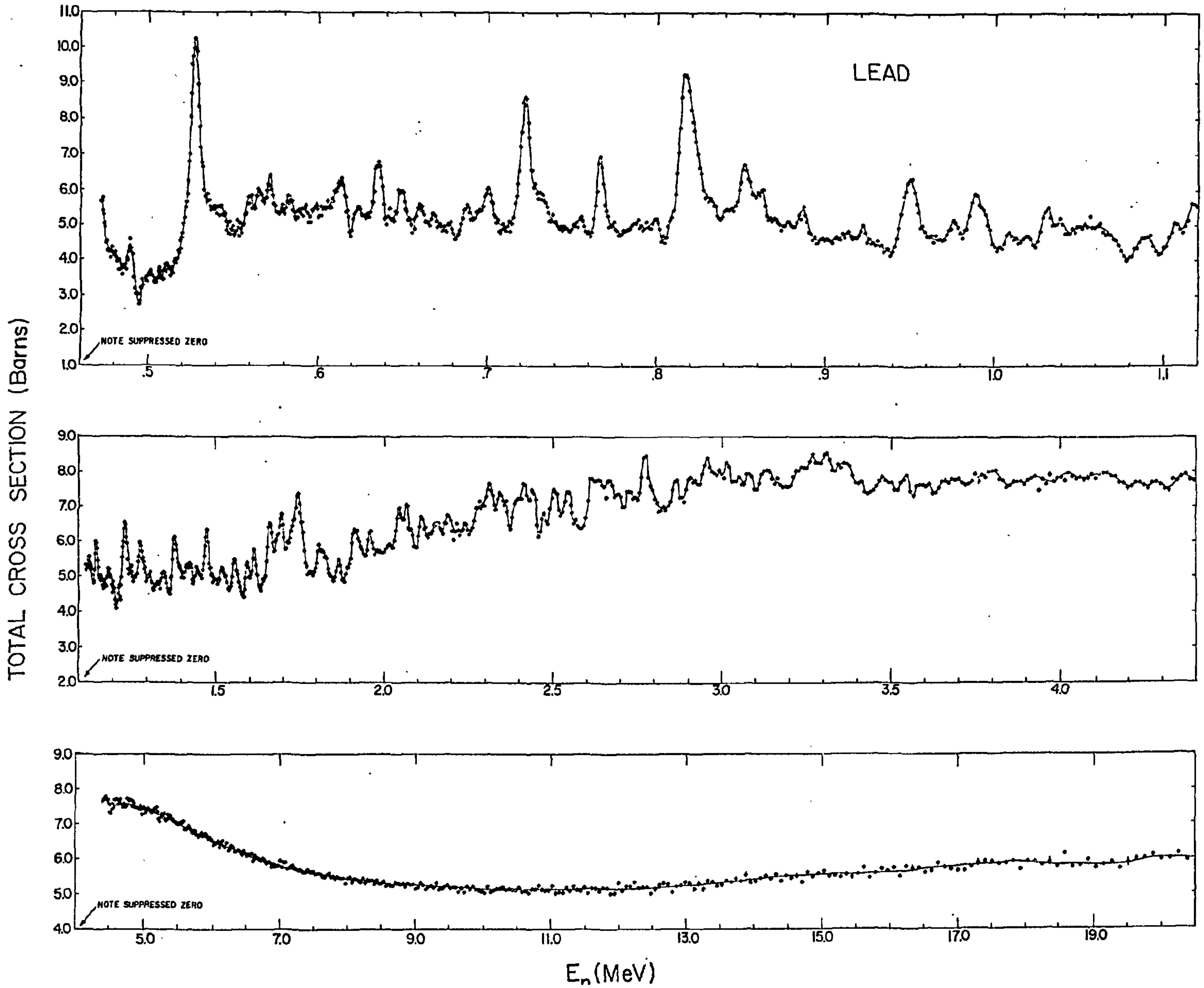

Figure A-1

DATA NOT FOR QUOTATION

NUCLEAR EFFECTS LABORATORY

A. SMALL-ANGLE ELASTIC SCATTERING OF FAST NEUTRONS (W. P. Bucher, C. E. Hollandsworth, R. D. Lamoreaux, and R. R. Sankey)

Data for the scattering of 7.55 and 9.5 MeV neutrons from C, N (N_2H_4) and O(H_2O) have been obtained for scattering angles of 3°, 7.5°, and 15° using the special-purpose collimator described in previous reports. Time-of-flight over a 2 meter flight path and neutron-gamma ray discrimination are used for background suppression. Reduction of the data is in progress. A Monte Carlo code to correct the data for multiple scattering effects has been written and is presently being checked.

Preliminary estimates of the corrections to be applied to the data indicate that the zero degree cross section for nitrogen will exceed previous estimates by approximately a factor of 2. Because of the importance of nitrogen in radiation transport calculations and the presence of a discrepancy in the existing nitrogen cross sections,[1] further measurements for nitrogen are planned. (Data pertinent to requests #31, #33, #39, #40, and #44; WASH 1144 - Draft Version).

Measurements will also be carried out for the following elements: Be, Al, S, Fe, Cu, and Pb. (Pertinent to Requests #22, #61, and #100; WASH-1144 - Draft Version).

B. DELAYED FISSION ISOMERS (D. Eccleshall, J. K. Temperley, J. A. Morrissey; S. L. Bacharach (Catholic Univ.))

Isomers with half-lives of about 100 ns and 900 ns in ^{237}Pu are being studied via the ^{237}Np(d,2n)^{237}Pu reaction. A pulsed and bunched beam from the tandem Van de Graaff accelerator is used, and the fission fragments are observed in surface barrier detectors. Data will be obtained for deuteron energies between 9 and 15 MeV. Data taken so far at 10, 11, and 12 MeV are consistent with a (d,2n) reaction. The isomers have comparable production cross sections, and the ratio of the two cross sections is relatively constant with energy. An abstract is being submitted to the New York American Physical Society meeting.

[1] J. K. Dickens and F. G. Perey, Nucl. Sci. Eng. 36, 280 (1969).

OAK RIDGE NATIONAL LABORATORY

A. Neutron Physics

1. Total Cross Sections

a. Total Cross Section for ^{16}O for 1.75- to 4.35-MeV Neutrons from a T(p,n) Source

(J. L. Fowler, C. H. Johnson, and R. M. Feezel)

A detailed knowledge of the neutron total cross section of ^{16}O is important for some shielding calculations; in particular, the minimum cross section at the well-known 2.35-MeV s-wave resonance is of interest because it is a "window" for escaping neutrons. Fowler et al.[1] and Johnson et al.[2] reported previously the neutron total cross section of ^{16}O as measured with 2- to 4-keV resolution over most of the energy region from 1680 to 4340 keV. The source for that work was the $^7Li(p,n)$ reaction induced by protons from the 5.5-MV Van de Graaff. We have now covered about the same energy region with the T(p,n) reaction at 30-keV resolution. The $^7Li(p,n)$ source has the advantage that it yields neutrons with accurately known energies and good resolution but the disadvantage that it has a second neutron group. At most energies the corrections which we made for this second group were small, but at some energies these were large, e. g. at the 2.35-MeV s-wave minimum the corrections exceeded 100%.

The data points in Fig. 1(1a) show our new measurements with the T(p,n) source, and the curve represents the earlier $^7Li(p,n)$ data except for the omission of five very narrow ($\Gamma < 2$ keV) resonances at 2888, 3006, 3212, 3438, and 3441 keV. We have adjusted the energy scale of the new work to agree with the older, more accurate scale. The cross sections are in good agreement except near narrow resonances. The new minimum for the s-wave resonance is 0.170 ± 0.006 barns; the correction for energy resolution reduces this to about 0.12 barns in excellent agreement with our earlier value (0.133 barns) for the $^7Li(p,n)$ source. At higher energies the two sets generally agree with each other and with the earlier work of Fossan et al.,[3] but there are certain regions where slight disagreements in the data from the two

[1] J. L. Fowler, C. H. Johnson, and F. X. Haas, Proc. Int. Symp. Nucl. Structure Contributions (Dubna, USSR, July 1969) p. 1 (1968).

[2] C. H. Johnson, J. L. Fowler, and R. M. Feezel, Report to the AEC Nuclear Cross Section Advisory Committee, ORNL-TM-2998, p. 12 (1970).

[3] D. B. Fossan, R. L. Walter, W. E. Wilson, and H. H. Barschall, Phys. Rev. 123, 209 (1961).

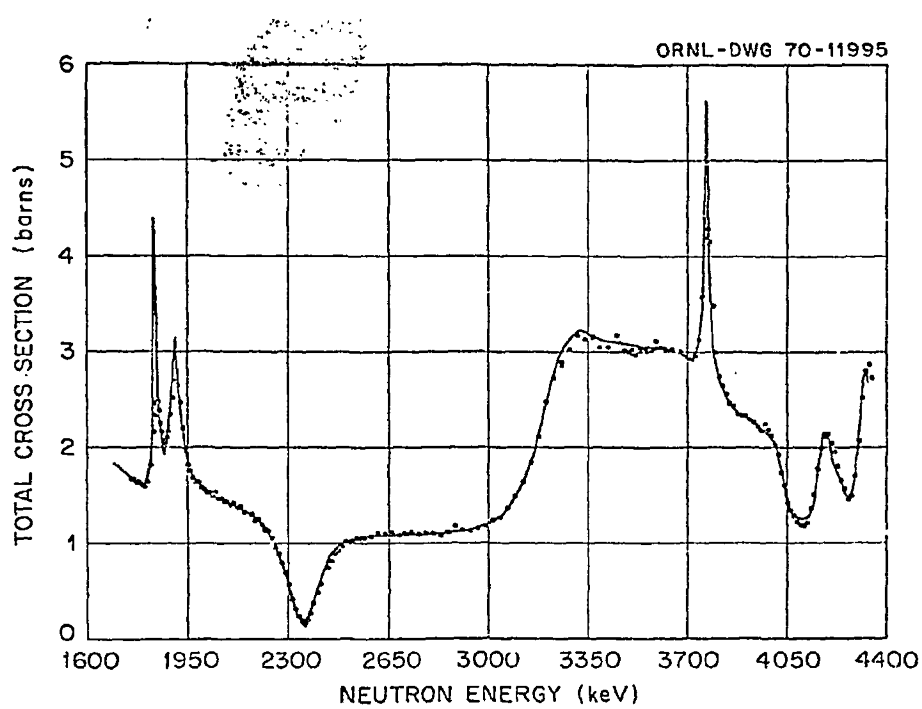

Fig. 1(1a). Neutron total cross section of ^{16}O as measured with T(p,n) neutrons with about 30 keV resolution. The curve represents earlier measurements with the ^{7}Li(p,n) source with 3- to 4-keV resolution. Five very narrow resonances are omitted from the curve.

DATA NOT FOR QUOTATION

sources suggest that the corrections for the second group from the $^{7}Li(p,n)$ reaction were not quite right. For example, it appears that the correction should have been larger at the 4.1-MeV minimum and smaller just above the 4.2-MeV peak. In this latter region we are not surprised that we over-corrected for the second group because the energy of the group happens to coincide with the strong 3.77-MeV resonance.

b. Transmission Measurements on Separated Isotopes
(W. M. Good, J. A. Harvey, and G. G. Slaughter)

Instrumentation is still in progress for transmission measurements on separated isotopes. Depending upon the amount of sample available, such measurements can be made at energy resolution figures of from 0.3% at 18 M to < 0.1% at 80 M. Natural lead has been used for preliminary studies at 80 M. Energy discrepancies and background uncertainties are still under investigation. There appears, however, essentially a one to one correspondence between the levels observed in transmission and those reported in capture by Block et al.[1] meaning that seemingly every level seen in capture has also been seen in transmission. With the completion of lead, measurements will begin on calcium.*

[1]WASH-1079, p. 146 (1967).

*Request No. 72.

c. Transmission Measurements upon ^{120}Sn and ^{118}Sn
(R. F. Carlton, J. A. Harvey, and G. G. Slaughter)

Transmission measurements have been made at ORELA upon 2.67" and 2" thick samples of ^{120}Sn and ^{118}Sn, respectively. A 4-1/2"-Dia. ^{6}Li glass scintillator was used with an 18-meter flight path resulting in neutron energy resolution of ~0.3%. Several moderately strong resonances were observed in the 10 keV energy region which did not show asymmetries and, hence, are not s-wave resonances. The transmission data are being analyzed by an area analysis program to obtain the neutron widths of the resonances. Measurements upon enriched samples of ^{124}Sn and ^{122}Sn will be made at both the 18-meter and 80-meter flight stations.

d. Parameters of Neutron Resonances in ^{243}Am
(J. A. Harvey and G. G. Slaughter; F. B. Simpson and O. D. Simpson;* R. W. Benjamin and C. E. Ahlfeld**)

Transmission measurements have been made on two small samples of ^{243}Am (99.73%) from 0.5 to 1000 eV using the Oak Ridge Electron Linear

*Idaho Nuclear Corporation.

**Savannah River Laboratories.

Accelerator. High resolution data ($\Delta E/E \sim 0.3\%$) were taken using 20 nsec bursts of 140 MeV electrons, 10 nsec channel widths, the SEL computer, and a flight path of 18.5 meters. The instrumental resolution was sufficiently good that Doppler broadening was the limiting effect in data analysis below 200 eV. Breit-Wigner single-level resonance parameters were obtained below 20 eV using a shape analysis program. The radiation widths of 17 resonances have been measured giving an $\bar{\Gamma}_\gamma$ of 39.0×10^{-3} eV. Area analysis was used above 20 eV where the Doppler width was too large to permit shape analysis. Preliminary results up to 60 eV were given in the last report to the NCSAC (NCSAC-31, page 69). Analysis of 156 resonances have now been completed up to 180 eV. The observed resonance spacing for both spin states is 0.70 ± 0.07 eV and the s-wave strength function ($10^4 \times \bar{\Gamma}_n^{\,0}/D$) is 0.88 ± 0.09. These values are in good agreement with earlier data based on resonances up to $\sim$25 eV. Transmission measurements upon other small samples of transplutonium isotopes are planned.

2. Radiative Capture Cross Sections and Spectra

a. Neutron Capture Cross Sections of ^{13}C and ^{16}O[1]

(B. J. Allen[*] and R. L. Macklin)

Measurements of the capture cross sections of ^{13}C and ^{16}O have been made at the Oak Ridge Linear Accelerator (ORELA). The accelerator was pulsed at 800 pps, with a beam pulse width of 50 ns. Targets used were a 1 gram, 58% enriched sample of ^{13}C and a 99.992% enriched $^{7}Li_2CO_3$ sample which yielded data on both ^{16}O and ^{7}Li. Measurements were made at 40 meters, with a pair of total energy detectors (TED) which have been described previously.[2] Figure 1(2a) which is given for illustration purposes is the relative yield of gamma rays from ^{13}C.

The capture areas and radiative widths are tabulated in Table I, together with the observed resonance energies and neutron widths. Also given are resonance parameters taken from the literature.

---

[*]On assignment from the Australian Atomic Energy Commission.

[1]Submitted for publication in Phys. Rev.

[2]R. L. Macklin and J. H. Gibbons, Phys. Rev. 159, 1007 (1967).

DATA NOT FOR QUOTATION

TABLE I

ISOTOPE	atom/barn	E_r(keV)	Γ_n(keV)	J^π	A_γ obs(beV)	$\Gamma_\gamma + k\Gamma_n$(eV)	Γ_γ(eV)	$\langle\sigma\rangle_{30}$ mb
^{7}Li	0.0139	254 ± 3	31 ± 7		89 ± 27	4.3 ± 1.3		
ref. 3,4 5,6		258	40	3^+			0.07	0.035
^{13}C	0.0020	152 ± 1	5 ± 1		112 ± 34	5.2 ± 1.6	4.6 ± 1.8	0.12
ref. 7		153 ± 5	13	1^+				
^{16}O	0.0209	426 ± 10	60 ± 15		106 ± 32	5.4 ± 1.6	2.6	0.0002
ref. 5,7,8 9,10		442	46	$3/2^-$				

[3] E. G. Bilpuch, J. A. Farrell, G. C. Kyker, P. B. Marks, and H. W. Newson, BNL-325, 1, Supplement 2 (1964).

[4] P. H. Stelson and W. M. Preston, Phys. Rev. 84, 162 (1951).

[5] R. O. Lane, A. S. Langsdorf, J. E. Monahan, and A. J. Elwyn, Ann. Phys. 12, 135 (1961).

[6] W. L. Imhof, R. G. Johnson, F. J. Vaughn, and M. Walt, Phys. Rev. 114, 4, 1037 (1959).

[7] H. O. Cohn, J. K. Bair, and H. B. Willard, Phys. Rev. 122, 534 (1961).

[8] A. Okazaki, Phys. Rev. 99, 55 (1955).

[9] R. K. Adair, Phys. Rev. 92, 1491 (1953).

[10] C. K. Bockelman, D. W. Miller, R. K. Adair, and H. H. Barschall, Phys. Rev. 84, 69 (1951).

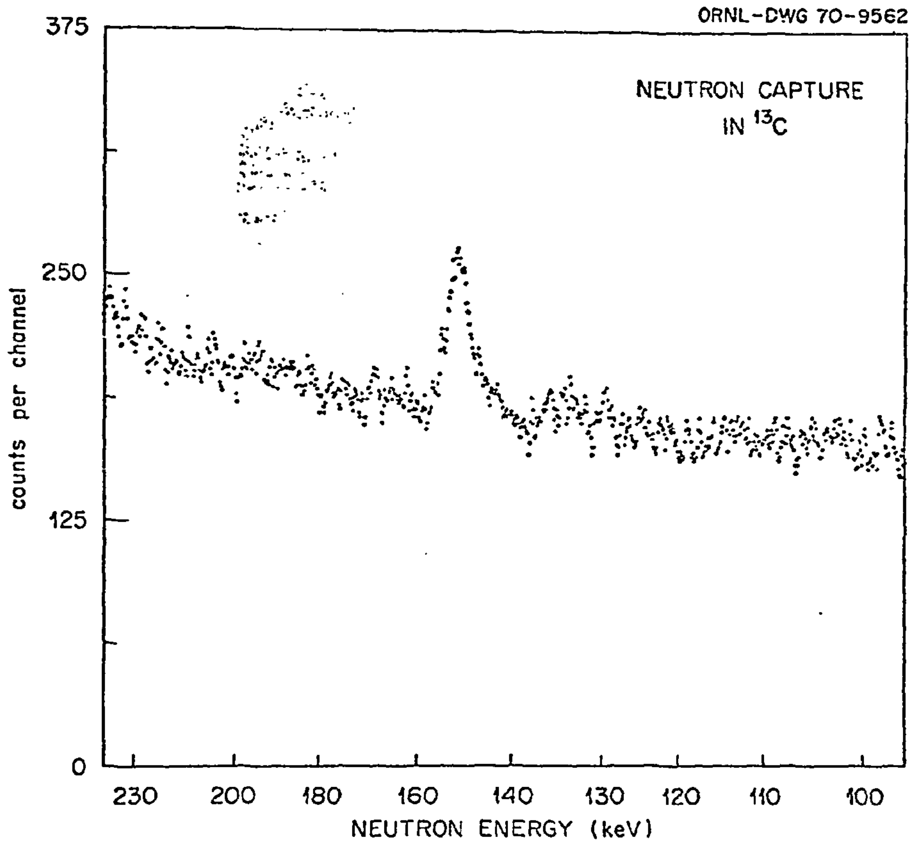

Fig. 1(2a)

DATA NOT FOR QUOTATION

b. Neutron Radiative Capture in Titanium[1]
(B. J. Allen* and R. L. Macklin)

The measurements have been completed for a determination of the capture cross section of natural titanium. The relative yield of capture gamma rays which has been observed is shown in Fig. 1(2b). The data are in process of being analyzed and interpreted.

---

[1]EANDC-85, Requests 232 and 233.

*On assignment from the Australian Atomic Energy Commission.

c. Neutron Radiative Capture in ^{207}Pb[1]
(B. J. Allen* and R. L. Macklin)

Preliminary data have been taken to determine the radiative capture cross sections of ^{207}Pb. Analysis and interpretation are not complete but Fig. 1(2c) is nevertheless a significant result which illustrates the superior resolution which is now attainable at ORELA. It will be seen that the yield returns to background between the 37 and the 41 keV resonances with no indication of the asymmetry observed at Livermore in the inverse reaction (See insert Fig. 1(2c)) and interpreted as an enhanced non-resonant capture. Note that the asymmetry in the n,γ yield (Fig. 1(2c)) is a consequence of multiple scattering in the sample; the observed shape of the resonance is consistent with a shape which is actually symmetrical.

---

[1]Submitted for publication in Phys. Rev. Letters.

*On assignment from the Australian Atomic Energy Commission.

d. Neutron Radiative Capture in ^{9}Be[1]
(R. L. Macklin and B. J. Allen*)

Measurements were made to determine if there exist any predominantly radiatively capturing levels in ^{9}Be and to determine the cross sections accordingly. Below 600 keV no levels were detected.

---

[1]EANDC-85, Requests 54, 55.

*On assignment from the Australian Atomic Energy Commission.

DATA NOT FOR QUOTATION

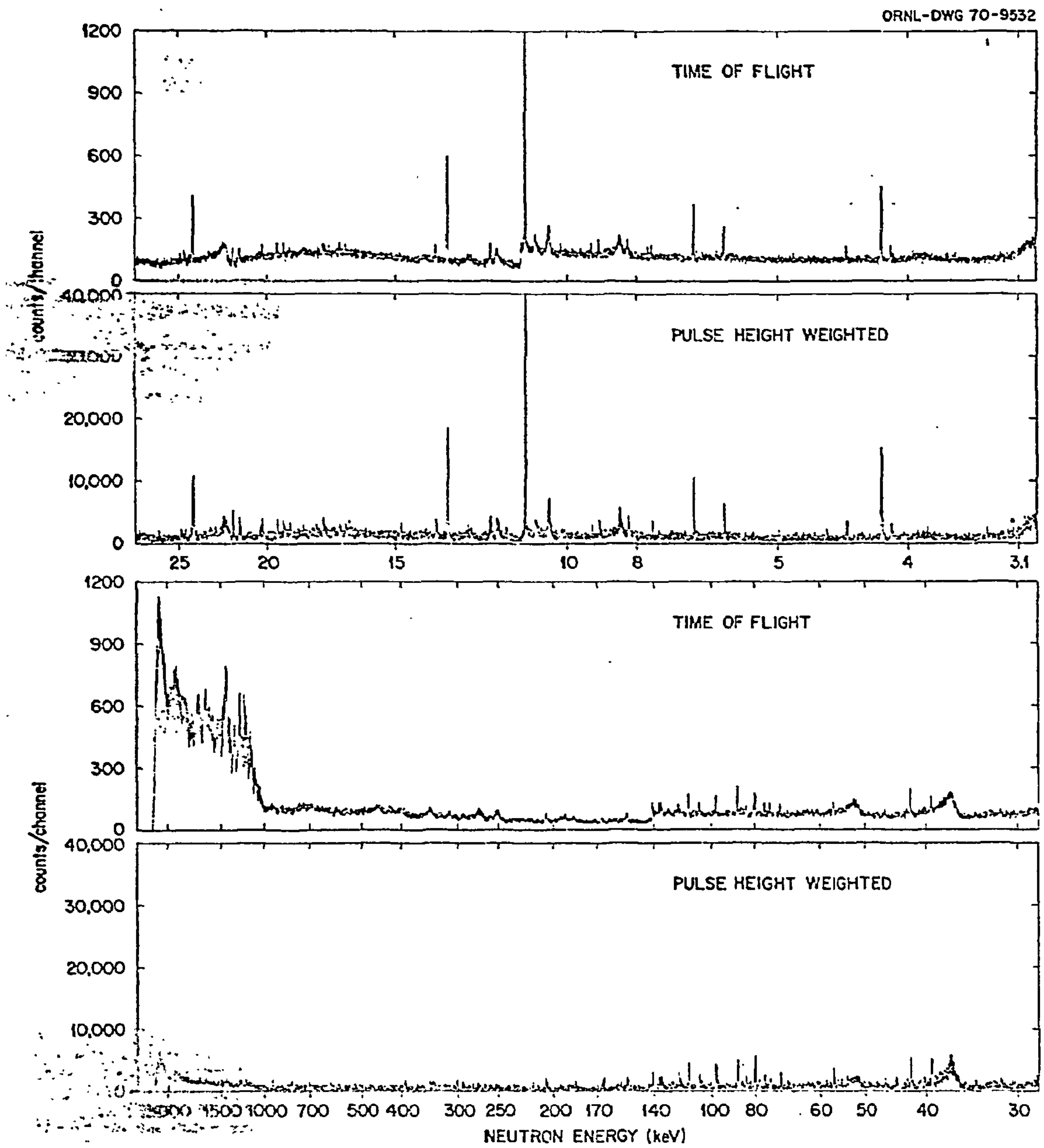

Neutron Capture in Titanium.

Fig. 1(2b)

DATA NOT FOR QUOTATION

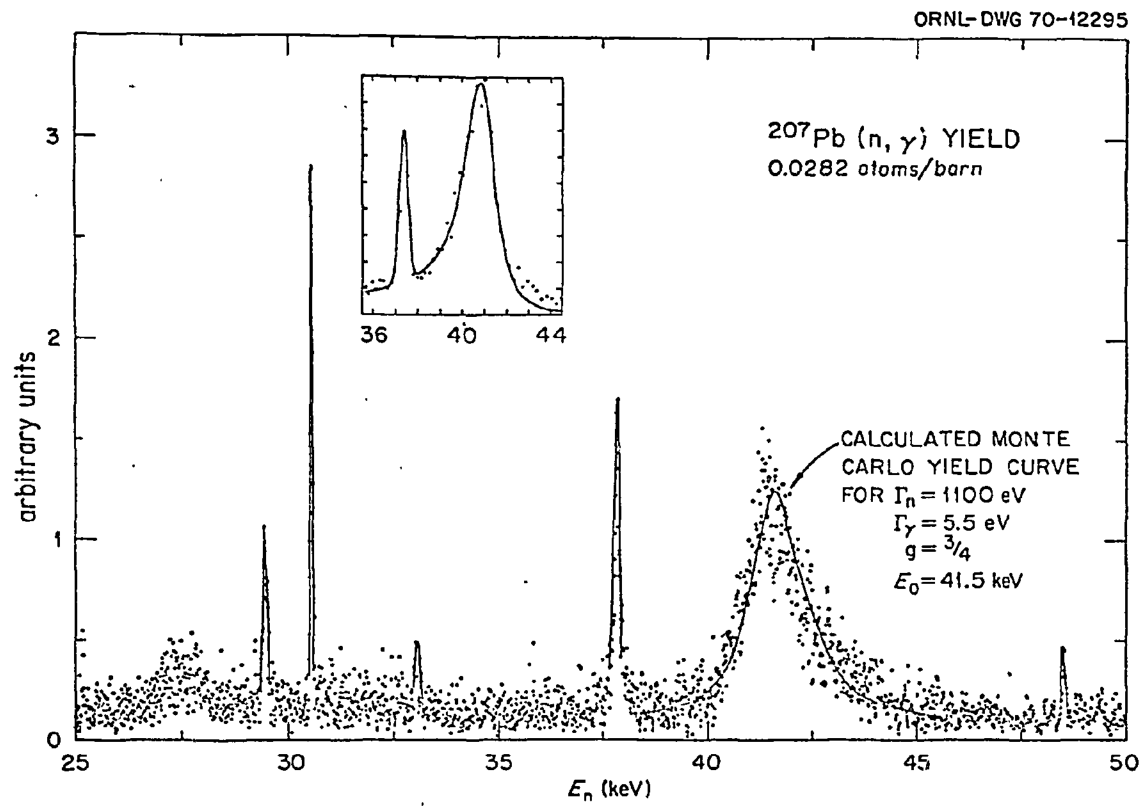

Fig. 1(2c)

DATA NOT FOR QUOTATION

e. Program for Measuring Neutron Radiative Capture Cross Sections at ORELA
(R. L. Macklin and B. J. Allen*)

The chromium isotopes (EANDC-85, Requests 267, 268, 269, 270, 271, 272) are in various stages of completion so far as the actual measurements are concerned. Ensuing measurements will then be on the separated isotopes of Ba, Te, Sr, Mg, ^{208}Pb, and $^{10}B(n,\alpha\gamma)$ (EANDC Requests 616, 75, 78, 79), as well as Hg, Mo, Ti (EANDC-85, Requests 515, 516, 525, 528, 529, 232, 233). Of less practical interest but of comparable interest otherwise are the monotopes (or near monotopes) F, V, Y, A, P, Sc, Mn, Co, As, Nb, Rh, La, Pr, Ta, Bi, and ^{238}U.

*On assignment from the Australian Atomic Energy Commission.

f. Distribution of Partial Radiation Widths in $^{238}U(n,\gamma)^{239}U$*
(O. A. Wasson[1] and R. E. Chrien[1], and G. G. Slaughter and J. A. Harvey)

The γ-ray spectra from neutron capture in 28 resolved resonances below 600 eV in ^{238}U were obtained at the 10m flight path of ORELA using a 10 cc Ge (Li) detector, with an γ-ray energy resolution, over the 10 day-run, of 5.2 keV at 4.6 MeV. (Figure 1(2f) shows the time spectra from which the resonances were chosen.) Several departures from a purely statistical decay of the compound nucleus have been noted. A strong correlation is observed between the intensities at the 3991 and 3982 keV γ rays while no correlation is observed between partial radiation widths and resonant reduced neutron widths. The average value of the M1 partial widths is within a factor of two of that for the E1 partial widths. The intensity variation over resonances of 7 of the 12 highest energy γ rays is consistent with a X^2 distribution with 1 degree of freedom while a somewhat narrower distribution is required for the others. The significance of these departures from the statistical model will be presented.

*Abstract submitted for the Fall Meeting of the American Physical Society, Houston, Texas, Oct. 15-17, 1970.

[1]Brookhaven National Laboratory.

DATA NOT FOR QUOTATION

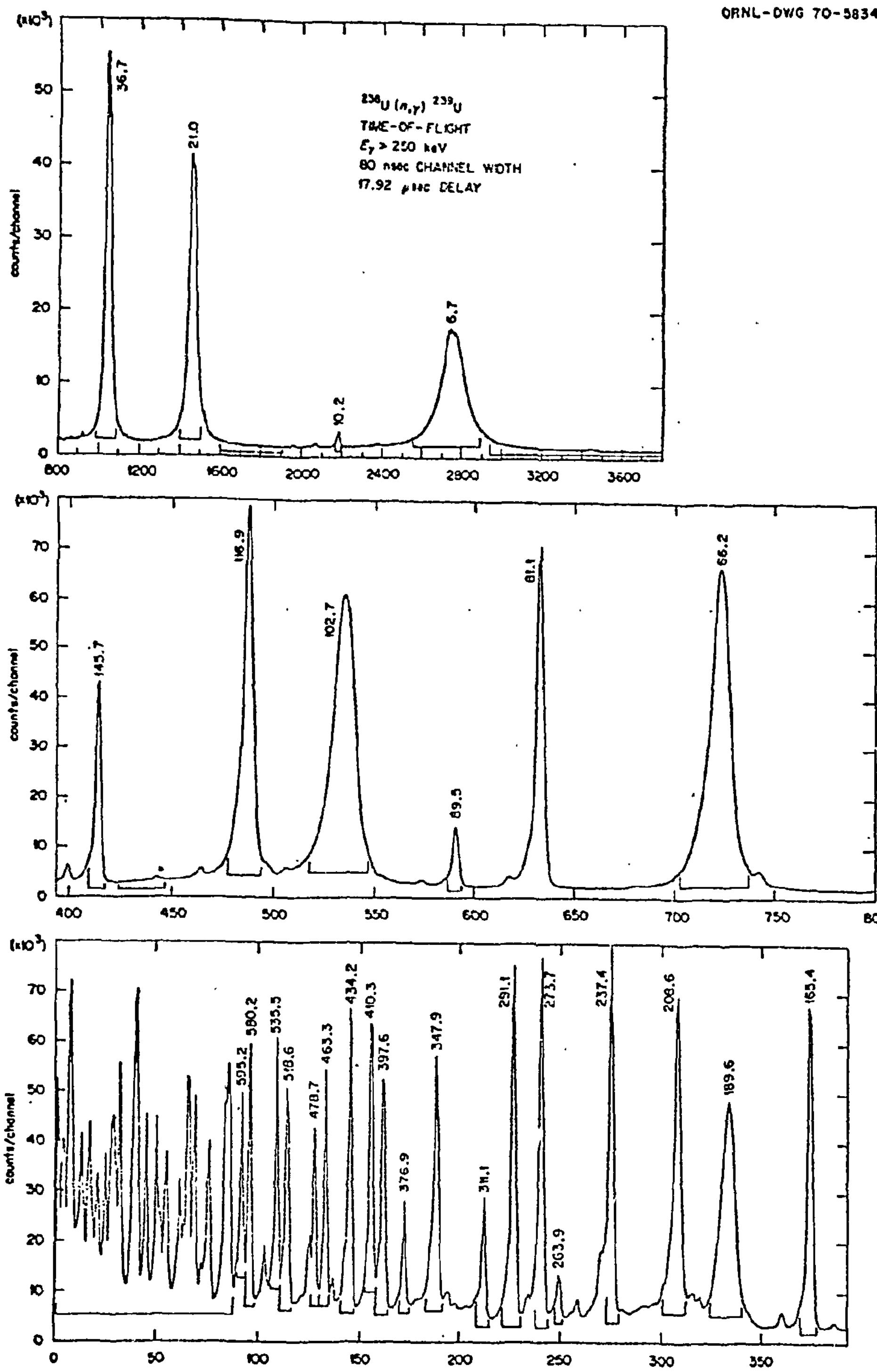

Fig. 1(2f)

DATA NOT FOR QUOTATION

3. Elastic and Inelastic Scattering Cross Sections

a. Neutron Inelastic Measurements at ORELA
(F. G. Perey, W. E. Kinney, and R. L. Macklin)

We have started a program of inelastic scattering cross section measurements at ORELA. The scattering sample is placed 40 meters from the neutron target in a well collimated flight path (the neutron beam is collimated to a dimension of 1" x 2"). The gamma rays from the inelastic scattering events are detected in two nonhydrogenous liquid scintillators placed on each side of the scatterer approximating a 4π geometry. The presently used detectors are fluorocarbon scintillators which are reasonably neutron insensitive and very adequate for the capture cross section measurement program.[1] The use of these detectors presents some inconvenience for the inelastic gamma-ray measurements because of the neutron sensitivity of the detector via inelastic scattering of the fluorine. The low-lying levels at 110 and 197 keV in fluorine impose a limit of about 200 keV on the lower bias of the Compton spectrum for inelastic gamma rays observed. There is also a need to correct the data for the sensitivity of the detector to the neutrons of higher energies due to the fluorine levels above 1.4 MeV. Deuterated benzine, although sensitive to neutrons via the detection of recoil deuterons, allows the possibility of pulse-shape discrimination to render the detector neutron insensitive[2] and is being investigated as a detector for these measurements. Because of the very good timing response of these detectors, and the very short intense burst capabilities of ORELA, inelastic cross sections can be measured with a few keV energy resolution at 1 MeV. The upper neutron energy limit of the method as presently used is about 4 MeV because of a combination of both lower neutron flux and greater neutron sensitivity of both scintillator materials via inelastic scattering in the carbon. Preliminary measurements have been performed by taking time-of-flight spectra as a function of pulse-height in the detectors for ^{7}Li, Na, Si, V, and Fe. Spectra were also taken using CF_2 and C as scatterers to determine the sensitivity of the detectors to neutrons and help in the background subtraction. Our present plans are to use the ^{7}Li measurements as a flux determination and measure the other cross sections relative to the ^{7}Li(n,n') cross section. Since this cross section should be slowly varying over our energy resolution function, it could be used as a secondary standard. Corrections to be applied to the raw data because of finite angle, finite sample, and the sensitivity of the efficiency of the detector to the angular distributions of the gamma ray are under investigation. As an example of the structure in the inelastic cross

---

[1] R. L. Macklin and B. J. Allen, Nuclear Instruments and Methods, in press (Oct. 1970).

[2] J. B. Czirr, Nuclear Instruments and Methods 72, 23 (1969).

section which such measurements reveal, time-of-flight spectra converted to counts detected, per keV neutron energy interval, are shown for Fe and V in Figures 1(3a) and 2(3a). No background subtraction or flux normalization was performed on the data shown in these figures. The overall timing resolution of the system was about 5 nsec for these measurements.

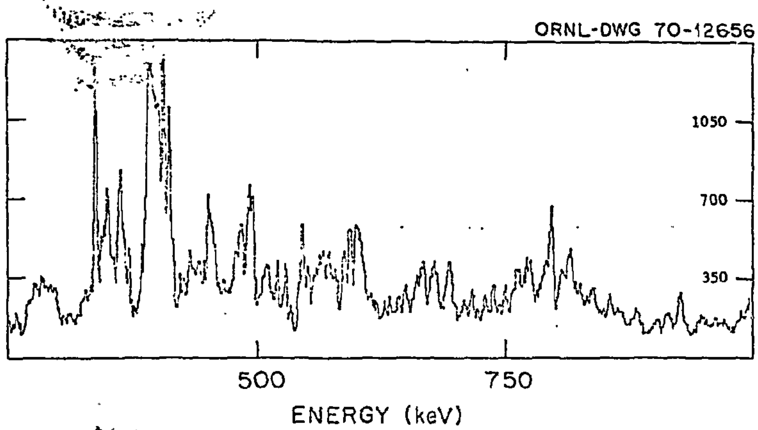

Fig. 1(3a)

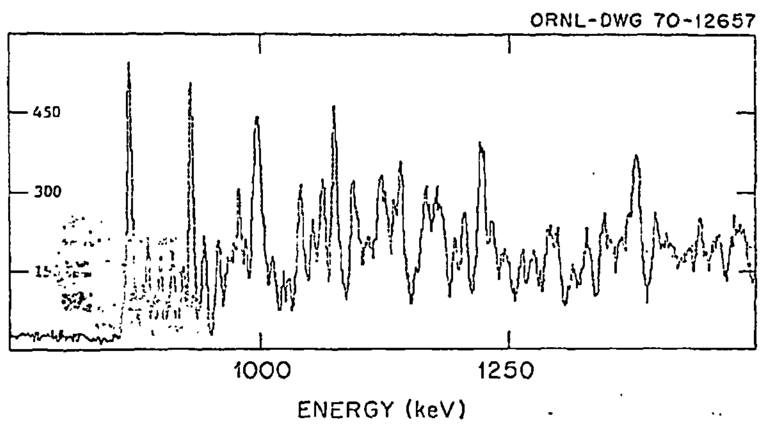

Fig. 2(3a)

4. Neutron Reaction and Gamma-Ray Production Cross Sections

a. The Fe(n,xγ) Reaction for $5.35 \leq E_n \leq 9.0$ MeV[1] (J. K. Dickens and F. G. Perey)

As part of a continuing program to obtain production cross sections for gamma rays produced by the interaction of neutrons with nuclei, we have measured differential cross sections for the reaction Fe(n,xγ) for nine bombarding neutron energies between 5.35 and 9.0 MeV.

Because of difficulties associated with the complex spectra that were observed, it was decided to concentrate on reducing the data for the well-known transitions whose cross sections were large enough to report with reasonable confidence. These differential cross sections are collected in Table I. The uncertainties assigned to the cross section data are as follows: 10% for $d\sigma/d\omega > 20$ mb/sr, 15% for $20 \geq d\sigma/d\omega \geq 2$ mb/sr and 20% for $d\sigma/d\omega < 2$ mb/sr. Our data are compared with previously published gamma-ray cross section data,[2] and with curves computed using compound-nucleus formalism;[3] the comparisons are shown in Figs. 1(4a) and 2(4a) for the 0.846-MeV transition from the first excited state in ^{56}Fe and the 1.238-MeV transition from the second excited state. The solid lines represent the calculations which include the known or probable contributions for gamma transitions from levels in ^{56}Fe up to 4.87 MeV excitation. As is seen for $E_n > 5.5$ MeV the calculations predict too little cross section for both transitions shown. We conjecture that nearly all of the levels in ^{56}Fe with $E_x > 4.87$ MeV decay through the first excited state. This conjecture is supported quite well by the nearly complete lack of gamma rays in our raw spectra which can be associated with ground-state transitions from highly excited states. The dashed curve in Fig. 1(4a) shows the predicted excitation junction for the 0.846-MeV gamma ray if the conjecture were completely valid.

It is evident, however, that a bigger detector with more efficiency for high-energy gamma rays and better resolution as well as a better understanding of the ^{56}Fe nucleus will be required before we can reliably obtain more complete results on this element.

[1] J. K. Dickens and F. G. Perey, ORNL-4592 (Sept. 1970).

[2] R. W. Benjamin, P. S. Buchanan, and I. L. Morgan, Nucl. Phys. 79, 241 (1966); W. E. Tucker, Phys. Rev. 140, B1541 (1965); D. L. Broder, et al., Izv. Akad. Nauk. SSSR, Ser. Fiz 31, 327 (1968). Translation Bull. of the Academy of Sciences of the USSR, Physical Series, Vol. 31 No. 2, 311 (Columbia Technical Translations, White Plains, New York 1968); D. M. Drake, et al., Nucl. Sci. and Eng. 40, 294 (1970).

[3] W. E. Kinney and F. G. Perey, Calculated ^{56}Fe Neutron Scattering and Gamma-Ray Production Cross Sections from 1.0 to 7.6 MeV, ORNL-4249 (1968); W. E. Kinney and F. G. Perey, Nucl. Sci. and Eng. 40, 396 (1970).

Table 1. Elemental Differential Cross Sections for Gamma-Ray Production Due to Neutron Interactions with Iron[a]

E_γ (keV)	Level (keV)	Cross Section (mb/sr) for E_n of – 5.35 ± 0.20 MeV		5.85 ± 0.02 MeV		6.40 ± 0.20 MeV		6.90 ± 0.15 MeV		7.45 ± 0.15 MeV		7.95 ± 0.10 MeV		8.50 ± 0.10 MeV		9.0 ± 0.1 MeV	
		55°	90°	55°	90°	55°	90°	55°	90°	55°	90°	55°	90°	55°	90°	55°	90°
								^{56}Fe Isotope									
846	846	85.0	81.7	86.6	83.2	88.0	82.0	89.2	84.2	84.6	77.5	94.6	84.2	93.4	85.1	101.0	88.8
1038	3123	5.7	5.7	5.6	5.6	6.5	6.1	6.5	6.4	6.3	5.8	7.0	5.3	7.9	6.4	7.4	7.3
1168 1175	3826 4298	2.1	2.2	2.2	1.9	2.5	2.1	1.6	1.8	1.9	1.8	2.6	1.8	2.2	1.9	1.8	2.0
1238	2085	23.9	22.6	27.0	23.5	28.9	24.5	30.0	25.3	29.6	27.5	33.2	27.2	34.5	31.1	40.0	33.7
1771	3857	2.2	3.2	2.4	3.3	2.4	2.4	2.6	3.1	1.9	2.2	2.0	2.0	2.3	2.3	2.4	1.8
1811	2658	9.3	10.6	11.2	9.6	9.9	8.9	11.0	9.5	9.6	8.2	9.6	8.1	9.2	8.5	9.6	9.0
2035	4120	1.4	1.9	2.8	2.1	2.4	2.3	1.6	1.7	2.2	2.5	2.0	1.4	2.8	2.2	2.6	2.4
2113	2960	5.5	5.9	5.1	5.2	5.4	4.9	5.2	4.7	4.2	4.2	4.3	3.7	4.1	3.7	4.3	4.4
2274	3123	3.3	3.4	2.4	2.9	2.1	2.6	2.2	2.6	2.5	2.8	2.3	2.0	1.7	1.6	2.4	1.8
2523[b]	3370	5.3	4.5	5.0	3.8	3.5	3.4	3.6	2.0	1.8	1.7	1.6	1.4	2.4	2.2	2.1	1.8
2599[c]	3445[c]	3.7	5.8	5.3	5.2	5.6	6.3	6.0	6.7	5.8	6.0	5.5	5.8	5.8	6.0	5.1	5.7
2759	3604	3.2	3.1	3.2	2.6	2.6	2.1	2.4	1.7	1.7	1.7	1.7	1.5	1.9	1.4	1.0	1.1
3202	4049	2.4	1.9	2.7	1.5	1.6	1.8	2.3	1.8	1.6	1.4	1.9	1.7	2.2	1.8	2.1	1.4
3445 3451	3445 4298	2.5	3.5	2.3	3.0	2.4	2.8	1.9	2.0	1.6	2.0	2.2	2.4	1.8	1.6	2.8	1.4
3548[b]	4395	2.0	2.2	2.9	2.6	2.2	2.5	1.7	1.9	1.5	2.2	1.1	1.5	2.0	1.4	2.8	1.9
3598[d]	3598[d]	2.6	3.3	2.9	2.6	2.4	2.5	2.4	1.9	1.8	1.6	1.5	1.4	1.6	1.2	1.2	1.4
								^{54}Fe Isotope									
1130	2538	1.3	1.1	1.0	1.0	1.2	1.2	1.1	1.3	1.6	1.3	2.1	1.5	1.6	1.3	1.4	1.3
1408	1408	3.8	4.2	3.7	3.0	4.1	3.3	4.4	3.5	3.7	3.3	3.3	2.8	4.2	3.7	4.4	3.5

[a] Not corrected for relative abundances of the isotopes.
[b] 2523- and 3548-keV lines each appear to be doublet.
[c] These data include contributions from 2599- and 2604-keV transitions from 3445- and 3450-keV levels.
[d] These data include contributions from 3598- and 3604-keV ground-state transitions.

DATA NOT FOR QUOTATION

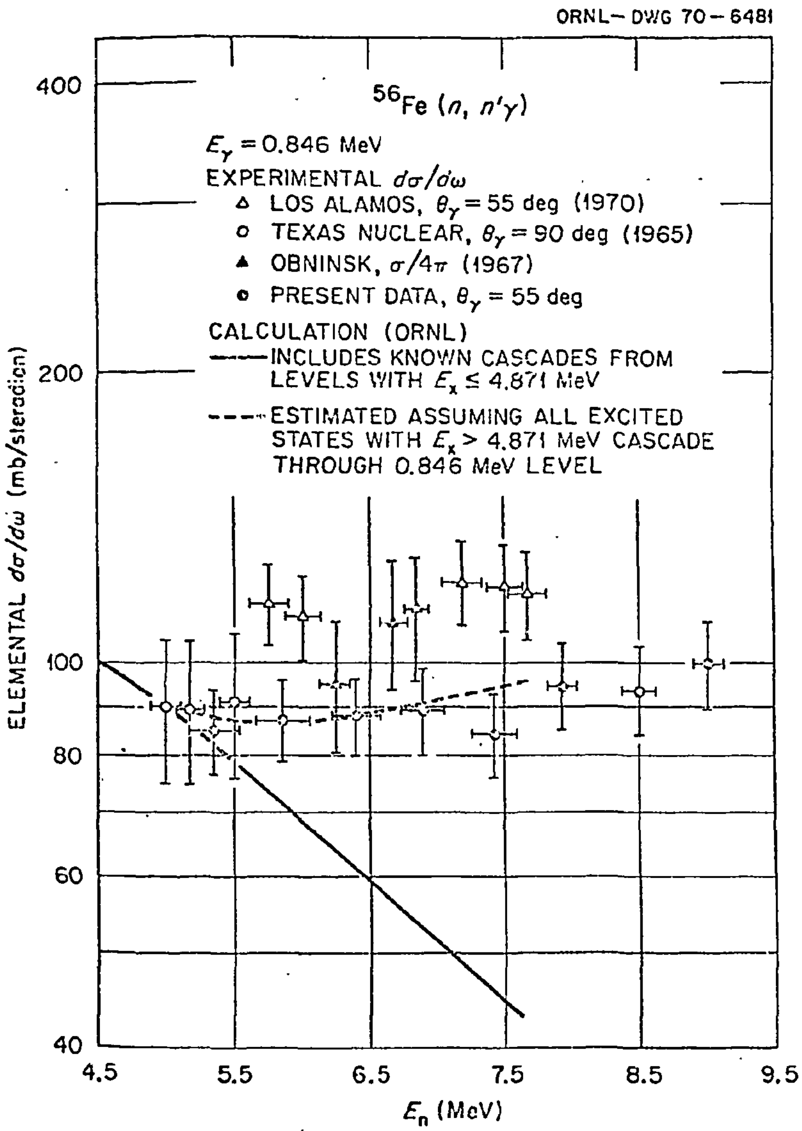

Fig. 1(4a). Elemental differential cross sections for gamma-ray production due to neutron excitation of the 0.846-MeV first-excited state in ^{56}Fe. The present data, for gamma-ray scattering angle of 55°, is compared with previously published data and with cross sections calculated using compound-nucleus formation combined with direct-interaction excitation (Ref. 3).

DATA NOT FOR QUOTATION

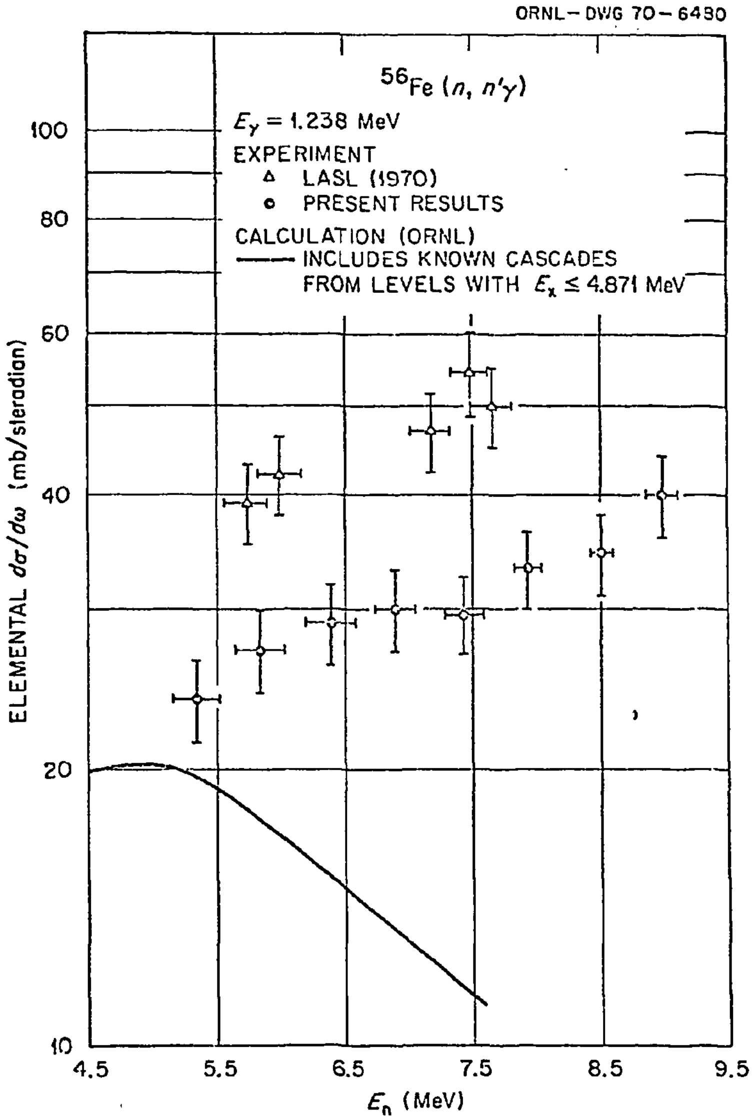

Fig. 2(4a). Elemental differential cross sections for gamma-ray production due to neutron excitation of the 2.084-MeV second-excited state in ^{56}Fe compared with previously published data and with cross sections calculated using compound nucleus formation. The difference between the data and calculated curve suggests that levels with $E_x > 4.871$ MeV de-excite through the 2.084-MeV level.

DATA NOT FOR QUOTATION

5. Properties of Fissile Nuclides

a. ^{238}U Capture Cross Section and ^{235}U Capture and Fission Cross Section Measurements
(G. de Saussure, R. B. Perez, and E. G. Silver)

Measurements are in progress to obtain accurate values for the neutron capture cross section of ^{238}U below 100 keV. This is an important parameter for the LMFBR Program. The measurements are done using the Oak Ridge National Laboratory Electron Linear Accelerator (ORELA) and a 800-gal. liquid-scintillator total-absorption gamma-ray detector installed on a 40-meter flight path.

Preliminary results are estimated to have an accuracy of 6% and are compared with the ENDF/B evaluation and with the data of M. Moxon (AERE-R-6074), Fig. 1(5a), and are summarized in Table I. These measurements were obtained with samples of .003 in. (4×10^{-4} a/b) and .025 in. (28×10^{-4} a/b).

Measurements with other sample thicknesses are in progress, as well as measurements of the fission and capture cross sections of ^{235}U obtained with the same equipment. The purposes of the measurements with ^{235}U are (1) to determine the capture cross section (and α) of that isotope over the range below 100 keV, and (2) to determine the ratio of the capture in ^{238}U to the fission in ^{235}U over the same energy range.

The following additional measurements are contemplated (1) transmission and self-indication measurements on ^{238}U below 100 keV. The results will be used with capture data described above, to derive resonance parameters up to about 5 keV. The transmission and self-indication measurements will probably be initiated in early 1971. (2) Capture, transmission, and self-indication measurements on ^{238}U and capture and fission measurements of ^{235}U on a flight path of 150 m are planned for the end of 1971. The purpose of the latter measurements will be to extend the work done at the 40-m flight path to cover the energy region of 100 to 300 keV.

DATA NOT FOR QUOTATION

Table I

Energy (keV)	Sample ".003"	Sample ".025"	"Average"	ENDF/B	ORNL/ENDF	Davey	ORNL/Davey
.5 – .6	5.19†	5.03	5.11	4.55	1.12		
.6 – .7	3.86	3.80	3.83	3.17	1.21		
.7 – .8	2.01	1.97	1.99	1.58	1.26		
.8 – .9	3.19	3.15	3.17	2.81	1.13		
.9 – 1.	4.39	4.45	4.42	3.89	1.14		
1. – 2.	2.02	1.98	2.00	1.80	1.11		
2. – 3.	1.54	1.49	1.52	1.32	1.15	1.31	1.16
3. – 4.	1.25	1.26	1.25	1.19	1.05	1.29	.97
4. – 5.	.955	.978	.966	1.10	.88	1.13	.85
5. – 6.	(1.41)*	.974	.974	1.01	.96	1.02	.95
6. – 7.	(.951)*	.930	.930	.950	.98	.945	.98
7. – 8.	.821	.812	.816	.894	.91	.885	.92
8. – 9.	.738	.718	.728	.845	.86	.839	.87
9. – 10.	.726	.728	.727	.809	.90	.803	.91
10. – 20.	.649	.643	.646	.687	.94	.672	.96
20. – 30.	.515	.505	.510	.527	.97	.528	.97
30. – 40.	.461	.462	.461	.443	1.04	.449	1.03
40 – 50	.394	.397	.396	.386	1.03	.394	1.01
50. – 60.	.328	.333	.330	.334	.99	.349	.95
60. – 70.	.274	.279	.277	.278	1.00	.287	.97
70. – 80.	.235	.244	.240	.230	1.04	.236	1.02
80. – 90.	.213	.224	.218	.211	1.03	.221	.99
90. – 100.	.186	.197	.191	.203	.94	.208	.92

*The data of the ".003" sample have a large uncertainty in the intervals 5. to 7. keV, associated with an Al capture resonance at 5.9 keV. The ^{238}U sample was held in an Al frame. New measurements without this Al frame are in progress.

†All cross-section values in barns.

DATA NOT FOR QUOTATION

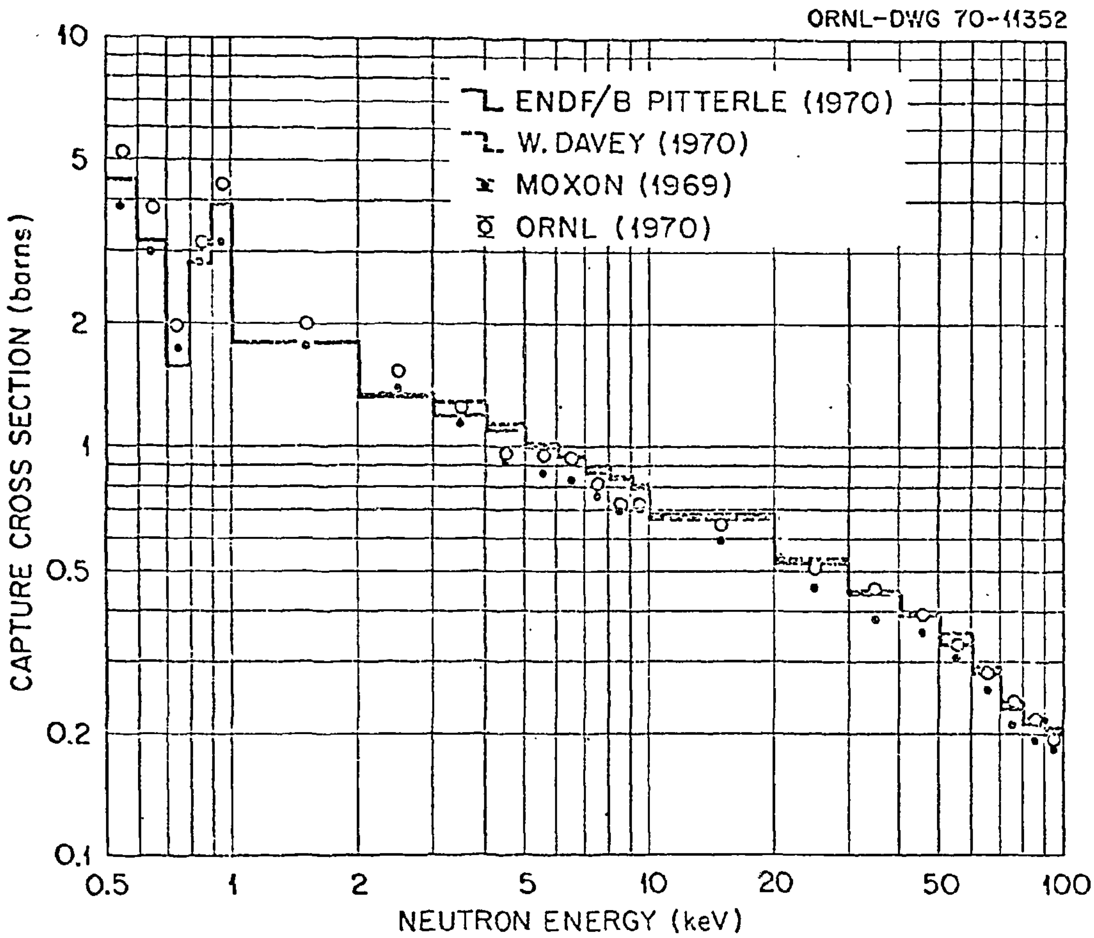

The ^{238}U Neutron Capture Cross Section in the Energy Range 0.5 to 100 keV.

Fig. 1(5a)

DATA NOT FOR QUOTATION

b. Measurement of $\bar{\nu}$ for ^{239}Pu
(L. W. Weston and J. H. Todd)

Preliminary measurements were carried out to attempt to resolve the discrepancy between Weinstein et al.[1] at Rensselaer Polytechnic Institute and Ryabov et al.[1] at Dubna. The method used for the present measurement was quite different from that previously used. Rather than counting thermalized neutrons following a fission with a high efficiency detector, the neutrons were detected with low efficiency using fast neutron detectors. Care was taken to avoid gamma-ray sensitivity. The ratio of the coincident count rate between the fast neutron detectors and a fission chamber and the total count rate in the fission chamber gave a relative measure of $\bar{\nu}$. Our preliminary data do not indicate a separation into two groups of values according to the spin state of the resonance but indicate a much weaker correlation. The correlation that does exist is in the direction indicated by Weinstein et al., rather than that indicated by Ryabov et al. Figure 1(5b) shows a comparison of our preliminary data with that of Weinstein et al.

[1] S. Weinstein, R. Reed, and R. C. Block, Physics and Chemistry of Fission, Proceedings of Vienna Conference, 1969, IAEA-SM-122/113.

c. Prompt Gamma Rays Emitted in the Thermal Neutron Induced Fission of ^{235}U
(Frances Pleasonton)

Preliminary results have been obtained for the average total number and average total energy of gamma rays emitted in the thermal neutron induced fission of ^{235}U. The work was carried out at the Oak Ridge Research Reactor as an extension of the experiment originally performed by Maier-Leibnitz, Schmitt, and Armbruster.[1] The early work was based on measurements of 3-fold coincidences of the fission fragments and the gamma rays, within a fixed resolving time of about 275 nsec. The present experiment duplicates their geometry of detection but measures in addition the time elapsing between the detection of one fragment and the detection of the gamma ray emitted in the same fission event.

The data are analyzed for various time intervals, as indicated in the table. The results given are probably reliable to about 7%, although all sources of uncertainties have not been evaluated pending the collection of further data. Good agreement is seen with the results of Peelle and Maienschein and with those of Verbinski and Sund for comparable times of observation.

[1] H. Maier-Leibnitz, H. W. Schmitt, and P. Armbruster, in Proceedings on the Symposium on the Physics and Chemistry of Fission, Salzburg, 1965 (IAEA, Vienna 1965) Vol. II, p. 143.

DATA NOT FOR QUOTATION

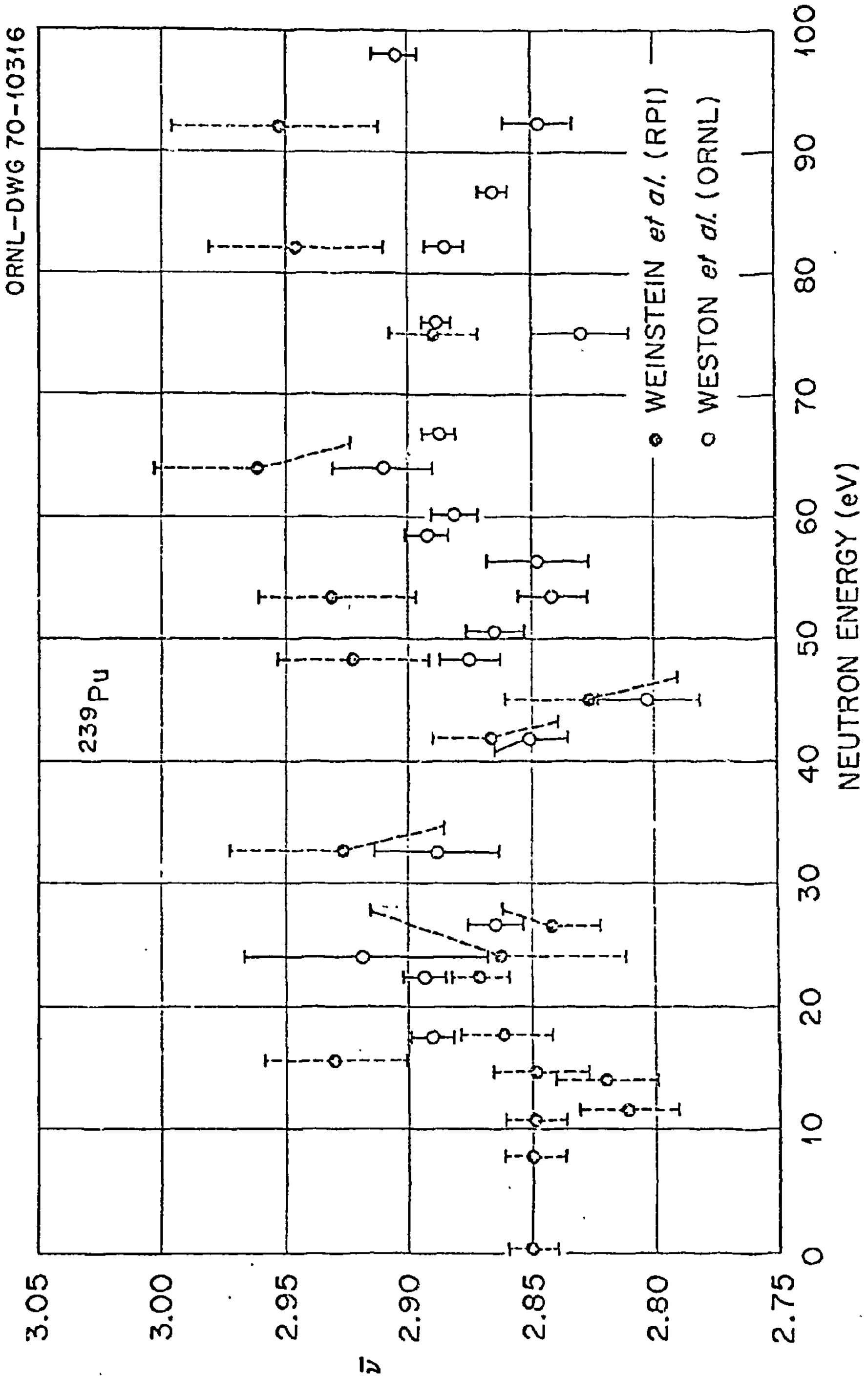

Fig. (15b)

DATA NOT FOR QUOTATION

Gamma energy (MeV)	Time interval (nsec)	Gammas/Fission	MeV/Fission	MeV/Gamma/Fission
0.030 - 10.4	10	6.19 ± 0.6	6.02 ± 0.6	0.97
"	next 60	1.89 ± 0.2	1.00 ± 0.1	0.53
"	sum 70	8.08 ± 0.8	7.02 ± 0.7	0.87
"	275	8.58 ± 0.8	7.36 ± 0.7	0.86
0.010 - 10.5[a]	69[a]	8.13 ± 0.35[a]	7.25 ± 0.26[a]	0.89[a]
0.14 - 10.0[b]	10[b]	6.69 ± 0.3[b]	6.51 ± 0.3[b]	0.97[b]

[a]R. W. Peelle and F. C. Maienschein, ORNL-4457, UC-34-Physics, April 1970.

[b]V. V. Verbinski and R. E. Sund, DASA Report No. 2234, GA-9148, April 1969.

d. High Resolution Cross Section Measurements for ^{234}U(n,f) and ^{236}U(n,f) at Neutron Energies Between 0.7 and 2 MeV (Helmut Rosler,* Franz Plasil, and H. W. Schmitt)

Experiments have been initiated at ORELA to measure the fine structure in the fission cross sections of ^{234}U and ^{236}U in the region of the fission threshold. The motivation is to find states that can be interpreted in terms of the double humped fission barrier.[1] The measurements are made with ionization chambers. The energy range is about 0.7 to 2 MeV and the energy resolution is about 7 keV. The ORELA neutron spectrum is monitored by a fast plastic scintillator and a ^{235}U fission ionization chamber identical to the ^{234}U and ^{236}U chambers. ^{234}U(n,f) and ^{236}U(n,f) cross sections relative to ^{235}U(n,f) can be extracted from the data. Estimated completion date is about October 1971.

*Guest assignee (NATO Fellowship) from Reaktorstation Garching, Munich, Germany.

[1]V. M. Strutinski, Nucl. Phys. A95, 420 (1967).

DATA NOT FOR QUOTATION

6. Theory and Analysis

a. Variation of the R Matrix[1]
(A. J. Mockel* and R. B. Perez)

The R matrix of Wigner and Eisenbud is a function of a set of parameters (channel radii, boundary numbers, etc.) as well as of the energy of the incoming particle. Invariant imbedding techniques have been applied, which give the variation of the R matrix with respect to changes of the parameters entering into the theory. A generalization of various formulas, derived originally by Wigner and Teichmann and Wigner, to the multichannel case has been obtained. Our general results apply also to deformations of the nucleus other than spherical. An application of the invariant imbedding technique is also shown concerning Robson's theory of the isobaric spin analogs.

[1]Abstract of paper submitted for publication in Phys. Rev.

*University of Florida, Gainesville, Florida.

7. Instrumental

a. Fast Neutron Capture Cross Section Facility[1]
(R. L. Macklin and B. J. Allen*)

The total energy weighting technique has been applied to measure fast neutron capture in small separated stable isotope samples at the Oak Ridge Electron Linear Accelerator (ORELA). Nonhydrogenous liquid scintillators provide low backgrounds below about 2.5 MeV neutron energy with time resolution better than 2 nanoseconds and gamma cascade efficiency typically 32% per neutron captured. The 40-meter flight path permits neutron energy resolutions ranging from $E_n/600$ at several keV (moderator thickness limited) to about $E_n/400$ at 2 MeV. On line data processing via multiple access computer allows (disc) storage to be reduced from over 4×10^6 channels $\sim$190,000. The usual corrections for sample thickness, purity, deadtime, and a transformation to capture cross section vs neutron energy are accomplished off-line in a larger digital computer.

[1]Abstract of paper submitted to Nuclear Instruments and Methods.
*On assignment from the Australian Atomic Energy Commission.

b. Gamma Flash Suppression for the ORELA Pulsed Neutron Source[1]
(R. L. Macklin)

A gamma ray flash suppression system for neutron time-of-flight experiments at the Oak Ridge Electron Linear Accelerator (ORELA) has been found very effective for partial cross section measurements. For capture cross section measurements at 40 m the residual pileup flash pulse from a typical sample is well within the neutron binding energy range, where the detector response is linear. This has allowed two parameter (time and pulse height) analysis down to 0.5 μsec after the flash.

---

[1]Abstract of paper to be published in Nuclear Instruments and Methods.

The Use of a Pulsed Van de Graaff Accelerator and Time-of-Flight Techniques to Reduce Backgrounds in (α,γ) Spectroscopy Experiments[1]

(Ronald J. Jaszczak and R. L. Macklin; F. E. Dunnam,* H. A. Van Rinsvelt* and R. H. Bloomer*)

A pulsed beam of alpha particles from a 5.5-MV Van de Graaff accelerator has been used to study radiative capture reactions. Time-of-flight techniques are used to discriminate against neutrons produced when the beam interacts with collimator/target contaminants, as well as against beam-independent background due to cosmic rays. With a beam pulse of less than 4 nsec (FWHM) duration and a repetition rate of 2 MHz, a portion of the $^{34}S(\alpha,\gamma)^{38}Ar$ excitation function was examined near $E_\alpha = 3.6$ MeV and the background found to be an approximate factor of 15 below that of the effective d.c. excitation function. In addition it is demonstrated that an angular distribution taken on resonance by this method requires substantially less background subtraction. The method has also been successfully applied to radiative capture studies in which the incident beam energy is above the neutron threshold for the target nuclei.

---

[1]Abstract of paper submitted for publication in Rev. Sci. Instr.

*Department of Physics, University of Florida, Gainesville, Florida.

d. A Proton Recoil Monitor for Neutron Flux Measurements[1]

(Ronald J. Jaszczak, R. L. Macklin, and M. C. Taylor*)

Time-of-flight techniques have been used with a silicon surface barrier detector and a polyethylene radiator to determine the neutron flux from the Oak Ridge Electron Linear Accelerator in the energy region between 200 keV and 7 MeV. The 200 mm^2 surface barrier detector at 40 meters and constant fraction timing electronics are used to measure time-of-flight, from which the neutron energies are inferred. A Monte Carlo program has been written to determine the efficiency, timing and energy characteristics of the monitor system.

---

[1]Abstract of a paper to be submitted for publication in the Rev. Sci. Instr.

*Saint Louis University, Saint Louis, Missouri.

e. Oak Ridge Electron Linear Accelerator (ORELA)
(J. A. Harvey and F. C. Maienschein)

From August 25, 1969, until March 26, 1970, the accelerator operated on a 5-day-per-week schedule and a total of 1780 research beam hours (71% of scheduled time) were used by experimenters. On May 1, 1970, operation was changed to a 7-day-per-week schedule. From April 1 to October 31, a total of 2121 hours was used by experimenters. This period included a major shutdown in July and August for installation of collimators, a new Ta target, and a Be target. During April and May difficulties were experienced with vacuum leaks in the electron guns and the operation time of the accelerator was below normal. However, electron gun 5-2 was installed May 29 and lasted until October 27 for a total of 1742.6 beam hours exceeding our previous record of 1600 hours for an earlier gun. Three klystrons still in operation in the accelerator have averaged over 5000 hours each. Two klystrons were replaced in March and October after $\sim$ 2700 hours average.

RENSSELAER POLYTECHNIC INSTITUTE

A. CROSS SECTION MEASUREMENTS

1. Total MeV Cross Sections on Na and C from 0.5 to 40 MeV* (J. C. Clement, R. Fairchild, C. G. Goulding P. Stoler and P. F. Yergin)

As of this report we have completed measurements of the neutron total cross section of sodium. A 90 MeV LINAC electron beam enabled reliable measurements to be carried out from about 0.5 to 40 MeV. A neutron burst width of 7 nsec and an analysis channel width of 10 nsec limited our resolution to 0.05 nsec/m. We used a newly fabricated metallic sodium sample with nl equal to 0.290 atoms/barn.

Thin layers of B_4C and Cd were used to filter out low energy neutrons. A 1-inch thick lead as well as a ½-inch thick tantalum filter reduced the gamma flash and neutron counting rate to a manageable number. A 1½-inch diameter brass collimator before the sample replaced the 1-inch diameter collimator used previously.[1] Other conditions remain identical to that reported earlier.

The cross sections thus obtained will be combined with our previous sodium cross sections to decrease the statistical error to the 1% range. The current run appears reliable from many points of view. The machine-independent background varies from 10% to 1% for sample in, with no more than 2% over most of the neutron energy spectrum. Examination of data taken at energies below the neutron threshold of our detector leads us to conclude that possible time-dependent background is below 1.5%. A more conclusive indication of reliability comes from excellent agreement between this run and previous ones made under somewhat different conditions. In comparing the cross sections with those obtained at Karlsruhe[2] we find the agreement is quite good, being generally within a couple of percent from 6 to 30 MeV. However,

---

* Pertinent to requests # 32 and 55.

in the region of [illegible]5 MeV, the present data are a few percent lower than Ref. 2 in the valleys, whereas the peak values are quite close. The sodium data are displayed in Figs. A1 to A4. Only the data from the 30 hour long sodium run are presented, as analysis is still progressing on the combined set of runs.

It is worthwhile to note that all the fine structure observed in the present data also appear in Ref. 2. The structure is quite dense. For example, there are between 50 and 60 resonances between 1 and 3 MeV.

In order to estimate overall capabilities of our system we measured the cross section of carbon from 0.5 to over 20 MeV. The 2.079 MeV resonance, and the other well known structures allow us to assess our resolution. We used a fairly thick sample with an nl of 0.425 atoms/barn. The excellent agreement with the National Bureau of Standards carbon measurements[3] lends credibility to the sodium data.

Our carbon data are presented in Figs. A5, A6 and A7. They represent the present data, including statistical fluctuations. The solid curve is the National Bureau of Standards cross section of Schwartz et al.[3]

---

[1] Linear Accelerator Project Progress Report April - June 1970, 52, RPI-328-190.

[2] S. Cierjacks, P. Forti, D. Kropp, J. Nebe and H. Unseld, "High Resolution Total Neutron Cross Sections Between 0.5 - 30 MeV," Karlsruhe, Euratom Report - KFK 1000.

[3] R. Schwartz, private communication.

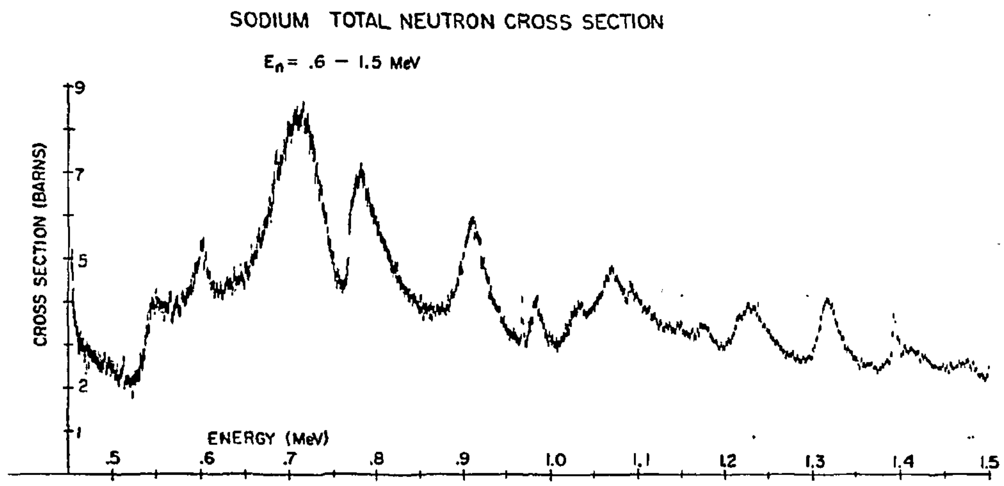

Figure A1

DATA NOT FOR QUOTATION

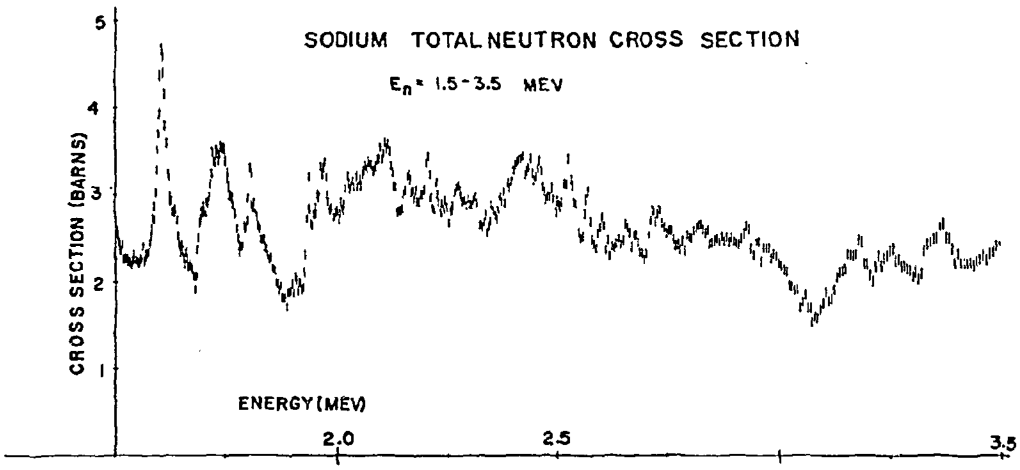

Figure A2

DATA NOT FOR QUOTATION

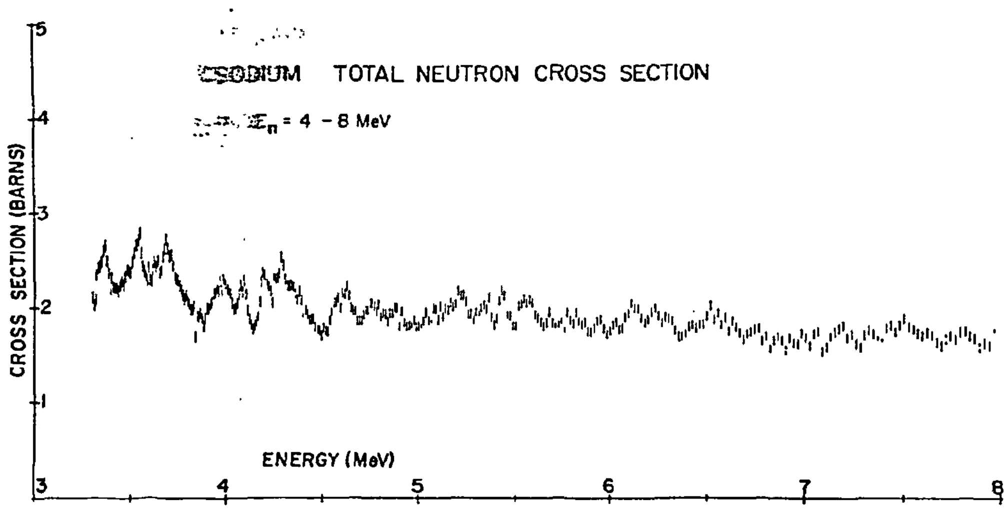

Figure A3

DATA NOT FOR QUOTATION

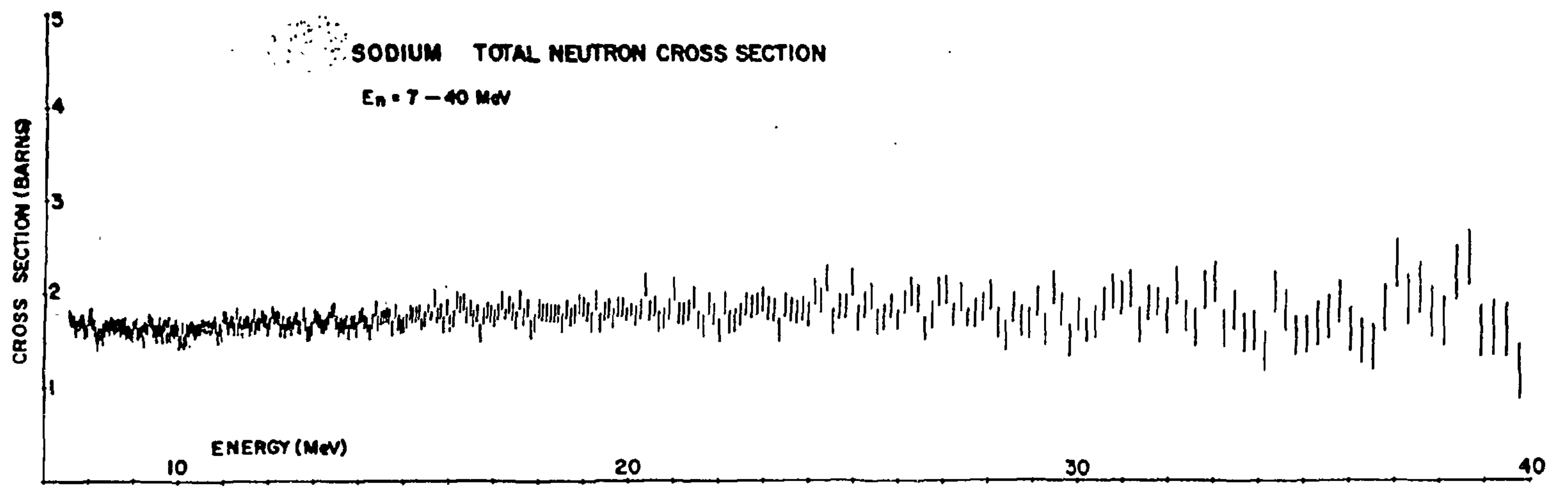
SODIUM TOTAL NEUTRON CROSS SECTION
En = 7 — 40 MeV
CROSS SECTION (BARNS)
1
2
3
4
5
ENERGY (MeV)
10
20
30
40

Figure A4

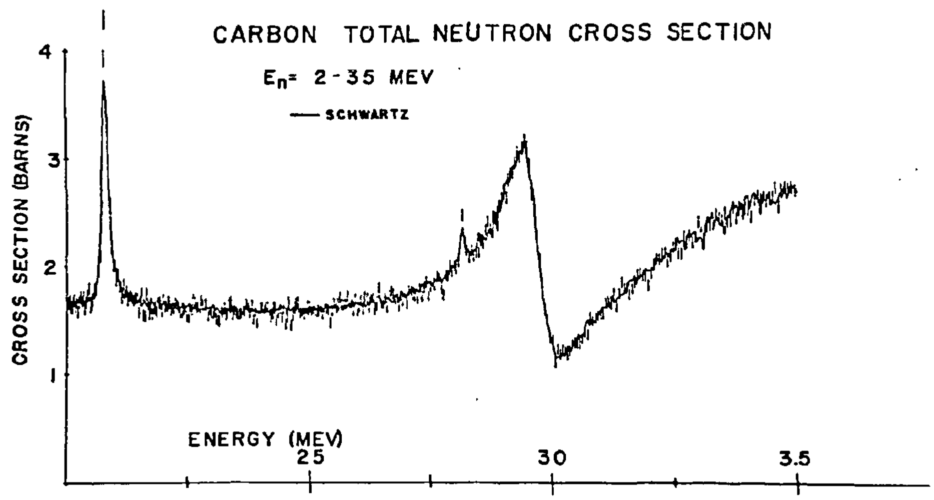

Figure A5

DATA NOT FOR QUOTATION

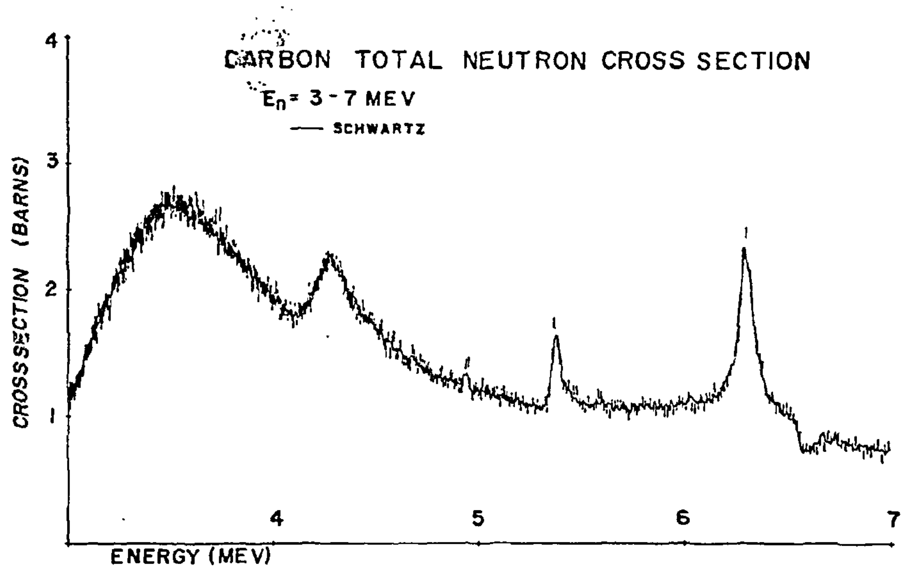

Figure A6

DATA NOT FOR QUOTATION

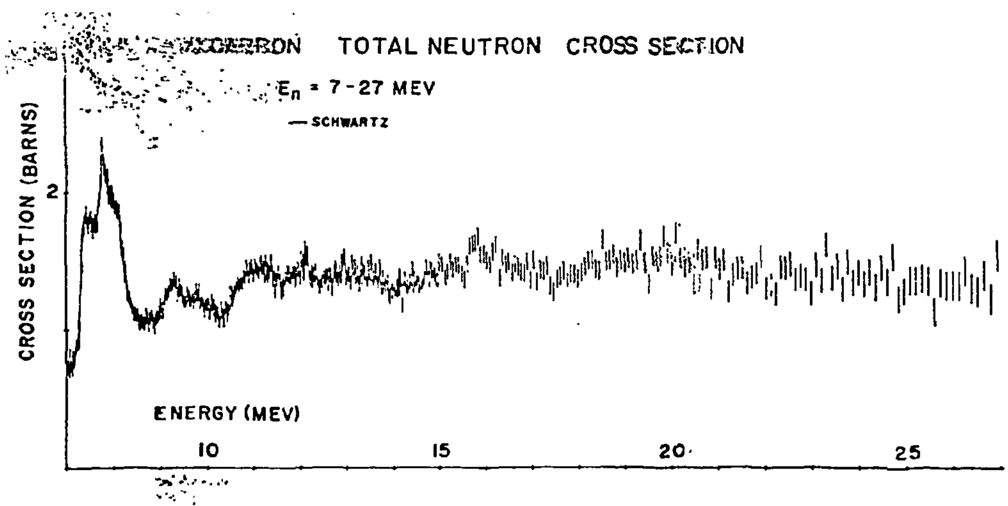

Figure A7

DATA NOT FOR QUOTATION

2. The Neutron Total Cross Section of ^{7}Li from 125 keV to 2 MeV* (R. C. Block, R. E. Slovacek and T. Y. Byoun)

The neutron total cross section of ^{7}Li has been determined by measuring the neutron transmission of ^{7}Li samples over the energy range from 125 keV to 2 MeV. Highly enriched metallic samples of ^{7}Li were prepared at the Los Alamos Scientific Laboratory by distilling metallic lithium into thin-wall (0.010-inch thick) 2-inch diameter stainless steel containers. Measurements were carried out with sample thicknesses of 0.0560, 0.1090, 0.3187 and 0.4675 atoms/barn, and the neutrons were detected with the ^{10}B-NaI detector located at the 27-meter flight station. The four ^{7}Li samples and a composite 'notch' filter package of Al, Na and Mn were alternately placed into the neutron beam under computer control, and the data were stored in the PDP-7 computer. A 10.5 gm/cm^2 sulfur sample was left in the neutron beam throughout the experiments to determine the background in the vicinity of the 111 keV sulfur resonance. The background in the energy region near the 260 keV ^{7}Li resonance was approximately 3% of the open beam counting rate. The transmission data have been reduced to total cross sections and preliminary results are shown in Fig. A8 for these four sample thicknesses. In general, the results overlap to within the counting statistics. These preliminary data are being compared with the recently reported ^{7}Li cross-section measurements by Meadows and Whalen.[1] Although it is premature to make a detailed comparison, there seems to be reasonable agreement between the two measurements, with the only exception being that this measurement is yielding a peak cross section slightly lower than that measured by Meadows and Whalen.

---

* Pertinent to request # 17.

1 J. W. Meadows and J. F. Whalen, Nucl. Sci. Eng. 41, 351 (1970).

DATA NOT FOR QUOTATION

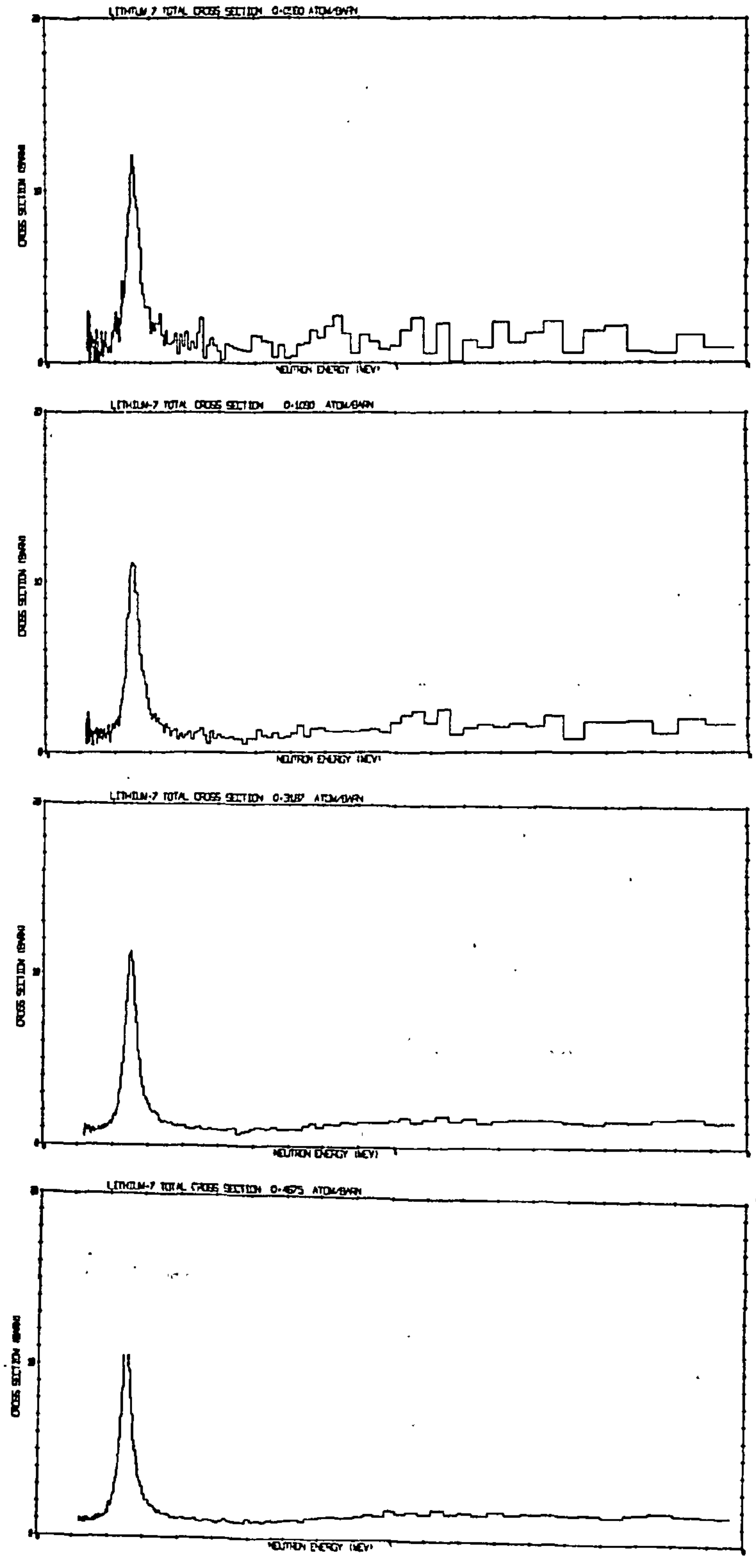

Figure A8

DATA NOT FOR QUOTATION

3. <u>KeV Neutron Capture and Transmission Measurements on ^{50}Cr, ^{52}Cr, ^{53}Cr, ^{54}Cr, ^{60}Ni and V*</u> (R. G. Stieglitz, R. W. Hockenbury and R. C. Block)

The following is an abstract of a paper submitted for publication in Nuclear Physics.

Neutron capture and transmission measurements were performed on vanadium and enriched samples of ^{60}Ni, ^{50}Cr, ^{52}Cr, ^{53}Cr, ^{54}Cr with an experimental resolution of 0.6 nanoseconds per meter. The capture measurements cover the energy range 0.1 to 200 keV while the transmission measurements extend to over 300 keV. Parameters are extracted for both s-wave and p-wave resonances. S-wave and p-wave strength functions, potential scattering radii, average capture cross sections and resonance absorption integrals are determined. The radiation width is found to vary widely among the s-wave resonances of each nuclide.

4. The Observation of Correlations Between Γ_n^o and Γ_γ in the Mass Range 50 to 60* (R. C. Block, R. G. Stieglitz and R. W. Hockenbury)

The following abstract has been submitted for presentation at the 1-4 February 1970 American Physical Society Meeting at New York City.

---

* Pertinent to requests # 84, 87 and 113, WASH 1144.

DATA NOT FOR QUOTATION

Neutron capture and transmission measurements[1] in the keV energy region upon ^{50}Cr, ^{52}Cr, ^{53}Cr, ^{54}Cr, V and ^{60}Ni have enabled 27 s-wave resonances to be analyzed for E_o, J, π, Γ_n and Γ_γ. The correlation coefficients between the neutron reduced width and the total radiation width, $\rho(\Gamma_n^o, \Gamma_\gamma)$, is: $\rho = 0.47$ for all 27 resonances, $\rho = 0.38$ for the 15 resonances in the odd (target) nuclei, and $\rho = 0.80$ for the 12 resonances in the even-even nuclei. The latter value of 0.80 is significantly different from zero. In addition, the resonance capture pulse-height spectra are dominated by strong high-energy gamma rays which we interpret as E1 transitions. The positive correlation, coupled with the strong E1 transitions, is interpreted as evidence of intermediate structure.

5. <u>KeV Neutron Capture Measurements on ^{240}Pu*</u>
(R. W. Hockenbury, J. D. Boice, W. R. Moyer and R. C. Block)

The ^{240}Pu data in the keV region have been reduced to capture and fission yields. The capture yield was normalized using the transmission data[1] for the 92.5 eV resonance where both capture and transmission data give the same quantity, $g\Gamma_n$, and where fission is negligible. The uncertainty in the absolute normalization is $\pm$ 12%, at present, due to cumulative errors in the transmission, capture and relative flux data. This uncertainty will be reduced by using other resonances in addition to the 92.5 eV resonance for normalization. This normalization method is not possible for the fission yield and the approximate detector efficiency for fission was used. The uncertainty in the fission yield is, at present, relatively large ($\pm$35%) due to possible errors in the detector efficiency, the large correc-

1 Stieglitz Hockenbury, and Block (to be published).

* Pertinent to requests # 459 and 461.

DATA NOT FOR QUOTATION

tion for the capture contribution, time-dependent and sample background corrections. Since the fission contribution is small relative to capture, the capture cross section is relatively insensitive to uncertainties in the fission cross section. For example, a 100% increase in the high bias correction to the low bias data results in ~10% change in the capture cross section. The data analysis is not yet complete; however, preliminary results are given in this report.

The yield divided by sample thickness (N) for the region from 800-1000 eV is shown in Fig. A9. Yield/N has the same units as cross section; however, they are not usually equivalent since the yield contains resolution, self-shielding and multiple scattering effects. The isolated cluster in fission at 800 eV is one of the sub-threshold fission groups (observed originally at Geel)[2]; the capture cross section has the typical structure for a heavy nucleus. The capture and fission yields divided by sample thickness are shown in Fig. A10 for the region from 4-30 keV. The gap in the data at 6 keV is due to a resonance in the Al sample container. In the keV region, corrections for self-shielding and multiple scattering effects will not exceed 10%. There the yield divided by sample thickness may be considered equal to the cross section for comparison purposes. The previously mentioned uncertainties in the fission cross section are large; however, we present it here to show the marked structure due to sub-threshold fission in the keV energy range. Using the fission cluster at 800 eV as a reference, the energy span of each fission group can be estimated. Above ~8 keV, with our experimental resolution, a fission group would show up as a single peak. Further analysis will be done to extract level spacing and, if possible, fission widths from these data. An evaluation by Yiftah[3] and a statistical ladder construction by Dyos[4] are superimposed on the measured cross section in Fig. A11. Detailed comparisons to these and other evaluations[5] will be made in a forthcoming report on this work.

DATA NOT FOR QUOTATION

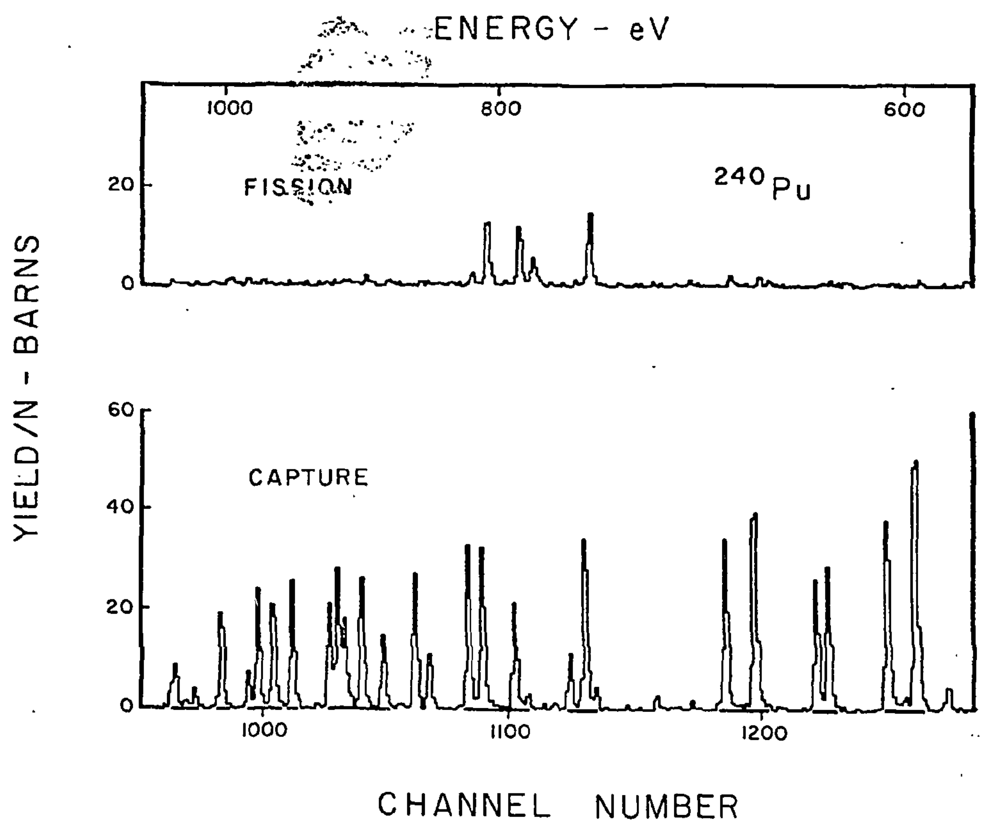

Figure A9

DATA NOT FOR QUOTATION

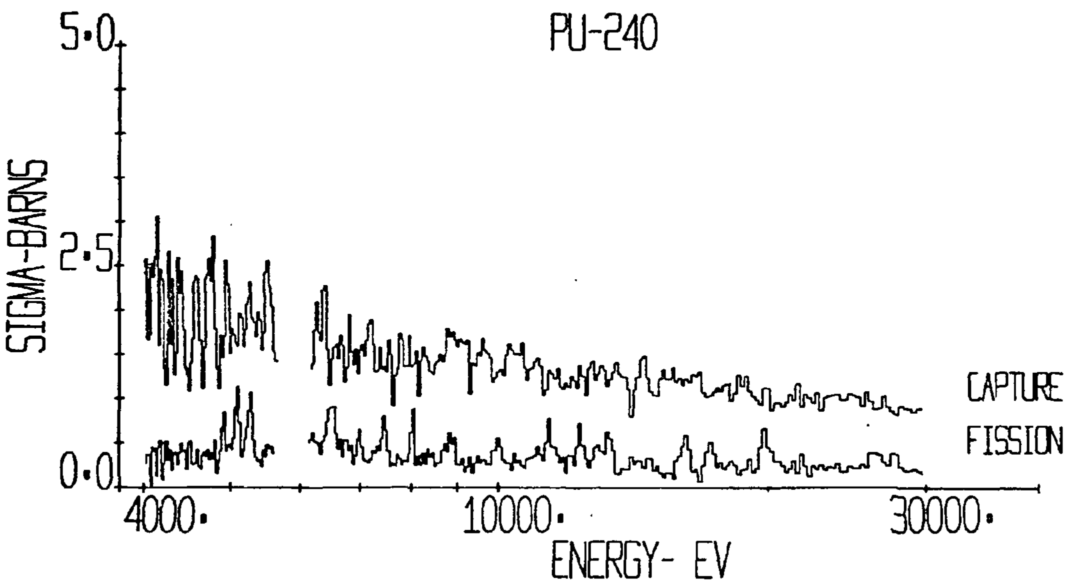

Figure A10

DATA NOT FOR QUOTATION

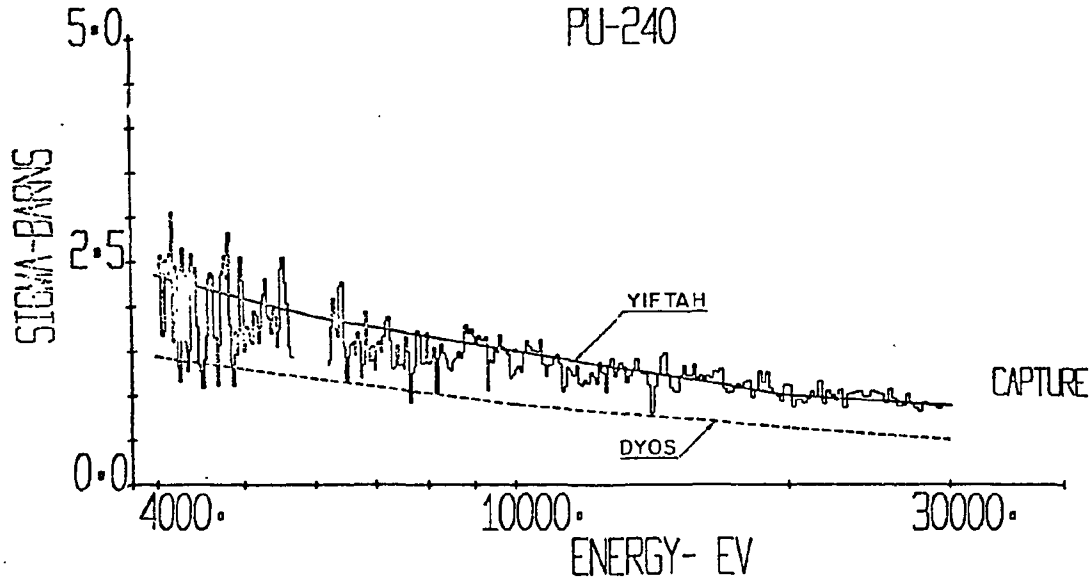

Figure A11

DATA NOT FOR QUOTATION

1. R. W. Hockenbury and R. C. Block, 20, RPI-328-187.

2. E. Migneco and J. P. Theobald, Proc. of Conf. on Neutron Cross Section and Technology, Washington, D. C., N.B.S. Special Publication 299, Vol I (1968).

3. S. Yiftah, J. J. Schmidt, M. Caner and M. Segev, Fast Reactor Symposium, Vol I, Karlsruhe (1967).

4. M. W. Dyos, Nucl. Sci. Eng., 34, 181 (1968).

5. T. Ishiguro, S. Katsuragi, M. Nakagawa and H. Takano, Nucl. Sci. Eng., 40, 25 (1970).

6. The Differential Elastic Scattering Cross Section of keV Neutrons from Iron and Nickel* (Ray Zuhr and K. Min)

In the program to measure the differential elastic scattering cross sections of keV neutrons the construction of the following experimental equipments was completed: (1) A scattering table which incorporates a scattering sample holder with two detector arms which can be rotated about the sample axis, (2) An eight-position automatic sample changer which can be used, with simple modifications, both for transmission and scattering measurements. (To fit the scattering geometry, only the alternate four sample positions are used.) The data acquisition capacity of this program was further improved by the feasibility of using a PDP-7 computer program originally written for the multiple-sample transmission experiments.

The time-of-flight neutron spectra scattered from natural iron, nickel and lead samples were measured with a ^{6}Li-glass scintillator mounted on a XP 1040 photomultiplier tube; a flight path of approximately 25 meters was used for this experiment. The spectra for iron and lead (to be used as a comparison target) were obtained at the scattering

* Pertinent to request # 119.

DATA NOT FOR QUOTATION

angles 135°, 110°, 90°, 70° and 45°, using the PDP-7 computer and the linac operating at 500 pps and producing 50-nsec wide pulses. The lead spectrum at 135° is shown in Fig. A12. The iron spectra at the same angle shows essentially the same features as reported previously in RPI-328-171, and it is not shown here. The Ni spectra shown in Fig. A13 were measured with 10 nsec beam pulse and the data were accumulated with a TMC time-of-flight unit.

With more accumulation of data for improved statistics, the iron and nickel cross sections will be extracted with respect to the known lead cross sections.

B. THEORY AND ANALYSIS

1. Temperature-Dependent and Multi-Level Effects On Neutron Resonance Cross Sections (T. E. Shea)

The following is an abstract of the doctoral thesis of T. E. Shea.

The effects of temperature-dependence and multi-level interference on neutron resonance cross sections and their manifestations on cross-section-dependent quantities are examined through the application of the Quasi-Resonance Multi-Level cross-section formalism. Cross-section expressions in this formalism are derived from the level matrix form of the R-Matrix formalism, and are given in terms of Lorentzian shape functions. The effects of nuclear thermal motion on the cross-section expressions are given in terms of the standard Doppler broadening functions.

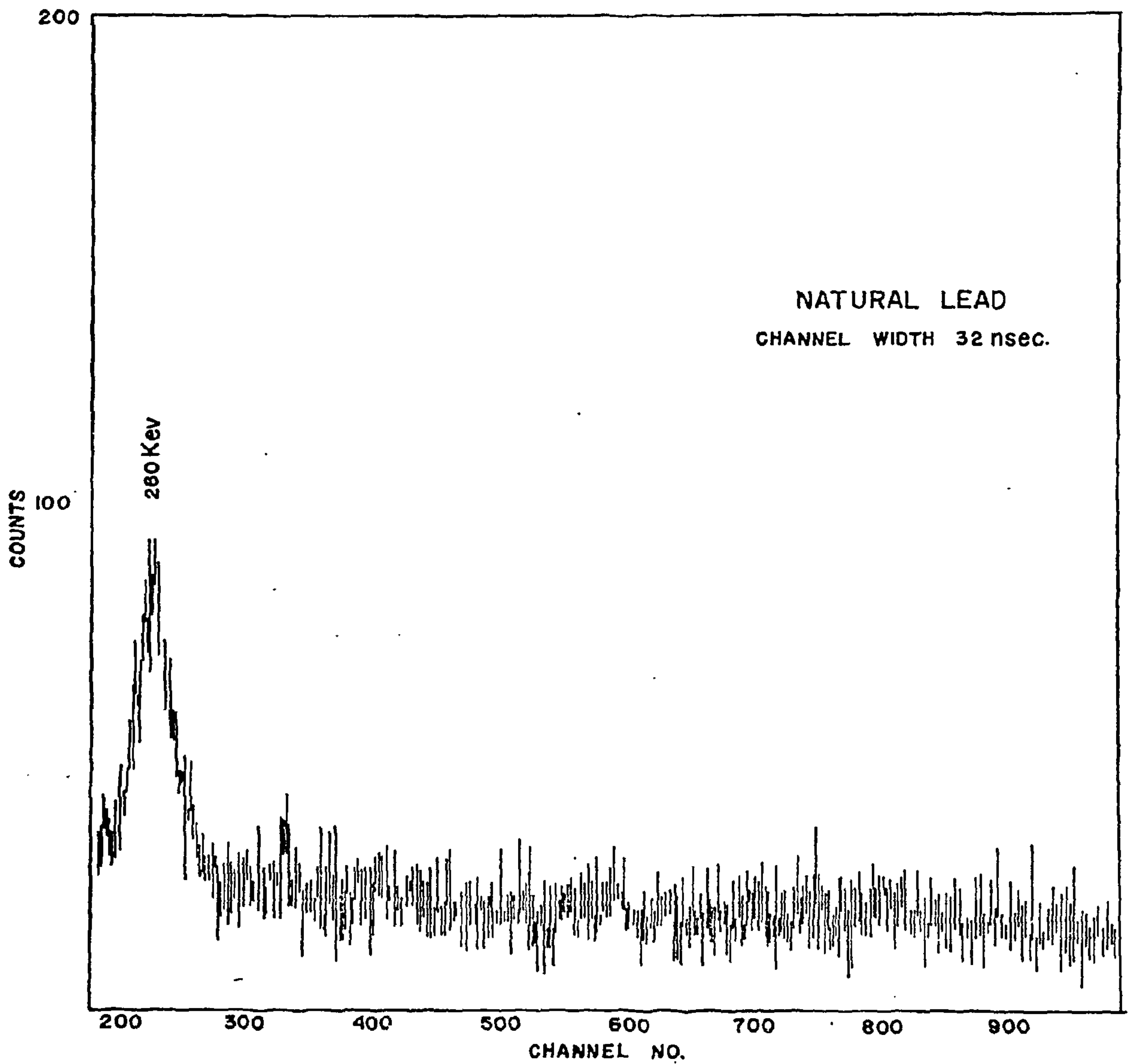

Figure A12

DATA NOT FOR QUOTATION

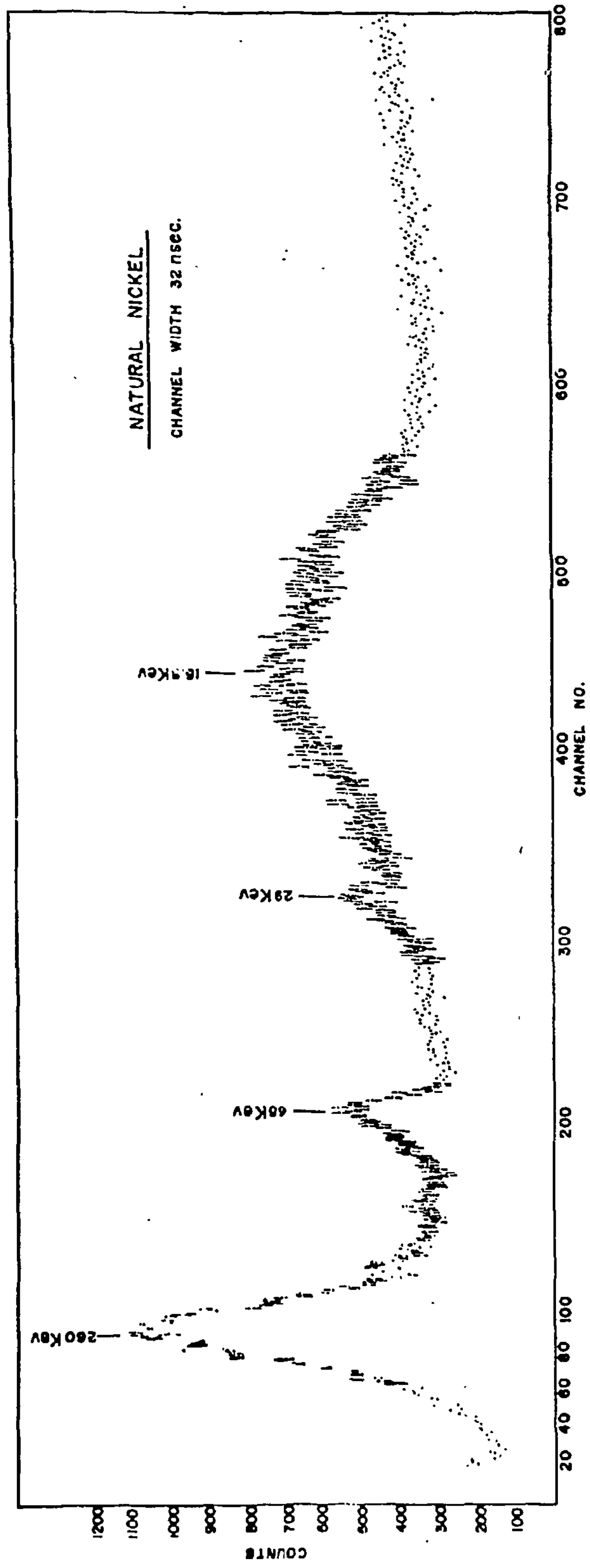

Figure A13

DATA NOT FOR QUOTATION

The Quasi-Resonance Triplet Approximation is introduced to facilitate the application of the formalism to the fissile nuclides. The Triplet Approximation fission parameters are studied in detail. For ^{235}U, they are determined to be negligibly intercorrelated and, in all cases studied, well represented by the chi-square frequency functions. The average symmetric fission parameter and its corresponding chi-square number of degrees of freedom are seen to be energy-dependent.

The Triplet Approximation is applied to the calculation of the ^{235}U fission cross section in the range from 18-66 eV. The approximation gives an improved representation of the cross-section line shape over the single-level type calculations. A weak- interference correction is introduced. When used with the Triplet Approximation, the comparisons with R-Matrix calculations are further enhanced. Fission integrals as well as point-wise cross sections are compared with experiment, with quite good agreement.

The average capture and fission cross sections and the average alpha for ^{235}U are computed in the energy range below 2.5 keV. Again, agreement between theory and experiment is quite good.

The Triplet Approximation is applied to be the Bramblett-Czirr experiment on shielded fission integrals for ^{235}U, in the resolved and unresolved resonance regions. The results indicate a need for additional cross-section measurements. Comparison calculations are in reasonable agreement with the data.

2. Analysis of Cross-Section Data Utilizing an Interactive Graphics Display (M. Lubert, N. C. Francis and R. C. Block)

The interactive graphics program permits a rapid analysis of the experimental data, eliminating the normal slow batch processing. The program MULTVL is modular in design with all pertinent data transmitted through labelled common blocks. The base overlay is a monitor program which executes a specified calculational path in which the final results are optionally displayed on a CRT. The basic program blocks are (1) an R-matrix cross-section routine, (2) a Doppler broadening code, (3) a resolution function routine, (4) a Monte Carlo program to treat multiple scattering effects and (5) an interactive graphics package. The user can modify the path as well as the physical parameters for all the modules while in display mode. The final results, in addition to necessary paper output, are viewed on the CRT and may be automatically transferred to computer-generated plots, microfilm and/or printer plots. A typical analysis, comprising several isotopes and one hundred resonances, computes the resolution-broadened transmission for two thousand energy points in approximately 1-2 minutes on a CDC-6600.

The analysis of the nickel, chromium and vanadium transmission experiments using R-matrix theory has yielded good results. However, the analogous comparison to the capture yield measurements for the same isotopes has been poor. In order to improve the theoretical calculation, the R-matrix formalism currently in use is being modified from two viewpoints. First, the collision matrix has been modified to use a representation of the Wigner level matrix which contains non-diagonal terms.[1] The level matrix is expanded to first order assuming random signs for the reduced width amplitudes. The collision matrix is then given by

$$U = O^{-1}\rho^{\frac{1}{2}}\Big[1 + \sum_{\mu,\nu} 2i\rho(\gamma_\mu x \gamma_\nu)\frac{\delta_{\mu\nu}}{E_\mu - E - \frac{i}{2}\Gamma_\mu}$$

$$+ \sum_{\mu,\nu}{}' 2i\rho(\gamma_\mu x \gamma_\nu)\Big\{(E_\mu - E - \frac{i}{2}\Gamma_\mu)^{-1} \sum_c \beta_{\nu c}\gamma_{\mu c}(E_\nu - E - \frac{i}{2}\Gamma_\nu)^{-1}\Big\}\Big]\rho^{-\frac{1}{2}}I$$

DATA NOT FOR QUOTATION

Lane and Lynn[2] have attempted to explain the direct mechanism contribution in neutron radiative capture. This model strongly selects those states which are single particle in nature. This can be included within the R-matrix representation by dividing the configuration space into an internal and external region and calculation the appropriate transition matrices. The contribution is largest for those transitions to low-lying single particle states and correlations between the partial radiative width and the final state reduced neutron width should exist. Several of the nickel and chromium isotopes have favored transitions to low-lying states. The contribution to the radiative capture cross sections should be evaluated.

The initial checkout of the program was performed by analyzing vanadium using the transmission data obtained by Stieglitz et al.[3] The resonance energies, widths, spins and strength functions have been determined. The strength functions for the 3^- and 4^- states in the energy interval 4.0 to 88.0 keV are 9.4×10^{-4} and 4.2×10^{-4} respectively, in good agreement with values previously reported,[4,5] The resonance parameters are summarized in Tables 1 and 2. The results of this report (column 5) agree quite well with the results reported by other workers, except for the spin assigned to the 17 keV resonance. Our analysis indicates that the spin for this level is 3^-.

---

[1] A.M. Lane and R.G. Thomas, Rev. Mod. Phys. 30, 257 (1958).

[2] A.M. Lane and J.E. Lynn, Nucl. Phys. 17, 563 (1960).

[3] R. G. Stieglitz, R.W. Hockenbury and R.C. Block, "KeV Neutron Cpature and Transmission Measurements on ^{50}Cr, ^{52}Cr, ^{53}Cr, ^{54}Cr, ^{60}Ni and V," (submitted for publication).

[4] M.C. Moxon and R.W.K. Firk, Proc. Phys. Soc. 82, 447 (1963).

[5] G. Rohr and E. Friedland, Nucl. Phys. A104, 1 (1967).

[6] J. Garg, private communication.

7 J. Morgenstern et al., Nucl. Phys. A123, 561 (1969).

DATA NOT FOR QUOTATION

TABLE 1

Resonance Parameters for ^{51}V

Resonance Energy (keV)

Rohr, Friedland[5]	J. Garg[6]	Morgenstern et al.[7]	R. Stieglitz[3]	This Report
4.17	4.16	4.169	4.16	4.17
6.89	6.8	6.886	6.79	6.85
11.81	11.68	11.81	11.52	11.68
16.6	16.23	16.6	16.24	16.26
17.4	16.99	17.4	17.0	17.0
21.65	21.75	22.32	21.67	21.75
29.45	29.63	29.44	29.66	29.6
39.3	39.54	39.37	39.63	39.6
48.15	48.15	48.43	48.37	48.4
49.55	49.48	49.28	49.63	49.79
51.95	51.98	51.69	52.22	51.95
53.0	53.0	52.73	53.15	53.0
62.9	63.9	62.7	63.14	63.2
68.1	68.6	68.3	68.5	68.3
83.0	82.6	82.2	83.0	83.0
87.6	87.5	87.0	87.6	88.3

TABLE 2

Resonance Parameters for ^{51}V

Neutron Widths (eV) and Spin

Rohr, Friedland[5]	J. Garg[6]	Morgenstern et al.[7]	R. Stieglitz[3]	This Report
508 (4)	500 (4)	508 (4)	520 (4)	500 (4)
1280 (3)	1230 (3)	1280 (3)	1280 (3)	1280 (3)
5500 (3)	5580 (3)	5500 (3)	4850 (3)	5580 (3)
350 (4)	350 (4)	350 (4)	360 (4)	350 (4)
350 (4)	350 (3)	90 (4)	350 (3)	350 (3)
790 (3)	960 (3)	950 (3)	680 (3)	950 (3)
191 (4)	150 (4)	160 (3)	130 (4)	190 (4)
570 (3)		480 (3)	540 (3)	480 (3)
150 (4)		100 (4)	30 (4)	100 (4)
630 (3)		550 (3)	560 (3)	550 (3)
115 (4)		88 (4)	55 (4)	90 (4)
980 (3)		800 (3)	830 (3)	800 (3)
3800 (3)		3600 (3)	4200 (3)	3600 (3)
4700 (4)		3900 (4)	4800 (4)	3900 (4)
1200 (4)		1000 (4)	1600 (4)	1000 (4)
3200 (4)		2700 (4)	3000 (4)	2700 (4)

C. "INTEGRAL" CHECKS ON CROSS-SECTION DATA

1. Fast Reactor Physics Studies (E. R. Gaerttner, M. W. Golay, N. N. Kaushal, B. K. Malaviya and M. Becker)

Time-of-flight studies of fast neutron spectra in large blocks of single materials are continuing. These measurements are compared with spectra calculated by means of DTF-IV code using cross-section data from the ENDF/B file. Analytical results of continuous slowing down theory are used as aids to interpretation of such comparisons.

At present, measurements on an aluminum assembly are in progress and are expected to be completed soon. Construction of a large cubical assembly of sodium is nearing completion and preliminary spectrum measurements on this assembly are expected to begin shortly.

Analysis of earlier measurements on iron and depleted uranium and current measurements on aluminum is being pursued concurrently. These analyses have revealed inconsistencies in various cross section compilations as well as programmatic errors in the codes used for this analysis. Our analysis of depleted uranium data indicates that the neutron spectra are quite sensitive to certain cross sections. Calculations are being performed using ENDF/B data and we expect to be able to make assessment as to the accuracy of these data. Our analysis of the measurements on iron has pointed out some deficiencies in the ENDF/B data and/or Karlsruhe (KFK-750) data. In particular, the following observations on the status of iron cross sections can be made on the basis of our analysis

1. ENDF/B data are not sufficiently resolved at high energies. However, the overall spectrum shape is not very sensitive to this lack of resolution. The main effect seems to be on the deep penetration problem at selected neutron energies.

2. There is a substantial discrepancy in the average values of the scattering cross sections in the range 30-300 keV between the ENDF/B data and the Karlsruhe data sets. The calculated spectra are quite sensitive to this discrepancy. The measured spectra are in better agreement with the calculations using ENDF/B data than those using Karlsruhe data.

3. In the neighborhood of and at the 27 keV resonance minimum, there is a clear discrepancy between the spectrum measurements and calculations using ENDF/B data.

Thus it appears that additional experimental and evaluation efforts are required for cross-section data in the 20-300 keV range. (These conclusions were presented at the (1970) Winter Meeting of the American Nuclear Society).

BONNER NUCLEAR LABORATORIES, RICE UNIVERSITY

A. NEUTRON PHYSICS

1. Fast Neutron Spectroscopy of (d,n) Reactions (Rendić, Mutchler, Sweeney, Sandler, and Phillips)

The angular distributions of fast neutrons from the $^{10}B(d,n)$ reaction at a bombarding energy of 11.8 MeV have been completed. The angular distributions from this reaction and the $^{11}B(d,n)$, $^{12}C(d,n)$, and $^{13}C(d,n)$ reactions, previously studied, have been analyzed in terms of zero range local DWBA, using the code DWUCK. Finite range and nonlocality effects have also been investigated. These results are now being prepared for publication.

2. The $^{2}H(p,pn)p$ Reaction at 9.0 MeV (Jackson, Emerson, Simpson, Joseph, Chen, Valkovic, Taylor, and Phillips)

The $^{2}H(p,pn)$ reaction has been studied at a bombarding energy of 9.0 MeV and several coincidence detection angles using the Rice University tandem Van de Graaff accelerator and computer-analyzer system. The energies of the detected, coincident particles were determined using a solid-state surface barrier detector for the proton and time-of-flight measurement on the neutron. The contributions of the neutron-proton final state interaction and neutron-proton quasi-free scattering have been observed. The final state interaction contribution has been reproduced using Phillips, Griffy, and Biedenharn theory. The shape of quasi-free scattering contribution spectrum is in reasonable agreement with simple impulse approximation prediction. The absolute value of cross section is a factor of two smaller than predicted by the spectator model calculations. This work has been accepted for publication in Nuclear Physics.

3. Preparation of a Monoenergetic d+d Neutron Beam at Tandem Energies (Hochberg, Rendić, and Phillips)

The study of combining neutron time-of-flight technology using simultaneously pulsed beam techniques and associated particle techniques for the d+d reaction at tandem energies has resulted in an M.A. thesis (for A. Hochberg). The conclusion was reached that the method is very promising since it eliminates 3- and 4-body final state neutron groups. However, it was concluded that neither the present scintillation nor the counter detection of the associated particle (He^3) is adequate to the necessary signal-to-noise and band width requirements.

B. MULTI-PARTICLE BREAK-UP REACTIONS AND FEW NUCLEON PROBLEMS

1. n-p and p-p Quasi-free Scattering for the p+d→p+p+n Reaction (Valković, von Witsch, Rendić, Otte, and Phillips)

Neutron-proton and proton-proton quasi-free scattering (QFS) has been studied in the reaction p+d→ p+p+n for proton bombarding energies 4.5 - 13.0 MeV, and in symmetric geometry $-\theta_{1p} = \theta_{2p} = \theta_n = 30^{\circ}$. The energy dependence (excitation curve) and the shapes of QFS peaks are reasonably well reproduced by spectator model calculations, although the absolute cross section is for a factor of 5 smaller than predicted by the simple impulse approximation.

2. Neutron-Deuteron and Proton-Deuteron Low Energy QFS in the d+d→ n+p+d Reaction (Sweeney, Valković, Otte, Andrade, and Phillips)

Neutron-deuteron and proton-deuteron quasi-free elastic scattering has been studied in d+d→ n+p+d reaction by coincidence detection of two outgoing particles and with dE/dx particle identification. Measurements were performed at deuteron bombarding energies 5.5 MeV $\leq E_d \leq$ 12.5 MeV with $\theta_d = -20^{\circ}$ and $\theta_p = \theta_n = 20^{\circ}$. Measured spectra show the contribution of nucleon-deuteron QFS process at all bombarding energies. The applicability of the impulse approximation has been considered. Comparison of n-d and p-d QFS was possible since no competing final state interactions were observed. The large cross section for n-d QFS offers the possibility of using d+d→n+p+d reaction as a source of the neutrons in the energy interval 3-8 MeV.

3. Comparison of p-p and n-p QFS in $p+d \rightarrow p+p+n$ Reaction
(Valković, Rendić, Otte, and Phillips)

Proton-proton and proton-neutron quasi-elastic scattering process contributions were measured simultaneously at proton energy of 12 MeV with $\theta_{1p} = -30^{\circ}$, $\theta_{2p} = \theta_n = 30^{\circ}$. The ratio of the peak cross sections $(\sigma_{np}/\sigma_{pp})_{exp}$ was found to be 2.0 ± 0.2, while the simple impulse approximation predicts $(\sigma_{np}/\sigma_{pp})_{imp} \approx 1.3$. No Coulomb effects were found to be significant. This work has been submitted for publication.

4. p-n and p-α QFS in the Reaction $p+{}^{9}Be \rightarrow p+n+\alpha+\alpha$
(Sweeney, Valković, and Phillips)

Measurements have been made of proton-neutron and proton-alpha QFS for 12-MeV protons incident on ^{9}Be. For the p-n QFS, we will compare the cross sections when the spectator ^{8}Be is in either its ground state or first excited state. The processes involving sequential decays through ^{9}Be, ^{8}Be, and ^{5}He states have been studied in order to obtain information on the reaction mechanism.

5. Four Body Break-up Reaction: $d + {}^{11}B \rightarrow \alpha+\alpha+\alpha+n$
(Rendić, Valković, Otte, von Witsch, and Phillips)

Break-up in four particles in the final state was investigated in the $d + {}^{11}B \rightarrow 3\alpha + n$ reaction. α-α and α-n coincidences have been detected at bombarding energy of $E_d = 12.0$ MeV. Preliminary results reveal the importance of sequential decay involving ^{8}Be and ^{12}C states and indicate $(n + {}^{8}Be)$ cluster structure of ^{9}Be rather than $(\alpha + {}^{5}He)$.

6. System for a Large Solid Angle Detection Chamber and Detector for Multi-Particle Break-up Studies
(D. Rendić, and G. C. Phillips)

A chamber that will allow the mounting of two large multiwire counters has been completed. Preparations are being made to make a system that uses two x-y wire planes to detect the break-up particles. Each multiwire counter will subtend about 1 steradian. Testing of the multiwire counters already used in high energy physics, and adapting it for use in low energy physics, is in progress.

7. <u>Neutron-Proton Coincidence Measurements in the Reaction $^{9}Be(p,pn)^{8}Be$</u> (Wilson, Sandler, Otte, and Phillips)

This work has been completed and is being prepared for publication.

8. <u>Investigation of the Reactions $^{9}Be(p;p,\alpha)^{4}HeN$ and $^{9}Be(p;p,N)^{8}Be$</u> (Hungerford, Ivanovich, Sandler, and Phillips)

Interpretation and collection of data of the neutron and alpha decay of the 2.43 MeV level of ^{9}Be is in progress. Preliminary analysis shows a broad double peak in the decay particle spectra which cannot be described by either a simple sequential decay through ^{8}Be or ^{5}He. This experiment supplies additional information to that of $^{9}Be(p,pn)^{8}Be$ reported above. This work is being continued.

C. INSTRUMENTATION

1. <u>IBM-1800 Computer Hardware and Software</u> (J. Buchanan, H. Jones, and M. Jones)

During this period (May 1 - October 31, 1970) development continued on the Bonner Nuclear Laboratories' data-acquisition system. The old experiment interface was abandoned with the new system put into exclusive service. The four old TMC ADC's were installed, bringing the total ADC's in the system to eight. Several experiments using all eight ADC's overlaid with off-process calculation have been accomplished. The BONER system is fully operational as originally designed. Major changes are being made to the print routine philosophy, including a streamed buffer counter. (This will facilitate the experimenter's correlation of multi-parameter streamed data with his single-parameter spectrum.) Also, we will soon have the option of double output buffers, which will speed up the maximum data rate by a factor of two. At the next major BONER update, we will load the latest modification of TSX version 3 - modification level 8.

2. <u>5.5 MeV Van de Graaff Improvement</u> (J. R. Risser, Cox, Windish, Hardy, and Phillips)

The new terminal was let to bids and High Voltage Engineering Corporation was awarded the contract. The new terminal should be installed in early 1971.

DATA NOT FOR QUOTATION

3. A Negative Ion Source for the tandem Van de Graaff (E. V. Hungerford and R. Y. Rodgers)

A negative ion source for injection into the Rice tandem Van de Graaff accelerator is being designed and built. A standard r-f source is used with acceleration of positive ions up to 100 keV. Charge exchange will be accomplished by means of Li vapor in the energy range 80-100 keV. The source will initially be used for ^4He, for which positive ion current is presently about 800 μA. Other ions to be investigated may possibly include carbon, neon, and nitrogen.

4. Multiwire Proportional Counter Camera for the Browne-Buechner Magnetic Spectrograph (Plasek, Buchanan, and Phillips)

A multiwire proportional counter with a backing scintillation counter has been designed, constructed, and tested in the Bonner Nuclear Laboratories' Browne-Buechner magnetic spectrograph. The position sensitive multiwire counter, coupled on-line to the 1800 IBM computer system, gives the $B\rho$ of the particles and the dE/dx is given by the linear signal. When used with a pulsed-bunched beam to measure time-of-flight to the scintillation detector, the system will be capable of giving magnetic spectra versus Z and m. Further testing of the system is proceeding.

5. Investigation of Multiwire Proportional Counters for Low Energy Nuclear Physics (N. D. Gabitzsch and G. C. Phillips)

Testing of low pressure multiwire proportional counters capable of detecting low energy (3-15 MeV) protons is now being conducted. These are very similar detectors as those used for (Task C) detection of high energy protons and π^+. Each M.W.P.C. will subtend a solid angle of one steradian and an angular resolution of the order of 10^{-3} steradians.

D. INTERMEDIATE ENERGY PHYSICS (TASK C)

1. Multiple Scattering of 600 MeV Protons (Hungerford, Mutchler, Scott, and Phillips (Rice University); J. C. Allred, Mayes (U. of Houston))

We have continued our investigation of the multiple scattering of 600 MeV protons from targets of C, Al, Cu, and

Pb at S.R.E.L. Preliminary studies showed a large deviation from the usual Moliere multiple scattering formulation for C and Al with decreasing deviations for the larger Z materials of Cu and Pb. Our latest, more definitive measurements, confirm these results. Calculations are in progress to support these results by theory.

2. Multiple Scattering of $\pi^{\pm}$ Mesons (Mutchler, Scott, Hungerford, and Phillips (Rice); Allred, Lee, and Mayes (U. of Houston))

Previous work[1,2] at S.R.E.L. had indicated that the small angle multiple scattering of 365 MeV/C π^- and 600 MeV protons is significantly effected by the interference between the nuclear and Coulomb amplitudes. We have extended these measurements to include an excitation curve spanning the (3/2, 3/2) resonance region for C, Al, Cu, and Pb using both π^- and π^+ mesons. Preliminary analysis indicates that the effect is much smaller than previously noted. The discrepancy with earlier results is attributed to improved experimental set-up and plane performance.

3. Determination of Pion Momenta and Beam Purity Using Multiwire Proportional Counters (Scott, Hungerford, Mutchler, and Phillips (Rice University); Mayes, Allred, and Goodman (U. of Houston))

$\pi^{\pm}$ beams of variable momentum have been produced with a CH_2 production target in the external 600 MeV proton beam at the Space Radiation Effects Laboratory. This beam contains $\pi^{\pm}$, $\mu^{\pm}$, $e^{\pm}$, and protons of various energies. The protons in the beam were differentiated by dE/dx and time-of-flight measurements. The π^+ flux is differentiated from the other relativistic particles by examining the meson distribution from the $\pi^+ \rightarrow \mu^+ + \bar{\nu}$ decay with thin multiwire proportional counters developed at Rice University. The opening angle of the muon distribution is used to determine the incidence π^+ momentum, and the integrated muon distribution is compared to a Monte Carlo calculation to determine the beam purity. The beam purity at a momentum of 330 MeV/C was found to be approximately 84% using this technique. The treatment of a π^- beam differs from the π^+ beam in that there are no protons to discriminate.

---

1 Report to the A.E.C. N.C.S.A.C., April 30, 1970, G.1

2 Ibid G.2

DATA NOT FOR QUOTATION

4. Elementary Particle and Intermediate Energy Physics Theory (R. Guertin and I. M. Duck)

We are performing a ρ bootstrap calculation including inelastic channels in an effort to extend the range of a rising ρ trajectory to higher energies where single channel calculations indicate a falling trajectory. This work is just underway and will continue through the summer of 1971.

5. π^- d Capture Theory (N. Carron and I. M. Duck)

We are re-examining the $\pi^- d \rightarrow nn\gamma$ final state interaction calculations of McVoy and Barden from which nn scattering length is determined. This work will use hard pion current algebra techniques and we hope to calculate the momentum dependent corrections to the shape of the endpoint of the gamma spectrum, thus providing a measure of the nn effective range.

6. Design of a Mobile On-Line Data Acquisition System for Intermediate Energy Physics (Buchanan, H.Jones, M. Jones, and Phillips)

In preparation for being a LAMPF user an on-line, mobile data acquisition system is being designed. Many small (mini) computers have been investigated, CAMAC studied, and one of our group (J. Buchanan) was a participant in the LAMPF summer study group that recommended specifications for the LAMPF computer systems.

A system concept, incorporating our experience with three prior Bonner Lab systems and the LAMPF study group conclusions, is under development. The design will emphasize a flexible mobile facility, capable of tying-in to various large laboratory computer and accelerator facilities (especially LAMPF) and capitalizing on our employment of large arrays of multi-wire proportional counters. The software, under development, is designed to be machine independent. The design will be completed, equipment purchased, and contracts let in early 1971.

TEXAS NUCLEAR

A. NEUTRON PHYSICS

1. Gamma-Rays from Nitrogen and Oxygen (W. E. Tucker, D. O. Nellis, P. S. Buchanan, and J. A. Stout)

(Work pertinent to requests #43, #47 WASH 1144)

Work is continuing on the gamma-ray measurements on oxygen and nitrogen at 14.8 MeV using both Ge(Li) and NaI(Tℓ) detectors. Most of the data have been obtained and a paper is in preparation.

2. Elastic and Inelastic Neutron Scattering from Nitrogen (P. S. Buchanan, T. C. Martin, W. E. Tucker, D. O. Nellis, and G. H. Williams)

(Work pertinent to requests #39, #40, #41 WASH 1144)

Neutron scattering measurements for nitrogen have been completed at 9 and 11 MeV incident neutron energies. The Los Alamos Tandem Facility was used to obtain these measurements. Elastic scattering data have been obtained at 9 and 11 MeV at about 15 angles between 30^0 and 120^0 to the incident beam. These data have been analyzed except for multiple scattering corrections, which are in progress. In addition, inelastic scattering cross sections are to be obtained at two or three scattering angles at each incident energy.

Figure A-1 shows a typical time-of-flight spectrum of scattered neutrons from nitrogen. This spectrum was obtained at an incident energy of 11 MeV and at a scattering angle of 70^0. The positions of the neutrons scattered inelastically to the various levels in ^{14}N are shown.

3. Elastic and Inelastic Scattering from Oxygen (D. O. Nellis, P. S. Buchanan, G. H. Williams, W. E. Tucker, and T. C. Martin)

(Work pertinent to requests #44, #45 WASH 1144)

Elastic and inelastic scattering measurements have been made for oxygen at 9 and 11 MeV neutron energies at a number of scattering angles. A water scattering sample was used in the measurements. Figure A-2 shows a spectrum obtained for water at 11 MeV and at $\Theta = 35^0$. The spectrum contains the resolved elastic peaks from ^{16}O and H and two inelastic neutron peaks corresponding to two pairs of excited doublets in ^{16}O. The analysis of the data is in progress.

4. Elastic and Inelastic Neutron Scattering from Iron, Aluminum, Calcium, and Silicon (G. H. Williams, W. E. Tucker, D. O. Nellis, T. C. Martin, and P. S. Buchanan)

(Work pertinent to requests #61, #62, #66, #67, #73, #74, #100, #101, #102 WASH 1144)

Neutron scattering data for Fe, Al, Ca, and Si are being obtained at 9 and 11 MeV at a number of scattering angles. The analysis of these data are in progress.

5. Compilation of Neutron-Induced Gamma-Ray Cross Sections (P. S. Buchanan, D. O. Nellis, W. E. Tucker, and G. H. Williams)

A compilation is currently being revised to include all measurements made at Texas Nuclear of cross sections and angular distributions of gamma rays from $(n,x\gamma)$ reactions. This compilation is to reflect Texas Nuclear research in this area from 1961 to the present and will include data for a large number of nuclei. It will supersede a previous 1969 compilation.[1]

[1] P. S. Buchanan, Texas Nuclear Report ORO-2791-28 (January 1969).

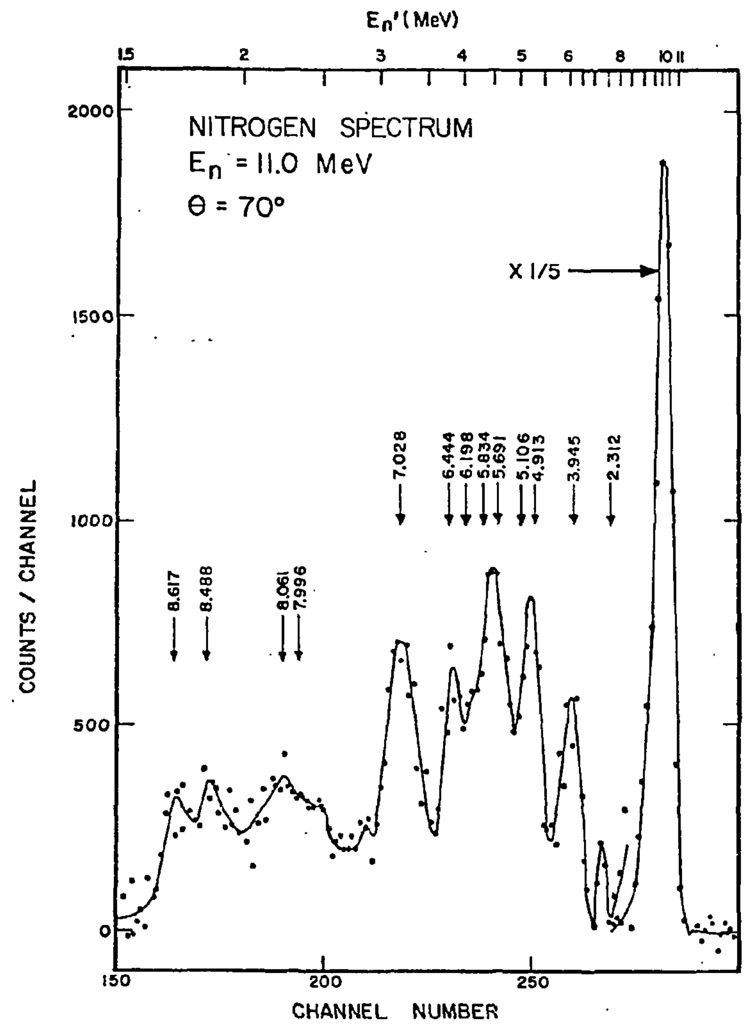

Figure A-1

DATA NOT FOR QUOTATION

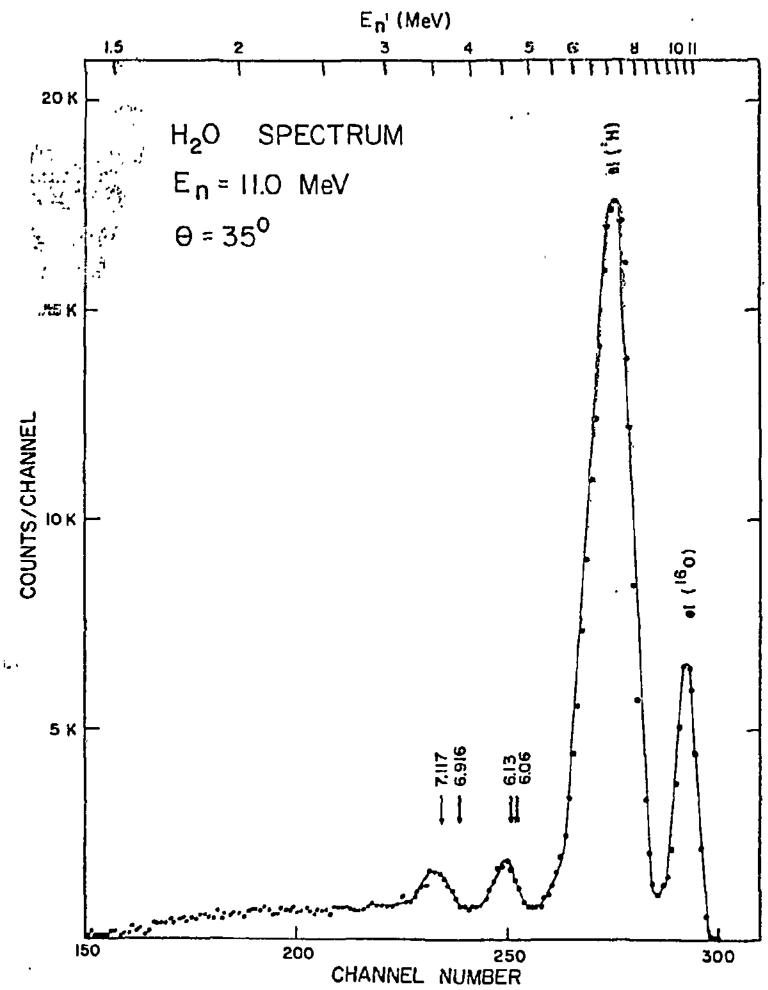

Figure A-2

DATA NOT FOR QUOTATION

TRIANGLE UNIVERSITIES NUCLEAR LABORATORY

A. NEUTRON PHYSICS AND FISSION

1. Resonance Cross Section Measurements with Continuous Beam (J. Malan, W. F. E. Pineo, E. G. Bilpuch, H. W. Newson, R. L. Walter)

The feasibility of using the $^{12}C(d,n)$ reaction as a neutron source to measure total neutron cross sections has been investigated. A liquid scintillator in open geometry (i.e., no collimator) was used with a pulse height discriminator to reduce the effect of scattered neutrons. The results indicate that this method is convenient for measuring cross sections in the energy region above 1.3 MeV which cannot be reached with the $^7Li(p,n)$ reaction at a 3 MeV accelerator. It will, however, be necessary to discriminate better against the high flux of scattered low energy neutrons which are present when a deuteron beam is used. The target chamber was redesigned to allow targets to be changed without breaking the vacuum. This arrangement was subsequently found to be very convenient. Using a high resolution deuteron beam of ~8 μA on C foils of ~5 μg/cm^2, a neutron energy resolution of less than 2 keV was obtained for neutron energies above 1.3 MeV. These techniques were applied to measurements of the total neutron cross section of radiolead (88% ^{206}Pb) from 1.3 to 1.9 MeV, a region in which some structure from doorway states is expected. Indications from the raw data, however, are that the structure is complicated and only partially resolved which renders the detection of a doorway state very difficult. The data are being processed, and further measurements on ^{206}Pb and possibly other elements are planned.

In order to facilitate higher resolution neutron measurements at energies below 1.3 MeV, a new type of LiF target was used. It is hoped that a "thickening" effect previously observed for Li targets on Ta can be eliminated by evaporating these targets on thin carbon backings, so that most of the heat is generated in the Ta beam stop rather than in the target. Targets of thickness ~.5 keV were made and found to stand up well to proton beams of ~6 μA. This technique is to be used in total neutron cross section measurements on Sr and other elements for which some doorway state predictions have also been made. See Section A6.

2. Average Total Neutron Cross Sections (W. F. E. Pineo)

Inactive.

DATA NOT FOR QUOTATION

3. Average Total Neutron Cross Sections and Strength Functions (W. F. E. Pineo, M. Divadeenam,* E. G. Bilpuch, H. W. Newson)

Preparation of papers on this topic based on the theses of M. Divadeenam and W. F. E. Pineo is in progress.

4. Analysis of Mo + n Resonances (M. Divadeenam, E. G. Bilpuch, H. W. Newson)

These data are being studied for signs of intermediate structure.

5. Theoretical Nuclear Structure Studies in ^{51}Ti and ^{209}Pb (M. Divadeenam, W. P. Beres**)

A paper on ^{51}Ti has been published.[1] A second paper has shown that the doorway state at 500 keV in Pb is due to an excited core rather than a 2p1h state.[2]

6. Shell Model Calculation of the Neutron Resonances and Intermediate Structure (F. T. Seibel,*** M. Divadeenam, W. P. Beres, H. W. Newson)

Feshbach, Kerman, and Lemmer's doorway-state theory of intermediate structure is applied to the investigation of neutron doorway escape widths, Γ_d. Assuming that the target nuclei in the ground state are spherical in nature, the three compound nuclei Zr^{91}, Sr^{89}, and Ca^{49} are considered as test cases. A basis of 2p-1h states in each of the above three compound nuclei is diagonalized via an effective two-body interaction. Doorway states of various angular momenta and of both parities are considered for the nuclei under investigation. Throughout the entire calculation proper Woods-Saxon potentials are used to generate both the neutron and proton wave functions. In the case of Sr^{89}, and Zr^{91}, the calculated p-wave escape widths are large compared to the s-wave widths in the low energy region. This is a manifestation of the single particle giant resonance phenomenon.

---

* Now at North Carolina Central University, Durham, North Carolina

** Now at Wayne State University, Detroit, Michigan

*** Now at Los Alamos Scientific Laboratory, Los Alamos, New Mexico

1) M. Divadeenam and W. P. Beres, Physics Letters 30B (1969) 598.

2) W. P. Beres and M. Divadeenam, Physical Review Letters 25, 596 (1970).

DATA NOT FOR QUOTATION

The effect of shell closure is evident in Ca^{49}; in that the spacing of levels is rather large and the lowest predicted s-wave doorway is around 1.5 MeV. These calculations predict correctly that there will be no observable s-wave resonances and also that most of the non s-wave resonances should be due to d-wave. These predicted J values are definitely confirmed for 4 out of 7 resonances and are consistent with all the data.

For comparison with low energy neutron scattering data, the sum rule $\Sigma \gamma_n^2 = \gamma_d^2$ is employed, and the effect of doorway states on the local strength function and the fine structure observed is discussed. The widths of the $1/2^+$ resonances of Pb^{207} have been determined well enough to confirm the sum rule which should hold if the isolated $1/2^+$ resonance in Pb^{208} acts as a doorway state for both Pb^{207} and Pb^{206}.

7. Charged Particle Induced Fission (F. O. Purser, J. R. Boyce, T. D. Hayward, E. G. Bilpuch, H. W. Newson, H. W. Schmitt*)

The total cross section for proton induced fission of ^{235}U has been measured for proton energies from 5.75 MeV to 30.0 MeV. Data have been accumulated at proton energy intervals of 250 keV over most of this region, and accurate fission fragment angular distributions have been measured at six energies. It is planned to extend this measurement to all of the available uranium isotopes in the immediate future. The first data for ^{235}U were reported at the Houston meeting of the Nuclear Physics Division of the American Physical Society.

For ^{235}U fragment mass and kinetic energy correlations have been obtained for selected proton energy regions to allow detailed study of energy dependent effects in the fission process at high excitation energies. This work will be continued and extended to the other uranium isotopes.

A corollary effort to the fission program has been instituted to measure proton elastic scattering and reaction cross sections for the actinide nuclei. The data available and optical model parameters applicable to these nuclei are extremely sparse. The systematic experimental study of this region has therefore been undertaken to facilitate analysis of our fission data.

Direct measurement of prompt neutron yields from proton induced fission is planned following the completion of development work currently in progress of the Cyclo-Graaff time of flight capability. This work would complement the

* Oak Ridge National Laboratory, Oak Ridge, Tennessee

DATA NOT FOR QUOTATION

neutron measurements currently available from $E_1E_2T_2$ correlations being performed at Oak Ridge and elsewhere.

The possibility of using coulomb induced fission to investigate sub-barrier resonance behaviour is being investigated.

8. Scattering of 8 MeV Polarized Neutrons from ^{4}He (Th. Stammbach,* J. Taylor, G. Spalek, R. L. Walter)

Published in Physical Review 2C, 2, 434 (1970).

9. Level Analysis of Nucleon-^{4}He Scattering (Th. Stammbach, R. L. Walter)

A paper on this work was presented at the International Symposium on Polarization Phenomena in Nuclear Reactions at Madison, Wisconsin, 8/31/70-9/4/70.

10. Comparison of the Analyzing Power for n-^{4}He Scattering Calculated from Several Sets of Phase Shifts (T. C. Rhea, Th. Stammbach, R. L. Walter)

A paper on this work was presented at the Madison Symposium on Polarization Phenomena.

11. The ^{9}Be(α,n) Reaction as A Source of Polarized Neutrons (Th. Stammbach, J. Taylor, G. Spalek, R. L. Walter)

A paper on this work has been published in Nucl. Instr. and Methods 80, 304 (1970).

12. Polarization in (^{3}He,n) Reactions on ^{9}Be, ^{11}B and ^{13}C (R. S. Thomason,** L. A. Schaller,*** Th. Stammbach, J. Taylor, R. L. Walter, R. M. Drisko (Univ. of Pittsburgh)).

This work is being prepared for publication.

---

* Schweiz. Inst. f. Nuklearf, Neunnbrunnenstf. 85, 8050 Zurich, Switzerland

** 6606 B Reider Court, Edgewood, Maryland

***

13. Polarization of Neutrons from the ^{6}Li(d,n) and ^{7}Li(d,n) Reactions (R. S. Thomason, G. Spalek, R. L. Walter)

A paper on this work has been submitted to Nuclear Physics.

14. Polarization in the ^{40}Ca, ^{24}Mg, and ^{28}Si(d,n) Reactions (J. Taylor, Th. Stammbach, G. Spalek, R. A. Hardekopf, R. L. Walter)

The neutron polarization angular distribution for the ^{40}Ca(d,n_0) reaction has been measured at 3.8 MeV, and the ^{24}Mg(d,n_0) and ^{24}Mg(d,n_1) polarizations have been obtained at 6 energies between 2.2 and 3.9 MeV. Neutron polarizations for the ^{28}Si(d,n_0) reaction were measured at 4 energies between 3.0 and 3.9 MeV and also at 8.1 MeV. DWBA calculations are being made for the ^{40}Ca and ^{28}Si(d,n) reactions and are essentially complete. A report of the ^{40}Ca(d,n) data was given at the Quebec Symposium on Nuclear Reaction Mechanisms and Polarization Phenomena, and a paper on all of these reactions is being prepared for publication.

15. A DWBA Study of the Polarization of Neutrons from The (d,n) Reactions in the 1p Shell (M. M. Meier,+ R. L. Walter, R. Seyler ((Ohio State Univ.)), T. R. Donoghue ((OSU)), R. M. Drisko ((Univ. of Pittsburgh))

This work will be published in Nuclear Physics.

16. Polarization of (d,n) Reactions on 1p-Shell Nuclei from 3 to 4 MeV (M. M. Meier, R. S. Thomason, G. Spalek, J. Taylor, R. A. Hardekopf, Th. Stammbach, R. L. Walter)

This work is inactive at present.

17. The j-dependence in The ^{11}B(d,n_0) and ^{11}B(d,n_1) Polarizations from 3 to 12 MeV (J. Taylor, G. Spalek, Th. Stammbach, R. A. Hardekopf, R. L. Walter)

The j-dependence in this study is observed by noting the difference between the n_0 polarization ($p_{3/2}$ transfer) and the n_1 polarization (mostly $p_{1/2}$ transfer). Previously reported polarizations measured at 9 angles at about 8, 10 and 12 MeV have been supplemented by reaction cross section measurements at 7, 10, and 12 MeV and deuteron elastic cross sections at 8, 10 and 12 MeV. DWBA

+ Now at National Bureau of Standards, Washington, D. C.

analysis of the data is proceeding and a preliminary report was submitted at the Madison Symposium. A more complete paper is being prepared for publication.

18. Remeasurement of The Neutron Polarization from The $^7Li(p,n)^7Be$ Reaction for 3 to 4 MeV Protons (R. A. Hardekopf, J. M. Joyce, R. L. Walter)

The polarization of the n_0 group was measured accurately to calibrate the reaction as a source of polarized neutrons. The trend of the n_0 polarization was verified and the polarization of neutrons leaving ^7Be in the first excited state was extracted from the data. Results were presented at the Madison Symposium on polarization phenomena.

19. Polarization of Neutrons from The $D(d,n)^3He$ Reaction (G. Spalek, J. Taylor, R. A. Hardekopf, Th. Stammbach, R. L. Walter)

The polarization of neutrons from this reaction has been measured for deuteron energies from 6 to 14 MeV. Polarizations were found to be consistently lower than polarizations of protons from the mirror $D(d,p)^3H$ reaction contrary to expectation based on charge symmetry of nuclear forces. The measurements are being extended to 20 MeV utilizing the Cyclo-Graaff deuteron beam. Results from 6 - 14 MeV were presented at the Madison Symposium.

B. GENERAL

1. IBM 360 and DDP 224 Programming (C. R. Gould, R. A. Hardekopf, J. M. Joyce, R. O. Nelson, C. E. Ragan)

The programs JIB3 (F. G. Perey), DWUCK (P. D. Kunz), SNOOPY (P. Schwandt), JUPITOR-2 (T. Tamura), M2 (D. J. Church) and FTAU (C. E. Ragan) mentioned in the last report continue to be used. The program BANDMIX (J. R. Erskine) now runs at TUCC. This program calculates Nilsson single particle wave functions for each band of a deformed nucleus and then mixes them through Coriolis coupling. Excitation energies, spectroscopic factors and stripping and pick-up cross sections are calculated for these mixed wave functions. The program CORPAR (T. P. Cardon) has been obtained for performing calculations based on intermediate coupling in the unified model. The program evaluates wave functions for a single particle coupled to a vibrating core. Up to three single particle orbitals and three phonon vibrations are considered and the program also calculates electromagnetic transition strengths between the levels.

A number of these programs have been chained into links to run on the 8K DDP-224. The program BANDMIX was adapted and displays experimental and theoretical energy levels after each calculation. Typewriter input facilitates parameter variation. An optical model code, utilizing subroutines from SNOOPY, has also been adapted for the DDP-224. This program is chained into four links on magnetic tape. Two links perform the optical model calculation for projectile spins of 0, 1/2 or 1 using up to 30 partial waves. A control link displays up to three sets of experimental and calculated cross sections and p variations on the 20 x 25 cm scope. The optional fourth link outputs calculated data on the lineprinter. A typical calculation takes about 10 sec.

2. Midstream Evaluation Conference (K. Way, S. M. Shafroth, J. Y. Park, H. W. Newson)

Three articles growing out of this conference are in process of publication in Nuclear Data Tables A8, No. 4. The titles and authors are "Midstream Evaluation, A = 88", C. D. Goodman, T. A. Hughes, M. W. Johns, and K. Way; "Midstream Evaluation, A = 89", M. W. Johns, J. Y. Park, S. M. Shafroth, D. M. Van Patter, and K. Way; and "Midstream Evaluation, A = 90", J. B. Ball, M. W. Johns, and K. Way.

Material in data journals edited at TUNL. Nuclear Data Tables and Atomic Data is listed in Appendix

3. Large-Capacity Foil Stripper for The Tandem Accelerator (T. B. Clegg, G. L. Morgan, T. G. Dzubay, G. Spalek)

The design has been completed. Construction will begin when shop time becomes available.

4. Tandem Energy Stabilization (T. Dzubay, F. O. Purser, E. G. Bilpuch, H. W. Newson)

An attempt is being made to minimize the energy spread in the tandem proton beam using a voltage correction signal of 0 to 6 KV applied to the target. A magnet at the exit of the accelerator deflects H^+ ions of energy E, which are then foccussed on a target in a conventional manner. A neutral beam of energy E/2 emerges undeflected through this first magnet, passes through a carbon stripping foil, and is then deflected by a 90° analyzing magnet. Signals from a pair of slits are amplified and applied to the target and stripping foil. A test of the beam transport system is ability to handle the two beams simultaneously has been satisfactorily completed. The electronic system has been bench tested, and the first test of the complete system in a closed loop mode is scheduled for the very near future.

5. Polarization Monitor for Polarized Proton Beams (E. J. Ludwig, T. B. Clegg, A. C. Watkins)

A ^{4}He gas cell has been constructed to use at the exit of the 24" scattering chamber to monitor continuously the polarization of proton beams produced by the polarized ion source. The gas cell will contain pressure up to 10 atmospheres of ^{4}He. Two detectors are placed in the gas cell, one to the left and one to the right of the beam. The spin quantization axis of the incident beam is vertical, perpendicular to the scattering plane. "Venetian blind"-type slits define the angular range of the scattered particles.

The polarimeter has been calibrated now for incident proton energies between 9.5 and 13.5 MeV. The efficiency of about 20 counts/sec and analyzing power of approximately 0.8 are satisfactory to provide accurate polarization monitoring for beam currents in the 1μA range. Further work is necessary to provide good isolation so the monitor will serve as a good Faraday cup to use in cross section measurements. Work is in progress also to find a good method to monitor the deuteron beam polarization.

6. Beam Chopper (P. Nettles, E. J. Ludwig, S. Shafroth, N. R. Roberson)

A computer-controlled beam chopper is being constructed in the Duke University machine shop. This is to be installed between the high resolution magnets and will be used for studies of nuclear processes producing short-half life radioactivities and for time-of-flight studies.

C. REPORTS OF PROJECT COMMITTEES

1. On-Line Data Acquisition And Analysis (S. E. Edwards, C. R. Gould, R. A. Hardekopf, J. Joyce, R. O. Nelson, N. R. Roberson)

The DDP-224 computer purchased by the University of North Carolina at Chapel Hill is being interfaced to an IBM Model 29 card punch. This feature should prove very useful for modifying or reproducing card decks and will facilitate transfer of data between different stages of analysis wither here or at the IBM 360 system at TUCC.

An automatic stabilization system for the 50 MH_2, 8K analog to digital converters is planned for the time share computer. This will primarily be for use in the acquisition of high resolution Ge(Li) spectra over long periods. Using an ultra stable double pulser, the computer will evaluate centroids of two reference peaks and make appropriate adjustments with stepping motors to the baseline and conversion gain of the ADC.

An interface to allow automatic read in and adjustment of the analyzing magnetic current and resonance frequency is also being constructed. This will be especially useful in the acquisition of yield curve data using the Cyclo-Graaff and will be a first step toward computer control of a number of Tandem and Cyclo-Graaff accelerator operations.

2. Scattering Chambers (E. J. Ludwig, T. B. Clegg, A. Watkins)

A second 24" scattering chamber is under construction at the Duke and UNC machine shops. This chamber will allow detectors on the top and bottom rotating plates to be continuously varied in position with respect to each other. It will be especially useful for high resolution studies of nuclear levels. The original 24" chamber will be altered so as to rotate around the beam axis. This feature will facilitate deuteron polarization measurements.

3. Lamb-Shift Polarized Ion Source (T. B. Clegg and G. A. Bissinger)

The Lamb-shift polarized ion source is now complete and is installed on the 7.5 MV Model FN tandem accelerator. The ion-source design follows largely that of two other such ion sources now operating at Los Alamos[1] and Wisconsin.[2] It utilizes the duoplasmatron, the extraction geometry, and the "spin-

1) G. P. Lawrence, G. G. Ohlsen and J. L. McKibben, Phys. Lett. 28B (1969) 594
2) T. B. Clegg and G. A. Bissinger, Bull. Am. Phys. Soc. 15 (1970) 598.

filter" scheme developed at Los Alamos. It utilizes the Wisconsin modular vacuum system. Polarized beams are injected into the accelerator with two electrostatic mirrors and two spin rotation solenoids similar to the scheme at the Wisconsin installation.

The duoplasmatron is a copy of the Los Alamos design with positive beam being extracted at energies up to 22 keV before being decelerated to 550 eV for protons or 1100 eV for deuterons. The magnetic lens is important to obtain high transmission of the positive beam into the cesium tube. The cesium oven will hold up to 200 grams and the cesium flow is regulated by a bakeable stainless steel valve. Under normal operation, however, the cesium deposited inside the vacuum system must be cleaned out long before 200 grams is evaporated. The cesium tube itself is 1.2 cm in diameter and 22.5 cm long. Surrounding the cesium oven assembly is a Freon cooled baffle. Following the cesium tube are deflection plates 12.5 cm long made from screen to avoid cesium buildup on the plates.

The beam then enters the uniform magnetic field region necessary for operation of the spin filter. The solenoid required to create this uniform magnetic field is 51 cm long and contains four separate coils. It produces an axial magnetic field variable between 535 and 605 G. which is uniform to 0.1 G over a 25 cm axial distance. A duplicate of the Los Alamos four-section radio-frequency cavity is placed in this uniform field region. The circuitry for r.f. frequency and amplitude stabilization follows plans developed at Los Alamos. In addition to providing the uniform field region, the four-coil solenoid arrangement provides a fringing field on either end with a maximum gradient of the axial field of about 80 G/cm. This slope is gradual enough to prevent significant quenching of the metastable beam upon entering and leaving the solenoid.

The beam leaving the spin filter region passes into the argon charge exchange tube which is 30 cm long and 6 cm in diameter. This is placed inside a solenoid which will make an axial magnetic field up to 200 Gauss. The negative polarized beam is then accelerated to energies up to 80 keV and focussed in a three-gap acceleration system similar to the Los Alamos design.

This accelerated beam then enters the first of two electrostatic mirrors where it is reflected through 90° into the first of two spin-rotation solenoids. The spin quantization axis can here be rotated through positive or negative angles. In particular, for proton and deuteron vector polarization measurements, the spin axis will be rotated alternately through $\pm 90°$ here. The beam is then focussed by an einzel lens into a second electrostatic mirror where it is reflected onto the tandem beam axis. Before entering the accelerator, the beam passes through a second spin rotation solenoid. The combination of two electrostatic mirrors and two spin rotation solenoids allows selection of any arbitrary direction for the spin quantization axis. The electrostatic mirrors used on the TUNL ion source are not alike. The first is a copy of the design developed at Brookhaven using three slotted plates.[3] The second is a copy of the electrostatic mirrors used on the Wisconsin ion source. Preliminary tests indicate the Wisconsin design is superior because it allows the beam to be reflected without the focusing associated with the Brookhaven design.

The main part of the vacuum system for the ion source consists of four welded aluminum vacuum chambers. These were precision machined after welding to assure that the boxes when bolted together would be self-aligning. Numerous holes for feedthroughs, windows, and pumps are provided. The tops of three of the boxes can be removed for easy access to the ion source components inside. A 4" diffusion pump is attached to the box housing the duoplasmatron. One 6" pump evacuates the cesium box and two 6" pumps are attached to the box containing the spin filter and the argon charge exchange region. A 4" pump evacuates the box containing the first electrostatic mirror and spin rotation solenoid. Water cooling for the pumps is provided with a closed deionized water system. Cooling for all the solenoids on the ion source is provided by a closed system circulating high dielectric strength transformer oil.

Construction began on the TUNL polarized source in September 1968 using funds granted by the U. S. AEC and the North Carolina Board of Science and Technology. The ion source was built in Chapel Hill and initial beam tests were made there in the spring of 1970. Metastable beam currents of 8nA of protons and 20 nA of deuterons were accelerated to 50 keV and focussed through a 0.63 cm diameter hole into the target chamber. With the spin filter operating, 2nA of polarized proton beam was observed in each of the α-states with an equal amount of unpolarized background current. It was later found that the magnetic field was accidentally not uniform in the spin-filter region causing the large unpolarized background beam.

In June 1970 the ion source was moved eleven miles to TUNL and was installed on the accelerator. In July initial tests showed that 2-3 nA of polarized proton or deuteron beam could be obtained at the high energy end of the accelerator. Since this time the polarized proton beam has been used. Beam currents of up to 4 nA with polarization of 68% have been obtained on target through 1 mm x 3mm slits. The proton polarizations were measured using p-^{4}He scattering. These target currents are approximately 10 to 15% of the current measured at the Faraday cup immediately following the spin rotation solenoid. To try to improve the transmission

3) J. A. Benjamin, D. Larsen, H. Wegner, Rev. Sci. Instr. 39 (1968) 272.

of the polarized beam through the accelerator, a measurement of the polarized beam emittance and a study of the optical properties of the present low-energy beam transport system are underway. Experiments are planned for the next few weeks to measure the deuteron polarization.

Remote controls for the lenses, mirrors, and spin rotation solenoids of the ion source are provided in the main accelerator control room. A system for changing the 575 Gauss coil current and the spin-rotation solenoid currents remotely has also been built and is now being installed. This will allow computer control of (1) the spin-state selection in the spin filter and (2) the orientation of the spin quantization axis.

4. Tandem Accelerator

The low energy extension has been modified to accept a spin precession solenoid for use with polarized beams. In the process of installing this solenoid a through realignment of the low energy extension was completed.

An oxygen beam capability has been developed using a helium-oxygen mixture in the duoplasmatron and Lithium exchange. 200 nanoamps of O^{5+} have been obtained at the analyzing magnet control slits.

All circuitry and hardware have been constructed to install a beam energy homogenizer on the tandem for ultra high resolution work. The arrangement utilizes the uncharged component of the beam which exists when gas stripping is employed. This neutral beam is transmitted through the first analyzing magnet undeflected then stripped and focused onto the input slits of the high resolution analyzing system. The energy error signal developed at the output slits of this system is then amplified and applied to both the target and the external stripping foil so that the system operates as a null device. The natural bandwidth of this method of cancelling tandem energy fluctuations is limited generally only by the capacitance of the target and/or stripper and thus avoids the frequency response difficulties introduced into voltage control systems by the slow response of the tandem terminal.

A complete cleaning of the columns and acceleration tubes and a thorough recheck of all resistors, spark gaps and associated components has just been completed. The previously reported terminal instability and sagging associated with the insert of high gamma fluxes in the vicinity of the terminal continue to limit available terminal energy and increase beam energy spread. Initial operation following the clean up indicates that the problem has not been alleviated by the massive overhaul. Present opinion points to the possibility of a very minor pressure leak too small to be evident in the tube vacuum gauges but producing sufficient gas flow to initiate tube flashing. This will be thoroughly checked out at the next tank opening.

5. Beam Transport System (F. O. Purser, T. D. Hayward, J. R. Boyce, R. L. Rummel, M. T. Smith)

The high resolution analyzing and beam transport system has been placed in routine operation. Reliability and energy calibration characteristics have proven excellent. Determination of the ultimate resolving power of the system has proven difficult since at tandem energies the tandem beam energy spread is generally less than the designed resolving power while for Cyclo-Graaff energies sharply defined resonances are not available. The best measurements to date indicate an energy resolution for the system of $\Delta E/E \leq 1/4000$. Operation in the high transmission mode has been entirely satisfactory with 100% transmission being routinely obtained.

New power supplies for the beam line x-y steerers have been designed and manufactured in order to increase reliability and smoothness of response. The new supplies have been installed and appear to perform well on initial tests.

6. Injector Cyclotron (F. O. Purser, T. D. Hayward, J. R. Boyce, H. W. Newson, R. L. Rummel, M. T. Smith)

A new power supply for the electrostatic deflector has been completed and tested. Based upon full curve rectification of a high frequency oscillator, the new supply minimizes ripple on the deflector voltage and also is compatible with feedback stabilization to insure positional stability of the beam injected into the tandem.

When the new deflector supply is installed it will be possible to resume development of dee voltage stabilization through use of a beam derived correction signal and an external feedback loop. All components and equipment necessary have been completed and on hand.

The hardware for the pulse suppression system for the cyclotron has been installed. Electronics required is nearing completion and will be tested in the near future. The pulse suppression device will allow time of flight studies with pulse repetition times ranging from 40 ns to 640 ns. Its initial use is planned in the charged particle fission program.

The variable azimuth resistor for the harmonic bump coils of the extraction system has been installed and is in normal use. An initial improvement in extraction efficiency from 35% to 50% was obtained.

A separate cooling water system for the cyclotron has been designed and is 80% installed. The present cooling system using a combination of iron and copper piping has proven most unsatisfactory for the low ion content water required to minimize power requirements for the various high voltage supplies. Iron leached from the pipes deposits in regions of high thermal or electric gradients and swiftly constricts cooling water flow to various critical regions. The new system is all copper and incorporates a separate freon chiller and heat exchanger to allow operation with deionized water at a reduced water temperature. Component lifetimes should be considerably extended.

YALE UNIVERSITY

A. NEUTRON TIME-OF-FLIGHT STUDIES

1. Photoneutron Reactions (F.W.K. Firk, C.P. Wu, and B.L. Berman*)

Evidence for isospin splitting of the dipole state in ^{26}Mg has been obtained by studying the energy spectra of photoneutrons emitted from the states. Intense and energetic transitions from T< states (T = 1) were observed below 18 MeV. Between 20 and 22.5 MeV, six states were positively identified as T> states (T = 2) whereas no decays were observed from states in this region to low-lying states of ^{26}Mg even though it is known that appreciable $(\gamma,1n)$ strength still exists up to 22.5 MeV. We conclude that this is clear evidence for isospin splitting of the dipole state in ^{26}Mg. We note that, in addition to the T-splitting, effects due to the possible deformation of the ground state of ^{26}Mg may obviously occur. However, our measurement cannot throw any light upon such effects.

2. Polarization Studies (F.W.K. Firk, R.J. Holt, R. Nath, H.L. Schultz, and F.D. Brooks**)

2.1 Photo-disintegration Studies

We have re-measured the differential polarization of photoneutrons from the reaction $^{16}O(\gamma,n)^{15}O$ at 45° and 90° using the liquid He polarimeter and nanosecond time-of-flight system described in a previous report. This time, however, a 1.2m long, 4KG solenoid was used to process the spins of the neutrons. Since all neutron energies between 2 and 30 MeV were measured in the experiment it was necessary to determine the angle of precession for a given

---

* On leave 1969-70 from LRL Livermore, California

** On leave from 1970-71 from University of Cape Town, South Africa.

neutron energy. This was deduced from accurately measured values of the magnetic field. In most of the present work, the field was set to precess the spin of a 6MeV neutron through 180°. The results agree well with those obtained earlier by switching left-right neutron counters in the traditional way.

Measurements of the polarization of photoneutrons from the D(γ,n)p reaction are now in an advanced stage. Identical targets of D_2O and H_2O (and also CD_2 and CH_2) have been used in these "difference" experiments. Preliminary measurements at 45° and 90° have been obtained in the photon energy range 5 to 30 MeV. The results are in general agreement with the predictions of Partovi.

2.2 Polarization in n-p Scattering

A neutron polarimeter, based upon direction-sensitive pulse shape discrimination properties of anthracene crystals, is being constructed. This will be used in conjunction with a pulsed polarized neutron beam from photodisintegration of ^{16}O to measure the polarization in n-p scattering in the 6-30 MeV range.

DATA NOT FOR QUOTATION